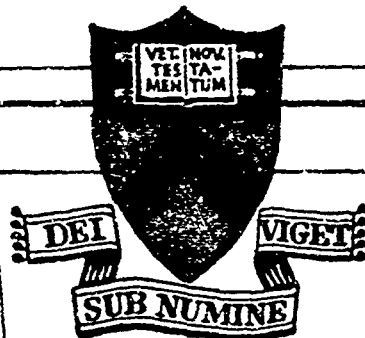
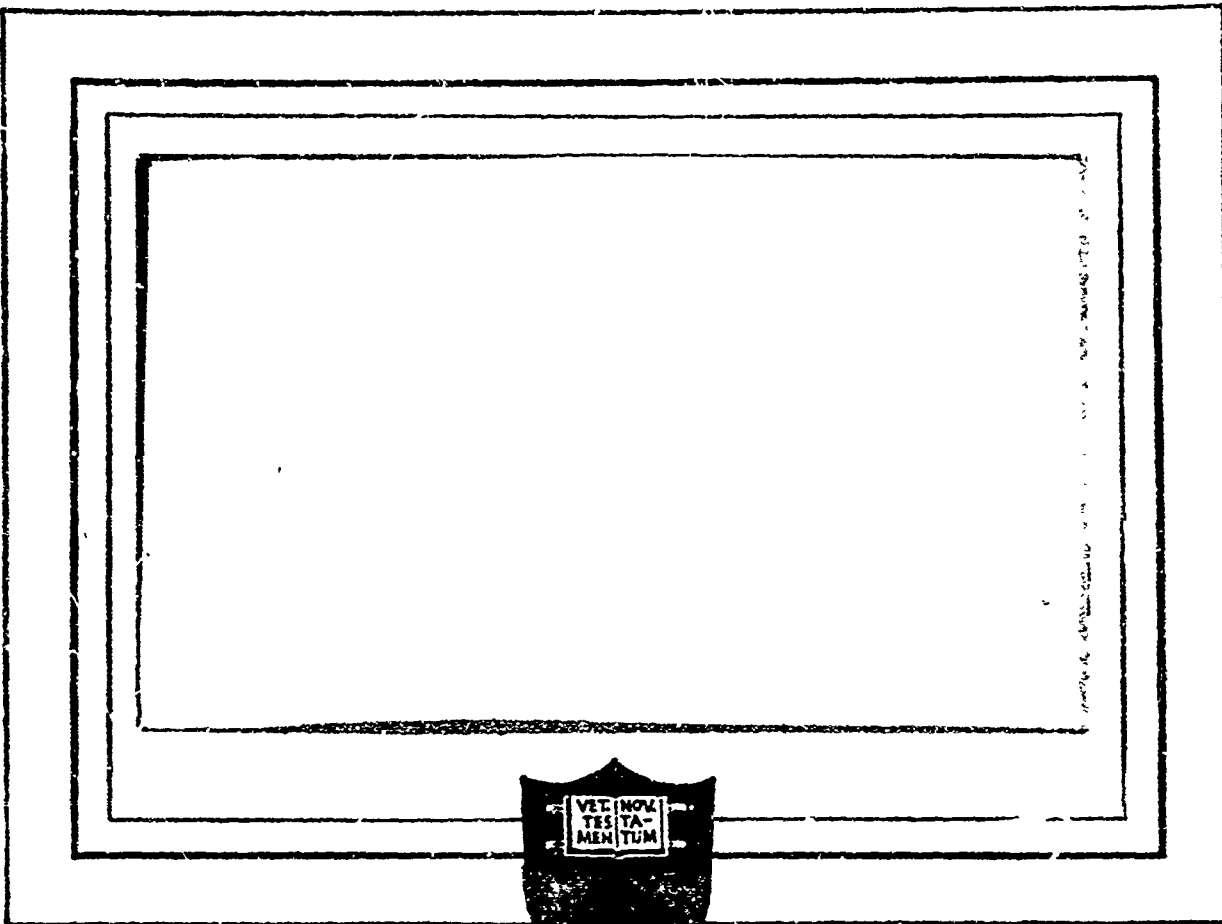


AD634277



CLEARINGHOUSE FOR FEDERAL SCIENTIFIC AND TECHNICAL INFORMATION			
Hardcopy	Microfilm	339	PL 48
\$ 7.00	\$ 1.75		
ARCHIVE COPY			

D  
JUN 27 1966  
C

PRINCETON UNIVERSITY  
DEPARTMENT OF  
AEROSPACE AND MECHANICAL SCIENCES

AFOSR SCIENTIFIC REPORT  
NO. 66-0855

AIR FORCE OFFICE OF SCIENTIFIC RESEARCH

Contract AF 49(638)-1268

THE HOMOGENEOUS GAS PHASE KINETICS OF  
REACTIONS IN THE HYDRAZINE-NITROGEN  
TETROXIDE PROPELLANT SYSTEM

BY

ROBERT F. SAWYER

Technical Report 761

Approved by:



Irvin Glassman  
Professor of  
Aeronautical Engineering  
Principal Investigator

Reproduction, translation, publication, use and disposal in  
whole or in part by or for the United States Government is  
permitted.

Guggenheim Laboratories for the Aerospace Propulsion Sciences  
Department of Aerospace and Mechanical Sciences  
Princeton University  
Princeton, New Jersey  
1965

The Homogeneous Gas Phase Kinetics of Reaction in the  
Hydrazine-Nitrogen Tetroxide Propellant System

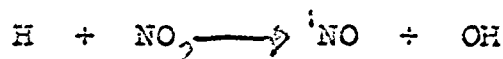
ERRATA, 7 April 1966

Page ii fourth line from bottom. change "reduction"  
to oxidation

Page 63 equation E3 (19) should read

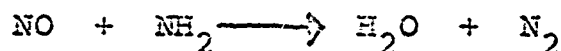
$$\log \left( - \frac{d[A_1]}{dt} \right) = \log k + \sum_{i=1}^m n_i \log [A_i]$$

Page 85 reaction R4 (6) should read

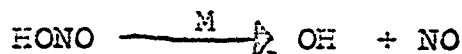


Page 87 fourth line from bottom should read: ....con-  
centration of the third body, M,

Page 141 sixth reaction under  $NH_3/NO_2$  should read



Page 168 reaction R7 (2) should read



Page 170 first equation should read

$$k_2' = k_2 [M]$$

Page 180 equation should read

$$\frac{d[O_2]}{dt} = -k_{21} [N_2H_4] \left\{ \frac{1 + \frac{k_{26}}{k_{29} [O_2]}}{1 + \frac{k_{25} [N_2H_4]}{k_{23} [O_2]}} \right\}$$

Page 259 Table 34, dimensions should read [(moles/cc) $\cdot^{.25}$  sec $^{-1}$ ]

ABSTRACT

The homogeneous gas phase reaction of hydrazine and nitrogen dioxide is of direct interest to rocket propulsion as it relates to the combustion of the propellants, hydrazine and nitrogen tetroxide. The reaction of these two gases is representative of a general, unresolved problem in combustion, the role of fuel pyrolysis in oxidation reactions. Both reactants of this combination have the potential for decomposition: hydrazine to ammonia, hydrogen, and nitrogen; and nitrogen dioxide to nitric oxide and oxygen.

A number of different homogeneous gas phase reactions arising from the possible combinations of the fuels: hydrazine, ammonia, hydrogen, and decomposed hydrazine with the oxidizers: nitrogen dioxide, oxygen, nitric oxide, and decomposed nitrogen dioxide were investigated in the same adiabatic flow reactor at temperatures falling between 800 and 1300°K. Heats of reaction, reaction orders, and reaction rates were determined. From the measured reaction rates, Arrhenius rate constants were calculated and overall activation energies determined. Based on the experimental observations and the work of other investigators on related reactions, reaction mechanisms were postulated.

The reaction of hydrogen and oxygen is about 10 times more rapid than the reaction of hydrogen and nitrogen dioxide. The hydrogen/nitrogen dioxide reaction produces nitric oxide which inhibits the further reduction of hydrogen. In small concentrations nitric oxide is observed to accelerate the reaction of hydrogen and oxygen. No reaction between hydrogen and nitric oxide



is observed.

Ammonia reacts about ten times more rapidly with nitrogen dioxide than with oxygen. This more rapid reaction is traced to the role of nitrogen dioxide in hydrogen abstraction from ammonia. The reaction of ammonia with decomposed nitrogen dioxide and with nitric oxide is slower than with oxygen is not observed.

The reaction of ammonia and hydrogen, corresponding to the reactive decomposition products of hydrazine, is much more rapid with nitrogen dioxide than with oxygen. No reaction can be obtained with decomposed nitrogen dioxide or with nitric oxide. Ammonia retards the reaction of hydrogen and oxygen in proportion to the amount of ammonia present. Hydrogen accelerates the ammonia/oxygen reaction, largely independently of the concentration of hydrogen. The reaction rate of the mixture of hydrogen and ammonia with nitrogen dioxide is similar to the hydrogen/nitrogen dioxide and to the ammonia/nitrogen dioxide reaction rates which are also comparable with each other.

Hydrazine and nitrogen dioxide react with a two step behavior. The rapid reduction of nitrogen dioxide to nitric oxide is followed by a slower reduction of nitric oxide. The first step reaction occurs without hydrazine decomposition. The second step requires the decomposition of hydrazine. The reaction of hydrazine and oxygen occurs with simultaneous decomposition and oxidation. The reaction of hydrazine and nitric oxide is similar to the second step of the hydrazine/nitrogen dioxide reaction.

SUMMARY OF MEASURED REACTION RATES

<u>reaction</u>	reaction rate = (concentrations in mole/cc)	<u>rate constant</u> $k = 10^A \exp(-E/RT)$	
		A	E (kcal/mole)
$H_2/NO_2$	$k \frac{[H_2]^{1.4}[NO_2]}{[NO_2]+[NO]}$	14.26	46.2
$H_2/O_2$	$k [H_2]$	10.96	38.2
$H_2/NO + \frac{1}{2}O_2$	$k [H_2]^*$	16.47	68.6
$H_2/NO$	no reaction	---	---
$NH_3/NO_2$	$k [NH_3][NO_2]$	15.85	33.8
$NH_3/O_2$	$k [NH_3][O_2]^*$	14.61	38.7
$NH_3/NO + \frac{1}{2}O_2$	no reaction	---	---
$NH_3/NO$	no reaction	---	---
$NH_3 + \frac{1}{2}H_2/NO_2$	$k [NH_3 + \frac{1}{2}H_2][NO_2]^*$	23.44	65.9
$NH_3 + \frac{1}{2}H_2/O_2$	$k [NH_3 + \frac{1}{2}H_2][O_2]^*$	19.64	61.9
$NH_3 + \frac{1}{2}H_2/NO + \frac{1}{2}O_2$	no reaction	---	---
$NH_3 + \frac{1}{2}H_2/NO$	no reaction	---	---
$N_2H_4/NO_2$ step I	$k [N_2H_4][NO_2]$	15.83	26.7
$N_2H_4/NO_2$ step II	$k [N_2H_4]$	10.17	39.6
$N_2H_4/O_2$	$k [N_2H_4]$	9.91	37.2
$N_2H_4/NO + \frac{1}{2}O_2$	$k [N_2H_4]^*$	10.35	39.1
$N_2H_4/NO$	$k [N_2H_4]$	11.48	45.4

---

\* assumed rate equations, others determined experimentally

### ACKNOWLEDGMENTS

The author thanks his advisor, Professor Irvin Glassman, for advice, guidance, and continued encouragement throughout the progress of this research. His eagerness and availability as a listener and discussor of the details of the investigations has been greatly appreciated. Dr. Alvin Gordon, Dr. Igor Eberstein, and fellow graduate students in the Guggenheim Laboratories also assisted in the research through numerous and helpful discussions.

The execution of the experimental work could not have been accomplished without the consistent and careful work of Mr. Joseph Sivo who maintained and rebuilt the experimental apparatus on more occasions than he or the author care to recall, handled the toxic and explosive reactants with strict adherence to safety procedures, and assisted in the gathering of the experimental data. Thanks are due to the entire Guggenheim staff, particularly to Mr. Anthony Bozowski, Mr. Donald Neiler, Mr. Lanny Hoffman and the computing group, and to Mr. Tony Poli and the design group for their assistance.

Dr. Wayne Solomon of the Air Force Rocket Propulsion Laboratory assisted in the flame studies. Dr. Roboz of the Air Reduction Research Laboratories performed the gas sample mass spectrometric analyses. Infrared equipment was made available by the Princeton University Chemistry Department.

Financial support and encouragement from the Air Force Office of Scientific Research, Propulsion Science Division under Air Force Grant 62-90, was essential in carrying out this investigation. Computer facilities used in this work were supported by National Science Foundation Grant NSF-GP 579. The author is proud to acknowledge fellow-

ship support received from the Daniel and Florence Guggenheim Foundation and from the Ford Foundation.

The careful attention of Miss Christine Walch to the typing of the manuscript has been appreciated greatly.

TABLE OF CONTENTS

	<u>PAGE</u>
TITLE PAGE	i
ABSTRACT	ii
ACKNOWLEDGMENTS	v
TABLE OF CONTENTS	vii
LIST OF FIGURES	xiv
LIST OF TABLES	xix
CHAPTER 1. <u>INTRODUCTION</u>	1
1.1 REACTION MATRIX	1
1.2 OBJECTIVES	2
1.3 OUTLINE OF PRESENTATION	4
CHAPTER 2. <u>THE REACTANTS</u>	6
2.1 HYDRAZINE AND ITS DECOMPOSITION PRODUCTS	6
2.1.1 Hydrazine	6
2.1.2 Hydrazine decomposition	12
2.1.3 Hydrogen	15
2.1.4 Ammonia	15
2.1.5 Decomposition of ammonia	16
2.2 NITROGEN TETROXIDE AND ITS DECOMPOSITION PRODUCTS	16
2.2.1 Nitrogen tetroxide	16
2.2.2 Nitrogen tetroxide decomposition	17
2.2.3 Nitrogen dioxide	18
2.2.4 Dissociation of nitrogen dioxide	20
2.2.5 Nitric oxide	21
2.2.6 Oxygen	22

	<u>PAGE</u>
2.3 EQUILIBRIUM COMPOSITIONS OF THE H-N-O SYSTEM	22
2.3.1 N-H systems	24
2.3.2 N-O systems	24
2.3.3 H-N-O systems	25
2.4 ENTHALPIES OF REACTION	26
CHAPTER 3. <u>EXPERIMENTAL TECHNIQUES</u>	30
3.1 THE FLOW REACTOR	30
3.1.1 Theory	31
3.1.2 Description of apparatus	33
3.1.2.1 Carrier gas system	34
3.1.2.2 Oxidizer system	39
3.1.2.3 Fuel system	39
3.1.2.4 Diluent nitrog. system	42
3.1.3 Experimental variables	44
3.1.3.1 Turbulence effects	44
3.1.3.2 Range of experimental parameters	45
3.2 CONTROLS AND MEASUREMENTS	47
3.2.1 Flows	47
3.2.2 Temperatures	47
3.2.3 Gas sampling	52
3.2.4 Velocity profile	52
3.3 EXPERIMENTAL PROCEDURE	52
3.3.1 General techniques	52
3.3.2 Safety precautions	53
3.3.3 Reproducibility of measured reaction rates	54
3.4 DATA REDUCTION AND ANALYSIS	54
3.4.1 Preliminary calculations	55
3.4.2 Calculation of the rate constant	57
3.4.3 Determination of reaction orders	62
3.4.4 Enthalpies of reaction	65
3.4.5 Statistical analysis of experimental data	65

	<u>PAGE</u>
3.5 ANALYSIS OF GAS SAMPLES	66
3.5.1 Gas chromatography	67
3.5.2 Infrared spectroscopy	67
3.5.3 Mass spectroscopy	68
3.6 REACTANTS AND CARRIER GASES	68
3.7 MASS SPECTROSCOPIC FLAME STUDY	70
CHAPTER 4. <u>HYDROGEN REACTIONS</u>	73
4.1 HYDROGEN/NITROGEN DIOXIDE	73
4.1.1 Stoichiometry	73
4.1.2 Experimental results, adiabatic flow reactor	74
4.1.3 Experimental results, flame studies	78
4.1.4 Results of other investi- gators	82
4.1.5 Reaction mechanism	85
4.2 HYDROGEN/OXYGEN	89
4.2.1 Stoichiometry	89
4.2.2 Experimental results	90
4.2.2.1 Nitrogen carrier (near stoichiometric composi- tion)	90
4.2.2.2 Air carrier (excess oxygen composition)	92
4.2.2.3 Comparison of nitrogen carrier and air carrier results	98
4.2.3 Wall effect	98
4.2.4 Results of other investi- gators	99
4.2.5 Reaction mechanism	103
4.3 HYDROGEN/NITRIC OXIDE-OXYGEN	107
4.3.1 Stoichiometry	107
4.3.2 Experimental results	108
4.3.3 Results of other investi- gators and reaction mechan- ism	109

	<u>PAGE</u>
4.4 HYDROGEN/NITRIC OXIDE	109
4.5 THE EFFECT OF NITRIC OXIDE ON THE HYDROGEN/OXYGEN REACTION	110
4.5.1 Stoichiometry	111
4.5.2 Experimental results	111
4.5.3 Results of other investigators	115
4.5.4 Reaction mechanism	115
4.6 COMPARISON OF HYDROGEN REACTIONS	117
CHAPTER 5 <u>AMMONIA REACTIONS</u>	122
5.1 AMMONIA/NITROGEN DIOXIDE	122
5.1.1 Stoichiometry	123
5.1.2 Experimental results	123
5.1.3 Results of other investigators	126
5.1.4 Reaction mechanism	129
5.2 AMMONIA/OXYGEN	
5.2.1 Stoichiometry	131
5.2.2 Experimental results	131
5.2.3 Results of other investigators	132
5.2.4 Reaction mechanism	134
5.3 AMMONIA/NITRIC OXIDE-OXYGEN	135
5.4 AMMONIA/NITRIC OXIDE	136
5.5 COMPARISON OF AMMONIA REACTIONS	137
CHAPTER 6. <u>AMMONIA-HYDROGEN REACTIONS</u>	142
6.1 AMMONIA-HYDROGEN/NITROGEN DIOXIDE	142
6.1.1 Stoichiometry	143
6.1.2 Experimental results	143
6.1.3 Results of other investigators and reaction mechanism	145
6.2 AMMONIA-HYDROGEN/OXYGEN	145
6.2.1 Stoichiometry	146
6.2.2 Experimental results	146
6.2.3 Results of other investigators and reaction mechanism	147



	<u>PAGE</u>
6.3 AMMONIA-HYDROGEN/NITRIC OXIDE-OXYGEN	148
6.4 AMMONIA-HYDROGEN/NITRIC OXIDE	148
6.5 COMPARISON OF AMMONIA-HYDROGEN REACTIONS	149
CHAPTER 7. <u>HYDRAZINE REACTIONS</u>	152
7.1 HYDRAZINE/NITROGEN DIOXIDE	152
7.1.1 Stoichiometry	153
7.1.2 Experimental results	157
7.1.2.1 Step I, reduction of nitrogen dioxide to nitric oxide	158
7.1.2.2 Step II, reduction of nitric oxide	162
7.1.2.3 Comparison of steps I and II	165
7.1.3 Results of other investigators	165
7.1.4 Reaction mechanism	167
7.1.4.1 Step I, reduction of nitrogen dioxide to nitric oxide	167
7.1.4.2 Step II, reduction of nitric oxide	170
7.2 HYDRAZINE/OXYGEN	173
7.2.1 Stoichiometry	174
7.2.2 Experimental results	174
7.2.3 Results of other investigators	177
7.2.4 Reaction mechanism	178
7.3 HYDRAZINE/NITRIC OXIDE-OXYGEN	181
7.3.1 Stoichiometry	181
7.3.2 Experimental results	182
7.3.3 Results of other investigators and reaction mechanism	182
7.4 HYDRAZINE/NITRIC OXIDE	183
7.4.1 Stoichiometry	184
7.4.2 Experimental results	185
7.4.3 Results of other investigators	185
7.4.4 Reaction mechanism	188

	<u>PAGE</u>
7.5 COMPARISON OF HYDRAZINE REACTIONS	189
CHAPTER 8. <u>COMPARISON OF THE REACTIONS STUDIED: THEIR RELATION TO THE HYDRAZINE/NITROGEN DIOXIDE REACTION</u>	195
8.1 COMPARISON OF EXPERIMENTAL RESULTS	195
8.1.1 Reaction orders	195
8.1.2 Heats of reaction and stoichiometry	197
8.1.3 Reaction rates	198
8.1.4 Overall activation energies	205
8.2 COMPARISON OF REACTION MECHANISMS	206
8.2.1 Oxidation by nitrogen dioxide	206
8.2.2 The oxidation of hydrazine	208
8.2.3 Other comments on reaction mechanisms	210
8.3 THE EFFECT OF NITROGEN DIOXIDE DECOM- POSITION UPON ITS SUBSEQUENT REACTION	211
8.4 THE EFFECT OF HYDRAZINE DECOMPOSITION UPON ITS SUBSEQUENT REACTION	212
REFERENCES	214
NOMENCLATURE	225
APPENDIX A. SUMMARY OF EXPERIMENTAL PARAMETERS, ARRHENIUS PARAMETERS, AND EXPERIMENTAL RATE DATA	228
APPENDIX B. DERIVATIONS	262
B.1 Determination of the rate constant from the reaction rate	262
B.2 Estimation of the uncertainty in the reaction rate constant from the uncertainties in the measured quantities	266
B.3 The relation between reaction rate and reaction time	270

	<u>PAGE</u>
APPENDIX C. DATA REDUCTION AND ANALYSIS PROGRAMS	276
APPENDIX D. INFRARED SPECTRA AND MASS SPECTROSCOPIC ANALYSIS OF GAS SAMPLES	300
APPENDIX E. HYDRAZINE/NITROGEN TETROXIDE AS ROCKET PROPELLANTS	305
E.1. General properties	305
E.2 Theoretical performance	307
E.3 Experimental performance	311

LIST OF FIGURES

<u>Figure</u>	<u>Title</u>	<u>Page</u>
1.	Reaction matrix for the gas phase reactions of hydrazine, nitrogen dioxide, and their decomposition products	3
2.	Comparison of hydrazine decomposition rates	14
3.	Dissociation of nitrogen tetroxide	19
4.	Composition according to the equilibria, $N_2O_4 \rightleftharpoons 2NO_2 \rightleftharpoons 2NO + O_2$ , pressure 1 (atm)	23
5.	Chemical kinetic flow reactor	35
6.	Experimental apparatus, test cell	36
7.	Experimental apparatus, control and instrumentation panels	37
8.	Flow schematic, carrier gas system	38
9.	Flow schematic, oxidizer system	40
10.	Temperature profile, cold nitrogen injection	41
11.	Flow schematic, fuel system	43
12.	Temperature profile, hydrazine/nitric oxide reaction	49
13.	Comparison of gas and wall temperature profiles, hydrogen/air, 3 (in) duct	51
14.	Schematic, experimental apparatus for hydrogen/nitrogen dioxide flame study	71
15.	Flame study apparatus: burner and sampling probe	72
16.	Hydrogen/nitrogen dioxide reaction rates, $T = 1000$ K, dependence on hydrogen concentration	76
17.	Mass spectrograph, air	79
18.	Mass spectrograph, $H_2/NO_2$ flame, $H_2$ rich	80

<u>Figure</u>	<u>Title</u>	<u>Page</u>
19.	Mass spectrograph, $H_2/NO_2$ flame, $NO_2$ rich	81
20.	Nitrogen dioxide/hydrogen reaction	84
21.	Determination of reaction order from statistical curve fit, hydrogen/oxygen, nitrogen carrier	91
22.	Hydrogen/oxygen reaction rates, $T = 990^\circ K$ , dependence on hydrogen concentration, $[O_2] \gg [H_2]$	94
23.	Effect of duct diameter on reaction rate, hydrogen/oxygen, air carrier	96
24.	Extrapolation of hydrogen/oxygen rate constant to infinite diameter, air carrier	97
25.	Comparison of experimental induction times for hydrogen/oxygen	102
26.	Effect of nitric oxide on the hydrogen/oxygen reaction rate, $T = 950^\circ K$ , $P = 1$ (atm), $[H_2] = 1.3 \times 10^{-7}$ (mole/cc)	113
27.	Reaction rate constants for $H_2/O_2 + NO$ , $P = 1$ (atm), $[H_2] / [O_2] = 1$ , $[H_2] / [N_2] = .01$	114
28.	Comparison of hydrogen reaction rates, nitrogen carrier	119
29.	Ammonia/nitrogen dioxide reaction rates, $T = 1000^\circ K$ , dependence on ammonia concentration	124
30.	Ammonia/nitrogen dioxide reaction rates, $T = 1000^\circ K$ , dependence on nitrogen dioxide concentration	125
31.	Nitrogen dioxide/ammonia reaction rate	127
32.	Ammonia/oxygen reaction rates, $T = 1163^\circ K$ , dependence on ammonia concentration	133
33.	Comparison of ammonia reaction rates, second order rate constant	138
34.	Comparison of ammonia reaction rates, first order rate constant	139
35.	Comparison of ammonia-hydrogen reaction rates	150

<u>Figure</u>	<u>Title</u>	<u>Page</u>
36.	Temperature profile, hydrazine/nitrogen dioxide	154
37.	Determination of reaction order from statistical curve fit, hydrazine/nitrogen dioxide (step I)	159
38.	Determination of reaction order from statistical curve fit, hydrazine/nitrogen dioxide (step I)	160
39.	Hydrazine/nitrogen dioxide reaction rates (step II), $T = 1000^{\circ}\text{K}$ , dependence on hydrazine concentration	163
40.	Hydrazine/nitrogen dioxide reaction rates (step II), $T = 1000^{\circ}\text{K}$ , dependence on nitric oxide concentration	164
41.	Hydrazine/oxygen reaction rates, $T = 1000^{\circ}\text{K}$ , dependence on hydrazine concentration	175
42.	Hydrazine/oxygen reaction rates, $T = 1000^{\circ}\text{K}$ , dependence on oxygen concentration	176
43.	Hydrazine/nitric oxide reaction rates, $T = 1020^{\circ}\text{K}$ , dependence on hydrazine concentrations	186
44.	Hydrazine/nitric oxide reaction rates, $T = 1020^{\circ}\text{K}$ , dependence on nitric oxide concentration	187
45.	Comparison of hydrazine reaction rates, nitrogen carrier	191
46.	Comparison of nitrogen dioxide reaction rates	200
47.	Comparison of oxygen reaction rates, first order rate constant	201
48.	Comparison of oxygen reaction rates, second order rate constant	203
49.	Comparison of nitric oxide-oxygen (decomposed nitrogen dioxide) reaction rates	204
50.	Hydrogen/nitrogen dioxide reaction kinetics, 2 (inch) quartz duct, nitrogen carrier	231

<u>Figure</u>	<u>Title</u>	<u>Page</u>
51.	Hydrogen/nitrogen dioxide reaction kinetics 4 (inch) quartz duct, nitrogen carrier	232
52.	Hydrogen/oxygen reaction kinetics, 2 (inch) quartz duct, nitrogen carrier	234
53.	Hydrogen/oxygen reaction kinetics, 4 (inch) quartz duct, nitrogen carrier	235
54.	Hydrogen/oxygen reaction kinetics, 2 (inch) quartz duct, air carrier	237
55.	Hydrogen/oxygen reaction kinetics, 3 (inch) quartz duct, air carrier	238
56.	Hydrogen/oxygen reaction kinetics 4 (inch) quartz duct, air carrier	239
57.	Hydrogen/oxygen reaction kinetics, 3.375 (inch) stainless steel duct, air carrier	240
58.	Hydrogen/nitrogen dioxide (decomposed) reaction kinetics, 2 (inch) quartz duct, nitrogen carrier, oxidizer injection port 4	242
59.	Ammonia/nitrogen dioxide reaction kinetics, 2 (inch) quartz duct, nitrogen carrier	244
60.	Ammonia/nitrogen dioxide reaction kinetics, 4 (inch) quartz duct, nitrogen carrier	245
61.	Ammonia/oxygen reaction kinetics, 4 (inch) quartz duct, air carrier	247
62.	Ammonia + hydrogen (2-1)/nitrogen dioxide reaction kinetics, 4 (inch) quartz duct, nitrogen carrier	249
63.	Ammonia + hydrogen (2-1)/oxygen reaction kinetics, 4 (inch) quartz duct, nitrogen carrier	251
64.	Hydrazine/nitrogen dioxide reaction kinetics, 4 (inch) quartz duct, nitrogen carrier (reduction of $\text{NO}_2$ to $\text{NO}$ )	253
65.	Hydrazine/nitrogen dioxide reaction kinetics, 4 (inch) quartz duct, nitrogen carrier (reduction of $\text{NO}$ )	254

<u>Figure</u>	<u>Title</u>	<u>Page</u>
66.	Hydrazine/oxygen reaction kinetics, 4 (inch) quartz duct, nitrogen carrier	256
67.	Hydrazine/decomposed nitrogen dioxide reaction kinetics, 4 (inch) quartz duct nitrogen carrier	258
68.	Hydrazine/nitric oxide reaction kinetics, 4 (inch) quartz duct, nitrogen carrier, $a = 1.0$	260
69.	Hydrazine/nitric oxide reaction kinetics, 4 (inch) quartz duct, nitrogen carrier, $a = .75$	261
70.	Reaction half-time for a first order reaction with temperature change	275
71.	Infrared spectrum, ammonia/nitrogen dioxide reaction products, excess nitrogen dioxide	302
72.	Infrared spectrum, hydrogen/nitrogen dioxide reaction products, excess nitrogen dioxide	
73.	Infrared spectrum, nitric oxide	304
74.	Theoretical specific impulse, nitrogen tetroxide/hydrazine	308
75.	Theoretical specific impulse, nitrogen tetroxide/hydrazine	309
76.	Theoretical characteristic velocity, nitrogen tetroxide/hydrazine	312
77.	Experimental performance, hydrazine/nitrogen tetroxide	315



LIST OF TABLES

<u>Table</u>	<u>Title</u>	<u>Page</u>
1	Physical properties of some H, N, O compounds	7
2.	Thermodynamic functions at 298.16°K for some gaseous H, N, O species	9
3.	Bond dissociation energies, H,N,O species	10
4.	Bond energies of H,N,O bonds	11
5.	Enthalpies of reaction for selected reactions involving H,N,O species	27
6.	Enthalpies of reaction for the oxidation of hydrogen, ammonia, hydrazine, and decomposed hydrazine by nitrogen dioxide, oxygen, nitric oxide, and decomposed nitrogen dioxide	29
7.	Summary of ranges of flow reactor experimental parameters	46
8.	Relative reaction rates, hydrogen reactions at 1000°K	118
9.	Summary of reaction mechanisms, hydrogen reactions	121
10.	Ammonia flame speeds, Andrews and Gray (102), 70 mmHg	134
11.	Relative reaction rates, ammonia at 1100°K	137
12.	Summary of reaction mechanisms, ammonia reactions	141
13.	Relative reaction rates, ammonia-hydrogen ( $\text{NH}_3 + \frac{1}{2}\text{H}_2$ ) at 1150°K	149
14.	Measured heats of reaction for hydrazine/nitrogen dioxide	153
15.	Hydrazine flame speeds, Gray and Lee (25) 40 mmHg	177

<u>Table</u>	<u>Title</u>	<u>Page</u>
16.	Relative reaction rates, hydrazine reactions at 1000°K	190
17.	Comparison of reaction orders and overall activation energies, hydrazine reactions	192
18.	Summary of reaction mechanisms, hydrazine reactions	193
19.	Summary of reaction orders for the general rate equation	196
20.	Summary of measured heats of reaction	198
21.	Relative reaction rates, summary of all reactions studied, temperature range, 800-1300°K.	205
22.	Overall activation energies, summary of all reactions studied	206
23.	Summary of hydrogen/nitrogen dioxide reaction rate constants	230
24.	Summary of hydrogen/oxygen reaction rate constants, near stoichiometric (nitrogen carrier)	233
25.	Summary of hydrogen/oxygen reaction rate constants, excess oxygen (air carrier)	236
26.	Summary of hydrogen/nitric oxide-oxygen reaction rate constants, $H_2/NO + \frac{1}{2}O_2$ , nitrogen carrier	241
27.	Summary of ammonia/nitrogen dioxide reaction rate constants, nitrogen carrier	243
28.	Summary of ammonia/oxygen reaction rate constants, air carrier	246
29.	Summary of ammonia-hydrogen/nitrogen dioxide reaction rate constants, nitrogen carrier	248
30.	Summary of ammonia-hydrogen/oxygen reaction rate constants, nitrogen carrier	250

<u>Table</u>	<u>Title</u>	<u>Page</u>
31.	Summary of hydrazine/nitrogen dioxide reaction rate constants, nitrogen carrier	252
32.	Summary of hydrazine/oxygen reaction rate constants, nitrogen carrier	255
33.	Summary of hydrazine/decomposed nitrogen dioxide reaction rate constants, nitrogen carrier	257
34.	Summary of hydrazine/nitric oxide reaction rate constants, nitrogen carrier	259
35.	Mass spectrometric analysis of some gas samples	301
36.	Theoretical performance of some common propellants	306
37.	Combustion parameters. $N_2H_4/N_2O_4, O/F = 1.5$	310

CHAPTER 1. INTRODUCTION

Although great interest exists in the use of the hydrazine/nitrogen tetroxide combination as a rocket propellant, their reaction has received little attention. The impossibility of obtaining the premixed combinations required for chemical kinetics studies in shock tubes, isothermal bombs, isothermal flow reactors, and premixed flames has no doubt contributed to this dearth of investigations. The only reported reaction studies are those based on droplet burning, for example (1, 2, 3, 4)\*, and, in a single case, upon a diffusion flame (4). Since reaction rates in both of these cases are likely to be diffusion limited, little understanding of the chemical kinetic processes and rates has resulted.

1.1 REACTION MATRIX

While the motivation for the present studies came directly from the application of these chemicals as rocket propellants, an understanding of the reaction of hydrazine and nitrogen dioxide sheds some light on a central, unresolved problem in combustion, the role of pyrolysis of a fuel in its subsequent or concurrent oxidation. In fact, the particular combination of hydrazine and nitrogen dioxide is representative even more broadly of the role of pyrolysis in combustion in that both the fuel and the oxidizer are subject to possible decomposition. The gas phase pyrolysis of hydrazine to ammonia, hydrogen, and nitrogen is well established. The decomposition of nitrogen tetroxide to nitrogen dioxide under most, if not all, conditions of a gas phase combustion reactions is so rapid that nitrogen

---

\*Numbers in parentheses indicate references, listed beginning page 214.

dioxide may be considered as the initial oxidizer. Nitrogen dioxide may undergo further decomposition to nitric oxide and oxygen, and under extreme conditions, the nitric oxide can thermally decompose to oxygen and nitrogen.

In addition to the reaction of hydrazine and nitrogen dioxide, a matrix of other possible reactions can result from the decompositions of these parent species. In all, a four by four matrix representing 16 separate reactions must be considered as relating to the reaction of the single precursor pair, see Figure 1. The mixed oxidizer,  $\text{NO} + \frac{1}{2}\text{O}_2$ , corresponding to the first step decomposition products of nitrogen dioxide, and the mixed fuel,  $\text{NH}_3 + \frac{1}{2}\text{H}_2$ , corresponding to the reactive decomposition products of hydrazine, have been treated as reactants distinct from their respective components.

## 1.2 OBJECTIVES

The task of sifting and distinguishing the details of the mechanism of a reaction as complex as that of hydrazine and nitrogen dioxide is beyond the capability of current kinetics experiments. It is both desirable and possible, however, to understand more about the reaction than can be learned from the gross features of its behavior in a rocket combustion chamber. While it is the nature of the adiabatic flow reactor experiments to conceal the details of individual reaction steps by surrounding them with the competing and influencing presence of reactants, intermediates, and products, the technique is suited particularly well to the task undertaken. The adiabatic flow reactor, while offering neither the precision of a molecular beam experiment nor the pragmatic applicability of a rocket chamber firing, lies between the two with the promise of learning something about the chemical kinetics of a complex reaction under conditions requiring only moderate

	$\text{N}_2\text{H}_4$	$\text{H}_2$	$\text{NH}_3$	$\text{NH}_3 + \frac{1}{2}\text{H}_2$
$\text{NO}_2$	+	+	+	+
$\text{NO} + \frac{1}{2}\text{O}_2$	+	+	—	—
$\text{O}_2$	+	+	+	+
$\text{NO}$	+	—	—	—

+ REACTION RATES MEASURED

— NO REACTION OBSERVED

REACTION MATRIX FOR THE GAS PHASE  
 REACTIONS OF HYDRAZINE, NITROGEN DIOXIDE,  
 AND THEIR DECOMPOSITION PRODUCTS

extrapolation to be applicable to a propulsion combustor.

The capability of the flow reactor experiments to yield homogeneous gas phase reaction rates and reaction orders was utilized fully. Hopefully, these results in themselves, especially as they represent several reactions whose rates have not been measured previously, will contribute to the growing knowledge of reaction kinetics. A more important objective, however, has been to study a number of related reactions in the same apparatus thereby eliminating the variable of experimental technique which usually plagues the comparison of chemical kinetic studies. Of the 16 reactions represented by the reaction matrix, 11 were found to have measurable rates. That these reactions were all investigated in the same experimental apparatus provided an uncommon opportunity for comparison with assurance that differences noted were attributable to the chemical kinetics of the reactions rather than the nature of the experiments represented.

### 1.3 OUTLINE OF PRESENTATION

The following two chapters are devoted to providing background material on the chemical and physical properties of the reactants studied and to presenting a review of the experimental technique including both the nature of the experimental measurements and the approach to their interpretation. The experimental results are then discussed in four chapters, grouped according to the fuel investigated, in the order: hydrogen, ammonia, hydrogen + ammonia, and hydrazine. In each of these chapters, the reaction of the particular fuel with each of the oxidizers is discussed (1) in terms of the measured stoichiometry, heat

of reaction, reaction order, and reaction rate, (2) in comparison with the results of other investigators, where available, and (3) in terms of a plausible reaction mechanism. A comparison of the various oxidations of each fuel concludes each of these four chapters. Finally, a comparison of all the reactions studied is attempted. Particular attention is given to general similarities and particular contrasts and to the effect of reactant decompositions upon their subsequent reaction.



## CHAPTER 2. THE REACTANTS

While the investigation is centered upon the reaction of hydrazine and nitrogen dioxide, the reactions of a number of other species resulting from the thermal decomposition of hydrazine and nitrogen tetroxide also are considered, especially as they relate to the hydrazine/nitrogen dioxide reaction. In this chapter the physical and chemical properties of these species and the nature of their decompositions are considered. The propellant performance characteristics of hydrazine and nitrogen tetroxide are discussed in Appendix E.

### 2.1 HYDRAZINE AND ITS DECOMPOSITION PRODUCTS

While the considerable recent attention paid to hydrazine is no doubt due in large part to its increased use as a rocket propellant, its ability to sustain a decomposition flame has attracted interest for a period dating back to the work of Murray and Hall (5) reported in 1951. Because hydrazine readily undergoes pyrolysis to other reactive species, ammonia and hydrogen, understanding of hydrazine oxidation must necessarily involve the consideration of the decomposition process and the properties of its decomposition products.

#### 2.1.1 Hydrazine

Hydrazine is a clear hygroscopic liquid with many physical properties resembling those of water, see Table 1. A saturated hydronitrogen, hydrazine has the structure,

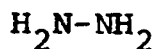
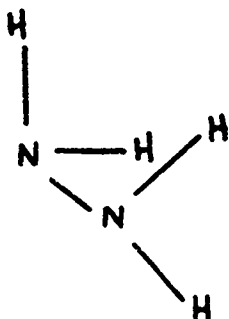


TABLE 1. Physical properties of some H, N, O compounds  
(6, 7, 8, 9, 10)

	H <sub>2</sub>	NH <sub>3</sub>	N <sub>2</sub> H <sub>4</sub>	H <sub>2</sub> O	$\begin{smallmatrix} 2\text{NO}_2 \\ \text{N}_2\text{O}_4 \end{smallmatrix}$	NO	O <sub>2</sub>
molecular weight	2	17	32	18	92/46	30	32
melting point (°C)	-259	-75	2	0	-11	-164	-219
boiling point (°C)	-253	-33	113	100	21	-152	-183
critical temperature (°C)	-240	132	380	374	158	-93	-119
heat of fusion (kcal/mole) at melting point	.03	1.8		1.4	3.0		.11
heat of vaporization (kcal/mole) at boiling point	.2	5.6	10.7	9.7	8.6		1.6
liquid density (gm/cc)	.07	.68	1.00	1.00	1.45	1.27	1.14

A high dipole moment, 1.83 to 1.90 Debye units, favors a cis-form.



Thermodynamic functions for hydrazine and other H-N-O species are summarized in Table 2. Little agreement appears to exist on the assignment of bond energies in hydrazine, or on the interpretation of bond dissociation energies. If one takes the N-N bond energy to be the bond dissociation energy measured by Diebler et al (14),  $D(\text{H}_2\text{N}-\text{NH}_2) = 60$  (kcal/mole), by electron impact studies, then the average N-H bond energy in hydrazine must be assigned as 88 (kcal/mole). As an example of the disparity in the assignment of bond energies, Jolly (12) has chosen to start with the standard N-H bond energy of 93 (kcal/mole) corresponding to the average N-H bond energy in ammonia, and assigns a 38 (kcal/mole) bond energy to the hydrazine N-N bond.

McHale et al (15) conclude from the decomposition kinetics of hydrazine that  $D(\text{H}_2\text{N}-\text{NH}_2) = 54$  (kcal/mole). Gray and Thynne (16) cite reported values of the N-H bond dissociation energy in hydrazine of from 76 to 117 (kcal/mole) but estimate from their experiments and analogy with iso-electronic species that  $D(\text{H}-\text{N}_2\text{H}_3) = 93$  (kcal/mole). Results of the present experiments would support a value less than the dissociation energy of the first N-H bond in ammonia, 104 (kcal/mole). Bond dissociation energies for H-N-O species are summarized in Table 3. Some H-N-O bond energy assignments are presented in Table 4.

TABLE 2. Thermodynamic functions at 298.16°K for some gaseous H, N, O species

specie	$S^\circ$	$\Delta H_f^\circ$	$\Delta F_f^\circ$	reference
	cal/mole °K	kcal/mole	kcal/mole	
H	27.39	52.10	48.59	(11)
NH	43.30	79.20	77.77	(11)
HNO	52.73	23.8	26.86	(11)
HNO <sub>2</sub> cis	59.59	-18.3	-10.02	(11)
HNO <sub>2</sub> trans	59.55	-18.8	-10.51	(11)
HNO <sub>3</sub>	63.66	-32.1	-17.69	(11)
HN <sub>3</sub>	56.7	70.3	78.5	(12)
OH	43.92	9.33	8.19	(11)
HO <sub>2</sub>	54.38	5.0	8.05	(11)
NH <sub>2</sub>	45.11	40.	42.98	(11)
NH <sub>2</sub> OH		-14.7 -18		(12) (13)
NH <sub>2</sub> NO		(25)		(estimated)
N <sub>2</sub> H <sub>2</sub>		48.7		(12)
H <sub>2</sub> O	45.11	-57.798	-54.64	(11)
H <sub>2</sub> O <sub>2</sub>	55.66	-32.53	-25.21	(11)
NH <sub>3</sub>	45.97	-11.04	-3.97	(11)
N <sub>2</sub> H <sub>3</sub>		(42)		(estimated)
N <sub>2</sub> H <sub>4</sub>	56.97	22.75	38.02	(11)
N	36.61	113	108.87	(11)
NO	50.35	21.58	20.70	(11)
NO <sub>2</sub>	57.34	7.91	12.25	(11)
NO <sub>3</sub>	60.36	16.95	27.36	(12)
N <sub>2</sub>	45.77	0	0	(11)
N <sub>2</sub> O	52.56	19.5	24.78	(11)
N <sub>2</sub> O <sub>3</sub>	74.12	19.99	33.45	(11)
N <sub>2</sub> O <sub>4</sub>	72.72	2.17	23.35	(11)
N <sub>2</sub> O <sub>5</sub>	75.67	3.1	30.67	(11)
O	38.47	59.56	55.40	(11)
O <sub>2</sub>	49.00	0	0	(11)

Table 3. Bond dissociation energies, H-N-O species

<u>bond</u>	<u>dissociation energy</u> [kcal/mole]	<u>reference</u>
H-H	104	(27)
H-NH <sub>2</sub>	104	(12)
H-NH	95	(12)
H-N	81	(12)
H-N <sub>2</sub> H <sub>3</sub>	93	(16)
	76	(14)
H-O	100.4	(28)
H-OH	120	(27)
	118.5	(28)
H-OOH	88	(29)
H-NO	48	(30)
N=N	226	(12)
HN=NH	119	(12)
H <sub>2</sub> N-NH <sub>2</sub>	60	(14)
	54	(15)
O <sub>2</sub> N-NO <sub>2</sub>	13	(29)
N=O	151	(12)
O-NO	72	(29)
O-NN	28	(29)
O=O	118	(12)
O-OO	24	(29)

Table 4. Bond energies for H, N, O bonds (12,27,31)

<u>bond</u>	<u>order</u>	<u>example</u>	<u>energy</u> [kcal/mole]
hydrogen-hydrogen	1	H <sub>2</sub>	104
hydrogen-oxygen	1	H <sub>2</sub> O	111
hydrogen-nitrogen	1	NH <sub>3</sub>	93
oxygen-oxygen	1	H <sub>2</sub> O <sub>2</sub>	33
	2	O <sub>2</sub>	118
oxygen-nitrogen	1	HNO <sub>3</sub>	57
	1.33	NO <sub>3</sub>	91
	1.75	NO <sub>2</sub>	112
	2	HNO <sub>2</sub>	146
	2.5	NO	151
nitrogen-nitrogen	1	N <sub>2</sub> H <sub>4</sub>	38
	1	N <sub>2</sub> O <sub>4</sub>	52
	2	N <sub>2</sub> H <sub>2</sub>	99
	3	N <sub>2</sub>	226

The bond distances and angles in hydrazine are (10)

N-H	1.04 Å	H-N-H	$108^{\circ} \pm 10^{\circ}$
N-H	1.47 Å	H-N-N	$108^{\circ} \pm 10^{\circ}$

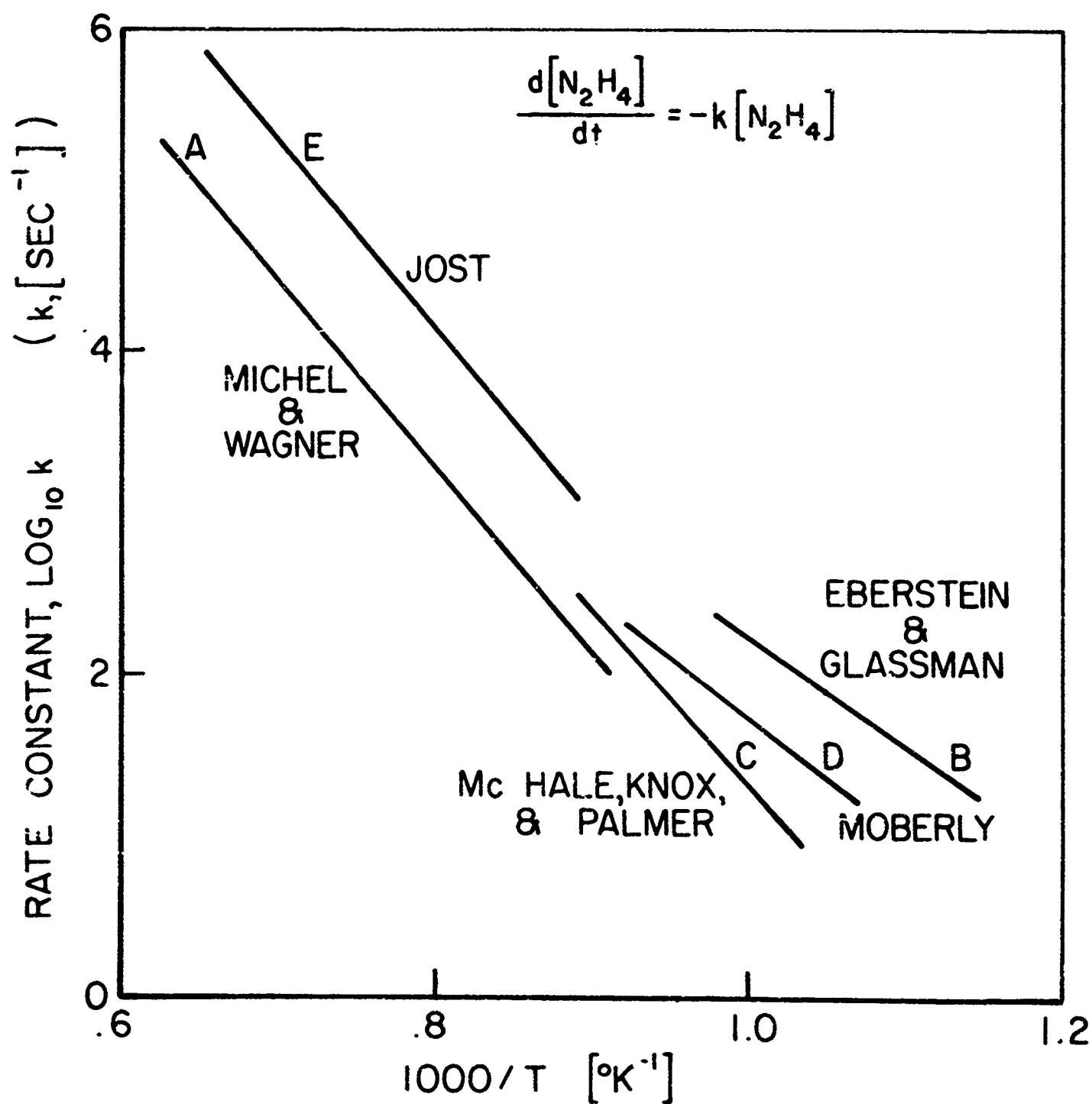
### 2.1.2 Hydrazine decomposition

The ability of hydrazine to sustain a decomposition flame has received the attention of a number of investigators (17,18,19, 20, 5, 21,22,23,24,25,26). Flame studies, usually at low pressures, have produced a general agreement that the decomposition proceeds with an overall kinetic order of two, and with a temperature dependence of the flame speed indicating an overall activation energy near 35 (kcal/mole). Several investigations of hydrazine decomposition have been conducted in shock tubes, generally at total pressures between 1 and 10 (atm) and large dilutions with argon or helium. These investigations (32, 15, 33,34,35,36,37) are in general agreement that the decomposition is first order in the hydrazine concentration as is consistent with the higher total pressures and diluted compositions of these studies. The rates measured by Eberstein and Glassman (38) in the same apparatus as for the present experiments are in agreement with the shock tube results. A comparison of measured hydrazine decomposition rates is made in Figure 2 from the results of the following experimenters.

<u>Curve</u>	<u>Experimenters</u>	<u>Description of experiment</u>
A	Michel and Wagner (32)	shock tube, 1100-1600°K, .03-.5% N <sub>2</sub> H <sub>4</sub> in argon, helium $k = 10^{12.4} \exp(-52000/RT)$ (sec <sup>-1</sup> )
B	Eberstein and Glassman (38)	flow reactor, 890-1010°K, 5% N <sub>2</sub> H <sub>4</sub> in nitrogen $k = 10^{10.33} \exp(-36170/RT)$ (sec <sup>-1</sup> )
C	McHale, Knox, Palmer (15)	shock tube, 970-1120°K 1%N <sub>2</sub> H <sub>4</sub> in argon $k = 10^{12.42} \exp(-50600/RT)$ (sec <sup>-1</sup> )
D	Moberly (33)	shock tube, 930-1090°K N <sub>2</sub> H <sub>4</sub> in argon $k = 10^{8.64} \exp(-31400/RT)$ (sec <sup>-1</sup> )
E	Jost (36)	shock tube, 1120-1550°K .3%N <sub>2</sub> H <sub>4</sub> in argon (rate constants calculated from Jost's data by Eberstein(39))

A lack of agreement in the observed activation energy is noted. Generally higher activation energies are reported for shock tube experiments than for the flow reactor experiment. Such an apparent inconsistency may result from the measurement of the initiation of reaction in the shock tubes and the measurement of the overall reaction rate in the flow reactor. All of the experiments, flame,





COMPARISON OF HYDRAZINE DECOMPOSITION RATES

FIGURE 2

TP13-4054-65

shock tube, and flow reactor studies, showed the decomposition to follow the approximate stoichiometry



### 2.1.3 Hydrogen

As a decomposition product of hydrazine, hydrogen would be expected to be reactive in subsequent oxidation processes. Hydrogen is thermally stable under flow reactor conditions. The physical properties of hydrogen are well defined, in particular the dissociation energy,

$$D(\text{H-H}) = 103.266 \text{ (kcal/mole)}$$

and the bond distance, .7417 Å.

### 2.1.4 Ammonia

Ammonia, a second decomposition product of hydrazine, has a pyramidal structure with the nitrogen atom at the apex and the hydrogen atoms at the corners of the base. The N-H bond distance is 1.014 Å and the H-N-H angle is 106.67°. The similarity between the bond distance and angle with those of hydrazine is noted. This similarity suggests a structure for hydrazine similar to ammonia with a hydrogen atom replaced by a  $\text{NH}_2$  radical. Under the flow reactor conditions, the decomposition of ammonia to nitrogen and hydrogen is thermodynamically favored.

FP/3-4054-65

### 2.1.5 Decomposition of ammonia

While the heterogeneous decomposition of ammonia has received extensive study, see, for example, (40), little information is available on the homogeneous decomposition of ammonia. Jacobs (41) has studied the decomposition of ammonia in argon using a shock-tube and infrared emission in the temperature range of 2000-3000°K. Extrapolation of his results to the temperatures of the present investigations indicates that thermal decomposition of ammonia does not occur in the flow reactor experiments. Temperatures in excess of 1500°K apparently are required to produce measurable ammonia decomposition. Therefore, while equilibrium considerations favor the decomposition of ammonia to hydrogen and nitrogen, kinetics considerations indicate that no significant decomposition occurs.

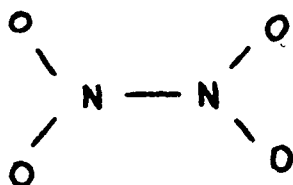
## 2.2 NITROGEN TETROXIDE AND ITS DECOMPOSITION PRODUCTS

As does hydrazine, nitrogen tetroxide possesses the potential for undergoing a series of decompositions which could affect its gas phase reactions. All of the gaseous nitrogen oxides have positive heats of formation and, therefore, the thermodynamic potential for decomposition to nitrogen and oxygen. The rates at which the various nitrogen oxides decompose will determine largely the role of oxidizer pyrolysis in combustion processes.

### 2.2.1 Nitrogen tetroxide

While in both the liquid and gaseous states, nitrogen

tetroxide and nitrogen dioxide always exist in the presence of each other, the solid state consists of pure  $\text{N}_2\text{O}_4$ . Physical properties generally refer to equilibrium mixtures of  $\text{N}_2\text{O}_4$  and  $\text{NO}_2$ . The nitrogen tetroxide molecule is planar having the structure



with the bond distances

N-N	1.75 Å
N-O	1.18 Å

and the O-N-O bond angle,  $134^\circ$ . The N-N bond length is seen to be much greater than the single N-N bond in hydrazine. This, together with the additional observation that the O-N-O angle is the same as that of  $\text{NO}_2$ , leads Jolly (12) to suggest that nitrogen tetroxide corresponds to a loosely joined pair of nitrogen dioxide molecules. While Jolly (12) assigns a N-N bond energy of 52 (kcal/mole), studies of the rate of dissociation of  $\text{N}_2\text{O}_4$  suggest that the dissociation energy,  $D(\text{O}_2\text{N}-\text{NO}_2)$ , is no more than 13 (kcal/mole). Schexnayder (29) reports a value of 13 (kcal/mole).

### 2.2.2 Nitrogen tetroxide decomposition

The decomposition of nitrogen tetroxide proceeds very

rapidly. The measured rates of Carrington and Davidson (42) made in a shock tube at from 250 to 300°K and of Wegener et al (43,44) made in a supersonic wind tunnel at from 210 to 300°K are in agreement. Carrington and Davidson, on the basis of experiments with nitrogen containing about 1% nitrogen tetroxide, propose a limiting first order rate constant for the rate equation

$$\frac{d[N_2O_4]}{dt} = -k[N_2O_4]$$

of

$$k = 10^{16} \exp (-13000/RT) \quad [\text{sec}^{-1}]$$

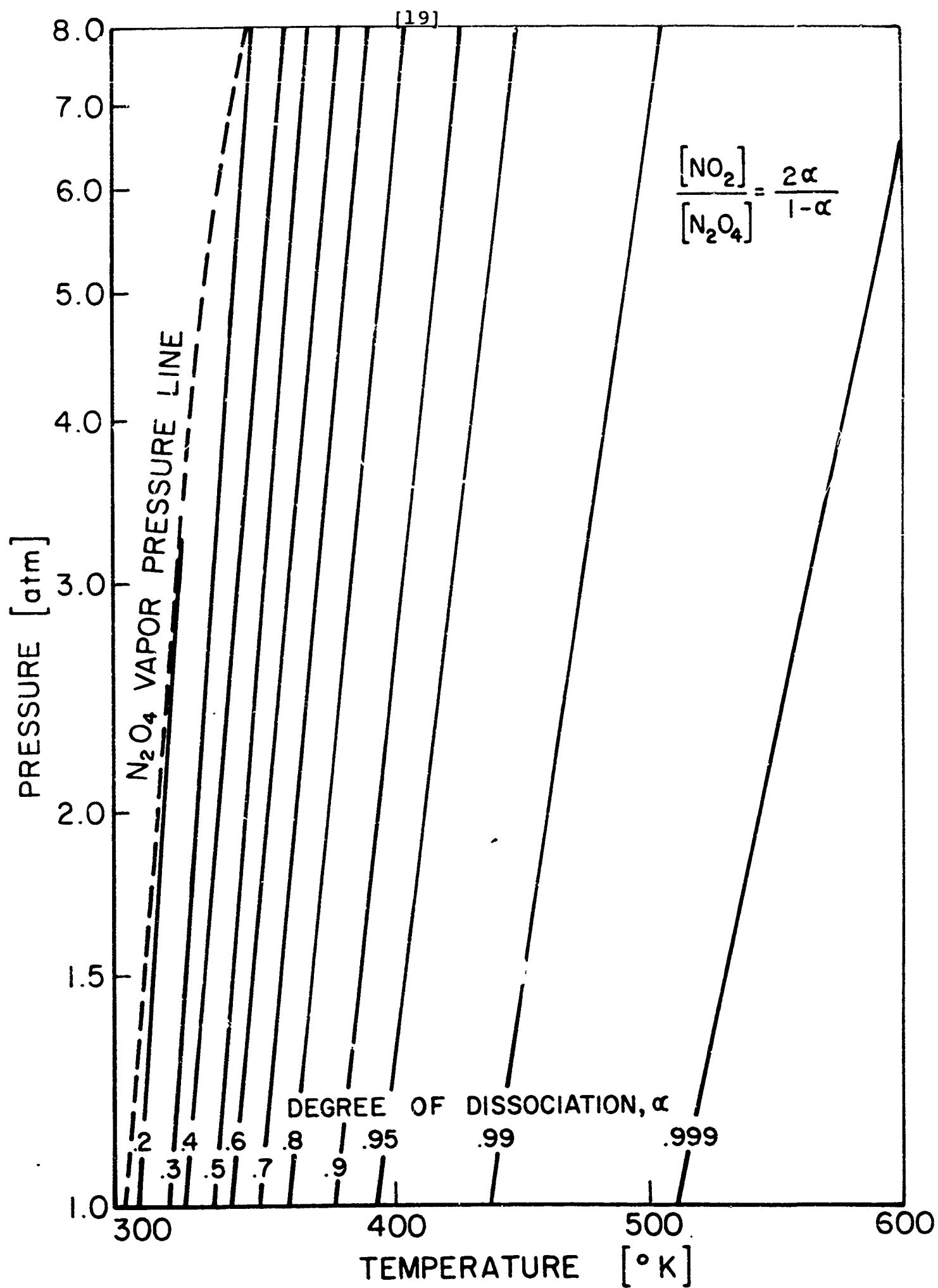
This rate is so rapid as to indicate that gas phase nitrogen tetroxide will dissociate to nitrogen dioxide (or to its equilibrium composition) in practically all conceivable combustion situations.

The equilibrium dissociation of nitrogen tetroxide to nitrogen dioxide was calculated on the basis of the thermodynamic data of Giauque and Kemp (45). Contours of the degree of dissociation as a function of temperature and pressure are presented in Figure 3.

### 2.2.3 Nitrogen dioxide

Nitrogen dioxide is a brown gas with the structure





DISSOCIATION OF NITROGEN TETROXIDE

FIGURE 3

with a N-O bond length of 1.18 Å and O-N-O bond angle of 134°. The bond dissociation energy,  $D(\text{O-NO}) = 72$  (kcal/mole) (29), makes the first oxygen atom from nitrogen dioxide much more readily available than an oxygen atom from oxygen,  $D(\text{O-O}) = 118$  (kcal/mole). Nitrogen dioxide is particularly toxic. The recommended maximum allowable concentration is five parts per million (40,46). The high absorbtivity of nitrogen dioxide in the visible range provides a convenient method of determining its disappearance in reactions through optical means. A thorough review of the reactivity and structure of nitrogen dioxide is presented by Gray and Yoffe (47).

#### 2.2.4 Dissociation of nitrogen dioxide

The dissociation of nitrogen dioxide according to the stoichiometry



while not as rapid as the dissociation of nitrogen tetroxide, is sufficiently rapid to occur in some combustion situations. Rosser and Wise (48) have measured the disappearance of  $\text{NO}_2$  in closed vessel between the temperatures of 630 and 1020°K in the presence of inert gases at total pressures up to one atmosphere. They found the reaction to be second order with respect to the nitrogen dioxide concentration

$$\frac{d[\text{NO}_2]}{dt} = -k[\text{NO}_2][\text{NO}_2]$$

with a specific rate constant given by

$$k = 10^{12.6} \exp (-26900/RT) \quad [\text{cc mole}^{-1} \text{ sec}^{-1}]$$

No effect of inert gases or surface coating was noted. Ashmore and Burnett. (19) have confirmed these results in similar experiments.

#### 2.2.5 Nitric oxide

While nitric oxide is a colorless gas, it rapidly reacts with oxygen in air to form nitrogen dioxide. The nitric oxide bond distance is 1.1508 Å; the bond dissociation energy  $D(\text{N-O}) = 151$  (kcal/mole). Although possessing a positive heat of formation, nitric oxide is relatively stable up to temperatures in excess of 2000°K.

Wise and French (50,51) have measured the dissociation of NO and reported a second order homogeneous dissociation rate

$$\frac{d[\text{NO}]}{dt} = -k[\text{NO}][\text{NO}]$$

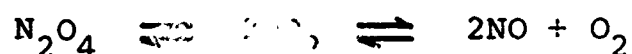
with the rate constant

$$k = 10^{14.34} \exp (-78200/RT) \quad [\text{cc mole}^{-1} \text{ sec}^{-1}]$$

Nitrogen was found to slow the dissociation at temperatures less than 1100°K. Oxygen was observed to accelerate the decomposition of nitric oxide.



Because of the slow dissociation of nitric oxide, a pseudo-equilibrium can be defined by the relations



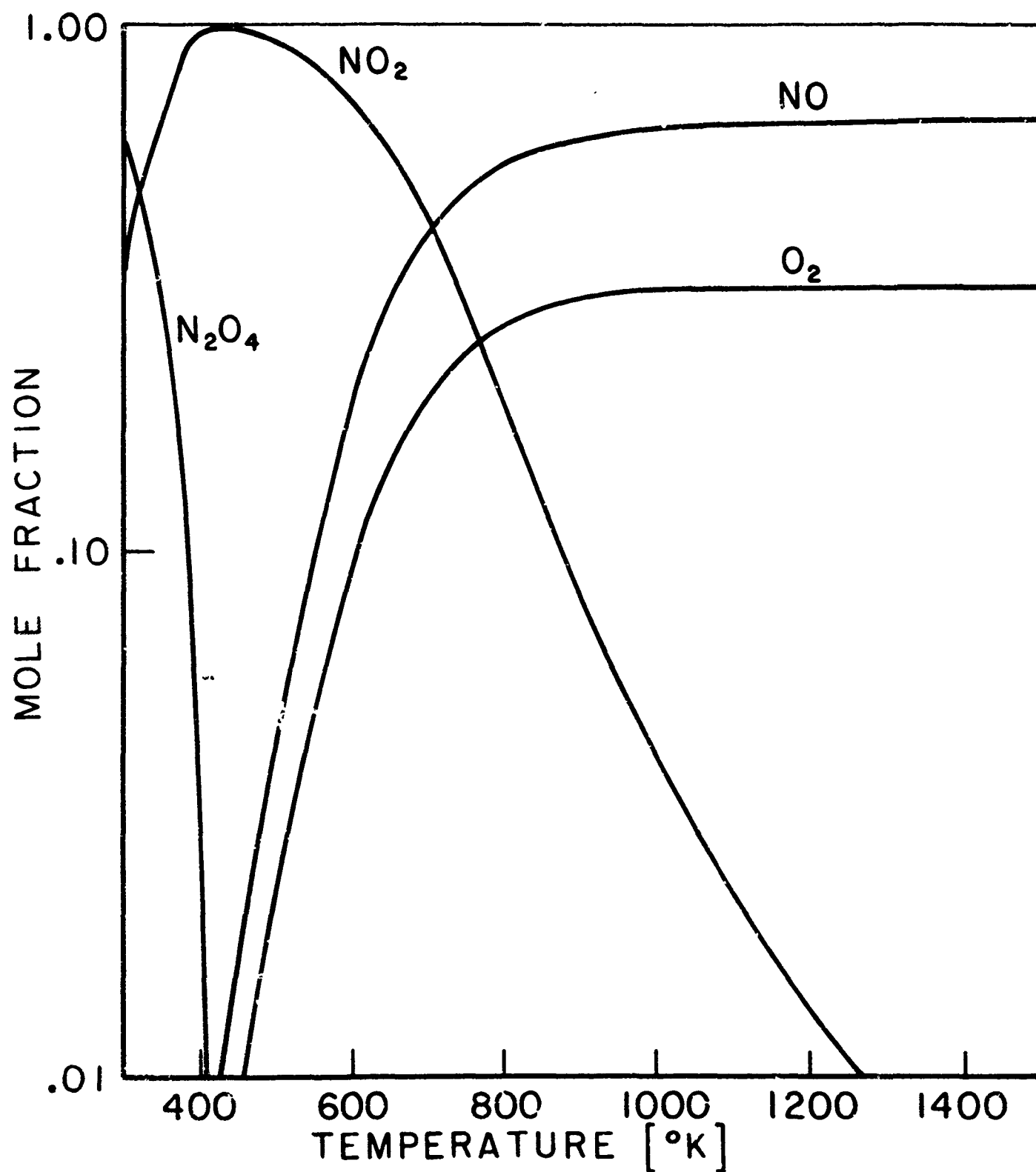
The composition according to such equilibria is presented in Figure 4 for a pressure of one atmosphere. The composition consists of approximately 100% nitrogen dioxide at 400°K and is largely dissociated to nitric oxide and oxygen at temperatures greater than 1000°K.

#### 2.2.6 Oxygen

As the second decomposition product of nitrogen dioxide, oxygen is a possible reactive specie in nitrogen dioxide combustion. The oxygen bond distance is 1.2074 Å and the bond dissociation energy  $D(\text{O}-\text{O}) = 118$  (kcal/mole). Oxygen therefore is more stable than nitrogen dioxide but less stable than nitric oxide.

### 2.3 EQUILIBRIUM COMPOSITIONS OF THE H-N-O SYSTEM

The probability of non-equilibrium reactions in the systems studied was both anticipated and observed. To provide a point of reference for following discussions of the reactions studied, some equilibrium compositions typical of H-N-O systems studied are presented for the conditions encountered in the flow reactor experiments. Calculations were made using the equilibrium thermodynamic program mentioned in Appendix E.

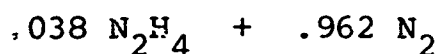


COMPOSITION ACCORDING TO THE EQUILIBRIA  
 $N_2O_4 \rightleftharpoons 2 NO_2 \rightleftharpoons 2NO + O_2$   
PRESSURE 1 [atm]

FIGURE 4

### 2.3.1 H-N Systems

Under flow reactor conditions, in equilibrium mixtures containing only nitrogen and hydrogen, these two elements appear predominantly in their diatomic forms with small amounts of ammonia at the lowest temperatures.



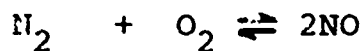
mole fractions

total pressure = 1 (atm)

temperature, °K	800	1000	1200
H <sub>2</sub>	.07263	.07270	.07271
N <sub>2</sub>	.92731	.92729	.92729
NH <sub>3</sub>	.00006	.00001	.00000

### 2.3.2 N-O Systems

As in the H-N system, nitrogen and oxygen appear predominantly in their molecular form. Small concentrations of nitric oxide are predicted at higher temperatures. The effect of the nitrogen is to increase the relative amount of oxygen appearing as NO as opposed to O<sub>2</sub>. This effect is as we would expect from consideration of the equilibrium



NO<sub>2</sub>

mole fractions

total pressure = .04 (atm)

temperature, °K	800	1000	1200
N <sub>2</sub>	.33333	.33331	.33321
O <sub>2</sub>	.66667	.66665	.66654

NO	.00000	.00004	.00025
----	--------	--------	--------

.0199 NO <sub>2</sub> + .9801 N <sub>2</sub>	mole fractions		
--	----------------	--	--

total pressure = 1 (atm)

temperature, °K	800	1000	1200
N <sub>2</sub>	.98010	.98009	.98007
O <sub>2</sub>	.01990	.01990	.01986
NO	.00000	.00001	.00007

### 2.3.3 H-N-O Systems

The equilibrium compositions of mixtures containing hydrogen, nitrogen, and oxygen contain primarily the species H<sub>2</sub>, H<sub>2</sub>O, N<sub>2</sub>, O<sub>2</sub> and, for some conditions, small amounts of NO or NH<sub>3</sub>. Under no conditions are both molecular oxygen and molecular hydrogen present, water always is the dominant specie in the presence of oxygen and hydrogen.

.943 N <sub>2</sub> + .019 H <sub>2</sub> + .038 NO <sub>2</sub> (1atm)	mole fractions		
temperature, °K	800	1000	1200
H <sub>2</sub> O	.00394	.00394	.00394
N <sub>2</sub>	.99016	.99015	.99014
NO	.00000	.00001	.00004
O <sub>2</sub>	.00591	.00590	.00589

In hydrogen rich systems, small concentrations of ammonia are predicted at the lowest temperatures.

## 2.4 ENTHALPIES OF REACTION

The standard enthalpies of reaction of a number of overall reactions involving H, N, O compounds are tabulated in Table 5 for future reference and for comparison with measured heats of reaction. The enthalpy of reaction is taken to be

$$\Delta H_{R_{298}} = - \left( \Delta H_{f_{298}}^{\circ} \text{ products} - \Delta H_{f_{298}}^{\circ} \text{ reactants} \right)$$

so that an exothermic reaction is recorded as having a positive heat of reaction corresponding to negative change (decrease) in heat of formation (products minus reactants).

Since the measured heats of reaction are obtained at elevated temperatures, comparison is properly made with the enthalpy of reaction at that temperature. This enthalpy of reaction is given by

$$\Delta H_{R_T} = \Delta H_{R_{298}} - (\Delta H_{f_T}^{\circ} - \Delta H_{f_{298}}^{\circ})_{\text{products}} + (\Delta H_{f_T}^{\circ} - \Delta H_{f_{298}}^{\circ})_{\text{reactants}}$$

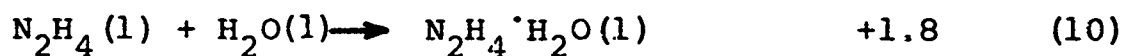
This effect, however, is usually small so that neglecting it is consistent with the experimental uncertainty in the measured heats of reaction. The enthalpies of reaction for the particular oxidations studied experimentally are summarized in the form of the "reaction matrix" in Table 6.

Table 5. Enthalpies of reaction for selected reactions involving H, N, O compounds\*

decompositions and phase changes

$\text{N}_2\text{H}_4$	$\longrightarrow$	$\text{NH}_3 + \frac{1}{2}\text{H}_2 + \frac{1}{2}\text{N}_2$	+33.80 [kcal/mole]	
$\text{N}_2\text{H}_4$	$\longrightarrow$	$2\text{H}_2 + \text{N}_2$	+22.75	
$\text{N}_2\text{H}_4 (l)$	$\longrightarrow$	$\text{N}_2\text{H}_4 (g)$	-10.7	(7)
$\text{N}_2\text{O}_4$	$\longrightarrow$	$2\text{NO}_2$	-13.72	
$\text{N}_2\text{O}_4 (l)$	$\longrightarrow$	$\text{N}_2\text{O}_4 (g)$	-9.11	
$\text{NO}_2$	$\longrightarrow$	$\text{NO} + \frac{1}{2}\text{O}_2$	-13.57	
$\text{NO}$	$\longrightarrow$	$\frac{1}{2}\text{N}_2 + \frac{1}{2}\text{O}_2$	+21.57	
$\text{NH}_3$	$\longrightarrow$	$1.5\text{H}_2 + \frac{1}{2}\text{N}_2$	-11.04	

hydration



oxidations of hydrogen

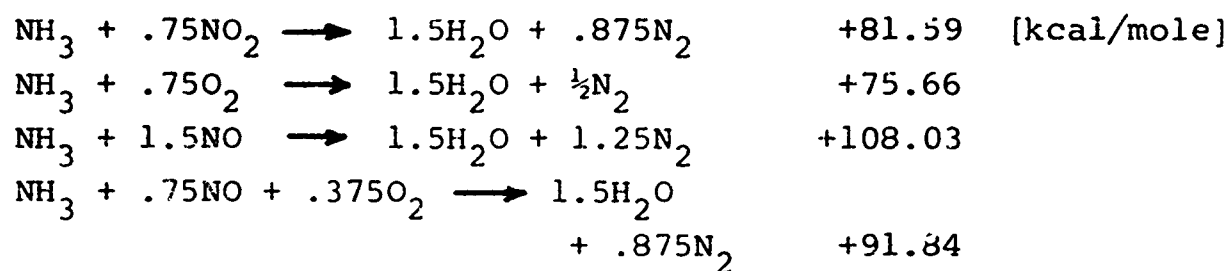
$\text{H}_2 + \text{NO}_2$	$\longrightarrow$	$\text{H}_2\text{O} + \text{NO}$	+44.13
$\text{H}_2 + \text{NO}_2$	$\longrightarrow$	$\text{H}_2\text{O} + \frac{1}{2}\text{N}_2 + \frac{1}{2}\text{O}_2$	+65.71
$\text{H}_2 + \frac{1}{2}\text{NO}_2$	$\longrightarrow$	$\text{H}_2\text{O} + \frac{1}{4}\text{N}_2$	+61.75
$\text{H}_2 + \frac{1}{2}\text{O}_2$	$\longrightarrow$	$\text{H}_2\text{O}$	+57.80
$\text{H}_2 + \text{NO}$	$\longrightarrow$	$\text{H}_2\text{O} + \frac{1}{2}\text{N}_2$	+79.38
$\text{H}_2 + \frac{1}{2}\text{NO} + \frac{1}{4}\text{O}_2$	$\longrightarrow$	$\text{H}_2\text{O} + \frac{1}{4}\text{N}_2$	+68.69

oxidations of ammonia

$\text{NH}_3 + 1.5\text{NO}_2$	$\longrightarrow$	$1.5\text{H}_2\text{O} + \frac{1}{2}\text{N}_2 + 1.5\text{NO}$	+55.15
$\text{NH}_3 + 1.5\text{NO}_2$	$\longrightarrow$	$1.5\text{H}_2\text{O} + 1.25\text{N}_2 + .75\text{O}_2$	+87.52

\*Calculated from values in Table 2, except as referenced.  
Gas phase unless otherwise indicated; (l) = liquid.

Table 5. (continued) Enthalpies of reaction for selected reactions involving H, N, O compounds.



oxidations of hydrazine

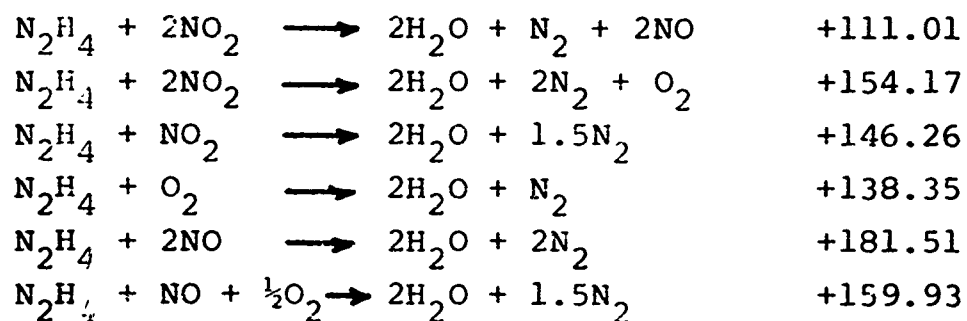


Table 6. Standard enthalpies of reaction for the oxidation of hydrazine, hydrogen, decomposed hydrazine, and ammonia by nitrogen dioxide, oxygen, decomposed nitrogen dioxide, and nitric oxide [kcal/mole fuel]

oxidizer	fuel			
	N	H <sub>2</sub>	NH <sub>3</sub> + $\frac{1}{2}$ H <sub>2</sub> **	NH <sub>3</sub>
NO <sub>2</sub>	111.01*	44.23	77.22	55.15
	146.26	61.80	112.47	81.59
O <sub>2</sub>	138.35	57.80	104.56	75.66
NO + $\frac{1}{2}$ O <sub>2</sub>	159.93	68.69	126.14	91.84
NO	181.51	79.39	147.72	108.03

\* First number refers to reduction of NO<sub>2</sub> to NO. The second number refers to the complete reduction of NO<sub>2</sub> to N<sub>2</sub>.

\*\*[kcal/ 1 mole NH<sub>3</sub> +  $\frac{1}{2}$  mole H<sub>2</sub>]



## CHAPTER 3      EXPERIMENTAL TECHNIQUE

The adiabatic flow reactor used in the present experiments is an evolved form of the reactors used by Crocco, Glassman and Smith (52) to study ethylene oxide decomposition by Swigart (53) to study the hydrogen/oxygen reaction, and by Eberstein (39,38) to study the decomposition of hydrazine and its methyl derivatives. Basically, the apparatus provides for the study of a reaction at temperatures of up to 1300°K under adiabatic conditions so that the progress of the reaction can be monitored by the temperature change through the reaction zone. By varying the temperature of the carrier gas, flow velocity, and reactant concentrations, one can measure reaction rates as a function of temperature and concentration to give overall activation energies and reaction orders, and heats of reaction. Gas samples taken from the flow reactor can be used to establish or confirm reaction stoichiometries.

### 3.1    THE FLOW REACTOR

While the concept of the flow reactor is basically simple, the equipment to insure the essential features of adiabatic flow at high temperatures, rapid mixing of reactant and carrier streams, the availability of steady vapor phase reactant flows, and the remote handling of explosive and/or toxic reactants in relatively large quantities (2 to 3 kilograms) has resulted in complex apparatus, controls, and instrumentation. The reactor itself is merely a heated cylindrical duct through which flows a hot carrier gas, into which the reactants have been injected.

### 3.1.1 Theory

In addition to elimination of heat transfer between the reactant gases and the reactor wall, a key feature of the flow reactor is maintenance of turbulent flow throughout the reaction zone. The turbulent flow allows rapid mixing of the reactant streams, generally less than 5 per cent by volume, with the hot carrier gas and the obtaining of relatively flat velocity, temperature, and concentration profiles in the radial direction thereby producing a one dimensional reaction zone. By properly spreading the reaction over the length of the reactor duct, one can keep longitudinal gradients of temperature and concentration small to insure that diffusion of heat and mass in the longitudinal direction is negligible.

The reaction rate may be related to measurable quantities in the following manner. The temperature rise of the carrier, reactant, and product gases is related to the consumption of reactant by

$$([A]_0 - [A])Q = \bar{C}_p \rho_{\text{total}} (T - T_0) \quad \text{E3 (1)}$$

where

$[A]_0$  initial reactant concentration (concentration of reactant not in excess if a mixture of two or more reactants in non-stoichiometric proportion is used)

$[A]$  local reactant concentration

$\rho$ total	total density (moles/cc)
$\bar{C}_p$	mean specific heat
$T_o$	initial temperature
$T$	local temperature
$Q$	heat of reaction

For a perfect gas the above expression may be written as

$$[A]_o - [A] = \left( \frac{\bar{C}_p \rho \omega P}{R Q} \right) \left( 1 - \frac{T_o}{T} \right) \quad \text{E3 (2)}$$

Since pressure is constant, the term in parentheses is a constant (neglecting the change in specific heat with temperature) and may be expressed in terms of the final condition, where  $[A] = 0$ , as

$$\left( \frac{\bar{C}_p \rho \omega P}{R Q} \right) = [A]_o \frac{T_f}{T_f - T_o} \quad \text{E3 (3)}$$

The reaction rate can be obtained by taking the time derivative of equation E3 (2) and substituting equation E3 (3)

$$\frac{d[A]}{dt} = -[A]_o \frac{T_o T_f}{T^2 (T_f - T_o)} \frac{dT}{dt} \quad \text{E3 (4)}$$

The quantities in the above expression are all measurable. The time derivative of the temperature is related to the space derivative in the longitudinal direction by the velocity,  $v$ ,

$$\frac{dT}{dt} = \frac{dT}{dx} \frac{dx}{dt} = \frac{dT}{dx} v$$

E3 (5)

For the simple case of a first order reaction, for which the reaction rate is expressed as

$$\frac{d[A]}{dt} = -k[A]$$

E3 (6)

the rate constant,  $k$ , is simply

$$k = \frac{T_f}{T} \frac{1}{T_f - T} \frac{dT}{dt}$$

E3 (7)

Determination of the rate constant from the reaction rate is more complex for reaction rates of other orders and dependence upon more than one specie concentration, see Section 3.4.1.

### 3.1.2 Description of the apparatus

A pictorial drawing of the apparatus is presented in


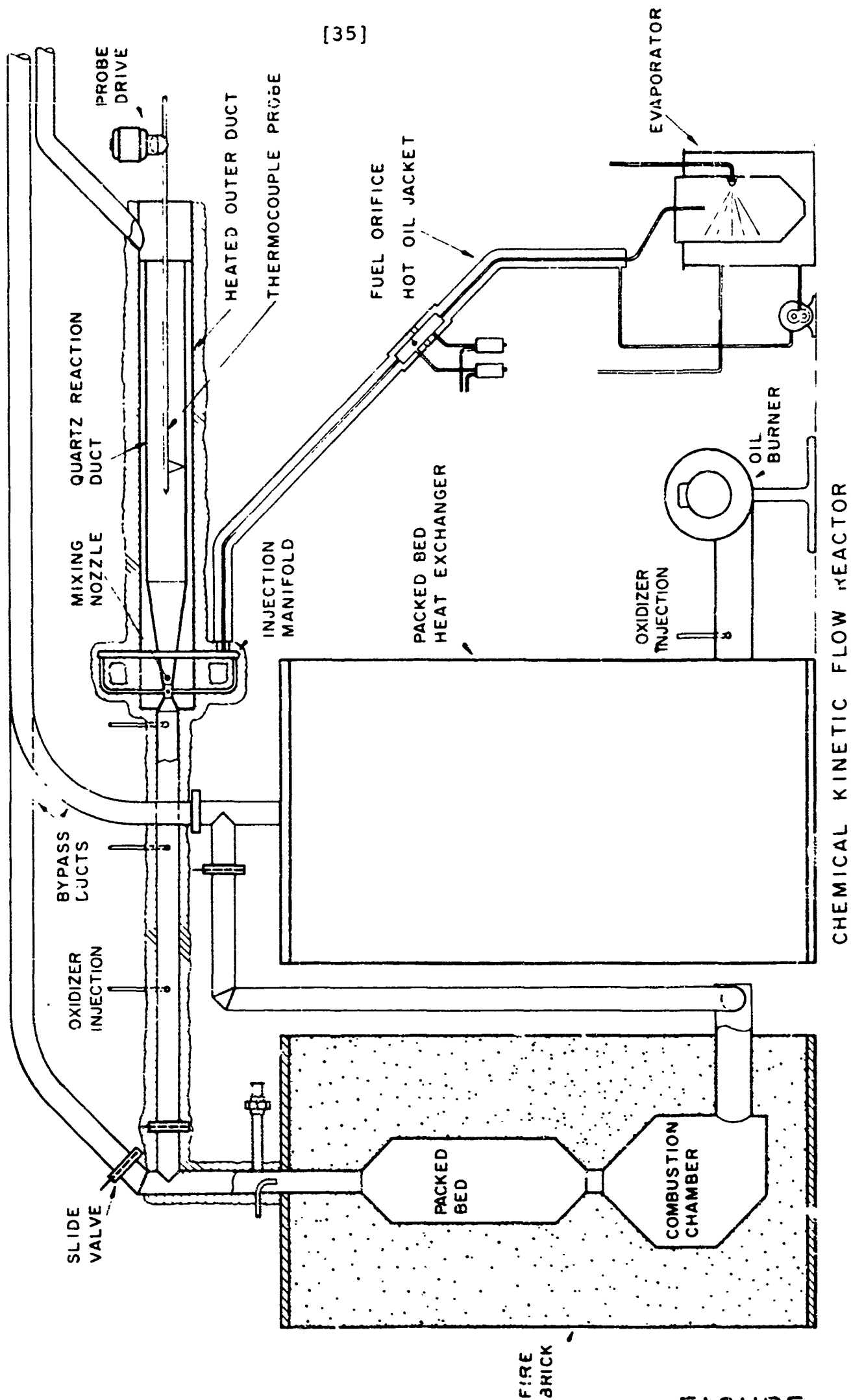


Figure 5. The reactor duct is a cylindrical tube of quartz or stainless steel, electrically heated, and with internal diameters varying from 5 to 10 centimeters. A fuel is injected into the hot carrier stream at the throat of a mixing nozzle one inch in diameter. Oxidizers are injected at locations varying from immediately upstream of the fuel injection point to upstream of the packed bed heat exchangers. Much of the associated apparatus is required to provide four separate gas flows and is discussed according to each gas flow. A more detailed description of previously developed features of the system is to be found in Reference (39). Two photographs of the apparatus are presented as Figures 6 and 7.

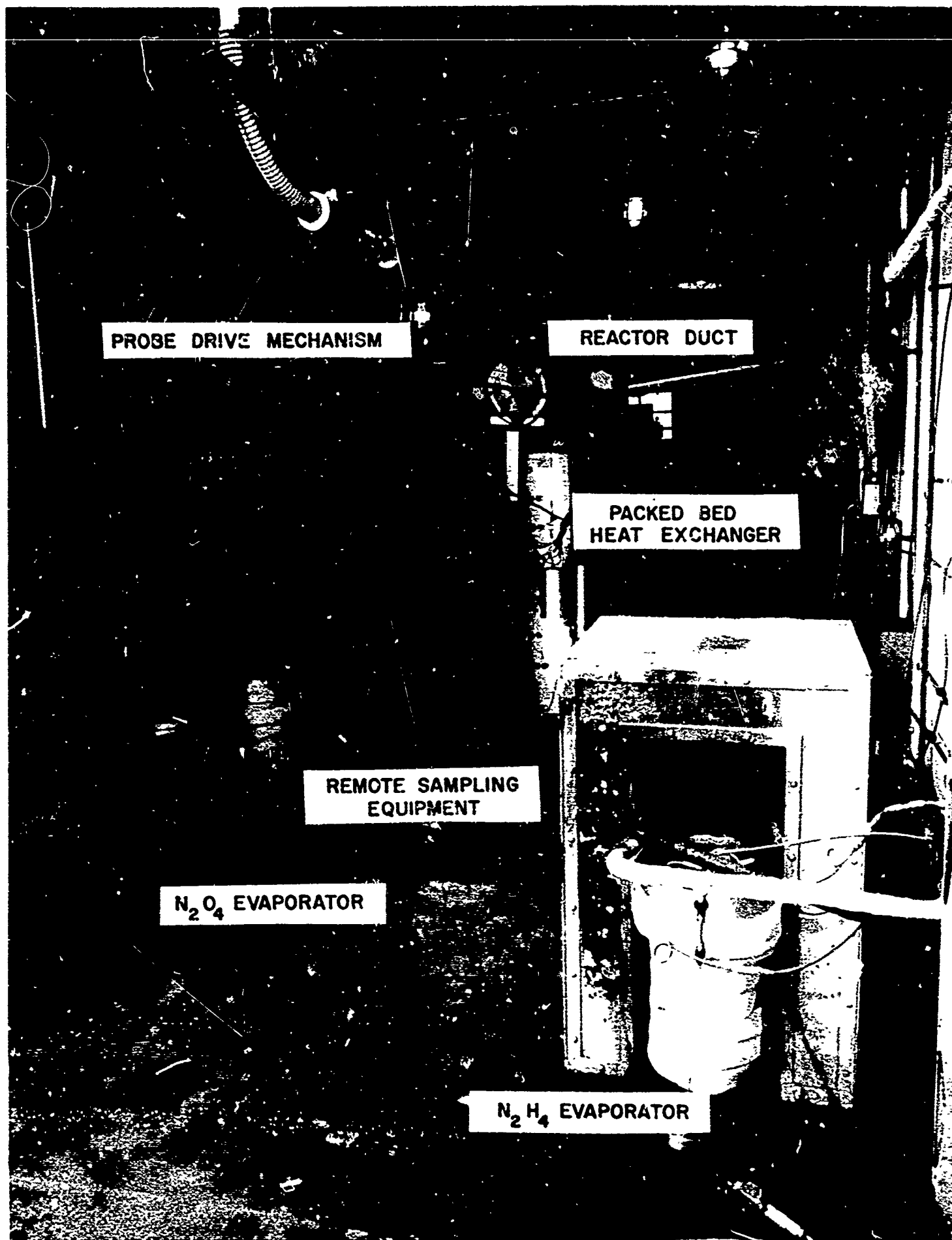
#### 3.1.2.1 Carrier gas system

Nitrogen or air is used as the carrier gas, which also serves as the oxidizer gas in the case of air. The carrier gas, which is obtained from a 2800 psi source, is exceptionally dry. The carrier gas pressure is dropped to less than 2 atmospheres before passing it through two packed bed heat exchangers having a thermal output in excess of 50 kilowatts. The oil fired beds are of sufficient thermal capacity to allow the obtaining of a data run requiring about one minute with less than a one degree K drop in the carrier temperature. An oxygen flow always is used following shut-down of the oil burners to insure removal of any residual carbon from the carrier flow system. The carrier gas and reaction products are vented through a roof stack to aid in the dissipation of toxic products. A schematic flow diagram of the carrier gas system is presented in Figure 8.



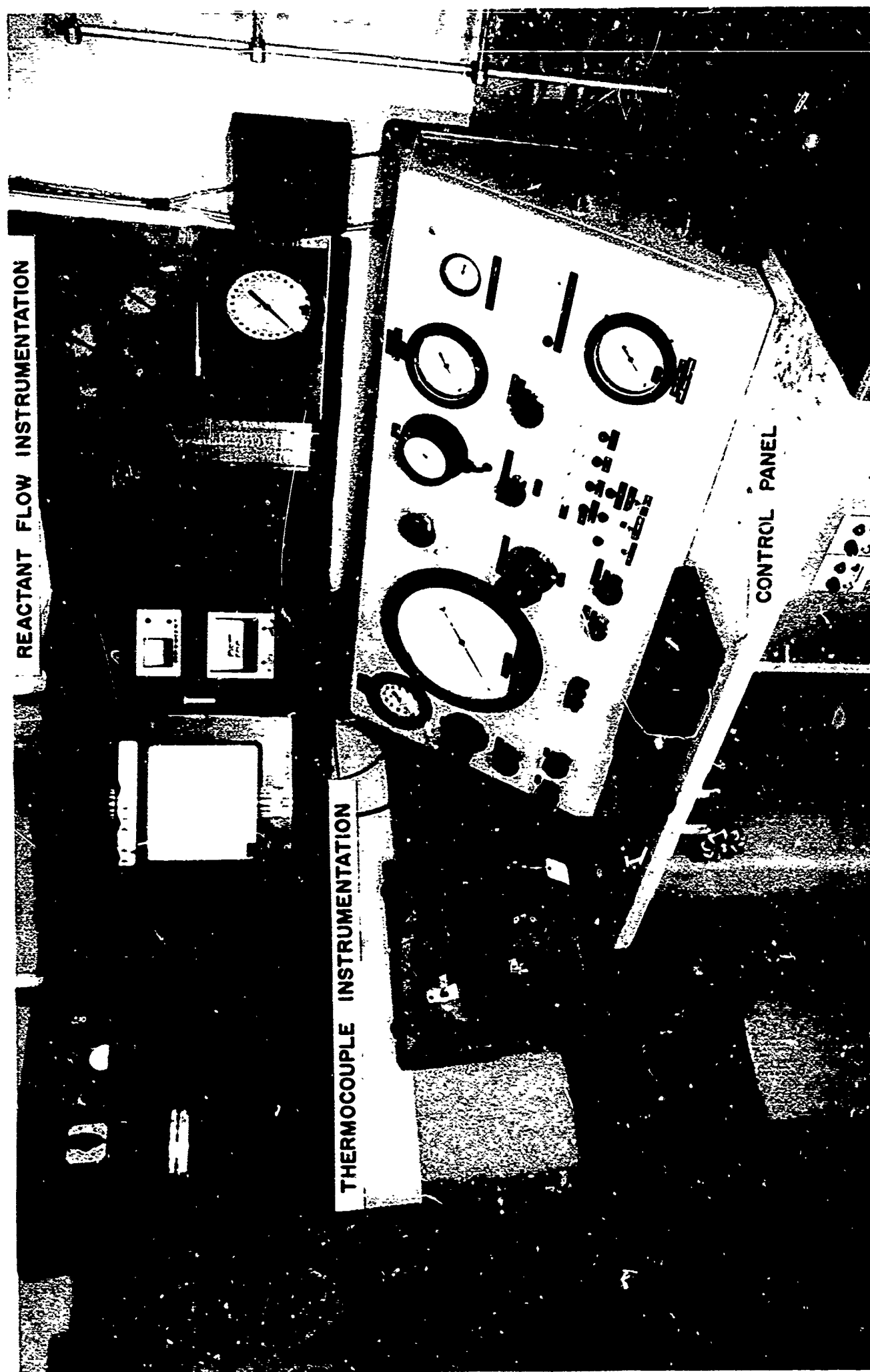
CHEMICAL KINETIC FLOW REACTOR

FIGURE



EXPERIMENTAL APPARATUS, TEST CELL

JP13-PIR 65

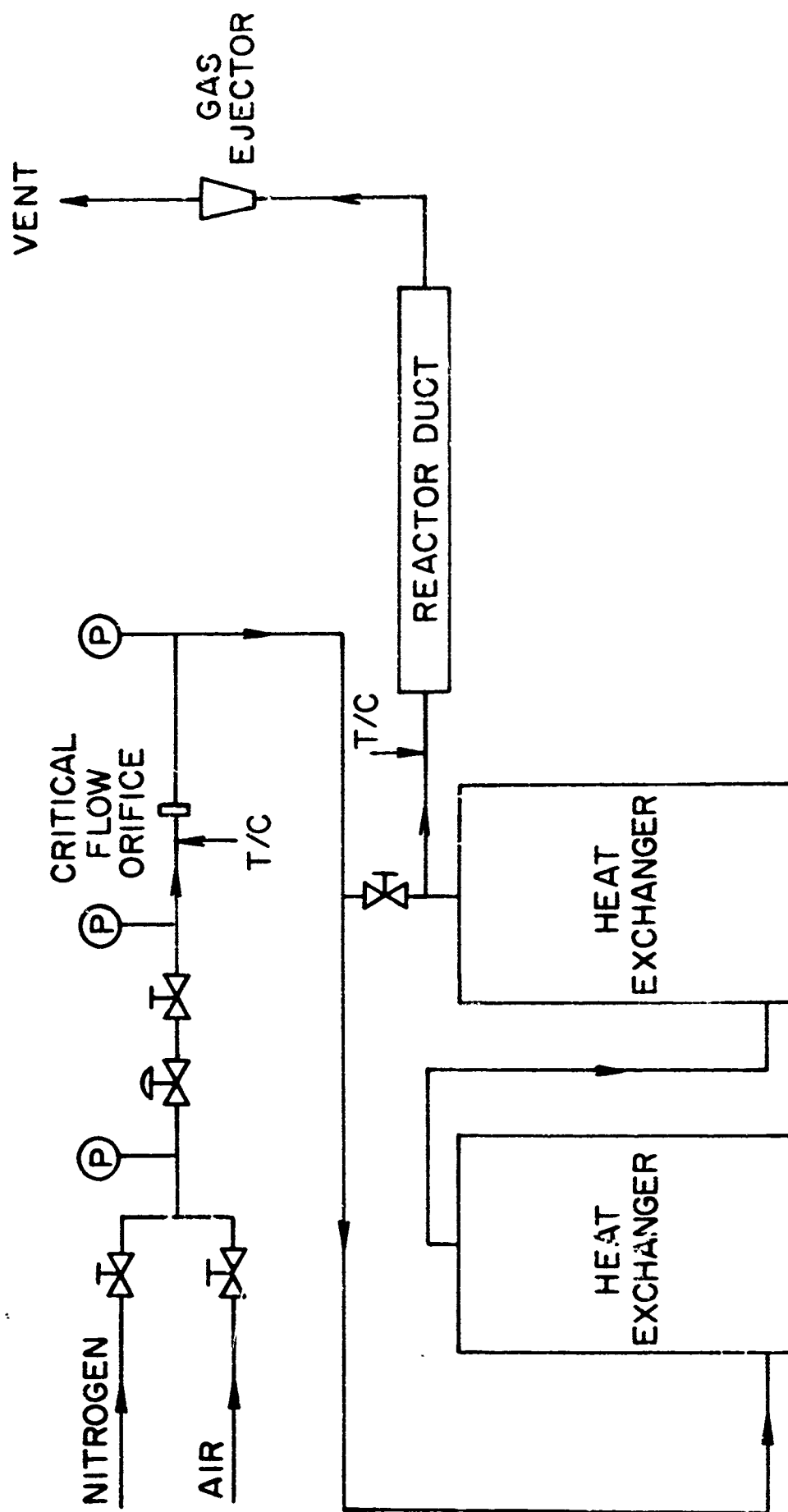


EXPERIMENTAL APPARATUS, CONTROL & INSTRUMENTATION PANEL



JP13-4051-65

[38]



FLOW SCHEMATIC, CARRIER GAS SYSTEM

FIGURE

### 3.1 2.2 Oxidizer system

When gaseous oxidizers are used, bottled sources are utilized and the gas is passed through a critical flow orifice flow meter, or meters, if two gases are used, and thence injected into the carrier gas upstream of the fuel injection point. Liquid nitrogen tetroxide is vaporized in a tank, with a capacity of about 3 kg, immersed in a hot water bath. The  $\text{N}_2\text{O}_4$ - $\text{NO}_2$  vapor is then superheated to about  $200^\circ\text{C}$  in an oil bath heat exchanger to effect complete conversion to nitrogen dioxide before passing it through a critical flow orifice. All lines, including pressure gage lines, are electrically heated to prevent internal condensation. The nitrogen tetroxide run tanks are filled by vacuum transfer to prevent contamination by exposure to the air. A schematic of the oxidizer system is presented in Figure 9.

### 3.1.2.3 Fuel system

Gaseous fuels are taken directly from bottled sources and are passed through a flow orifice into the fuel injection manifold. Consisting of four injection ports, evenly spaced about the circumference of the mixing nozzle, the fuel injectors provide a high flow velocity required for rapid mixing. Mixing of the fuel is obtained in a short distance as is indicated by the flow reactor temperature profile with nitrogen as the injected gas, Figure 10.

The handling of anhydrous hydrazine presents continuous and largely unresolved problems. Approximately a 2 kg quantity of liquid hydrazine is placed in a run tank located in a blast pit removed from the test cell. The

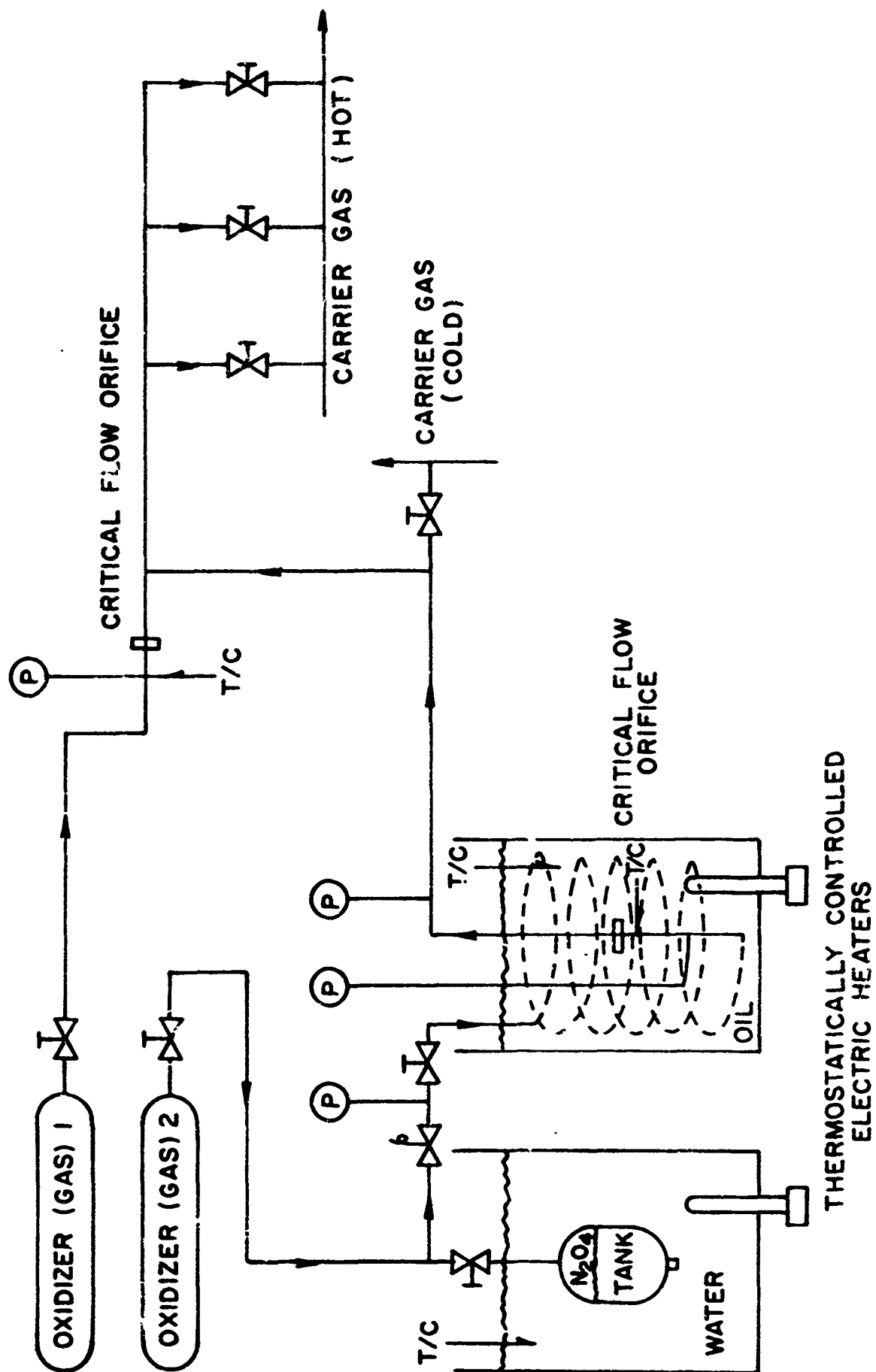
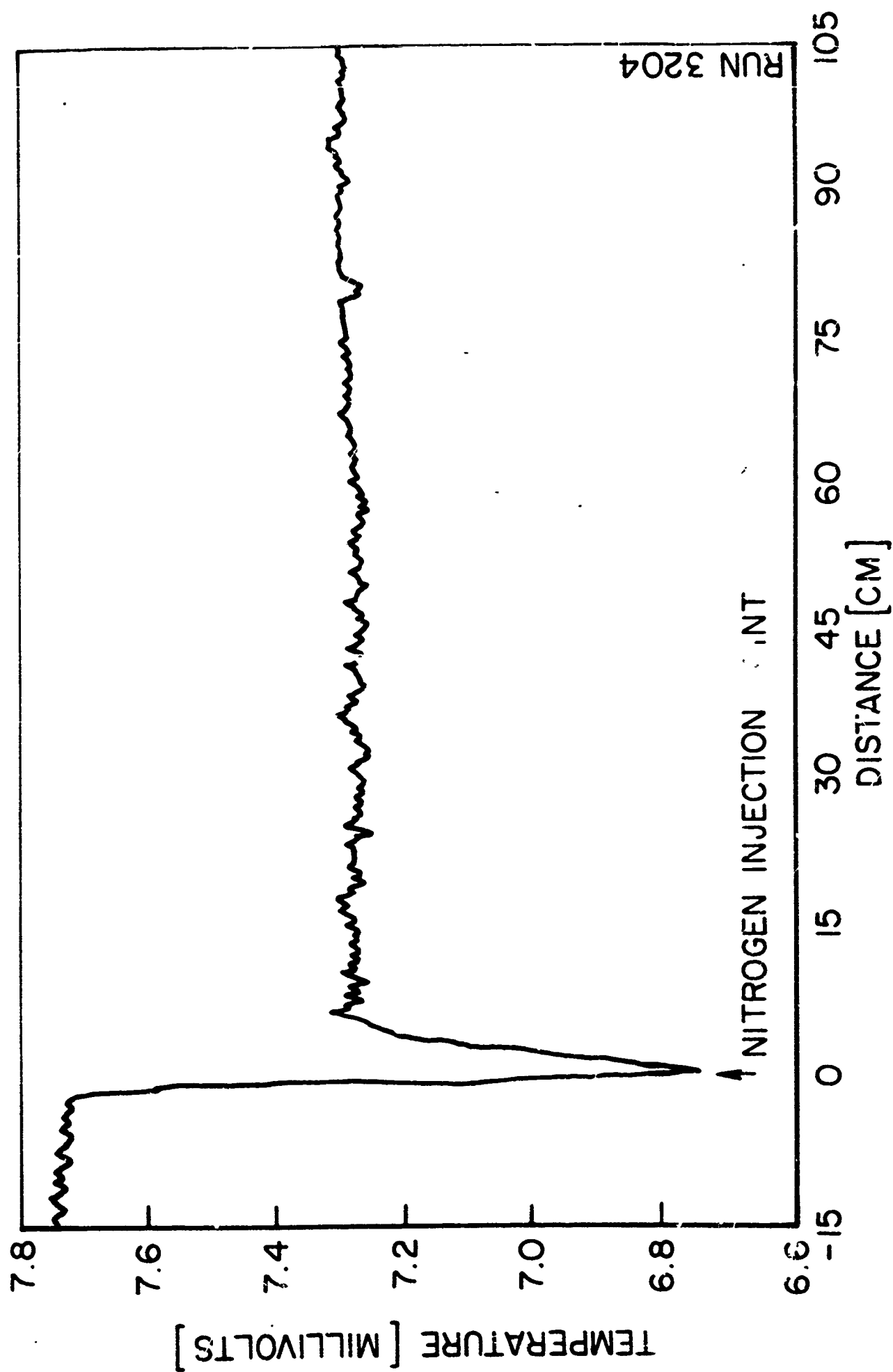


FIGURE 9

FLOW SCHEMATIC, OXIDIZER SYSTEM

JP13-4049-65



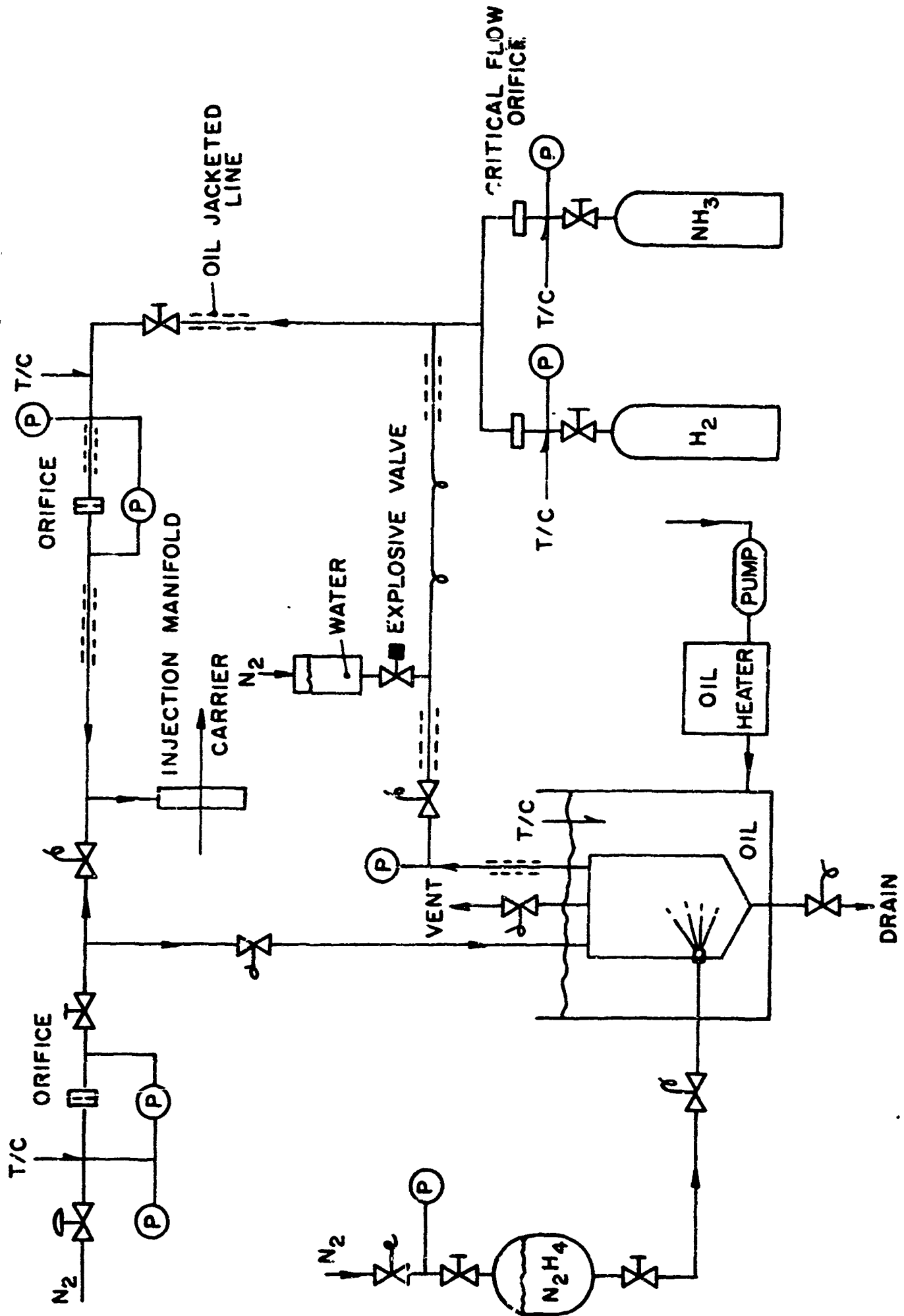
[41]

TEMPERATURE PROFILE, COLD NITROGEN INJECTION

liquid hydrazine is transferred under 100 pounds pressure to an oil bath evaporator into which it is injected through one to three spray nozzles. Practically all surfaces and lines in contact with hydrazine vapor are teflon, teflon coated, or, in the case of the injector manifold, quartz and glass. Nitrogen is also injected into the hydrazine evaporator in an attempt to reduce explosive tendencies by dilution and to reduce the hydrazine partial pressure and therefore the temperature required to obtain fully vaporized or superheated hydrazine. A nitrogen dilution of about 5 to 1 by volume is used. The evaporator oil bath is maintained at 150°C giving a nitrogen/hydrazine flow at about 100°C and 1.5 atm. The vapor transfer line is also oil jacketed to maintain this flow temperature up the injection point. The mixed hydrazine plus nitrogen flow rate is metered by the pressure drop across an orifice. Loop-type detonation traps and a continuity circuit-explosive valve-water injection automatic shutdown system are used, without complete success, to prevent propagation of detonations from the manifold to the evaporator. Provisions for remote purging of all parts of the hydrazine system have been made. A simplified schematic of the fuel flow system appears as Figure 11.

#### 3.1.2.4 Diluent nitrogen system

Diluent nitrogen is metered and injected into the hydrazine evaporator in the hydrazine experiments. In the hydrogen experiments it is necessary to inject nitrogen with the hydrogen to obtain satisfactory mixing. In this latter case, the nitrogen is injected into the hydrogen flow downstream of the hydrogen flow metering orifice as is shown on the fuel flow schematic, Figure 8.



FLOW SCHEMATIC, FUEL SYSTEM (SIMPLIFIED)

### 3.1.3 Experimental Variables

#### 3.1.3.1 Turbulence effects

The advantages of turbulence in producing one dimensional flow and in speeding the mixing process have been mentioned previously. Glassman and Eberstein (54) have paid particular attention to the possible adverse effects of turbulence upon the flow reactor measurements. They concluded that the turbulence level in the reactor is such that the chemical kinetics measurements are not affected by the turbulence; in particular, they demonstrated that the turbulence time scale is sufficiently long to insure attainment of steady state kinetics. That no effect upon the reaction rate by changing the flow velocity, and therefore, Reynolds number and turbulence level, is observed in the present experiments is consistent with the conclusions of Glassman and Eberstein.

It also should be noted that the character of the mixing process seems to have little effect upon the measured reaction rates. Hydrogen in particular demonstrates a tendency to react in the injection region before complete mixing. The reaction rates measured downstream of this mixing-reaction region are the same as are measured when careful attention is paid to the obtaining of mixing before the onset of any reaction. An important characteristic of the turbulent flow reactor seems to be its insensitivity to processes which occur prior to the measured reaction, for example, an onset of reaction in the mixing zone.

### 3.1.3.2 Range of experimental parameters

The temperature, reactant concentrations, and flow velocity are available as experimental controls to be used in maintaining a reaction zone spread out over at least half the length of the reactor duct. If the reaction takes place too rapidly, an excessively steep reaction profile is produced which introduces high temperature and concentration gradients. If the reaction takes place too slowly, a final temperature cannot be identified and the reaction rates cannot be calculated. Note that it is necessary that the reaction "go to completion" only in the sense that a steady temperature is reached indicating the completion of an energy release process is attained; not in the sense that the fuel or oxidizer is oxidized or reduced fully. The reaction rate, depending exponentially upon the temperature, is most responsive to the temperature as a control. The maximum temperature is limited by structural failure of the apparatus components, for example, warping of the quartz duct which occurs at about  $1300^{\circ}\text{K}$ . The reactant concentrations can be varied only within the limits that the temperature rise produced by their reaction be between about 50 to  $200^{\circ}\text{K}$ . The minimum flow velocity is limited by the maintenance of turbulent flow. The maximum flow velocity is limited by the pressure at which the packed bed heat exchangers can be operated.

In practice, it is possible to make reproducible rate measurements of the first order reaction rate in the range of from 10-1000 ( $\text{sec}^{-1}$ ), or over a range of reaction rates varying by a factor of about one hundred. As a consequence, the widely different reaction rates of the various



combinations which are studied, it is not possible always to measure reaction rates of different reactions at the same temperatures. Since at temperatures in the range of  $1000^{\circ}\text{K}$ , the observed reaction rates roughly double with every 30 to  $40^{\circ}\text{K}$  increase in temperature (compared to the "doubles every  $10^{\circ}\text{K}$ " rule at room temperature), the maximum temperature range for investigation is about  $200^{\circ}\text{K}$ . More typically, temperature ranges of about  $100^{\circ}\text{K}$  are investigated for a given reaction. A summary of the range of experimental parameters is presented in the following table.

---

TABLE 7. Summary of flow reactor experimental parameters

pressure	1 (atm)
partial pressure, reactants	10-150 (mmHg)
total gas density	$.9-1.3 \times 10^{-5}$ (moles/cc)
duct diameter	5-10 (cm)
duct length, overall	115 (cm)
reaction zone	about 80 (cm)
temperature	800-1300 ( $^{\circ}\text{K}$ )
flow velocity	400-4500 (cm/sec)
Reynolds number (diameter)	3500-39000
stay time	22-250 (millisec)
mixing time	1-20 (millisec)
reaction time	8-250 (millisec)
thermocouple probe traverse time	60 (sec)
flow Mach number	less than .1

---

### 3.2 CONTROLS AND MEASUREMENTS

Measurement of the reaction rates requires only a knowledge of the temperature profile, local flow velocity, and initial reactant concentration (see equations E3(4) and E3(5)). With the exception of the experiments involving hydrazine, the uncertainty in the experimental results is attributable preponderantly to the temperature measurements.

#### 3.2.1 Flows

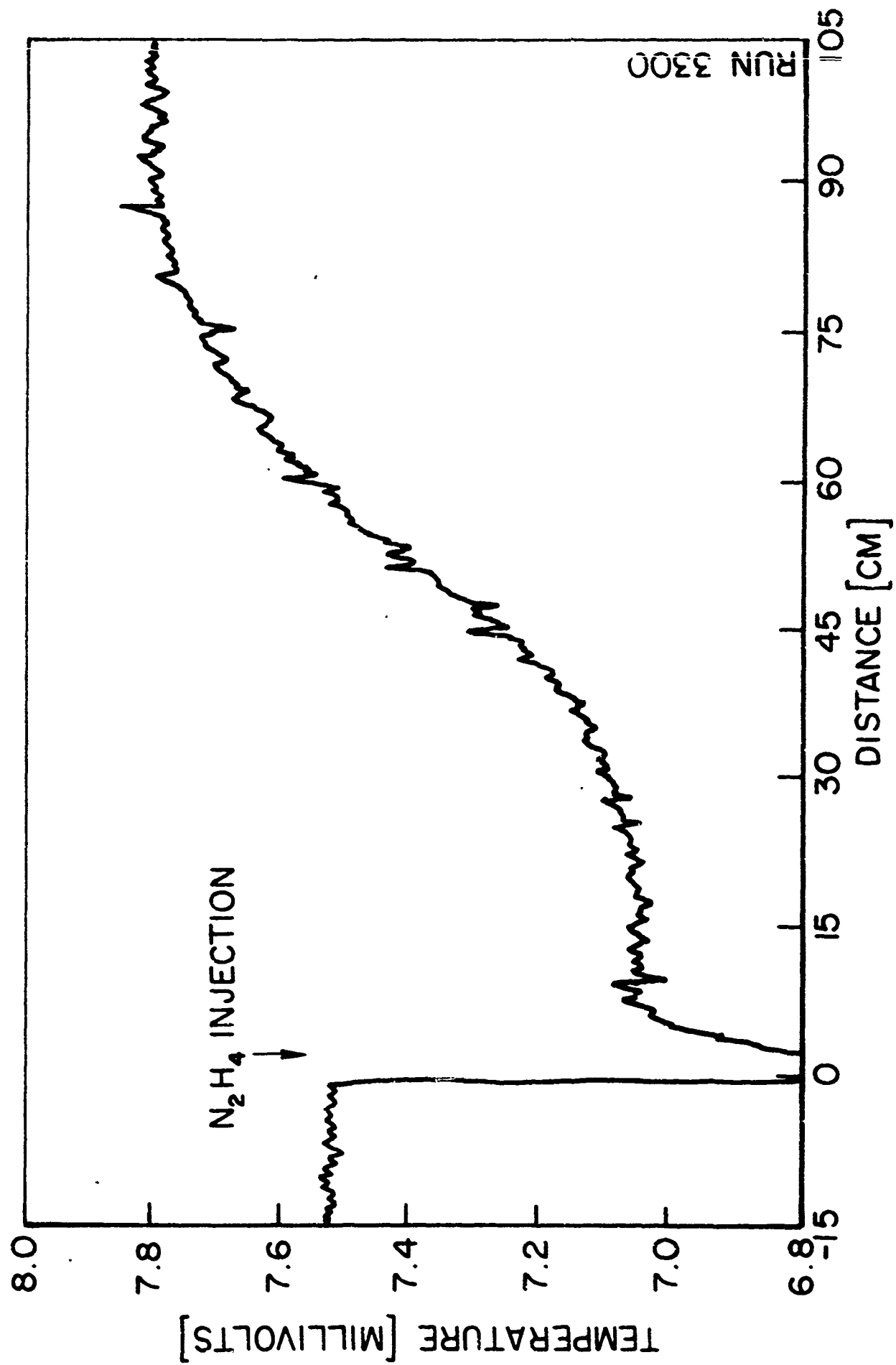
All flows are metered by calibrated orifices, either critical flow or non-critical flow. Flow rates are controlled by hand valves, remotely operated in the case of the reactants, except for the hydrazine flow which is "accepted" rather than controlled. The hydrazine evaporator is operated at whatever conditions are required to prevent the collecting of liquid and/or exceeding a maximum evaporator pressure of about 2 atmospheres. The hydrazine flow, being calculated from the difference of the measured mixed flow of hydrazine vapor and nitrogen and the measured nitrogen dilution flow, is subject to larger uncertainties than the other flows measured.

#### 3.2.2 Temperatures

Temperatures are monitored, as required for control and in the flow measurements, at a number of locations in and about the flow reactor. The critical temperature measurement, however, is in the reactant zone. An uncooled,

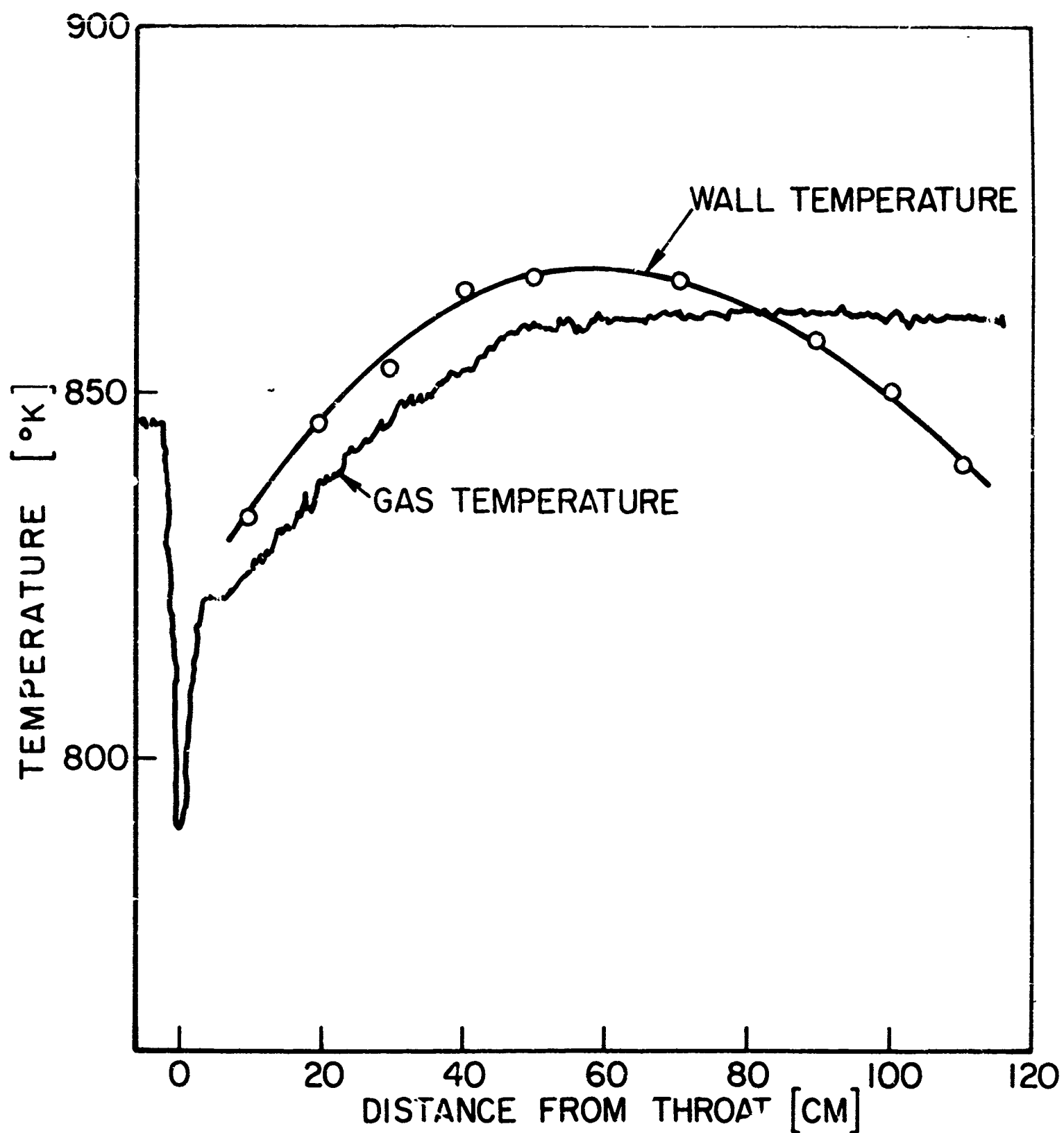
traversing probe one-half inch in diameter is employed with an in or out traverse time of about 60 seconds. Since the probe travel velocity is much less than the flow velocity, rate measurements can be made traversing either in or out. A silica coated, .0015 inch platinum--platinum 13% rhodium wire thermocouple is used with a bead diameter held to less than about .002 (inch). The silica coating is applied in a flame seeded with hexamethyldisiloxane to prevent the catalytic property of platinum from affecting the experiments. Cookson et al (55) have published the results of a study on identical thermocouples in hydrogen-air flames from which they conclude that silica is an effective catalysis inhibitor. They also report that small diameters, less than about .004 (inch), are required to "reduce the effect of recombination in the boundary layer surrounding the thermocouple." The smaller diameter thermocouples produce smaller thermal gradients in the boundary layer (because the probe temperature is closer to the gas temperature) and thereby reduce boundary layer recombination. Sample thermocouples are calibrated against a National Bureau of Standards calibrated standard thermocouple.

A typical temperature profile without reaction was presented as Figure 10, and with reaction is presented in Figure 12. The uncertainty in the temperature profile measurement does not arise solely from the measuring technique, but also from the failure of the flow reactor to attain adiabatic operating conditions. Ideally, if the wall temperature were to match the gas temperature, not only would the flow be truly adiabatic, but additionally a much smaller potential for radiation heat transfer



TEMPERATURE PROFILE, HYDRAZINE / NITRIC OXIDE REACTION

between the thermocouple and its surroundings would exist. While an estimate of this diabatic effect can be made from a gas temperature trace without reaction present, which shows little heat transfer between wall and gas, a thermocouple instrumented duct is used to determine the ability of the wall to adapt to the gas temperature profile. Times of the order of 20 to 30 minutes are found necessary for the duct wall temperature to come to a steady state condition. A comparison of the wall temperature and gas temperature profiles is presented in Figure 13. While in this particular case radiation heat transfer to and from the thermocouple and diabatic effects are relatively unimportant, such is recognized not to be the case for many of the experimental measurements. At higher temperatures radiation heat transfer effects become greater. With some of the reactants, particularly hydrazine, equilibration times of 20 to 30 minutes are not available. As a net result of the uncertainty in the measured gas temperature and of heat transfer between the gas and the wall, the uncertainty in the calculated rate constant can be as high as 100% (see Appendix B) although uncertainties of less than 50% can be attained in most cases. The hydrazine experiments are further complicated by the high uncertainty in the measured hydrazine flow rates. Fortunately, for a first order dependency upon the hydrazine concentration and an excess of oxidizer, the reaction rate constant calculation is not dependent upon the hydrazine concentration. Accurate knowledge of the hydrazine flow, therefore, is not required. The measurement of the heat of reaction, on the other hand, depends directly on the reactant flow rate, and, therefore, does reflect uncertainties in the measured flow.



COMPARISON OF GAS AND WALL TEMPERATURE PROFILES  
HYDROGEN / AIR REACTION, 7.5 [CM] DUCT

### 3.2.3 Gas sampling

Gas samples are taken from the reactor using a water cooled stainless steel probe with an expansive quench through a .015 (inch) throat diameter nozzle. Quench times of less than one millisecond are calculated. Samples are taken directly into glass bottles, with a sampling time of about two minutes, and stored until analyzed by one of the techniques discussed in Section 3.5.

### 3.2.4 Velocity profile

A direct determination of the radial velocity profile was made at operating temperatures using a stagnation pressure rake. The results confirm a turbulent velocity profile. A previous investigation of the radial temperature variation (53) has shown a similar "flat" profile.

## 3.3 EXPERIMENTAL PROCEDURE

### 3.3.1 General techniques

While the procedures followed depend upon the particular reaction studied, certain standard techniques are found necessary to obtain reproducible data. Following the establishment of a reaction in the reactor duct, the reaction is maintained for 20 to 30 minutes before recording of experimental data to insure thermal equilibrium. Within a temperature range, the concentration of fuel and oxidizer are varied independently.

### 3.3.2 Safety precautions

The combination of the toxic properties of nitrogen dioxide and nitric oxide and the explosive character of hydrazine demands strict adherence to safety procedures. The test cell atmosphere is monitored for nitrogen dioxide and personnel are not allowed in the cell with concentrations in excess of one part per million. Protective clothing, checked for non-reactivity with the reactants, is worn when handling hydrazine, nitrogen tetroxide, and nitric oxide. Esso Humble-Therm 500 is used as the heat transfer fluid in both the nitrogen tetroxide and the hydrazine evaporators. Its compatibility with liquid and vapor nitrogen tetroxide at temperatures of up to 200°C was checked to insure that no dangerous reaction would occur should a leak develop in the oxidizer system. Emergency breathing apparatus is available should the necessity of entering the test cell arise under conditions of a contaminated atmosphere. Stainless steel lines, fittings, and gages are used throughout the oxidizer system and standard "oxygen-clean" procedures are employed to condition the system following possible contamination.

The ability to handle hydrazine vapor without unpredictable explosions was never attained. In addition to the handling features outlined in section 3.1.2.3, a lengthy conditioning of the apparatus is found to be mandatory. Following the cleaning and assembly of all parts, the hydrazine system is purged for several days with dry nitrogen. A series of "fuels" are then run, leading up to anhydrous hydrazine, in an attempt to passivate the system. Generally the sequence used is: dis-



tilled water, monomethyl hydrazine, 50% water--50% hydrazine, 25% water--75% hydrazine, 10% water--90% hydrazine, anhydrous hydrazine. Damage resulting from the hydrazine explosions generally precludes positive determination of the cause of the explosions. In general the explosions are traced to the vapor phase part of the system. Handling procedures for nitrogen tetroxide and hydrazine are discussed in detail in the following references (56,57,7,58,40,59,60,61,62).

### 3.3.3 Reproducibility of measured reaction rates

All of the reactions investigated were studied on at least two separate days, generally more, to insure the reproducibility of the measured rates. Some, but not all, of the reactions were studied in different duct sizes to determine possible wall effects. A total of 1768 runs were made, of which approximately half represented measurable reactions, and resulted in about 5000 data points. An important feature of the flow reactor technique is the attendant ability to produce a large quantity of valid experimental data.

### 3.4 DATA REDUCTION AND ANALYSIS

Because of the quantity of experimental data, computer reduction and analysis is mandatory. Repetition of experimental points provides additional statistical advantages in determining the reaction rate parameters. A summary, rather than a detailed accounting and explanation of the relations used in the data reduction and analysis, is presented in the following sections. The

details of the data reduction and analysis are available in Appendix C in compact but complete form as listings of the FORTRAN statements of the computer programs employed.

### 3.4.1 Preliminary calculations

The basic technique for determining the reaction rate was developed in Section 3.1.1. The measurements required to establish the reactor flows (pressures, pressure drops across orifices, temperatures) are recorded by hand during each run or probe traverse. This information is then transferred to punched cards and converted through application of the appropriate calibrations and corrections, to flow rates, concentrations, mole fractions, equivalence and reaction ratios, and flow velocity. The temperature profile similarly is read "by hand" from the strip chart record in terms of millivolts of thermocouple output and slopes. This information is then card punched and converted to temperatures and temperature-time gradients with application of corrections for changes in flow velocity through the reaction zone due to temperature change and possible net change in total volume in going from reactants to products.

The equivalence ratio,  $\phi$ , used throughout is that defined by the fuel to oxidizer ratio divided by the fuel to oxidizer ratio corresponding to that stoichiometry for which the fuel and oxidizer are oxidized and reduced, respectively, to their standard valency states.

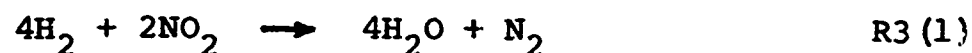
$$\phi = \frac{\frac{[F]}{[O]}}{\left(\frac{[F]}{[O]}\right)}$$

standard stoichiometry

For reactions which ordinarily proceed to a state other than the standard state, a second ratio, which herein is termed the "reaction ratio,"  $\xi$ , is useful. Definition of this ratio requires reference to a particular reaction (as does also definition of the equivalence ratio),

$$\xi = \frac{\frac{[F]}{[O]}}{\left(\frac{[F]}{[O]}\right)_{\text{reaction stoichiometry}}}$$

For example, hydrogen and nitrogen dioxide have a standard stoichiometry of



while under the conditions of the present experiments these same reactants exhibit a reaction stoichiometry



An equivalence ratio of  $\phi = 1$  therefore implies a hydrogen to nitrogen dioxide ratio of 2, while a reaction ratio of  $\xi = 1$ , where the reaction is understood to be according to R3(2), implies a hydrogen to nitrogen dioxide (molar) ratio of 1. The necessity of distinguishing between these two cases arises from definition of what is meant by "fuel rich" and "oxidizer rich". If fuel rich is to mean that additional fuel will go unreacted, then the appropriate description is  $\xi > 1$ , not  $\phi > 1$ .

#### 3.4.2 Calculation of the rate constant

The relation for determining the rate constant from the reactor temperature profile for a first order reaction depending on a single specie only, that is, one for which the rate is given by

$$\frac{d[A]}{dt} = -k_1[A]$$

E3 (8)

was shown by Crocco, Glassman and Smith (52) to be

$$k = \frac{1}{T_f - T} \frac{T_f}{T} \frac{dT}{dt}$$

E3 (9)

where:

[A]	concentration of reactant A	(moles/cc)
$k_1$	first order rate constant	(sec <sup>-1</sup> )
T	local temperature	(°K)
$T_o$	initial temperature	(°K)
$T_f$	final temperature	(°K)
t	time	(sec)

Eberstein (39) extended the rate constant relation, E3(9), to a nth-order reaction depending on a single specie only, that is, one for which the rate is given by

$$\frac{d[A]}{dt} = k_n [A]^n \quad \text{E3 (10)}$$

and showed that

$$k_n = \left( \frac{Q}{\rho_o C_p T_o} \right) \frac{1}{T} \left( \frac{1}{T_f - T} \right)^n \frac{T_f}{T} \frac{dT}{dt} \quad \text{E3 (11)}$$

where:

Q	heat of reaction	(cal/mole)
$\rho$	molar density	(mole/cc)
$C_p$	molar specific heat constant pressure	(cal/mole °K)
n	reaction order	

For reactions involving more than one reactant and with rate dependencies involving products and possibly inerts in addition to reactants, a more general relation is required.

$$\frac{d[A_1]}{dt} = -k[A_1]^{n_1}[A_2]^{n_2}\dots[A_m]^{n_m}$$

E3 (12)

or, more compactly

$$\frac{d[A_1]}{dt} = -k \prod_{i=1}^m [A_i]^{n_i}$$

E3 (13)

It is understood that specie  $A_1$  is chosen so that its disappearance is a measure of the reaction rate. Generally  $A_1$  is one of the reactants. Particularly, since the reactions studied involve two reactants, the following convention is used throughout.  $A_1$  refers to the reducing reactant and  $A_2$  to the oxidizing reactant, or, as is common to the rocket propulsion and combustion fields, the "fuel" and "oxidizer", respectively.  $A_3$ ,  $A_4$ , and so forth refer to other species, the presence of which may affect the reaction rate. Note also that

$$\frac{d[A_1]}{dt} = (\text{constant}) \frac{d[A_2]}{dt}$$

E3 (14)

The dimensions of the rate constant,  $k$ , are

$$\left[ \left( \frac{\text{cc}}{\text{mole}} \right)^{-1 + \sum_{i=1}^m n_i} \frac{1}{\text{sec}} \right]$$

The rate constant thus depends not only on the reaction rate but also on the form of the rate equation E3(13), hence

$$k = k \left( \frac{d[A_i]}{dt}, [A_i], n_i \right) \quad \text{E3 (15)}$$

The details of the derivation of the relation for determining the rate constant from the temperature profile and justification of the necessary simplifying assumptions are presented in Appendix B. The general form of the expression for determining the rate constant is

$$k = \left( \rho^{-1 + \sum_{i=1}^m n_i} x_1^{n_1-1} \prod_{i=2}^m x_i^{n_i} \right)^{-1} \frac{T_f}{T} \frac{1}{T_f - T} \frac{dT}{dt} \quad \xi \leq 1 \quad \text{E3 (16)}$$

where:

$x_i$  mole fraction of specie  $A_i$

Specie  $A_1$  must be chosen so that the condition of a completed reaction is described by  $x_1 = 0$ . For the case of a binary reaction this implies an excess of specie  $A_2$  over that required for the reaction stoichiometry, or, in other terms, "oxidizer rich," or, the reaction ratio,  $\xi \leq 1$ . For the "fuel rich" case, ie.  $\xi \geq 1$ , a new expression for the rate constant is required. Such an expression is obtained by exchanging the subscripts "1" and "2" in Equation E3(16) to give

$$k = \left( \varphi^{-1 + \sum_{i=1}^m n_i} x_1^{n_1} x_2^{n_2-1} \prod_{i=3}^m x_i^{n_i} \right)^{-1} \frac{T_f}{T} \frac{1}{T_f - T} \frac{dT}{dt}$$

$$\xi \geq 1$$

E3(17)

Equations E3(16) and E3(17) reduce to the first order, single specie dependency Equation E3(9) upon substitution of  $n_1 = 1$  and  $n_2 = n_3 = \dots = n_m = 0$ . Similarly, they reduce to the nth-order, single specie dependency equation E3(11) upon substitution of

$$n_1 = n, \quad n_2 = n_3 = \dots = n_m = 0$$

$$x_1 = x_{10} \frac{T_f - T}{T_f - T_0} = \frac{\bar{C}_p T}{Q_0} \frac{T_f - T}{T_f - T_0}$$

$$\varphi = \varphi_0 \frac{T_0}{T}$$



The assumptions implicit in the general reaction rate constant equations are:

- (1) one dimensional (radially uniform properties, composition, and flow parameters)
- (2) adiabatic
- (3) no longitudinal diffusion of heat or mass
- (4) perfect gas equation of state
- (5) constant pressure
- (6) reaction rate (or energy release rate) is proportional to the temperature rise (that is, constant specific heat)

In addition to measuring the temperature profile, flow velocity, and initial reactant concentrations, determination of the rate constant requires knowledge of the reaction stoichiometry and of the reaction orders with respect to each relevant specie. Determination of the reaction stoichiometry is based on the measured heat of reaction, variation of the flow stream temperature rise with reactant ratio, measured product composition (where available), and the work of other investigators. Determination of the reaction orders,  $n_i$ , is discussed in the following section.

#### 3.4.3 Determination of reaction orders

Before the rate constant,  $k$ , can be calculated, the reaction orders,  $n_i$ , appearing in the general rate equation introduced in the previous section

$$\frac{d[A_i]}{dt} = -k \prod_{i=1}^n [A_i]^{n_i}$$

E3 (18)

must be determined. Several experimental and analytic approaches are available. The direct approach of holding all parameters constant except for the concentration of the specie  $A_i$  and noting the change of the reaction rate with changing concentration of  $A_i$  is the best technique for determining the reaction orders. Unfortunately since concentrations and temperatures change during a given run, it is difficult to obtain data for which all parameters except for one concentration are constant. Where possible, experiments were run with one reactant in large excess so that its concentration would change little during reaction. By then selecting reaction rates at a given temperature, sufficient data generally can be obtained to allow the plotting of rates versus concentrations on log-log plots from which the slope is the reaction order.

$$\log \frac{d[A_i]}{dt} = -\log k + n_i \log [A_i]$$

E3 (19)

Where such data cannot be obtained, two other approaches are available. If the orders with respect to all but one specie are known, then the effect of variations in these concentrations on the rate can be accounted for and the order with respect to the concentration of the specie of interest determined as above.

The statistical analysis of the rate constants provides yet another technique. By assuming various reaction orders, calculating the corresponding rate constants, and statistically determining which set best fits an Arrhenius type rate expression, one may determine the "best" reaction order. Some care must be used in this approach as there is a bias resulting from the experimental uncertainty in the temperature measurements. The uncertainty in the reaction rate is least for an overall reaction order,

$\sum n_i = 0$ . As the overall reaction order departs from this value, the uncertainty in the temperature,  $T_f - T$ , is reflected more strongly in the resulting uncertainty in the rate constant,  $k$  (see equation E3(16) and Appendix B). This technique is biased, therefore, in favor of an overall reaction order of zero.

Several other "clues" are available to confirm the selection of the proper reaction orders. Since the concentrations of the reactants (and products) change through the reaction zone, the selection of a wrong reaction order will produce apparent disagreement between the temperature dependence of the rate constant for a single run and the temperature dependence of the rate constant as averaged for a number of runs with different initial conditions. The feature of higher apparent activation energy for individual runs than for a number of runs taken together, is reported by Eberstein (39). He attributes the effect to heat transfer losses. The present investigations confirm that heat transfer losses can produce such an effect and therefore indicate the necessity of attaining thermal equilibrium prior to measuring reaction rates. The selection of incorrect reaction orders has a similar effect and can result in single run apparent activation energies

which are either greater or less than the activation energy obtained from rate data representing a number of runs. Careful attention to the attainment of thermal equilibrium and the selection of the proper reaction orders generally results in agreement between activation energies as calculated for single runs and as calculated for a number of runs. Selection of a wrong reaction order is often immediately recognizable in terms of the large scatter which results in the rate constants as plotted as a function of the reciprocal temperature. One also should note that the choice of the reaction order has a strong effect on the calculated overall activation energy, i.e., dependence of the rate constant upon temperature. For this reason, care is necessary in the interpretation of differences of activation energies of reactions with different orders.

#### 3.4.4 Enthalpies of reaction

The enthalpies of reaction generally are calculated simply on the basis of the flow rates, temperature rise, and a mean specific heat. Where justified, the variation of specific heat with temperature and composition is considered. In general, no correction is applied to reduce the enthalpy of reaction measured at a high temperature to an enthalpy of reaction at standard temperature. This effect is small compared to the uncertainty in the measured value. Because of the difficulty in identifying the initial temperature in many of the runs, the flow reactor is not an accurate device for measuring reaction enthalpies. Thermodynamic data, as required, is taken from the JANAF tables (11).

#### 3.4.5 Statistical analysis of experimental data

The calculated rate constant data are analyzed

statistically for their mean variation from a least squares fit to a straight line representing the logarithm of the rate constant as a function of the reciprocal of the absolute temperature. This is in accordance with an Arrhenius type rate expression

$$k = 10^A \exp(-E/RT) \quad E3 (20)$$

from which

$$\log_{10} k = A - \frac{E}{(\log_e 10) RT} \quad E3 (21)$$

The use of a temperature dependent preexponential factor is neither justified nor necessary to correlate the experimental results. The range of temperatures studied and the experimental uncertainties are not consistent with such a refinement. Standard deviations of the preexponential factor exponent, A, and the overall activation energy, E, are calculated according to standard techniques of the statistics of linear relations, eg., Nalimov (63).

### 3.5 ANALYSIS OF GAS SAMPLES

Ideally, the reactor gases should be sampled and analyzed in a fashion which would give quantitative identification of the species present at the reaction conditions. The difficulty of accomplishing this arises from the basic problem of maintaining the sample composition upon removing it from the high temperature reactor. While a sampling probe was designed and is used which gives rapid quenching of possible high temperature reactions, the problem of

preventing low temperature reactions until the gas can be analyzed remains unsolved. Reaction products which condense at room temperature, for example water, also will be lost or reduced in concentration. Three different techniques are employed in the gas analysis and are discussed below.

### 3.5.1 Gas chromatography

A Beckman GC-1 Gas Chromatograph is used with a Linde molecular sieve column. Because of the low concentration and high reactivity of many of the product gases, the only identifiable species are nitrogen, oxygen, and hydrogen. Of these nitrogen is the carrier gas and its presence as a reaction product is, therefore, not discernible. Oxygen and hydrogen are detected only as reactants when they are present in concentrations in excess of their stoichiometric values. Oxygen and hydrogen are not detected as possible reaction products, as might be expected in the reaction of ammonia and nitrogen dioxide.

### 3.5.2 Infrared spectroscopy

An infrared spectrometer is much more useful in the identification of reaction products. Two different models are used, a Perkin Elmer Model 21 and a Perkin Elmer Model 237B, both grating spectrophotometers. A ten centimeter, single pass cell with sodium chloride windows is employed. A problem of the reactivity of nitrogen dioxide and the sodium chloride windows is encountered as is evident in

in the spectra showing nitrosylchloride and sodium nitrate. This difficulty also is reported by Pierson, Fletcher, and Gantz (64). Species such as  $\text{NO}_2$ ,  $\text{NO}$ ,  $\text{N}_2\text{O}_4$ ,  $\text{NH}_3$ ,  $\text{N}_2\text{O}$  are found to be identifiable. Not all are found as reaction products, but some, rather, in reactant samples. Unfortunately nitric oxide is only weakly absorbing, as is expected from its near homo-polar character, and is difficult to detect at low concentrations. Some typical infrared spectra of the product gas samples are presented in Appendix D.

### 3.5.3 Mass spectroscopy

A small number of gas samples taken from the reactor were analyzed using a CEC 21-130 cyclodial focusing mass spectrometer. The operating conditions were about 78 volts ionizing potential and  $10^{-7}$  mmHg pressure. Gaseous species present in concentrations down to about 5 parts per million or .0005% were detectable.

### 3.6 REACTANTS AND CARRIER GASES

In all cases the reactants studied are used as received from the manufacturer without purification. The manufacturers' specifications for the reactants are summarized below

material	supplier	minimum purity	impurities
$\text{N}_2\text{O}_4$	Allied Chemical	99.5%	.1% $\text{H}_2\text{O}$ .08% Cl as NOCL .01% ash

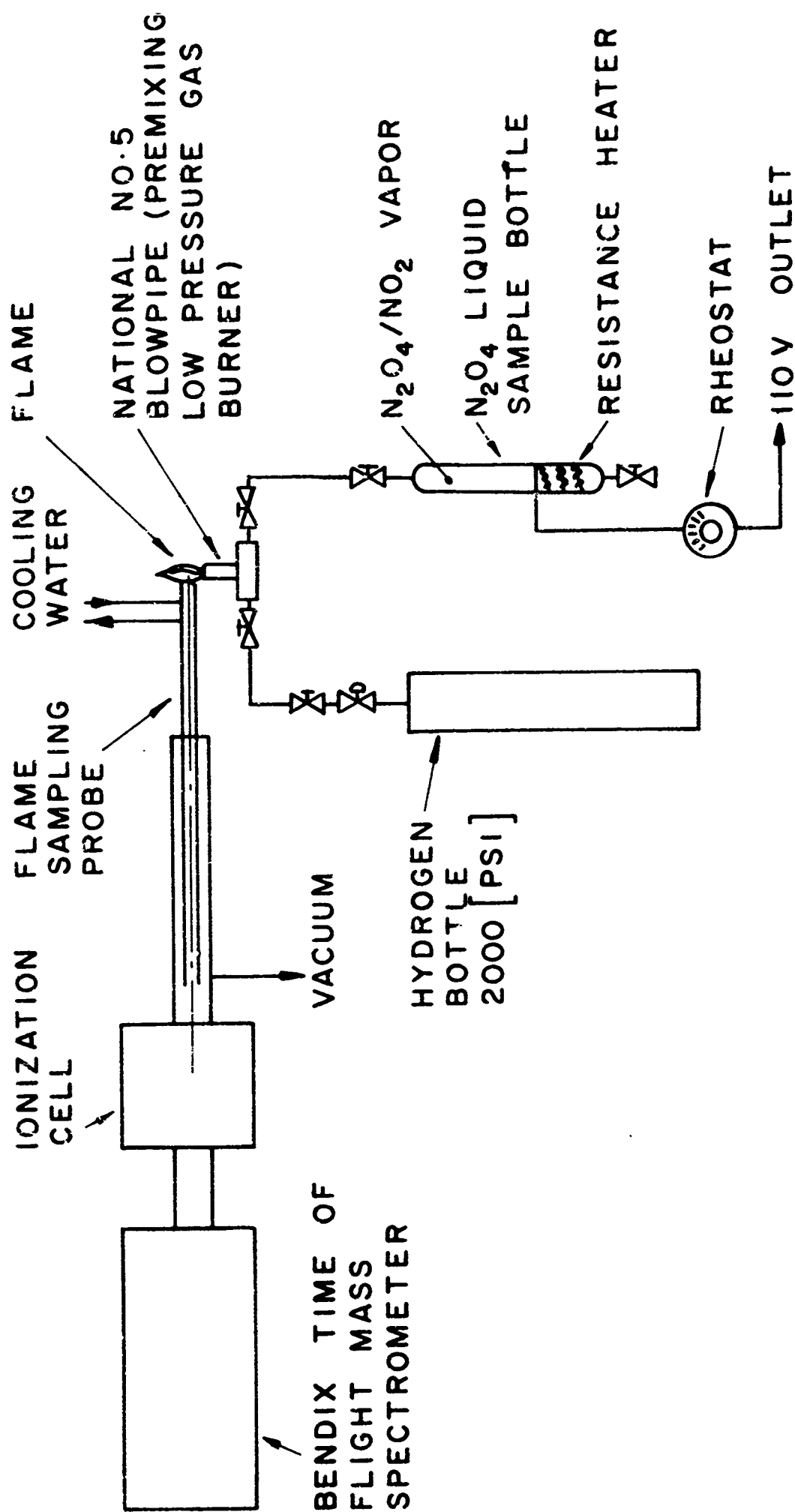
material	supplier	minimum purity	impurities
NO	Matheson	99.0%	CO <sub>2</sub> N <sub>2</sub> O
NH <sub>3</sub>	Matheson	99.99%	H <sub>2</sub> O
H <sub>2</sub>	General Dynamics	99.8	H <sub>2</sub> O, O <sub>2</sub> , CO <sub>2</sub>
	Matheson	99.95	
N <sub>2</sub>	Air Products (liquid)	99.95	
air	local supply, high pressure, dried		
N <sub>2</sub> H <sub>4</sub>	Olin, technical anhydrous	97 %	H <sub>2</sub> O, NH <sub>3</sub> , aniline
O <sub>2</sub>	Matheson	99.6	Ar N <sub>2</sub>

In addition to the difficulty of undertaking the purification of the relatively large quantities of gases and liquids used, most of the impurities present are either in such small quantities as to be negligible or would not be expected to have a noticeable effect upon the measurements. The fact that the rate measurements are always made under conditions wherein substantial quantities of the product gases are present, renders the presence of small quantities of such impurities as water unimportant. Water is a major reaction product in all of the reactions studied.

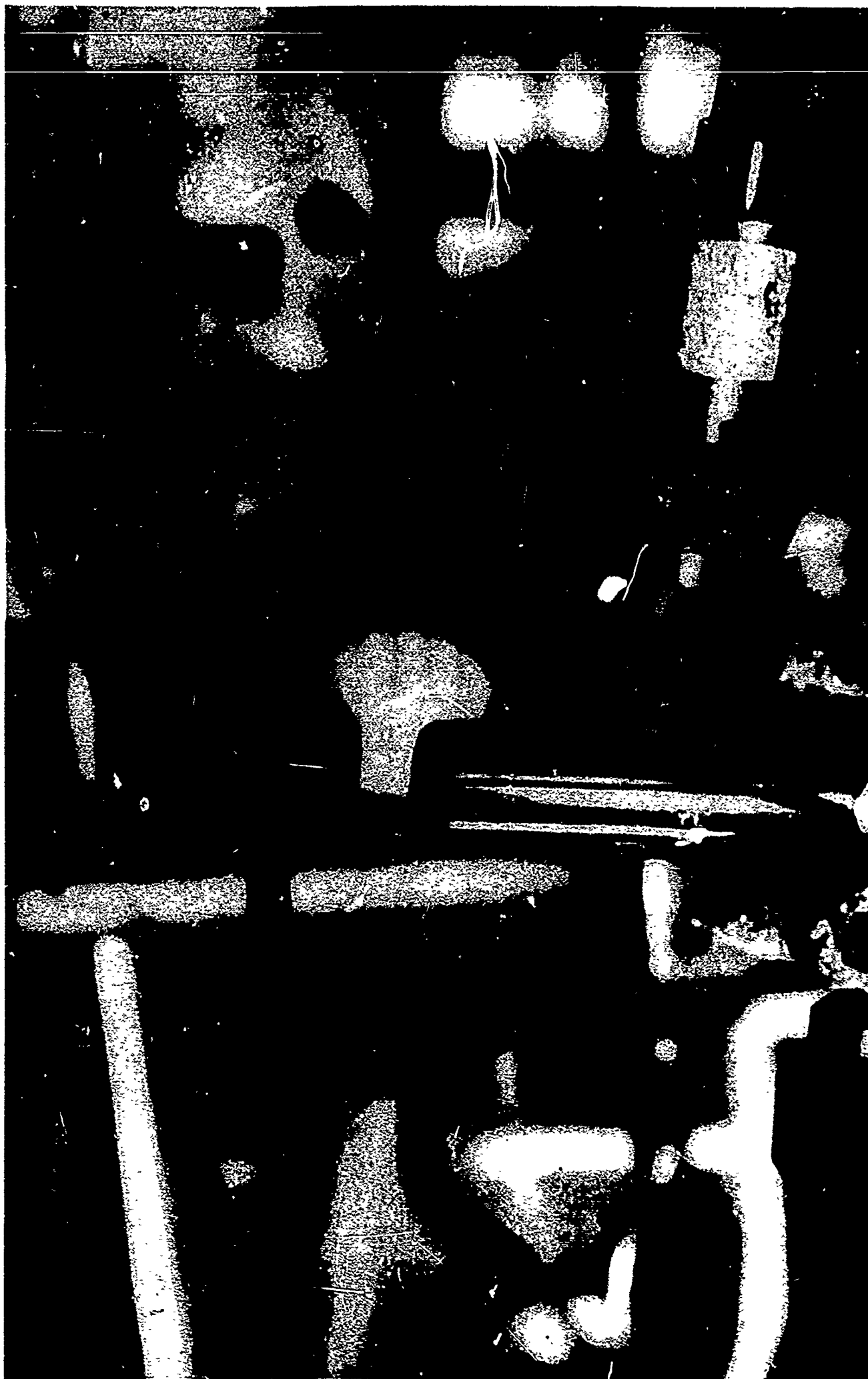


### 3.7 MASS SPECTROSCOPIC FLAME STUDY

A study of a premixed hydrogen/nitrogen tetroxide flame was conducted by the author using apparatus at the Air Force Rocket Propulsion Laboratory, Edwards AFB, California. A premixed gas flame was obtained using a National No. 5 blowpipe in air and a flow system presented schematically in Figure 14. The water cooled sampling probe was positioned approximately in the center of the flame cone and samples taken for flows with excess hydrogen and with excess nitrogen dioxide. A photograph of the burner and sampling probe is presented as Figure 15. The gas sample was ionized in a commercial Knudsen Cell operated at a potential of 70 electron volts. A Bendix time of flight mass spectrometer was operated at pressures less than  $10^{-5}$  millimeters of mercury. A detailed description of the system is to be found in Reference (65).



SCHEMATIC, EXPERIMENTAL APPARATUS FOR HYDROGEN DIOXIDES FLAME STUDY



FLAME STUDY APPARATUS: BURNER & SAMPLING PROBE

## CHAPTER 4

HYDROGEN REACTIONS

Hydrogen is a major constituent of the decomposition products of hydrazine. The reaction of hydrogen with nitrogen dioxide and the products of nitrogen dioxide decomposition is therefore of interest. By determining the character of the reaction of hydrogen with nitrogen dioxide, oxygen, decomposed nitrogen dioxide, nitric oxide, and oxygen plus varying amounts of nitric oxide, an increased understanding of the effect of nitrogen dioxide decomposition on its subsequent reaction with hydrogen, and, therefore, with decomposed hydrazine, has been obtained. For each reaction, experimental evidence has been secured to determine the stoichiometries, reaction rate orders, and reaction rates. From the study of the reactions of hydrogen and similar investigations of the reactions of ammonia, ammonia and hydrogen, and hydrazine, reported in the following three chapters, a thorough picture of the hydrazine/nitrogen dioxide reaction may be drawn.

4.1 HYDROGEN/NITROGEN DIOXIDE

The reaction of hydrogen and nitrogen dioxide was studied experimentally using two techniques: adiabatic flow reactor reaction rate measurements and a mass spectroscopic investigation of a premixed flame.

4.1.1 Stoichiometry

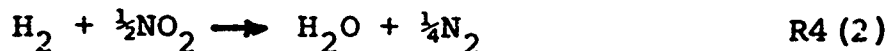
The stoichiometry of the overall reaction occurring in the two experiments is different as a result of the

difference in reaction temperatures. In the flow reactor, where reactions are studied at about 1000°K, the reaction involves the reduction of the nitrogen dioxide only to nitric oxide,



Evidence that such is the case is found in the detection of nitric oxide in the infrared absorption spectra and mass spectra of the product gases. Additionally, the heat of reaction is measured to be 45 [kcal/mole H<sub>2</sub>] which is in good agreement with the calculated value of 44.13 [kcal/mole H<sub>2</sub>] for the above reaction. Even a ten per cent consumption of NO would give an 8 [kcal/mole H<sub>2</sub>] increase in the heat of reaction which could be detected readily.

In the flame studies, however, where the temperature approaches the adiabatic flame temperature of 2660°K, no nitric oxide is detectable in the products of the hydrogen rich flame, indicating that the overall stoichiometry is approximately

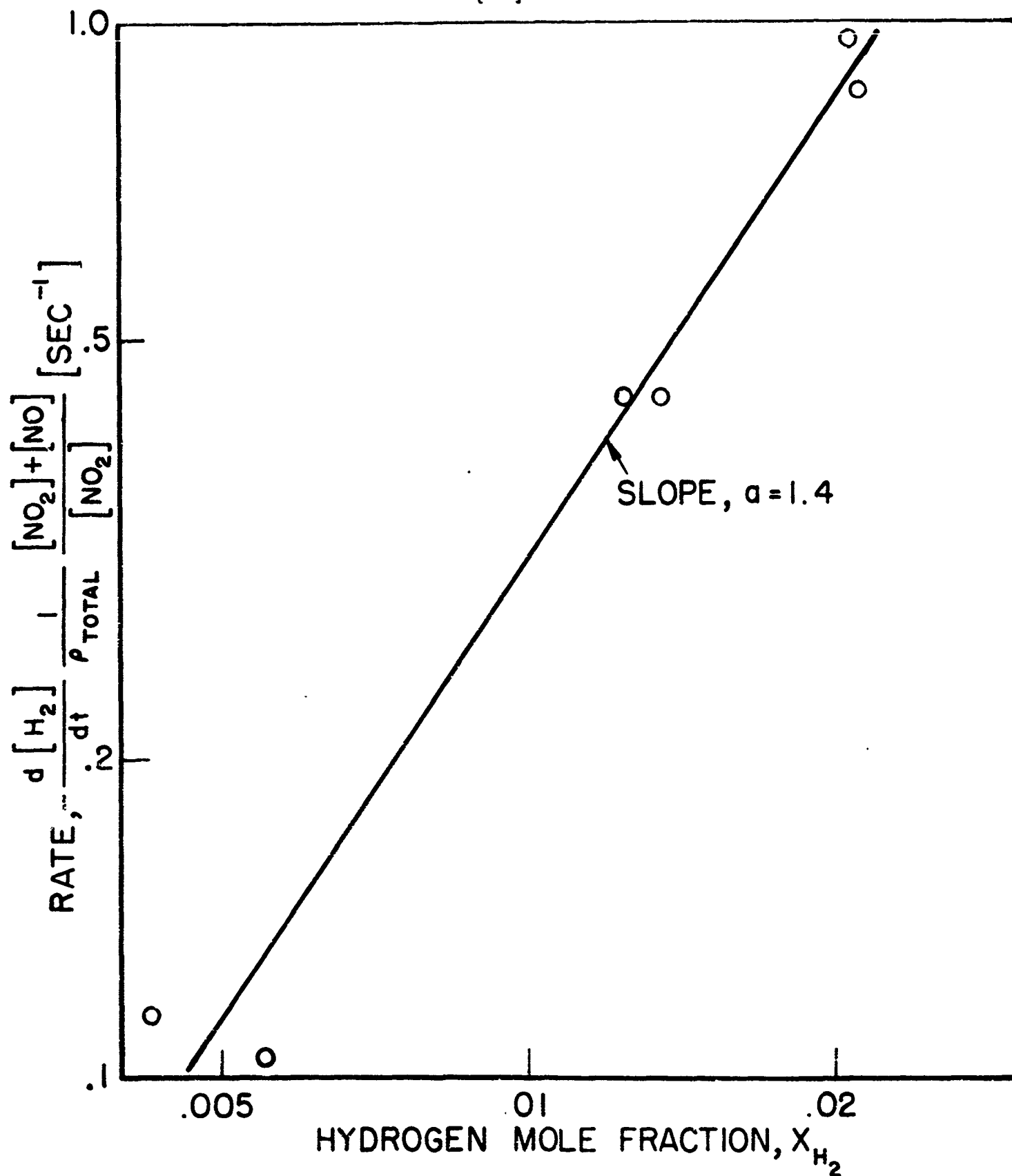


#### 4.1.2 Experimental results, adiabatic flow reactor

Determination of the reaction orders is difficult because of the large number of experimental parameters affecting the rate. Rosser and Wise (66, 67, 68) and Ashmore and Levitt (69,70) found the reaction rate to depend on the hydrogen concentration, nitrogen dioxide concentration, and sum of nitrogen dioxide and nitric oxide concentration. These investigators found nitrogen

dioxide to be both a reactant with hydrogen and an inhibitor to the reaction of hydrogen. Nitric oxide was found to inhibit the reaction. In the present experiments, temperature also must be added as an experimental parameter. The problem of isolating each of these effects is approached in the following manner. In each case rates are selected (from the rate as a function of temperature) at a single temperature. The rate dependence upon the hydrogen concentration is obtained by holding the initial concentration of nitrogen dioxide constant. This procedure gives a constant concentration of nitrogen dioxide plus nitric oxide through the reaction zone. It is necessary also to assume that the rate dependence upon the nitrogen dioxide concentration is first order as is reported by both groups of investigators mentioned above. This technique gives a hydrogen dependence,  $a = 1.4$ , see Figure 16. It is not possible, using nitrogen dioxide, to separate adequately the rate dependencies on local  $\text{NO}_2$  and initial  $\text{NO}_2$  concentrations. By assuming one dependency, however, the other could be determined, but this approach at best can give only a qualitative check on the rate orders. The dependency upon the initial nitrogen dioxide concentration (or sum of local nitrogen dioxide and nitric oxide concentrations) is found to be  $c = -0.8$  and the dependency upon local nitrogen dioxide concentration,  $b = 1.0$ . The reaction orders are summarized below.

$$\frac{d[\text{H}_2]}{dt} = -k[\text{H}_2]^a[\text{NO}_2]^b([\text{NO}_2 + \text{NO}])^c$$



HYDROGEN / NITROGEN DIOXIDE REACTION RATES  
 $T = 1000^\circ \text{K}$ , DEPENDENCE ON HYDROGEN CONCENTRATION

FIGURE 16

	a	b	c
Rosser and Wise	1.4	1.0	-1.0
Ashmore and Levitt	1.5	1.0	-1.0
present investigation	1.4	1.0	-0.8

Reaction rates were measured in 2 and 4 [inch] quartz ducts over the temperature range  $850 \leq T \leq 1110^\circ\text{K}$  and equivalence ratio range  $0.33 \leq \phi \leq 5.5$ , or a reaction ratio range of  $0.66 \leq \frac{1}{2} \leq 11.0$ . Reaction rate constants are calculated from the experimentally measured reaction rates using the following dependency.

$$\frac{d[\text{H}_2]}{dt} = -k[\text{H}_2]^{1.4}[\text{NO}_2]^{1.0}([\text{NO}_2] + [\text{NO}])^{-1.0}$$

The order  $c = -1$  is selected, rather than the observed  $c = -0.8$ , to facilitate comparison with the results of other investigators. The rate constant,  $k$ , is the Arrhenius rate constant which is used throughout this thesis in its simplest form to characterize the temperature dependence of the reaction rates.

$$k = 10^A \exp(-E/RT)$$

Plots of the logarithms of the experimental rate constants are presented as a function of  $1/T$  in Figures 50 and 51\* for the 2 and 4 [inch] ducts respectively.

\*Graphical presentation of the experimental rate data in terms of calculated rate constants is made in Appendix A for all of the reactions studied. Information summarizing the experimental parameters and the least squares curve fits to these rate constants also are presented in Appendix A. The rate equations and Arrhenius parameters selected as best representing each reaction studied are summarized in the main text. Figure numbers greater than 50 refer to figures located in the appendices.

VP 13-4039-65



Experimental parameters, the Arrhenius parameters, A and E, and the uncertainties in A and E are summarized in Table 23. The overall activation energies measured in the two ducts are approximately the same, 48.0 and 46.2 [kcal/mole] for the 2 and 4 [inch] ducts; the rates, however, are slightly higher in the smaller duct. The differences are attributed to a wall effect which is discussed in the following section on the hydrogen/oxygen reaction. The rate constant for the hydrogen/nitrogen dioxide reaction is selected to be that measured in the 4 [inch] duct,

$$k = 10^{14.26} \exp(-46200/RT) \quad [(\text{moles/cc})^{-.4} \text{sec}^{-1}]$$

#### 4.1.3 Experimental results, flame studies

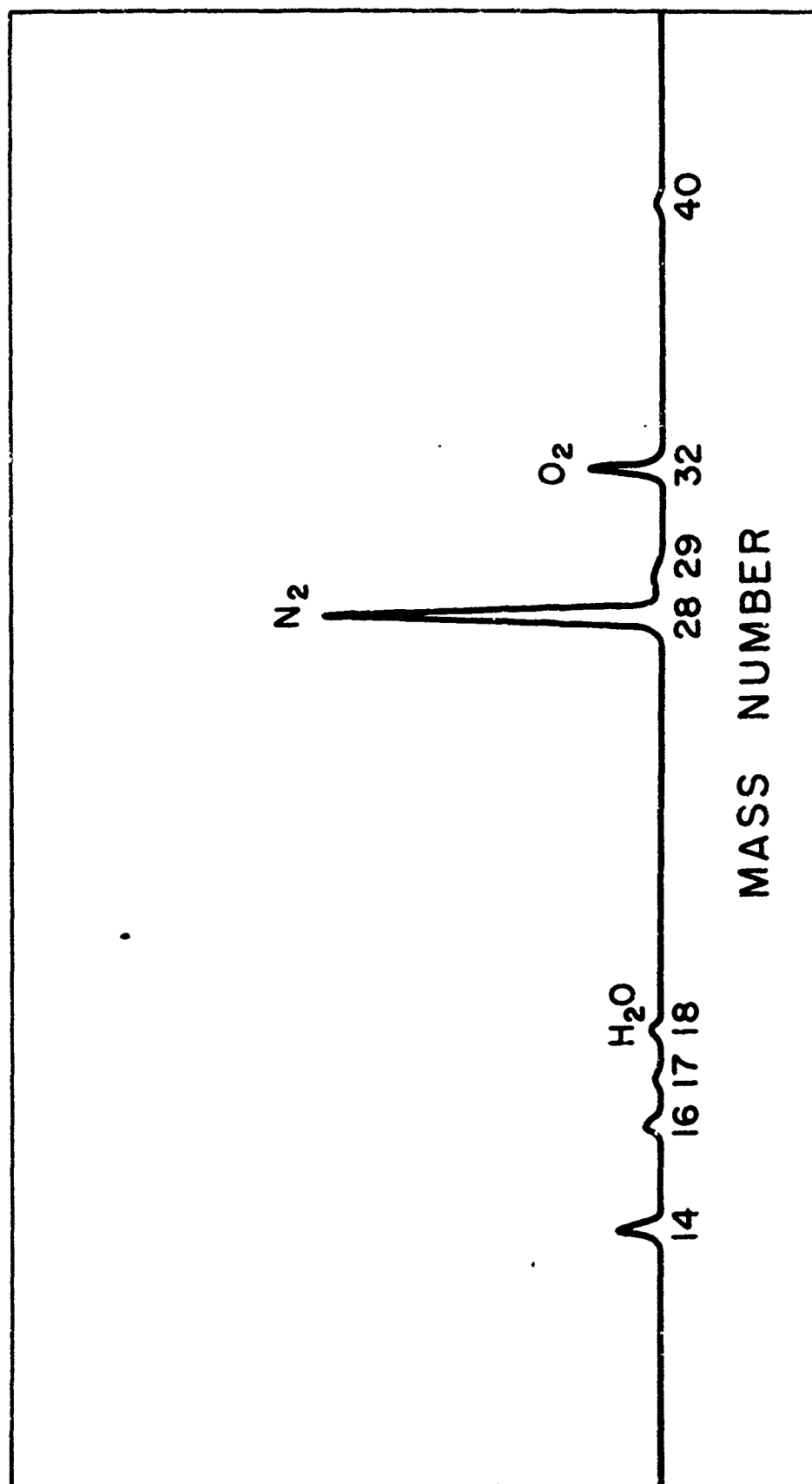
A premixed hydrogen/nitrogen dioxide flame was studied using a time of flight mass spectrometer to identify species present in samples taken directly from the flame. Three series of samples, air, hydrogen rich flame, and nitrogen dioxide rich flame, were taken and characteristic mass spectra obtained, see Figures 17, 18, and 19.

In the air sample, identifiable peaks occur at mass numbers 14, 16, 17, 18, 28, 29, 32, 40, and 44 which are consistent with the species  $\text{N}_2$ ,  $\text{O}_2$ ,  $\text{H}_2\text{O}$ , Ar, and  $\text{CO}_2$ , all normally constituents of air.

The mass spectra for the hydrogen rich flame is characterized by a strong water peak. No nitric oxide or nitrogen dioxide is present indicating that the

---

\*Tables beginning with Table 23 are found in the appendices.



MASS SPECTROGRAPH, AIR

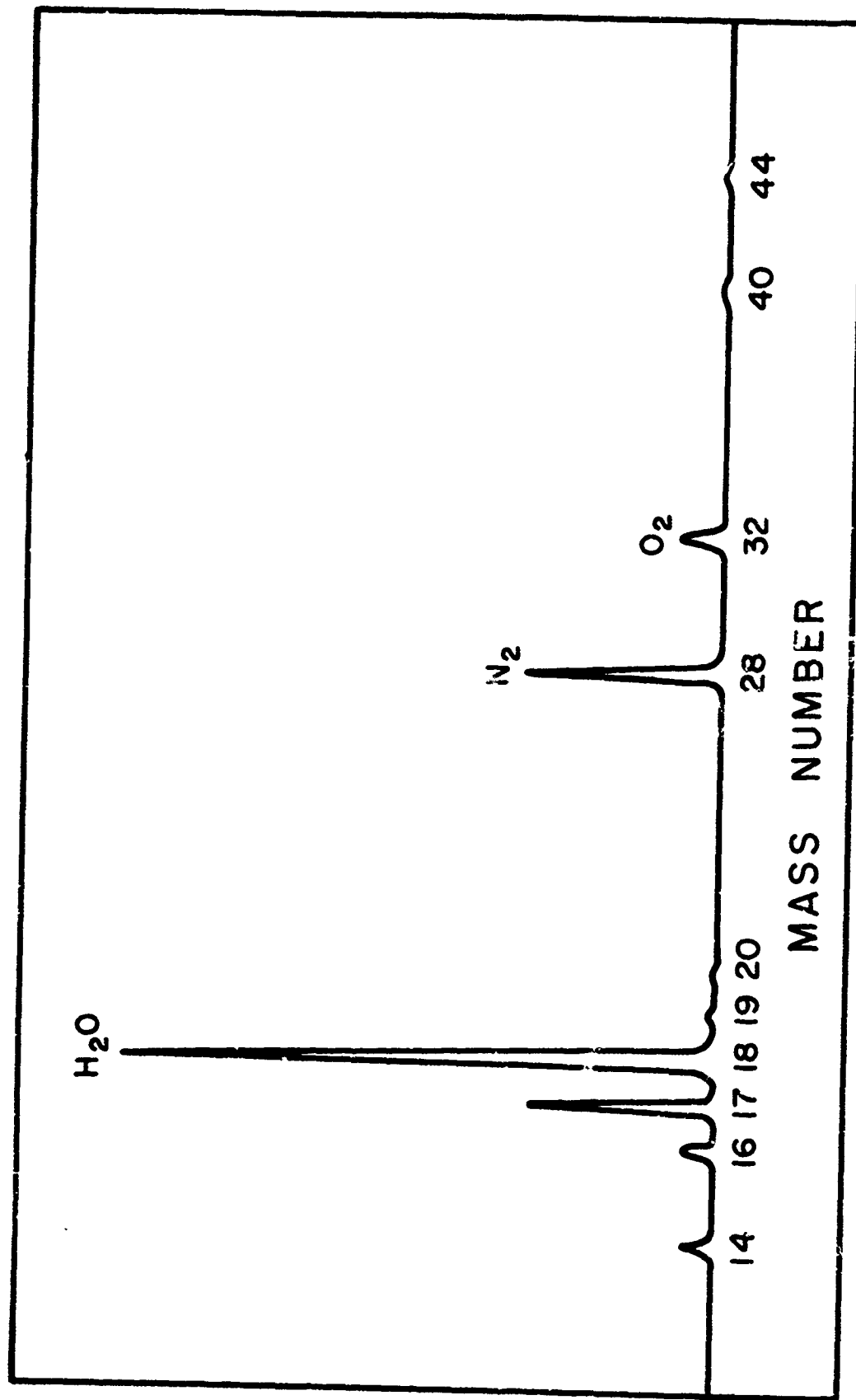
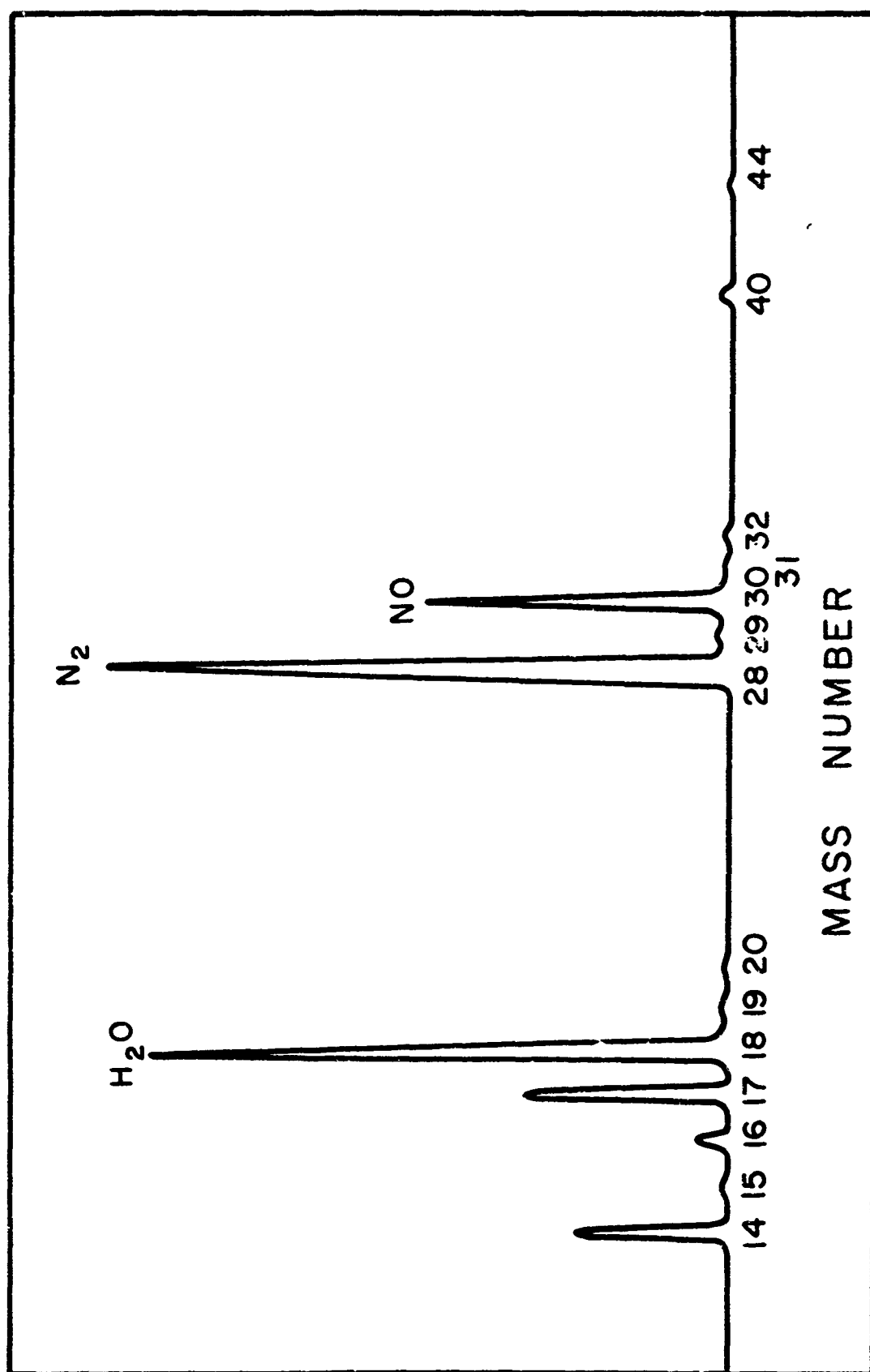
MASS SPECTROGRAPH,  $H_2/NO_2$  FLAME,  $H_2$  RICH

FIGURE 18

MASS SPECTROGRAPH,  $H_2/NO_2$  FLAME,  $NO_2$  RICH

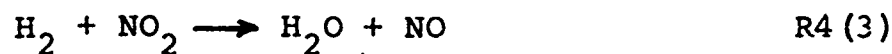
nitrogen dioxide is completely consumed. Since the experiment is conducted in air, the oxygen peak is probably largely attributable to diffusion of air into the flame. The presence of hydrogen atoms and molecules is indicated (not shown in the figure). The possible presence of OH radicals is masked by the water cracking pattern. While the presence of O radicals is similarly hidden by the water and oxygen cracking patterns, the mass number 16 peak height is somewhat proportionately greater than would be expected from the water and oxygen alone and, therefore, the presence of O atoms probably is indicated.

In the nitrogen dioxide rich flame mass spectra, the strong presence of nitric oxide, mass number 30, is noted. The continued absence of nitrogen dioxide, mass number 46, confirms that the reduction of nitrogen dioxide always proceeds through NO, either by direct reaction or by dissociation. Once again the presence of hydrogen atoms is established. The height of the mass number 31 peak is greater than would be expected from  $N^{15}O$  and is to be attributed to HNO. Another possibility would be  $N_2H_3$  but it is not reasonable that such a species could form in the hydrogen/nitrogen dioxide reaction. Also significant is the absence of any peaks corresponding to  $HNO_2$  or  $HNO_3$ .

#### 4.1.4 Results of other investigators

Rosser and Wise (57,68) have measured the hydrogen/nitrogen dioxide reaction rate between 600 and 700°K in a closed vessel using a technique of determining the nitrogen dioxide disappearance by change in light absorption.

They conclude that the reaction follows the stoichiometry



and report the disappearance of  $\text{NO}_2$  to be given by

$$\frac{d[\text{NO}_2]}{dt} = -k[\text{H}_2]^{1.4}[\text{NO}_2]([\text{NO}_2] + [\text{NO}])^{-1}$$

where the rate constant,  $k$ , has the form

$$k = 10^{14.2} \exp(-46000/RT) \quad [(\text{moles/cc})^{-0.4} \text{sec}^{-1}]$$

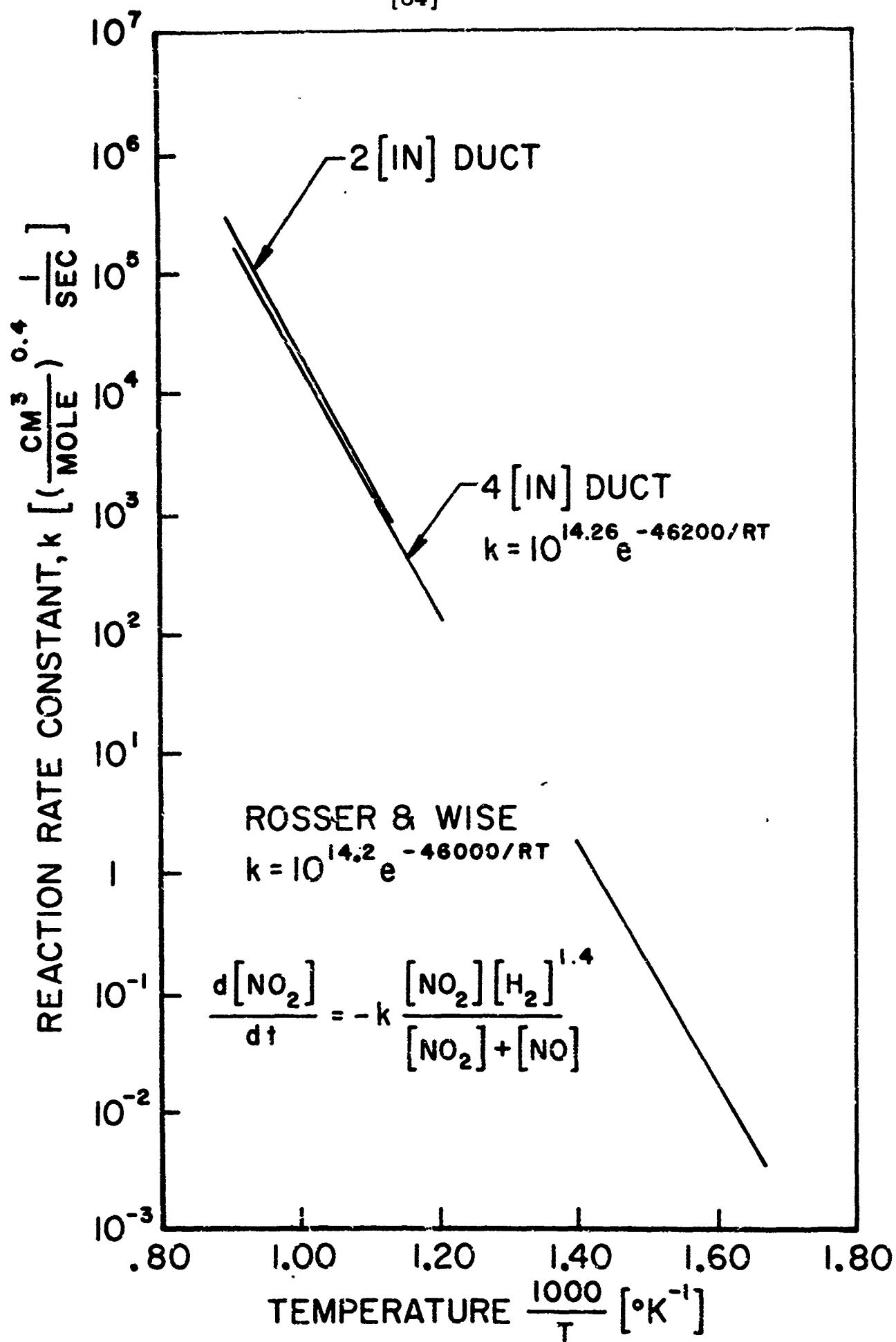
Ashmore and Levitt (69,70) used a similar technique to investigate this reaction in the temperature range of 640 to 700°K and also conclude that the stoichiometry is as given by R4(3). They find a similar rate dependence,

$$\frac{d[\text{NO}_2]}{dt} = -k_1[\text{H}_2]^{1.5}[\text{NO}_2]([\text{NO}] + k_2[\text{NO}_2])^{-1}$$

and the rate constant

$$k_1 = 10^{14.0} \exp(-43000/RT) \quad [(\text{moles/cc})^{-0.5} \text{sec}^{-1}]$$

The present results, for temperatures of 850 to 1110°K, are in surprisingly good agreement with rates measured at much lower temperatures by Rosser and Wise. A comparison of these rates, Figure 20, shows a good correlation over eight orders of magnitude in the rate constant.



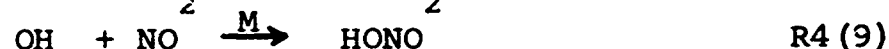
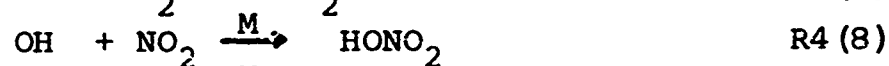
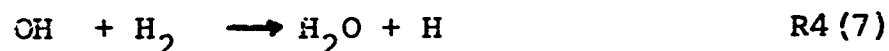
NITROGEN DIOXIDE / HYDROGEN REACTION RATE

FIGURE 20

The low flame temperature,  $1550^{\circ}\text{K}$ , obtained by Wolfhard and Parker (71) in their hydrogen/nitrogen dioxide flame studies, indicates that the reaction is incomplete, probably with  $\text{NO}_2$  being reduced only to  $\text{NO}$ . The difference from the present flame study may be attributed to the lower pressure at which Wolfhard and Parker conducted their experiments.

#### 4.1.5 Reaction mechanism

Rosser and Wise, and Ashmore and Levitt, independently proposed the following chain mechanism to describe the hydrogen/nitrogen dioxide reaction.



Reaction R4 (6) has been studied directly by Clyne and Thrush (72). They found that the vibrationally excited hydroxyl radicals produced in this reaction then reacted appreciably with molecular hydrogen to give water and hydrogen atoms, R4 (7).

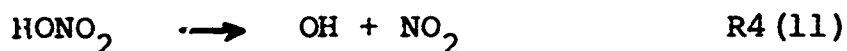
The reactions, in a steady state analysis, yield the rate expression (66)

$$\frac{d[\text{H}_2]}{dt} = \frac{d[\text{NO}_2]}{dt} = \frac{-k_5 k_7 [\text{H}_2]^2 [\text{NO}_2]}{k_8 [\text{NO}_2] + k_9 [\text{NO}]} \quad \text{E4 (1)}$$

JPR2498



At the higher pressure of the present experiments, the last two reactions can proceed independently of a third body. The calculated lifetimes of excited HONO and HONO<sub>2</sub> exceed the mean time to a collision with a deactivating particle. At the higher temperatures of the present experiments, the back reactions



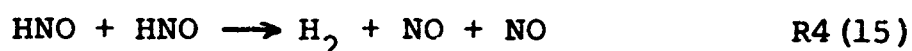
are likely to become more important. One difficulty with the mechanism proposed by the other investigators is that it is shown to give a second order dependence upon the hydrogen concentration, E4(1). Rosser and Wise attribute this difference to a removal of chain carriers at the wall and an inhibiting effect of the large excess of hydrogen used in their experiments. Neither of these arguments applies here: approximately stoichiometric mixtures are used and no change in order with respect to hydrogen is noted between the 2 and 4 (inch) results, even though a small wall effect on the rate is found.

As a limiting case, consider the termination to be dominated by the reaction



This reaction has been postulated to explain the inhibiting effect of NO addition on hydrocarbon oxidations, see, for example, (30). Under the reactor conditions, the lifetime of a newly formed (excited) HNO molecule is calculated, using the RRK model (73) to be about the same as the mean

time for collision, therefore at least a partial third body dependency is indicated. If we additionally assume that HNO is removed in a manner which does not affect the concentration dependence of R4(12), as Rosser and Wise did for reactions R4(8) and R4(9), for example, as



then we may now calculate the steady state concentration of OH

$$[\text{OH}] = \frac{k_5 k_6}{k_7 k'_{12}} \frac{[\text{NO}_2]^2}{[\text{NO}]}$$

and of H

$$[\text{H}] = \frac{k_5}{k'_{12}} \frac{[\text{H}_2][\text{NO}_2]}{[\text{NO}]}$$

The substitution

$$k'_{12} = k_{12} [\text{M}]$$

has been made since the concentration of third body, primarily the carrier nitrogen, is approximately constant. Assuming the propagation reactions to be much faster than the termination reaction one finds that the overall rate

is now given by

$$\frac{d[\text{NO}_2]}{dt} = - \frac{k_5 k_6}{k'_{12}} \frac{[\text{H}_2][\text{NO}_2]^2}{[\text{NO}]}$$

While this particular rate expression does not give the proper concentration dependencies, as a limiting case, it does point out that a termination step involving elimination of an H atom, as by the formation of HNO, serves to reduce the reaction order with respect to  $\text{H}_2$ . This observation suggests that reaction R4(12) should be added to the mechanism of Rosser and Wise. In other respects, the results of the flow reactor experiments appear consistent with the mechanism proposed by the other investigators.

At the higher temperatures encountered in the flame experiment, the mechanism is quite different from that just proposed. The complete reduction of the nitrogen dioxide must be accounted for, in particular, the breaking of the NO bond. At these temperatures possible reactions are



Of these, the first, R4(16), is highly endothermic while the last, R4(18), is four-center and would have a poor steric factor. A likely candidate is reaction R4(17).

The nitrous oxide and oxygen would then be free to react with hydrogen. The formation of species such as HNO and HONO, while to be expected, does not aid in the breaking of the NO bond and therefore is not helpful in explaining the high temperature reaction of hydrogen and nitrogen dioxide.

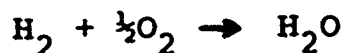
#### 4.2 HYDROGEN/OXYGEN

The kinetics of the hydrogen/oxygen reaction probably has been investigated more thoroughly and by more investigators than the kinetics of any other reaction. It is not intended that this section present an exhaustive review of this work or report on a thorough experimental investigation of this reaction. The intent, rather, is to provide experimental data which can be compared validly with similar data for the other reactions studied.

Two series of experiments were performed on the hydrogen/oxygen reaction. First, reaction rates were measured in four different reactor ducts, with a broad range of mixture ratios, and, second, reported in Section 4.4, the effect of the addition of nitric oxide was studied. Comparison of these results with work of other investigators is made and the relation of the hydrogen/oxygen reaction to the other hydrogen "reaction matrix" reactions is noted.

##### 4.2.1 Stoichiometry

The hydrogen/oxygen reaction proceeds in the reactor to completion as



R4 (19)

The measured heat of reaction at  $1000^{\circ}\text{K}$  of 59.3 (kcal/mole  $\text{H}_2$ ) is in good agreement with the heat of formation of water at this same temperature, -59.246 (kcal/mole) (11).

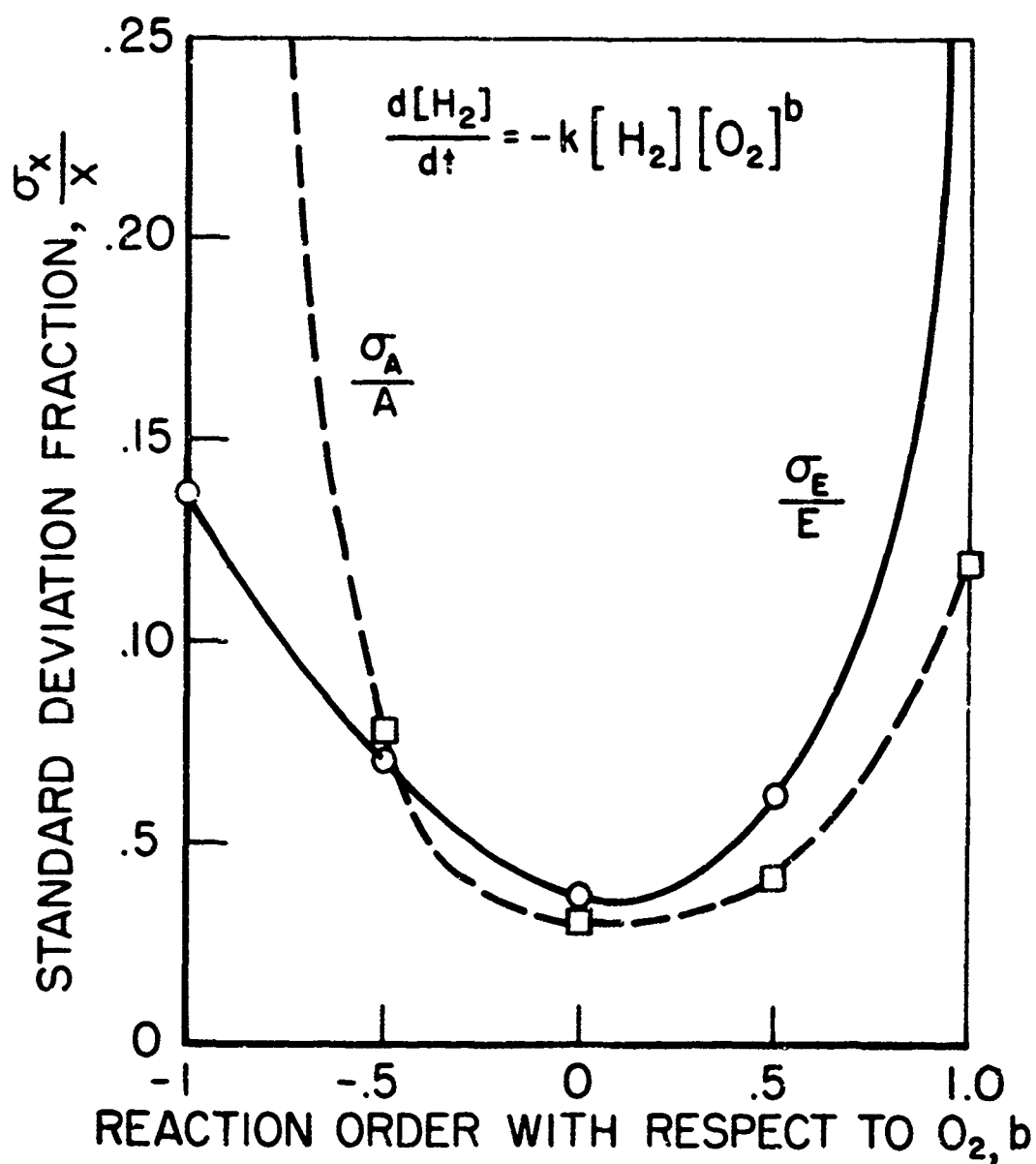
#### 4.2.2 Experimental results

Two general classes of compositions were studied, one with a nitrogen:hydrogen:oxygen mole ratio of approximately .98:.01:.01 and the other with the composition, expressed in the same terms of .79:.01:.20. These correspond to experiments where the carrier was nitrogen or air, respectively. The two cases are discussed separately.

##### 4.2.2.1 Nitrogen carrier (near stoichiometric composition)

From the experiments conducted with a large excess of oxygen, it is established that the hydrogen/oxygen reaction is first order with respect to hydrogen (see section 4.2.2.2). Using this first order dependency upon hydrogen, the experimental rates are analyzed statistically for a range of orders with respect to oxygen of from -1.0 to +1.0. These results, plotted in Figure (21), show approximately zero order dependency upon the oxygen concentration.

Reaction rates were measured in both the 2 and 4 (inch) diameter quartz ducts. The experimental rate constants for these two series of experiments are plotted in Figures (52) and (53). The corresponding Arrhenius parameters for the least squares fits to these data are summarized in Table (24). The 2 (inch) duct results represent only a small number of data points, however,



DETERMINATION OF REACTION ORDER FROM STATISTICAL CURVE FIT, HYDROGEN/OXYGEN, NITROGEN CARRIER

FIGURE 21

it is noted that the overall activation energies obtained in the two ducts are in good agreement and that there is a slight increase in the rate for the smaller duct. The representative experimental rate constant for the reaction of hydrogen and oxygen near stoichiometric conditions is selected to be that obtained in the larger duct, that is

$$\frac{d[A_2]}{dt} = -k[H_2]$$

$$k = 10^{10.96} \exp(-38200/RT) \quad [\text{sec}^{-1}]$$

#### 4.2.2.2 Air carrier (excess oxygen composition)

By measuring reaction rates with a large excess of oxygen, initial equivalence ratios in the range of  $.026 \leq \phi \leq .062$ , it is possible to establish the reaction order with respect to hydrogen. Since the local hydrogen concentration depends both upon the initial concentration and upon the extent to which the reaction has approached completion, a large concentration variation is obtainable. The change in the oxygen concentration under these conditions is less than 10 per cent thereby allowing expression of the reaction rate as

$$\frac{d[H_2]}{dt} = -k[H_2]^a$$

E4 (2)

that is, without expressed dependence upon the oxygen concentration. Now, defining the reduced rate,  $R'$ , and rewriting the above expression we obtain

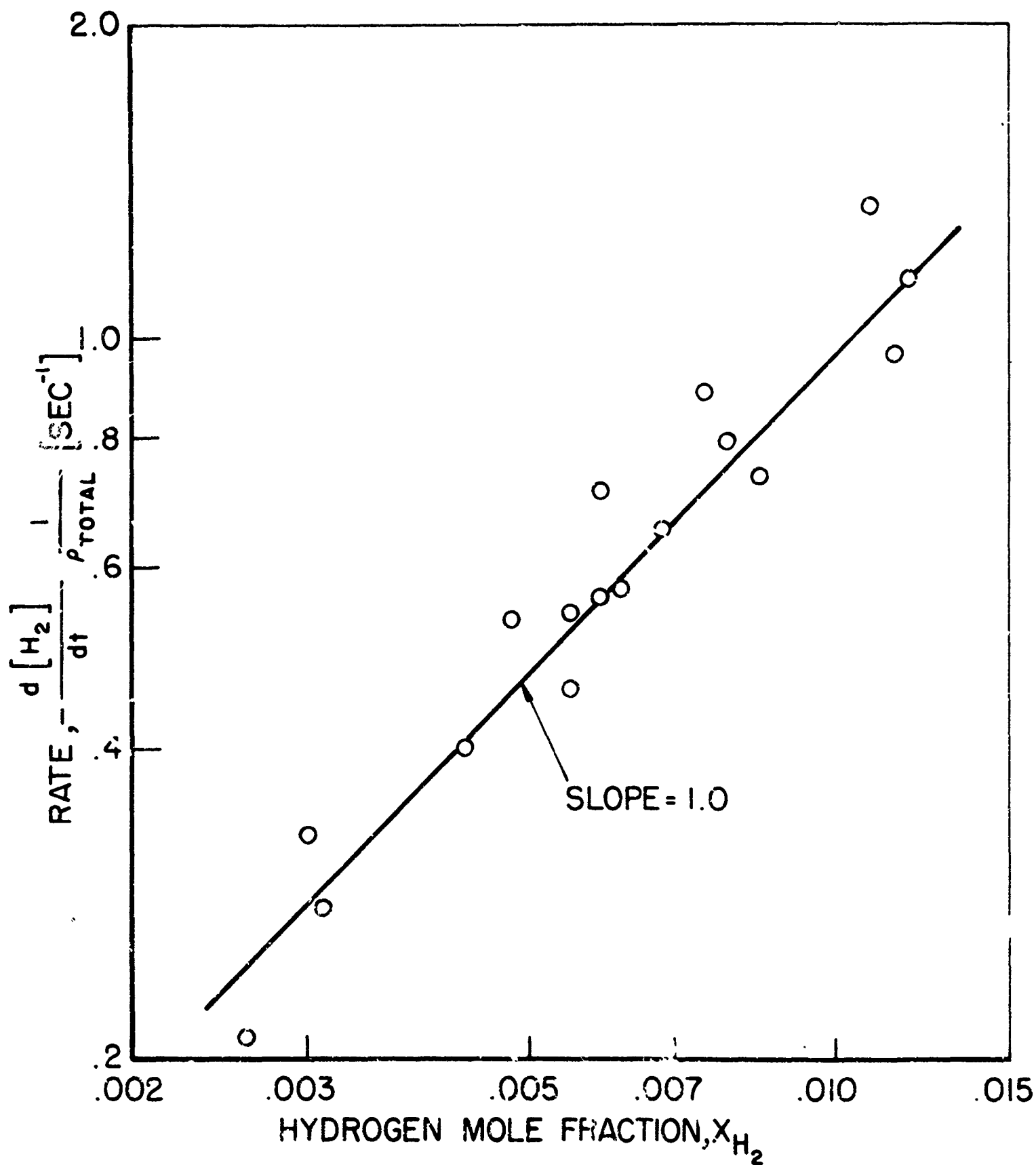
$$\begin{aligned}
 R' &= - \frac{d[H_2]}{dt} \frac{1}{P_{total}} \\
 &= k \frac{1}{P_{total}} P_{total}^a \left( \frac{[H_2]}{P_{total}} \right)^a \\
 &= (k P_{total}^{a-1}) x_{H_2}^a
 \end{aligned}
 \tag{E4 (3)}$$

By selecting rates at a fixed temperature and since the pressure throughout the reaction zone is constant, we see that the term in parentheses is a constant. The slope of a log-log plot of  $R'$  versus  $x_{H_2}$  therefore gives the reaction order,  $a$ . From such a plot, see Figure (22), the reaction is found to exhibit approximately first order dependence upon the hydrogen concentration, that is,  $a = 1.0$ .

Reaction rates were measured in quartz ducts with inside diameters of 2, 3, and 4 (inches) and in a stainless steel duct with an inside diameter of 3 3/8 (inches). The experimental rate constant data points for each of these four cases are plotted as a function of  $1/T$  in Figures (54), (55), (56), and (57) respectively. The corresponding Arrhenius parameters for the least squares fits to these data are summarized in Table (25).

While the overall activation energies,  $E$ , are seen to be in good agreement for all four ducts, +36.2, +39.8, +39.5, and +38.2 (kcal/mole), a consistent trend toward higher rates with decreasing duct diameters is noted. A comparison





HYDROGEN / OXYGEN REACTION RATES,  $T = 990^\circ K$ ,  
 DEPENDENCE ON HYDROGEN CONCENTRATION,  $[O_2] \gg [H_2]$

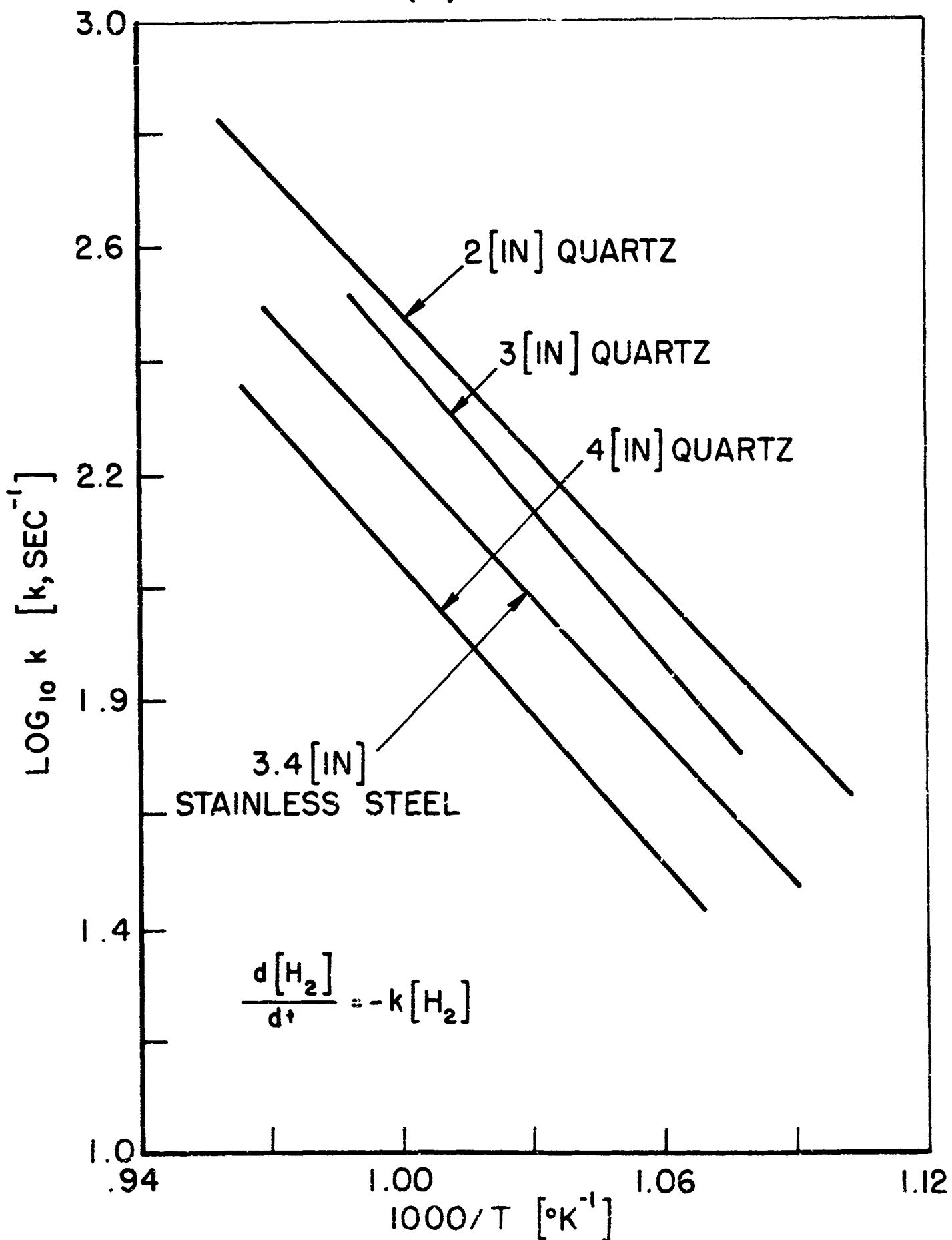
FIGURE 22

of the rates obtained in the different ducts is presented in Figure (23). This result is interpreted as a wall effect, in particular, one for which the wall serves as a positive catalyst for the reaction. The rates obtained with the stainless steel duct are in good agreement with those obtained in the quartz ducts--no wall material effect is noted.

Since rate data are available for several diameters, extrapolation to an infinite diameter, or zero wall effect can be made with some validity. Characterizing the wall effect simply by the surface to volume ratio, or, equivalently, in proportion to (diameter)<sup>-1</sup>, one may extrapolate the rate constant to the limit of 1/d = 0. The pre-exponential factors, A, adjusted for differences in activation energies, are plotted for the four ducts in Figure (24) as a function of 1/d. The magnitude of the wall effect, while definitely present, is not much greater than the uncertainties in A, expressed as plus and minus one standard deviation,  $\sigma_A$ . Extrapolation to infinite diameter gives a result close to that for the 4 (inch) duct. The rate constant measured with the four inch quartz duct is chosen as being representative of the hydrogen, oxygen reaction rate with a large excess of oxygen, that is,

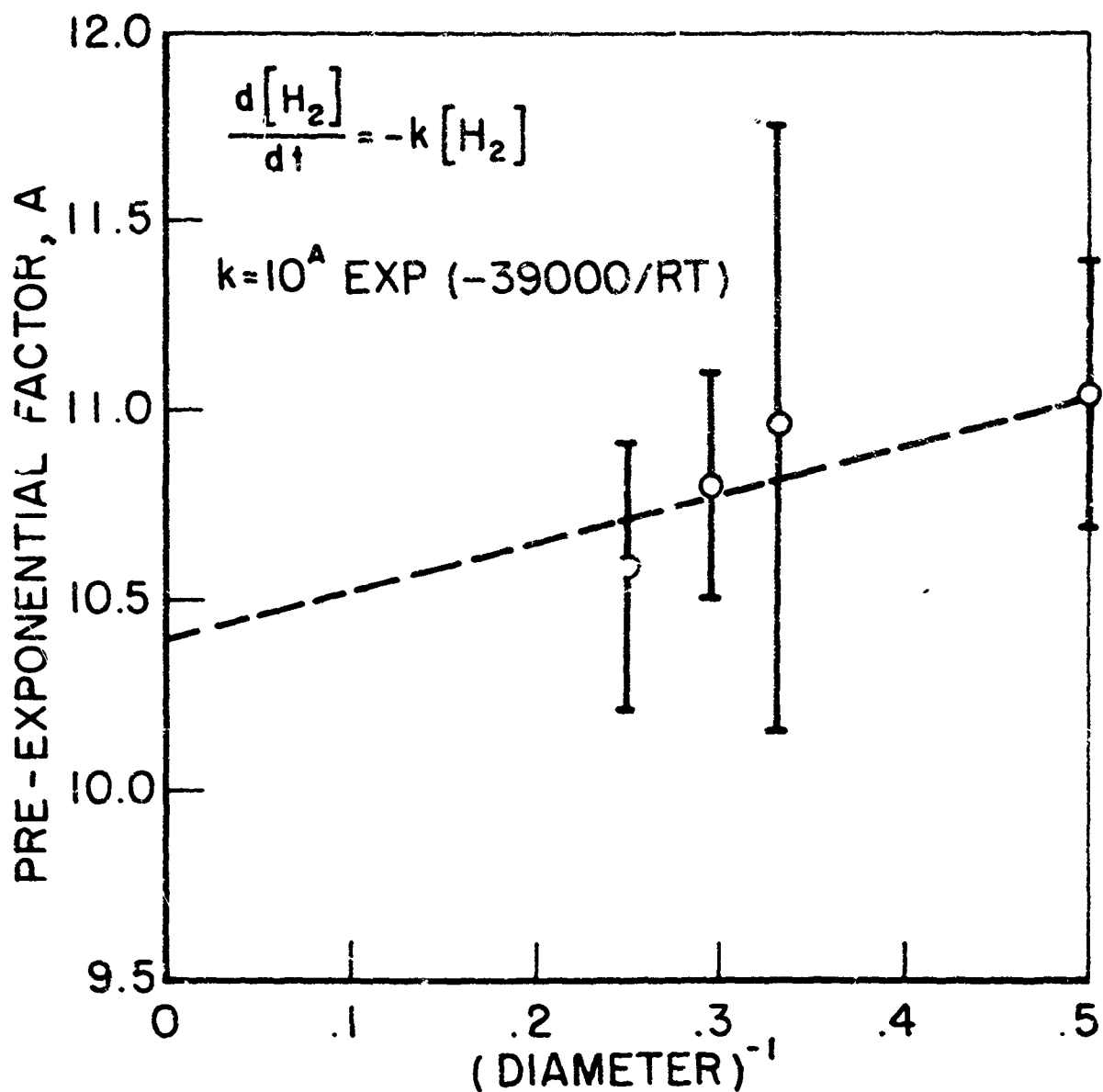
$$\frac{d[H_2]}{dt} = -k[H_2]$$

$$k = 10^{10.71} \exp(-39500/RT) \quad [\text{sec}^{-1}]$$



EFFECT OF DUCT DIAMETER ON REACTION RATE,  
HYDROGEN/OXYGEN, AIR CARRIER

FIGURE 23



EXTRAPOLATION OF HYDROGEN/OXYGEN RATE  
CONSTANT TO INFINITE DIAMETER DUCT, AIR CARRIER

#### 4.2.2.3 Comparison of nitrogen carrier and air carrier results

The overall activation energies for all cases are found to be in good agreement. The rates, however, are larger with nitrogen as a carrier, or, equivalently oxygen as a diluent is found to slow the reaction. That oxygen is not observed to depress the reaction rate when nitrogen is used as the carrier may be attributed to the limited range of oxygen concentrations which were studied (compared to the factor of 20 increase in oxygen concentration obtained by using air as the carrier). To bring the cases into agreement requires a reaction order dependency upon oxygen of  $b = -0.4$ .

The wall is noted to act as a positive catalysis to the overall combustion reaction in both cases. The catalytic is larger when air is used as the carrier.

#### 4.2.3 Wall effect

That the wall should act as a positive catalyst is contrary to observations made at lower temperatures and pressures by other investigators, particularly Lewis and von Elbe (74) who conclude that chain breaking occurs at the wall. They do find that the chain breaking efficiency of quartz is low. Swigart (53), who studied the same reaction in stainless steel ducts, observed similar catalytic wall effects. Benson (73) argues that the formation of H atoms at the wall is an important reaction. In particular, he suggests that "active sites on the walls are covered with  $O_2$  and that  $H_2$  can react with them.....and liberate an H atom into the gas phase." Such a mechanism explains not only the observed catalytic wall effect but additionally the observation that the wall effect is stronger

for the case in which a large excess of oxygen is present. The present experimental results would equally as well support a mechanism such as oxygen dissociation at the wall.

#### 4.2.4 Results of other investigators

In the extensive study of the kinetics of the hydrogen/oxygen reaction, most of the earlier investigators were concerned with detonation limits including the effects of wall coatings, inert diluents, and additives. Minkoff and Tipper (75) present a good review of this work through about 1960. More recently, investigations have centered on a study of induction times, particularly at high temperatures, and upon related free radical reactions.

Comparison of the present investigation with the results of experimenters who have studied induction times is necessarily difficult. While the reactants are the same, the phenomena observed are essentially different. Most of the induction time experiments have been conducted in shock tubes or related devices and the initiation reaction followed by the onset of a free radical build-up (generally OH) or the beginning of a pressure or density change. The adiabatic flow reactor has proved unsuitable to direct measurement of induction times for the hydrogen/oxygen reaction. Small changes in experimental parameters related to the hydrogen injection, primarily the nitrogen dilution but also the carrier flow rate and temperature, produce large variations in the observed induction times. As suggested by Swigart (53), these variations are probably attributable to heterogeneous

reactions occurring in the injection region. The overall reaction rates which can be measured independent of the nature of the induction process, characterize the overall or global hydrogen/oxygen reaction in a regime where the presence of reaction products, primarily water, must be considered to affect the reaction. This situation is recognized to be basically different from the induction time experiments in which the presence of products is negligible. It is felt, none-the-less, to be worthwhile to compare the present results and "induction time" results by the technique of calculating the induction time from the measured global rates. While no particular correlation with the buildup of OH radicals would be expected, some similarity would be hoped for with induction experiments in which a later phenomenon was observed, for example, the pressure rise.

The relation between reaction times and reaction rates is discussed in Appendix B. In particular, the error introduced by failing to account for temperature rise in experiments based on the measurement of reaction time is considered.

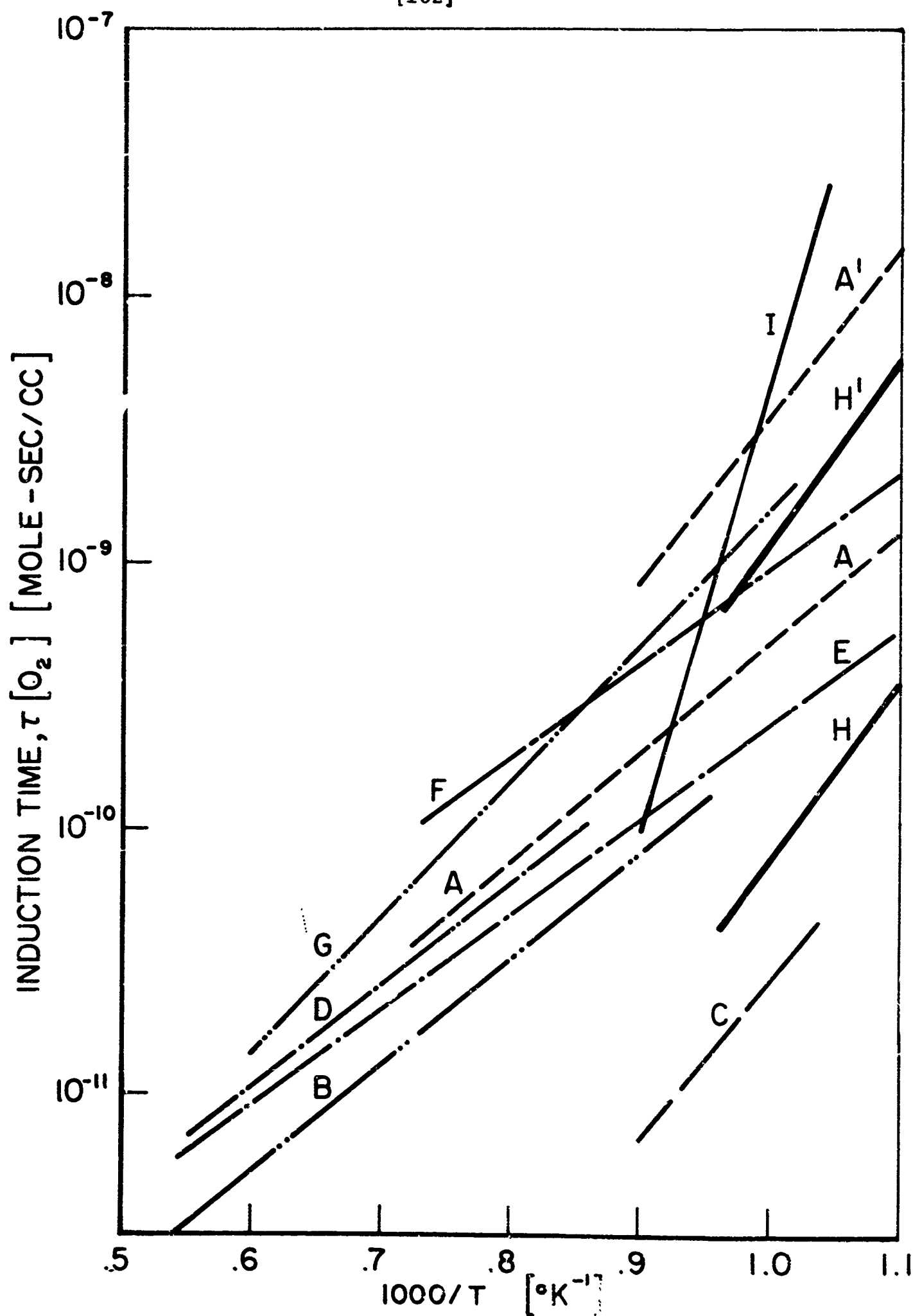
Several additional experimental investigations of hydrogen/oxygen induction times have been reported since the reviews of Patch (76) and of Nicholls, Adamson, and Morrison (77). The results of a number of these investigations are compared in Figure (25) and the nature of the experiments outlined below.

<u>curve</u>	<u>experimenters</u>	<u>description of experiment</u>
A	Miyama and Takeyama (78)	shock tube, OH absorption

A'	Miyama and Takeyama (78)	shock tube, pressure rise $.25 \leq \phi \leq 1.0$ , 70- 90% argon
B	Shott and Kinsey (79)	shock tube, OH absorption $.12 \leq \phi \leq 2.5$ , 83- 99.6% argon
C	Rhodes and Chriss (80)	supersonic wind tunnel
D	Ruegg and Dorsey (81)	ballistic range, schlieren $\phi = 1.0$ , 56% nitrogen (air)
E	Strehlow and Cohen (82)	shock tube, schlieren $\phi = 1.0$ , 25-34% argon
F	Fujimoto (83)	shock tube, OH emission
G	Mullaney, Ku, Botch (84,85)	shock tunnel, schlieren $\phi = 1.0$ , 56% nitrogen (air) or 57% argon
H	present investigation	adiabatic flow reactor temperature rise, $\phi \approx 1.0$
H'	present investigation	$\phi \approx .04$
I	Skinner and Ringrose (86)	shock tube, OH emission $\phi = 2.0$ , 90% argon

Induction times based on 10 per cent reaction as calculated from the rates obtained in the present investigation are also presented in Figure 25. As pointed out by Mullaney, Ku, and Botch (84), the use of the oxygen concentration in correlation of induction times is useful only for





COMPARISON OF EXPERIMENTAL INDUCTION TIMES  
FOR HYDROGEN/OXYGEN

FIGURE 25

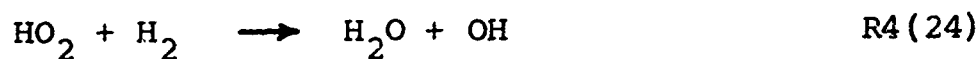
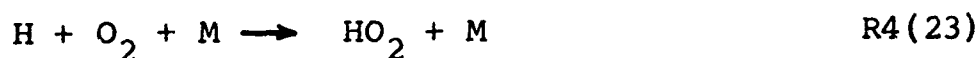
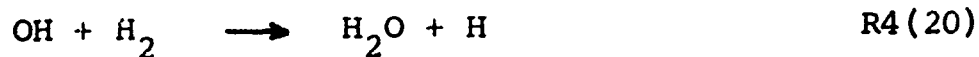
purposes of comparison, except in the case of hydrogen rich mixtures,  $\phi \gg 1$ . Miyama and Takeyama (78) found induction time dependence upon the hydrogen concentration in agreement with the present observations, at temperatures less than  $1100^\circ\text{K}$ . The same investigators also found that the activation energy was higher for the induction time as measured by the pressure rise than as measured by the OH concentration, 29 [kcal/mole] versus 19 [kcal/mole]. In comparing the present results to those of other experimenters, one notes that the calculated induction times are of the right order of magnitude but that the activation energies are higher than those found in most of the induction time experiments. From the second observation one would conclude that the observed overall reaction rate is not controlled by the formation of OH radicals as is the induction time.

Norrish and Porter (87) from explosion studies, conclude that while hydrogen accelerates the reaction, oxygen in excess has an effect similar to an inert gas, it decreases the rate. This would appear to be consistent with the present observation of a weak rate dependence, probably slightly negative, upon the oxygen concentration. Swigart (53) reports a  $-\frac{1}{2}$  power dependence of the reaction rate upon the oxygen concentration but no such effect is noted in the present experiments.

#### 4.2.5 Reaction mechanism

The reaction mechanism of Willbourn and Hinshelwood (88) has been adopted with slight modification by most subsequent investigators of the hydrogen/oxygen reaction. They propose the following steps which are shown to explain the three explosion limits of hydrogen/oxygen.

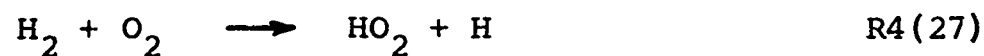
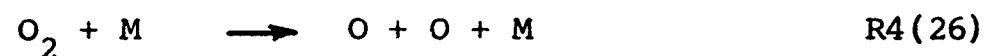
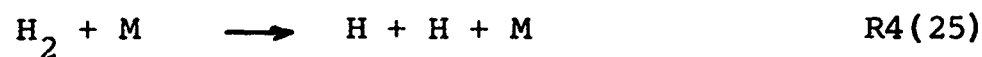
JP13-4045-65



The formation of hydrogen peroxide provides a reaction which is preferable to R4(24).



The mechanism is noted to be highly branched. Possible initiation reactions would include



Reaction R4(26) is the most endothermic of the above and therefore probably the least important. In the present investigation, as argued in Section 4.2.3, the heterogeneous reactions



are likely to be important.

The reaction mechanisms generally proposed for the supersonic combustion of hydrogen and air differ from the above scheme in several respects. The first three propagation and branching reactions above, R4(20), R4(21), and R4(22) are postulated also to be important reactions in the supersonic combustion problem. Hydroperoxide, as appears in Reactions R4(23) and R4(24), is not considered to play an important role. Finally, termination reactions involving the following free radical recombinations usually are invoked. See, for example, Reference (89).

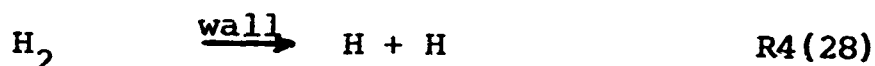


That excess oxygen slows the reaction was observed also by Swigart (53). Lewis and von Elbe (74) state, however, that "kinetically the effect of oxygen is essentially that of diluent." This observation must be rejected on the basis of the present experiments. That the addition of oxygen does not accelerate the reaction indicates that the initiation reactions R4(26) and R4(27) are not rate controlling. The effect of  $\text{O}_2$  in slowing the reaction is consistent with the behavior predicted by the termination reaction R4(23). The similarity of the vibrational frequency of oxygen ( $1555 \text{ cm}^{-1}$ ) and the bending mode frequency of water ( $1595 \text{ cm}^{-1}$ ) has been observed to produce a highly efficient resonant exchange of energy (90). Dixon-Lewis and Williams (91) have speculated that oxygen in oxygen rich flames may cause apparent catalysis of radical recombination (which is interpreted to mean that excess oxygen will slow the reaction).

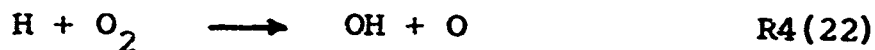
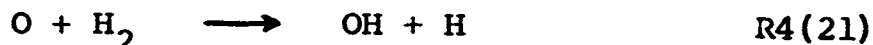
Skinner and Ringrose (86) recently have reported the results of shock tube experiments at the same temperatures as the present investigation. They report induction times which are much longer and apparent activation energies which are much larger than those expected from experiments at higher temperatures. They attribute these observations to the role of  $\text{HO}_2$  radicals in slowing the reaction and demonstrate the agreement of their experimental results with a proposed reaction mechanism (similar to that above) through numerical integration of the rate equations.

In summary, the important steps in the hydrogen/oxygen reaction kinetics, as pertinent to the present investigation, are suggested to be the following.

#### initiation

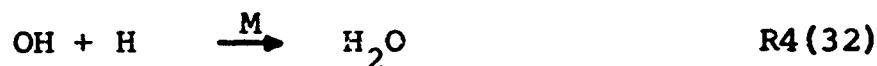


#### branching



#### propagation



termination4.3 HYDROGEN/NITRIC OXIDE-OXYGEN

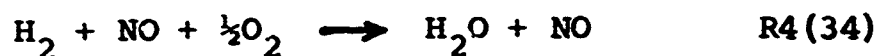
A reaction of particular interest is that of hydrogen with decomposed nitrogen dioxide. As discussed in Section 2.2.4, nitrogen dioxide decomposes to nitric oxide and oxygen according to the stoichiometry



Such a mixture can be obtained conveniently in the reactor by injecting nitrogen dioxide into the nitrogen carrier upstream of the pebble-bed heat exchangers. A second method is to inject both nitric oxide and oxygen. Both techniques were used but the second is presented as a special case of the study of the effect of the addition of nitric oxide on the hydrogen/oxygen reaction and is discussed in Section 4.5.

4.3.1 Stoichiometry

The reaction is concluded to involve only the oxygen without the consumption or decomposition of the nitric oxide.



The evidence for this conclusion is based on the results of the study of the effect of nitric oxide on the hydrogen/oxygen reaction (Section 4.5) and comes primarily from the observation that the heat release is unaltered by addition of NO, even when excess  $H_2$  is present.

#### 4.3.2 Experimental results

All reaction rate measurements were made in the 2 [inch] quartz duct with nitrogen carrier. Equivalence ratios of  $.44 \leq \phi \leq .64$ , or, equivalently, reaction ratios of  $.88 \leq \lambda \leq 1.29$  were studied. These mixtures correspond to small variations about the stoichiometry expressed in R4(34). No attempt was made to make an independent determination of reaction orders with this particular reactant combination, rather, a rate dependence similar to that used to correlate the hydrogen/nitrogen dioxide reaction rates was used arbitrarily. The rate equation used is

$$\frac{d[H_2]}{dt} = -k[H_2]^{1.4}[O_2]^{1.0}[NO]^{-1.0}$$

for which the rate constant was found to be

$$k = 10^{25.71} \exp(-98300/RT) \quad [(\text{mole/cc})^{-.4} \text{sec}^{-1}]$$

For comparison with the hydrogen/oxygen reaction the rate dependence used and rate constant determined were,

$$\frac{d[H_2]}{dt} = -k[H_2]$$

$$k = 10^{16.47} \exp(-68600/RT) \quad [\text{sec}^{-1}]$$

The Arrhenius parameters for this reaction are summarized in Table (26) and the experimental rate constants are plotted in Figure 58. No chemical significance is to be attached to the "activation energies" reported above. The reaction rate equations were selected arbitrarily to allow comparison of the rate constants with the rate constants of the related hydrogen reactions. The "activation energies" in this case are no more than curve-fit constants.

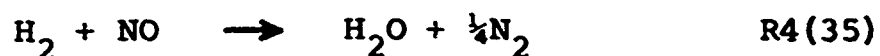
#### 4.3.3 Results of other investigators and reaction mechanism

While the effect of nitric oxide on the reaction of hydrogen has been studied by other investigators, the writer is aware of no experiments involving NO concentrations which are as high as the NO concentration corresponding to decomposed nitrogen dioxide. The reaction mechanism is discussed in Section 4.5.

#### 4.4 HYDROGEN/NITRIC OXIDE

Attempts to establish a measurable reaction between hydrogen and nitric oxide in either the 2 or 4 [inch] quartz duct with nitrogen carrier were not successful at temperatures of up to 1170°K. A range of hydrogen to nitric oxide ratios,  $.2 \leq \phi \leq 3.0$ , with hydrogen concentrations of up to  $4 \times 10^7$  [moles/cc] was used.

Wolfhard and Parker have studied premixed hydrogen/nitric oxide flames (71). Experimental flame temperatures were measured to be 2820°C, indicating that at high temperatures, the reaction proceeds as





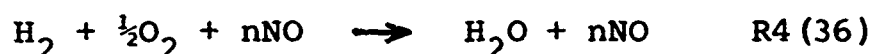
They conclude that the reaction of nitric oxide requires either the presence of radicals such as  $\text{NH}$  or  $\text{NH}_2$  or the thermal decomposition of the nitric oxide and state that the process will occur only at temperatures approaching about  $2800^\circ\text{C}$ . Neither of these conditions were met in the present experiment. If hydrogen atoms were present, as from the catalytic decomposition of hydrogen at the walls, the formation of  $\text{HNO}$  apparently does not provide a route for the reaction of hydrogen and nitric oxide. It is important to note the strong resistance nitric oxide shows to reduction at temperatures below its dissociation temperature. Even the presence of such radicals as  $\text{H}$ ,  $\text{OH}$ , and  $\text{O}$  and the likely formation of such species as  $\text{HNO}$ ,  $\text{HONO}$ , and  $\text{ONO}$  does not result in the breaking of the  $\text{NO}$  bond.

#### 4.5 THE EFFECT OF NITRIC OXIDE ON THE HYDROGEN/OXYGEN REACTION

As may be noted from the results reported in the first three sections of this chapter, the oxidations of hydrogen by  $\text{NO}_2$ ,  $\text{O}_2$ , and  $\text{NO} + \frac{1}{2}\text{O}_2$  are similar in that essentially all of the hydrogen is oxidized to water, but distinctively different in terms of the rate at which this oxidation takes place. A large concentration of nitric oxide is found to be an inhibitor to the oxidation of hydrogen by both nitrogen dioxide and by oxygen. Additional information on this effect was obtained by measuring the reaction rate of hydrogen/oxygen with varying amounts of nitric oxide added.

#### 4.5.1 Stoichiometry

The controlling stoichiometry of the hydrogen/oxygen reaction appears to be unchanged by the presence of NO. That the nitric oxide is neither consumed nor decomposed to any great extent is evidenced by the failure of the addition of nitric oxide to produce any change in the energy release. This effect was noted to be true for all hydrogen/oxygen mixture ratios, that is, for  $\phi \geq 1$ . That no reaction between nitric oxide and hydrogen alone is obtainable and that nitrogen dioxide is reduced by hydrogen only to nitric oxide is further evidence that nitric oxide is not consumed. Any decomposition of nitric oxide would be evidenced by a heat release of 21.6 [kcal/mole] which is neither observed nor expected at these temperatures. Nitric oxide is detected in the infrared absorption spectra of the products of both the reaction of  $H_2/NO_2$  and of  $H_2/NO + \frac{1}{2}O_2$ . The hydrogen/oxygen reaction in the presence of nitric oxide then has the overall behavior



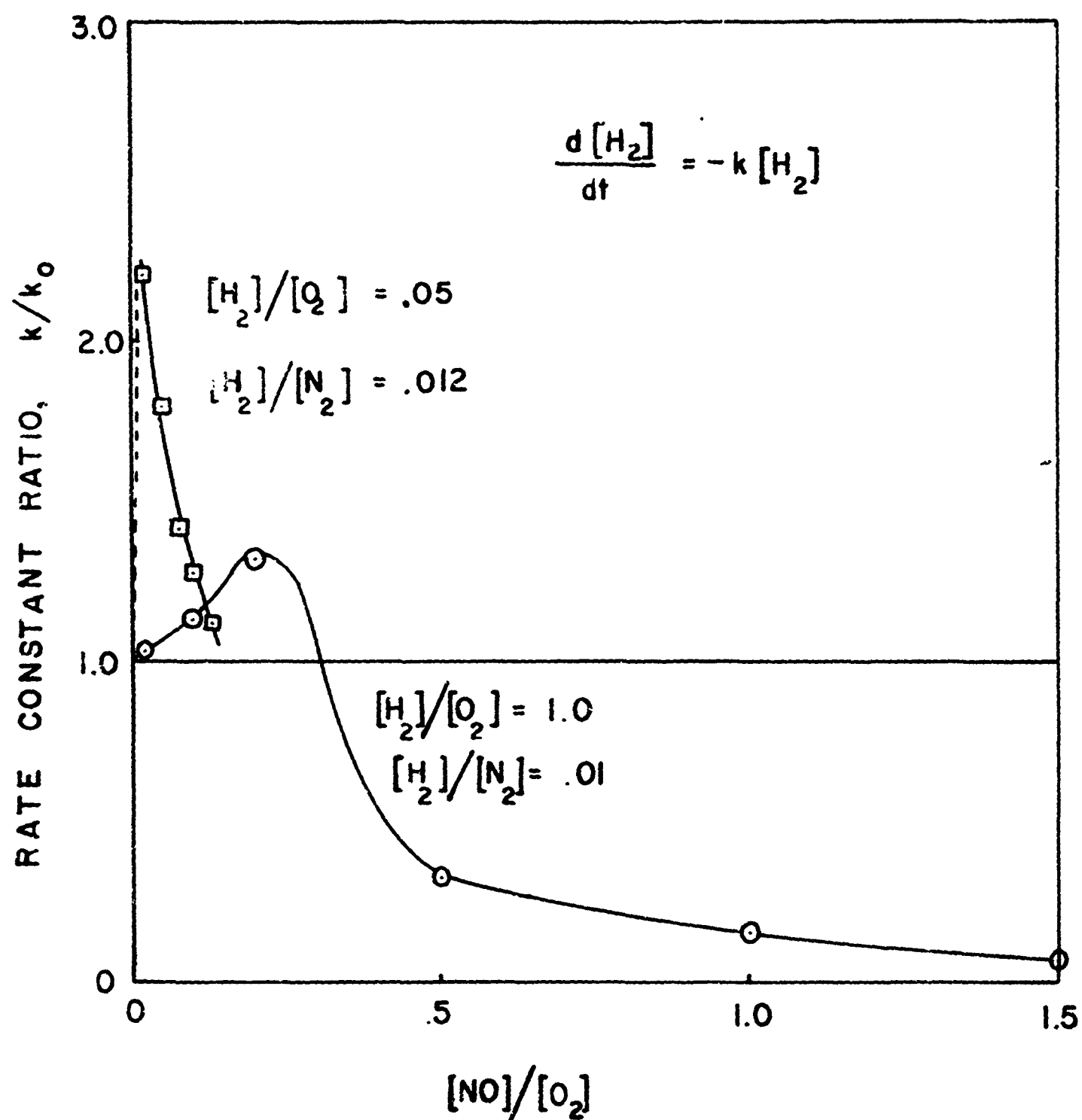
#### 4.5.2 Experimental results

A series of experiments were made in the 4 [inch] quartz duct with two general reactant compositions similar to those described in the section on the hydrogen/oxygen, that is, corresponding to nitrogen carrier and to air carrier. Approximate mole fractions for these two cases are indicated below.

	N <sub>2</sub>	H <sub>2</sub>	O <sub>2</sub>	NO
N <sub>2</sub> carrier	.98	.01	.01	0 to .015
air carrier	.79	.01	.20	0 to .01

The results for the two cases are different. In both cases the addition of small quantities of nitric oxide accelerates the hydrogen/oxygen reaction. The addition of large quantities slows the reaction. For purposes of comparison, all rates are determined on the basis of a simple first order dependency on the hydrogen only. It is recognized that a better correlation of experimental data is obtained, when large quantities of NO are added, with the more complex dependency used in Sections 4.1 and 4.3 .

The effect of nitric oxide addition for the two cases of  $[H_2]/[O_2] = 1$  and  $[H_2]/[O_2] = .05$  are compared at a temperature of 950°K in Figure 26. Increases in the reaction rate by a factor of about 1.3 are obtained in the first case and by greater than 2.0 in the second case. As seen in Figure 27, the addition of small amounts of nitric oxide produces only an increase in the rate while the addition of large amounts produces both a decrease in the rate and a change in the overall activation energy. The magnitude of the inhibition effect of nitric oxide is found to be approximately proportional to the NO concentration. The special case of  $[NO]/[O_2] = 2$ , corresponding to the dissociation of nitrogen dioxide, is consistent with the trend shown in these results.



EFFECT OF NITRIC OXIDE ON THE HYDROGEN  
OXYGEN REACTION RATE,  $T = 950^\circ K$ ,  $P = 1$  (atm),  
 $[H_2] = 1.3 \times 10^{-7}$  (mole/cc)

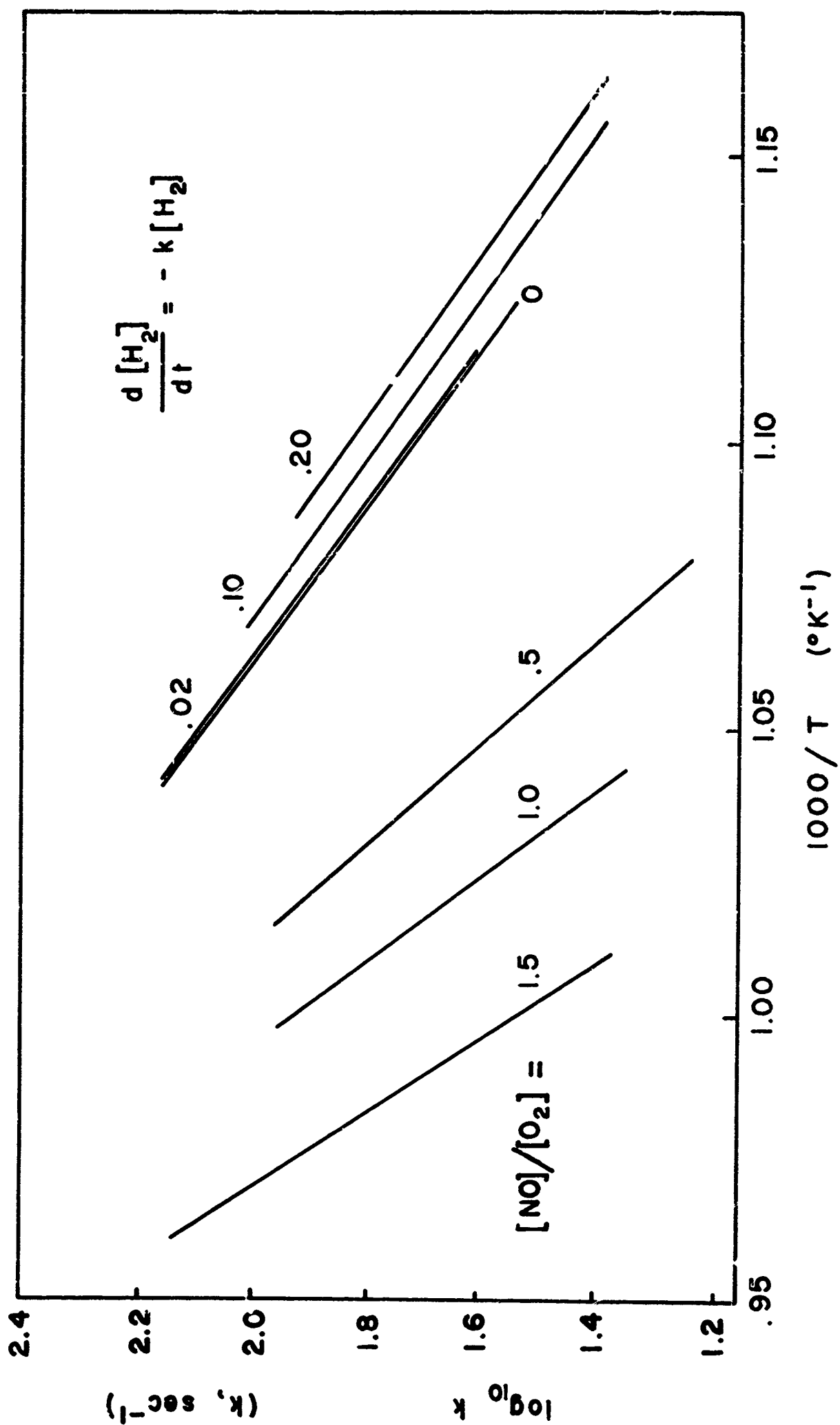


FIGURE 27

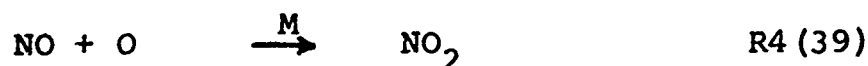
REACTION RATE CONSTANTS FOR  $H_2/O_2 + NO$ ,  $P = 1 \text{ (atm)}$ ,  
 $[H_2]/[O_2] = 1$ ,  $[H_2]/[N_2] = .01$

#### 4.5.3 Results of other investigators

Ashmore (92,93) studied the sensitizing effect of small amounts of NO on the hydrogen/oxygen reaction in terms of ignition limits. He found that the sensitizing limits were the same whether NO, NOCl, or NO<sub>2</sub> was used and interpreted the widely different induction periods associated with these three sensitizers to correspond to the different times for the additives to decompose to yield nitric oxide. Crist and Wertz (94) concluded from an earlier investigation that the sensitization of the hydrogen/oxygen reaction by nitrogen dioxide was due to NO<sub>3</sub> rather than NO. Recently, Skinner (95), in shock tube studies, has observed qualitatively an acceleration of the hydrogen/oxygen reaction by the addition of small amounts of NO. The author is not aware of any other investigation of the effect of large amounts of nitric oxide on the hydrogen/oxygen reaction.

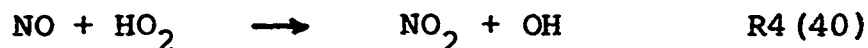
#### 4.5.4 Reaction mechanism

The primary behavior which any proposed reaction mechanism should predict is the quenching effect of NO at large concentrations and the accelerating effect at small concentrations. The former is the easiest to postulate. The effect is, no doubt, to remove free radicals, in particular, those important to the hydrogen/oxygen reaction, H, OH, and O. Nitric oxide long has been recognized as an inhibitor of reactions involving free radicals, see, for example, Lewis and von Elbe (74) or Trotman-Dickenson (96). The following termination reactions involving NO can account for the observed inhibition.

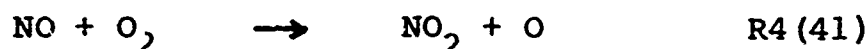


The first reaction, the formation of nitrous acid, is the most plausible. The possibility of the second reaction acting as an important quenching reaction has received little attention in the literature, but, none-the-less, seems reasonable, especially in light of the detection of HNO in the nitrogen dioxide rich hydrogen/nitrogen dioxide flame. This reaction is only slightly more exothermic than the first, 51.6 versus 49.8 [kcal/mole]. Clement and Ramsay (97) report the H-NO bond energy to be 48.6 [kcal/mole] which allows classification of nitroxyl as a relatively stable molecule, similar to hydroperoxyl. Reaction R4(38) is reported also by Ashmore and Tyler (98).

The function of NO in sensitizing the hydrogen/oxygen reaction is difficult to establish. Ashmore and Tyler (98) have suggested that NO can convert the  $\text{HO}_2$  to the more active specie, OH.

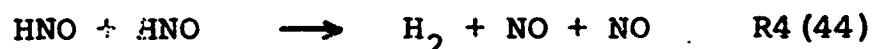
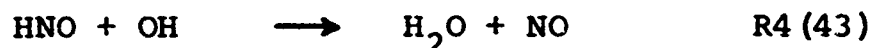
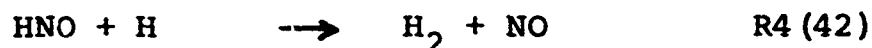


Another possibility is for NO to introduce O atoms by the reaction



Both reactions, as well as the observation of Wise and French (51) that oxygen accelerates the decomposition of NO, are in agreement with greater sensitization with large oxygen concentrations. The first reaction, R4(40), is exothermic in the amount of 17 [kcal]; the second, R4(41) is endothermic in the amount of 46 [kcal]. Reaction R4(40) therefore is favored.

Both the suggested NO quenching and accelerating reactions appear to be first order in NO, which would fail to account for the observed change in the function of NO from a catalyst to an inhibitor as its concentration is increased. To agree with the observation, the order of NO as an inhibitor should be greater than as a catalyst. This might arise through a secondary reaction, such as the consumption of the unstable HNO molecule, with might occur as



Reaction R4(44) would give the quenching reaction an apparent higher order dependence on the NO concentration.

#### 4.6 COMPARISON OF HYDROGEN REACTIONS

The hydrogen reactions studied are ordered in terms of their reaction rates in the following table.



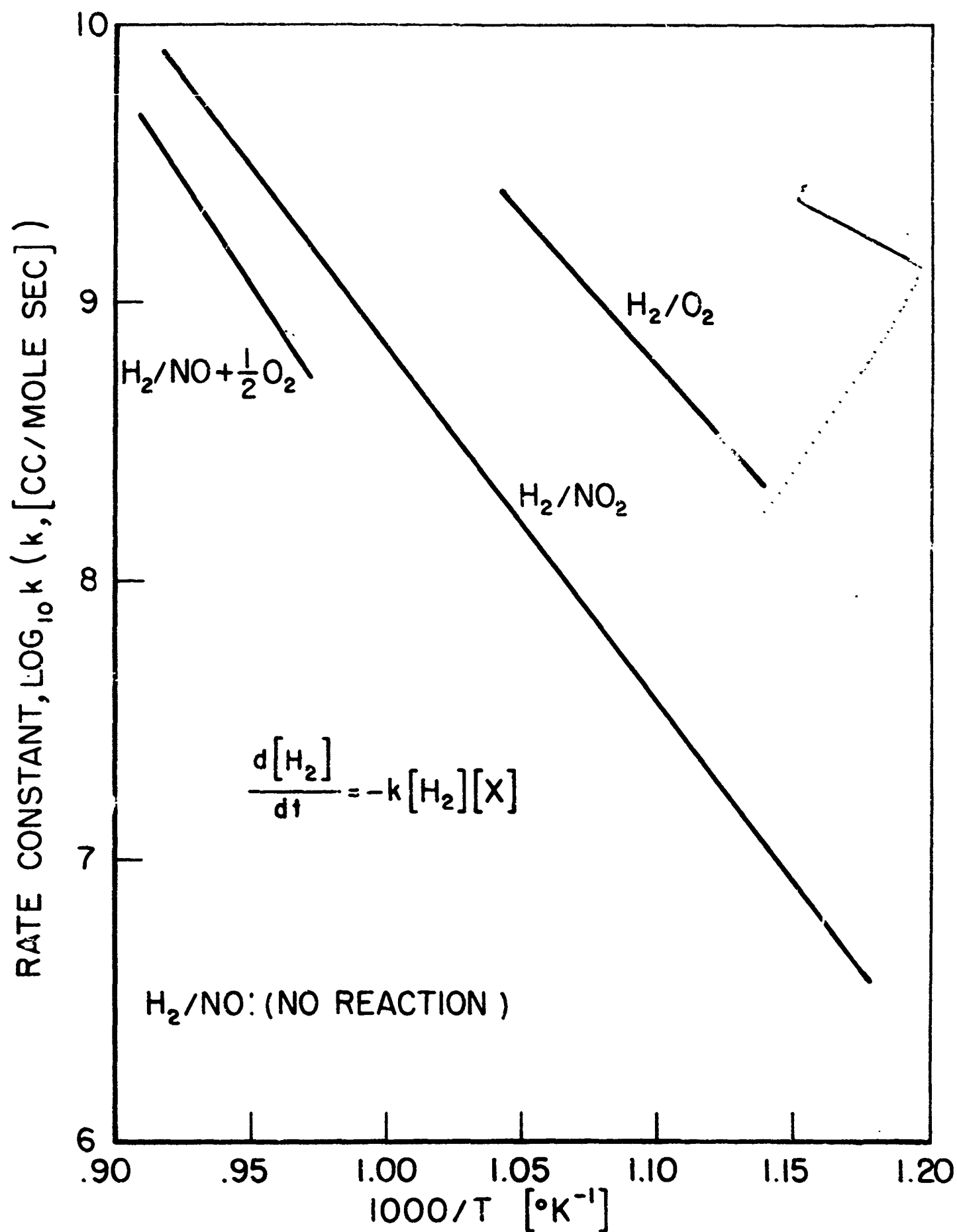
TABLE 8. Relative reaction rates, hydrogen reactions at 1000°K

oxidizer	relative rate
O <sub>2</sub>	40
NO <sub>2</sub>	3
NO + ½O <sub>2</sub>	1
NO	no reaction

In other terms, the hydrogen/oxygen reaction is found to proceed about 14 times faster than the hydrogen/nitrogen dioxide reaction. The hydrogen/nitrogen dioxide reaction is found to be about 3 times as fast as the reaction of hydrogen with a 2:1 mixture of nitric oxide to oxygen. No reaction is obtained between hydrogen and nitric oxide.

In another form, the measured reaction rates are compared in Figure 28. Since the reactions are found to follow different orders with respect to hydrogen and the oxidizer, to compare the rates it is necessary to impose an artificial, common rate constant dependency. A first order dependency on both the hydrogen and appropriate oxidizer is used. That is, rate constants are calculated on the basis of the rate equation,

$$\frac{d[H_2]}{dt} = -k[H_2][X]$$



COMPARISON OF HYDROGEN REACTION RATES,  
NITROGEN CARRIER

FIGURE 28

[X] refers to the concentration of  $O_2$ ,  $NO_2$ , or, in the case of the mixture of  $NO + \frac{1}{2}O_2$ , to  $O_2$ .

The most important steps of the reaction mechanism are compared in Table 9. The explanation of the great difference between the hydrogen reaction rate with oxygen and with nitrogen dioxide is due to the basic character of the reaction mechanisms: the hydrogen/oxygen reaction proceeds by a chain branching mechanism while the hydrogen/nitrogen dioxide reaction proceeds by a chain propagating mechanism. From the experimental results, it is to be concluded that, in the case corresponding to dissociated nitrogen dioxide, the nitric oxide destroys the chain branching character of the hydrogen/oxygen reaction through efficient destruction of OH and H radicals. These same effects are reflected in the higher overall activation energy of the slower reacting combinations. That the  $H_2/NO + \frac{1}{2}O_2$  reaction is even slower than the  $H_2/NO_2$  reaction probably is due to the larger concentration of NO in the former case. The  $H_2/NO$  reaction, which is not observed, depends on the breaking of the NO bond which does not occur at the experimental temperatures (except in the presence of certain radicals, as discussed later).

TABLE 9. Summary of reaction mechanisms, hydrogen reactions.

	$H_2/O_2$	$H_2/NO_2$	$H_2/NO + \frac{1}{2}O_2$
initiation	$H_2 \xrightarrow{\text{wall}} H + H$ $H_2 + O_2 \rightarrow HO_2 + H$	$H_2 + NO_2 \rightarrow H + HONO$	$I_2 \xrightarrow{\text{wall}} H + H$ $H_2 + O_2 \rightarrow HO_2 + H$ $NO + O_2 \rightarrow NO_2 + O$
branching	$O + H_2 \rightarrow OH + H$ $H + O_2 \rightarrow OH + O$		$O + H_2 \rightarrow OH + H$ $H + O_2 \rightarrow OH + O$
propagation	$OH + H_2 \rightarrow H_2O + H$ $HO_2 + H_2 \rightarrow H_2O_2 + H$	$OH + H_2 \rightarrow H_2O + H$ $H + NO_2 \rightarrow NO + OH$	$OH + H_2 \rightarrow H_2O + H$ $HO_2 + NO \rightarrow NO_2 + OH$ $HO_2 + H_2 \rightarrow H_2O + OH$
termination	$H + O_2 \xrightarrow{M} HO_2$ $OH + H \xrightarrow{M} H_2O$	$OH + NO \rightarrow HONO$ $OH + NO_2 \xrightarrow{M} HONO_2$ $NO + H \xrightarrow{M} HNO$	$NO + OH \rightarrow HONO$ $NO + H \xrightarrow{M} HNO$

## CHAPTER 5

AMMONIA REACTIONS

The second hydrazine decomposition product to be discussed is ammonia. If hydrazine decomposition to hydrogen, ammonia, and nitrogen precedes oxidation, then the reactions of ammonia become important, especially since three times as much hydrogen appears bound in ammonia as appears in molecular hydrogen. Of the fuels studied, ammonia was the least reactive, and required high temperatures to obtain ignition and measurable reaction rates. Thermodynamic equilibrium favors the decomposition of ammonia to nitrogen and hydrogen at the temperatures of the present investigations. The ammonia decomposition rate, however, is much slower than its reaction rate and, therefore, ammonia decomposition is not of concern in the present experiments.

5.1 AMMONIA/NITROGEN DIOXIDE

Ammonia and nitrogen dioxide react readily at room temperature to form ammonium nitrate, nitrogen, and water, according to the stoichiometry, reported by Falk and Pease (99)



This reaction prevented the obtaining of a premixed gas flame, as was used in the study of the hydrogen/nitrogen dioxide reaction. The products of this low temperature reaction plugged the burner shortly following the observation of an apparent flame.

### 5.1.1 Stoichiometry

At higher temperatures, that is those of the present investigations, the reaction involves the complete oxidation of the ammonia to water but the reduction of the nitrogen dioxide only to nitric oxide. The heat of reaction is measured to be 52 [kcal/mole  $\text{NH}_3$ ] which is to be compared to the theoretical value of 55 [kcal/mole  $\text{NH}_3$ ] for the following stoichiometry



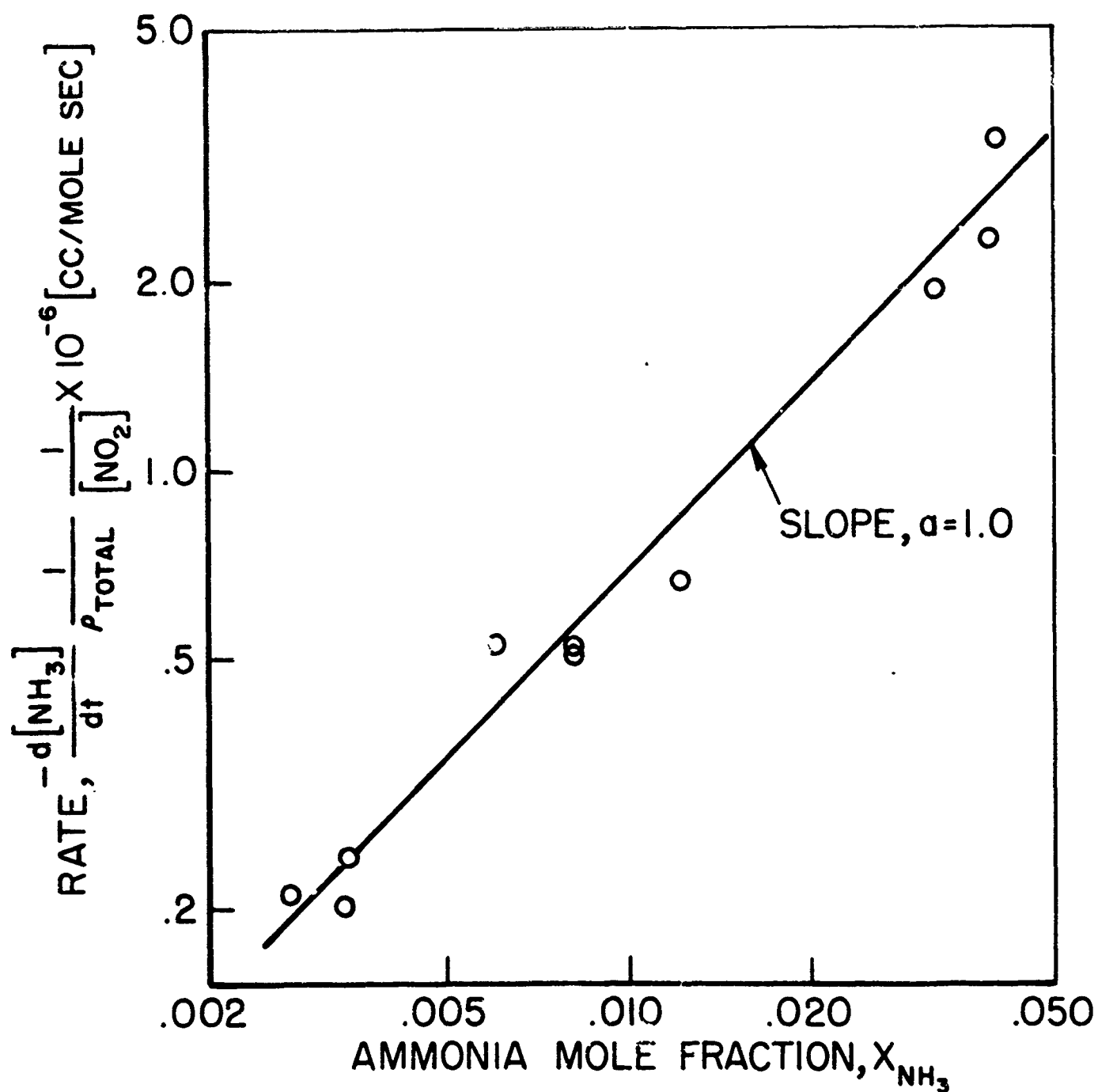
Nitric oxide is detected in both the infrared spectra and mass spectra of the reaction products (Appendix D).

### 5.1.2 Experimental results

The reaction orders for the ammonia/nitrogen dioxide reaction are determined by noting the change in reaction rate with concentration of ammonia, Figure 29, and with concentration of nitrogen dioxide, Figure 30, at a selected temperature of  $1000^\circ\text{K}$ . The reaction rate is found to be first order with each reactant, that is, the rate equation is found to be

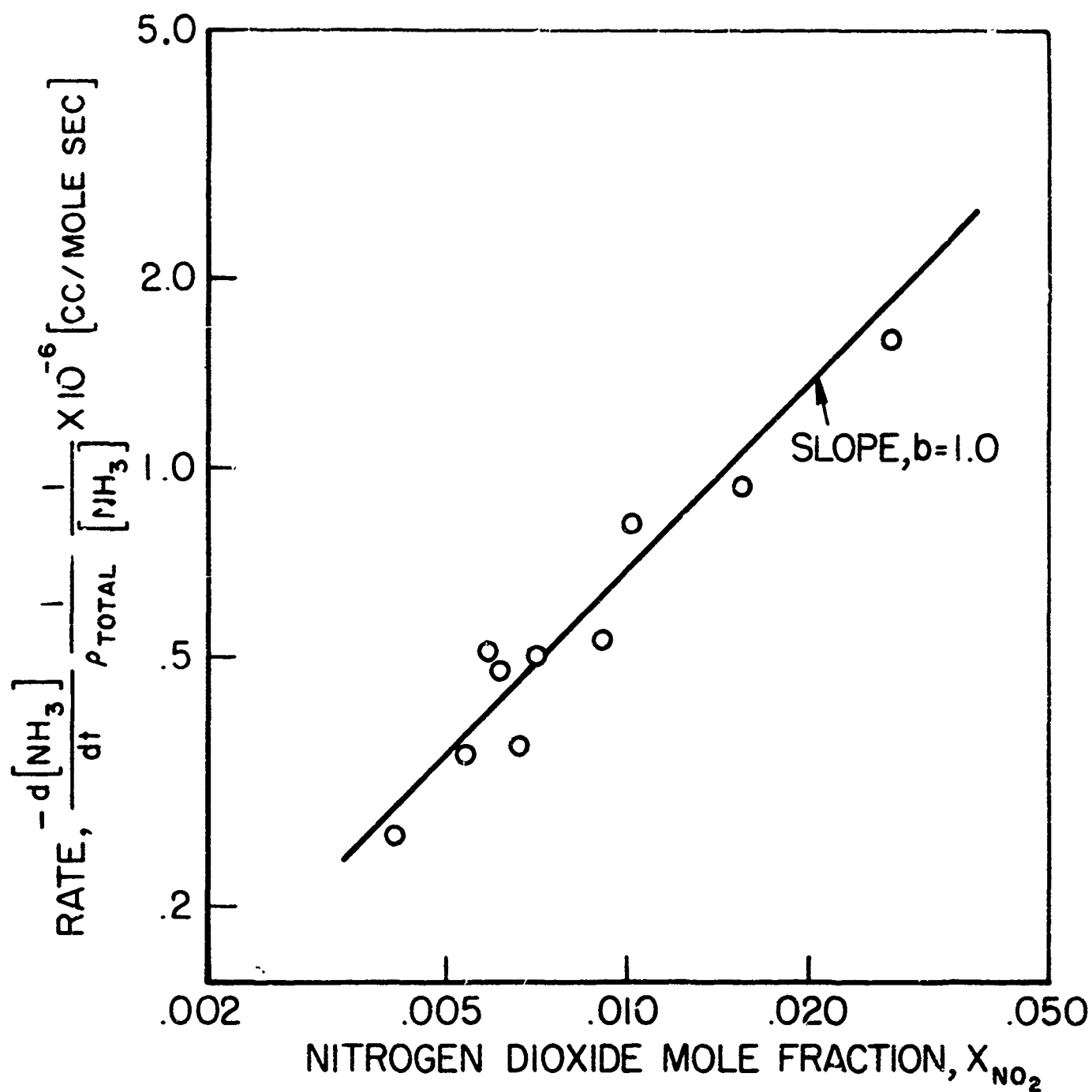
$$\frac{d[\text{NH}_3]}{dt} = -k[\text{NH}_3][\text{NO}_2]$$

Rates were measured in both the 2 and 4 [inch] quartz ducts. While the measured rates are approximately the same, a higher overall activation energy is found for the smaller duct. The experimental parameters are summarized in Table 27 and the rate constants calculated



AMMONIA/NITROGEN DIOXIDE REACTION RATES,  
 $T=1000^\circ\text{K}$ , DEPENDENCE ON AMMONIA CONCENTRATION

FIGURE 29



AMMONIA / NITROGEN DIOXIDE REACTION RATES,  
 $T=1000^\circ\text{K}$ , DEPENDENCE ON NITROGEN DIOXIDE  
 CONCENTRATION

FIGURE 30

JP13-4063-65



from the measured reaction rates are plotted in Figures 59 and 60. The Arrhenius expression for the rate constant calculated from rates measured in the larger duct is

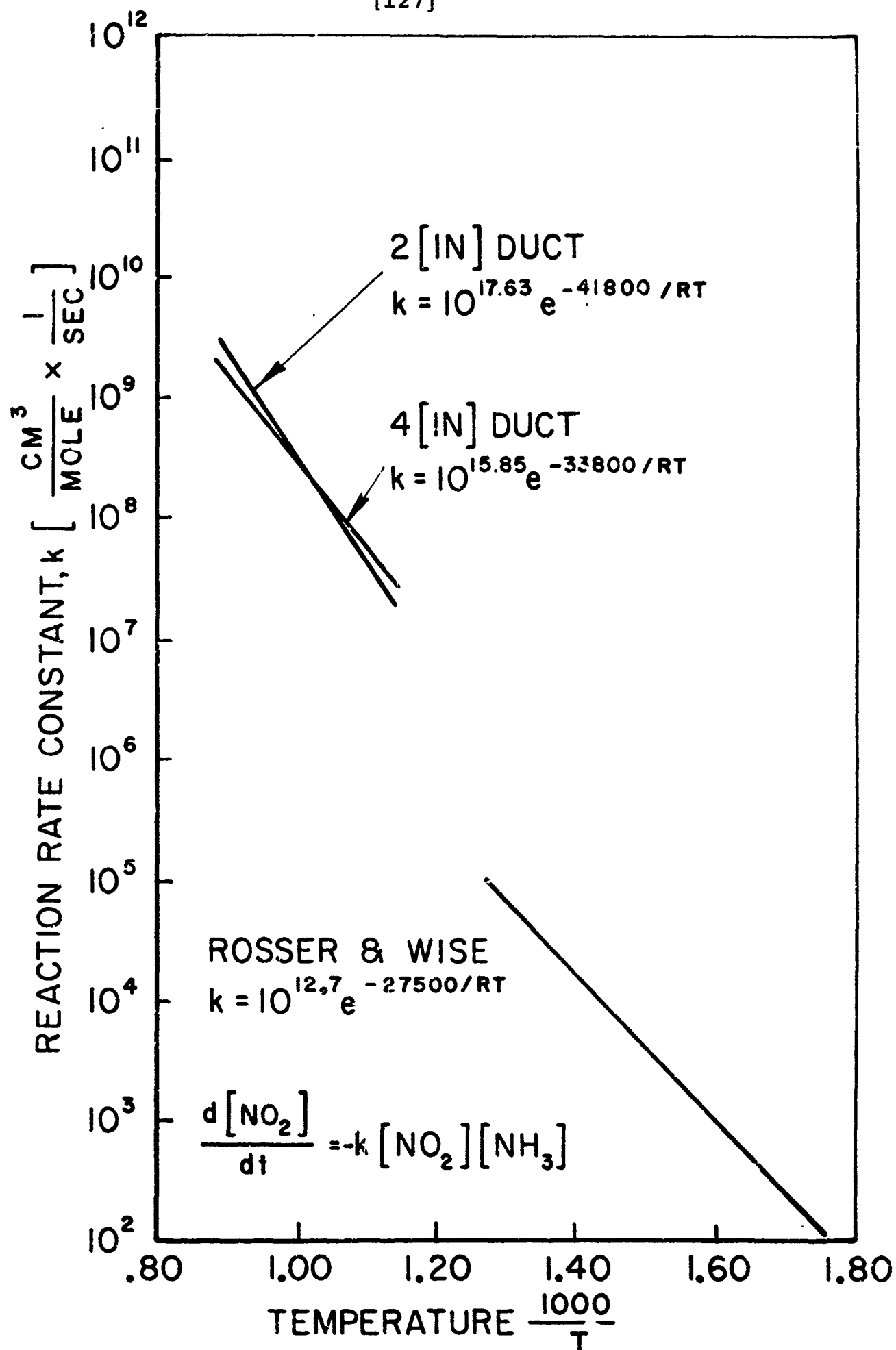
$$k = 10^{15.85} \exp(-33800/RT) \quad [\text{cc mole}^{-1} \text{sec}^{-1}]$$

### 5.1.3 Results of other investigators

Besides the low temperature work of Falk and Pease (99, 100), the only other known investigation of the ammonia/nitrogen dioxide reaction is the work of Rosser and Wise (13). These investigators measured the reaction rate in a closed vessel by means of an optical determination of the disappearance of nitrogen dioxide. This experiment was similar to their investigation of the hydrogen/nitrogen dioxide reaction. As in the present investigation, they found the reaction to be first order with respect to both nitrogen dioxide and ammonia. Their reported rate constant of

$$k = 10^{12.7} \exp(-27500/RT) \quad [\text{cc mole}^{-1} \text{sec}^{-1}]$$

and the results of the present investigation are not in good agreement. As shown in Figure 31, extrapolation of the reaction rates of Rosser and Wise, measured at lower temperatures than the present experiment, gives a lower reaction rate than found in the present experiments. Since the experiments were conducted at different temperatures, it is difficult to establish whether the apparent inconsistency represents a change in the reaction mechanism or is a result of the difference in measuring technique. The good agreement obtained between the



NITROGEN DIOXIDE / AMMONIA REACTION RATE  
 FIGURE 31

present investigation of the hydrogen/nitrogen dioxide reaction and the work of these two investigators on the same reaction suggests that either a change in the reaction mechanism or interaction of thermal decomposition explains the difference, rather than a difference in measuring technique.

The work of Rosser and Wise was complicated by a parallel disappearance of nitrogen dioxide by thermal dissociation, a problem not encountered under the operating conditions of the flow reactor. That their measured value for the decomposition rate of nitrogen dioxide (48) is approximately the same as the above rate for the reaction of nitrogen dioxide and ammonia

$$\frac{d[\text{NO}_2]}{dt} = -k[\text{NO}_2][\text{NO}_2]$$

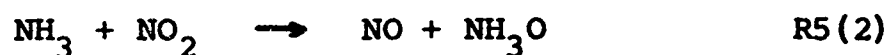
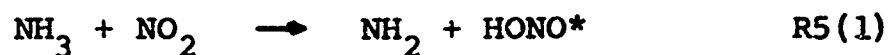
$$k = 10^{12.6} \exp(-26900/RT) \quad [\text{cc mole}^{-1}\text{sec}^{-1}]$$

would seem to raise some question about the interpretation of their results. Since they measure the progress of the reaction by the disappearance of nitrogen dioxide, it would seem difficult to distinguish between the case of ammonia and nitrogen dioxide reacting directly and the case of nitrogen dioxide decomposing, perhaps only to  $\text{NO} + \text{O}$ , then reacting with ammonia.

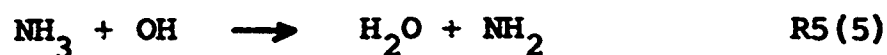
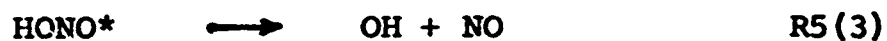
Rosser and Wise found that high pressures of inert gases, such as  $\text{Ne}$ ,  $\text{N}_2$ , and  $\text{CO}_2$ , had no effect on the reaction. They reported the primary reaction products to be  $\text{N}_2$ ,  $\text{NO}$ , and  $\text{H}_2\text{O}$ , in agreement with the present observations.

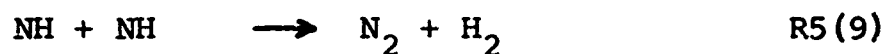
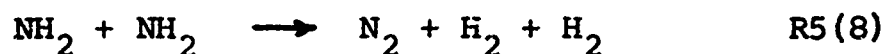
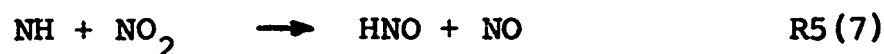
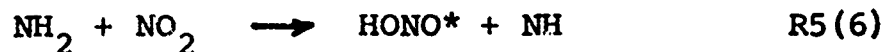
5.1.4 Reaction mechanism

Rosser and Wise propose two reaction mechanisms based on the two initiation reactions,



The primary difficulty with their two subsequent reaction mechanisms is that they both involve  $\text{NH}_2$  as a primary chain carrier and therefore predict the reaction of a large fraction of the nitric oxide. As discussed in Chapter 7 on hydrazine reactions, hydrazine, unlike ammonia, is reactive with nitric oxide, an effect probably attributable to the presence of reactive  $\text{NH}_2$  radicals. If the reaction of ammonia and nitrogen dioxide depends upon  $\text{NH}_2$  as a primary chain carrier, one would expect that reduction of nitric oxide would also occur. No such reduction of nitric oxide occurs. Since the oxidation of ammonia occurs primarily by hydrogen abstraction, the formation of  $\text{NH}_2$  radicals is an unavoidable consequence. By postulating that  $\text{NO}_2$  is more effective than  $\text{NO}$  in removing  $\text{NH}_2$ , a reaction mechanism evolves which depends strongly upon  $\text{OH}$  radicals as the primary chain carriers. In addition to the first initiation step above, R5(1), the following steps are suggested.





The second hydrogen abstraction, reaction R5(6) is endothermic by only 14 [kcal]; the breaking of the second N-H bond in ammonia is easier than the first (see Table 3). On the basis of a simplified scheme involving only reactions R5(1), R5(3), R5(4), R5(5), R5(6) and R5(7), the steady state assumption of constant radical concentrations gives, for the reaction rate

$$\frac{d[\text{NH}_3]}{dt} = -k_1 \left( 1 + \frac{2k_3k_5}{k_4} \right) [\text{NH}_3][\text{NO}_2]$$

The above expression gives the right order with respect to the reactants. The overall activation energy is that of the initiation reaction, R5(5), if  $k_4 \gg 2k_3k_5$ . If  $k_4 \ll 2k_3k_5$ , the overall activation energy is  $E = E_1 + E_3 + E_5 - E_4$ . Since  $E_3 \approx E_5 \approx 0$ , the overall activation energy in this second case would be predicted to be less than  $E_1$ .

Inclusion of the bimolecular termination steps, R5(8) and R5(9) in the reaction mechanism would serve to reduce the overall activation energy. As discussed by Frost and Pearson (101), the apparent activation energy of a chain propagation reaction is

$$E = E_{\text{propagation}} + w^{-1}(E_{\text{initiation}} - E_{\text{breaking}})$$

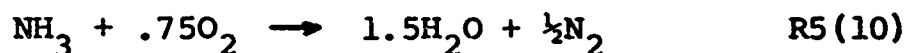
where  $w$  is the order of the chain breaking process with respect to the chain carrier.

## 5.2 AMMONIA/OXYGEN

The ammonia/oxygen reaction is very difficult to initiate in the flow reactor at temperatures less than  $1100^{\circ}\text{K}$ . Even at these temperatures high oxygen concentrations are required. To obtain a measurable reaction, it is necessary to use air as the carrier gas, giving oxidant rich mixtures.

### 5.2.1 Stoichiometry

That the ammonia is fully oxidized is evidenced by the observed heat of reaction which is measured to be 74 [kcal/mole  $\text{NH}_3$ ]. This value is in agreement with a theoretical value of 75.66 [kcal/mole  $\text{NH}_3$ ] for the reaction



Additionally, no ammonia is detected in the infrared absorption spectra of a sample of the reacted gases.

### 5.2.2 Experimental results

Since large excess quantities of oxygen are necessary to obtain a measurable reaction, it is not possible to determine the order of the reaction with respect to the oxygen concentration. This requirement of high oxygen concentration itself, however, does indicate a positive reaction rate order with respect to oxygen. The rate dependence upon the ammonia concentration is

determined directly by noting the variation of the reaction rate with ammonia concentration at a selected temperature of 1163°K. A log-log plot of the rate versus ammonia mole fraction, Figure 32, shows a first order dependence upon the ammonia.

Reaction rates are calculated according to the rate equation

$$\frac{d(\text{NH}_3)}{dt} = -k[\text{NH}_3][\text{O}_2]$$

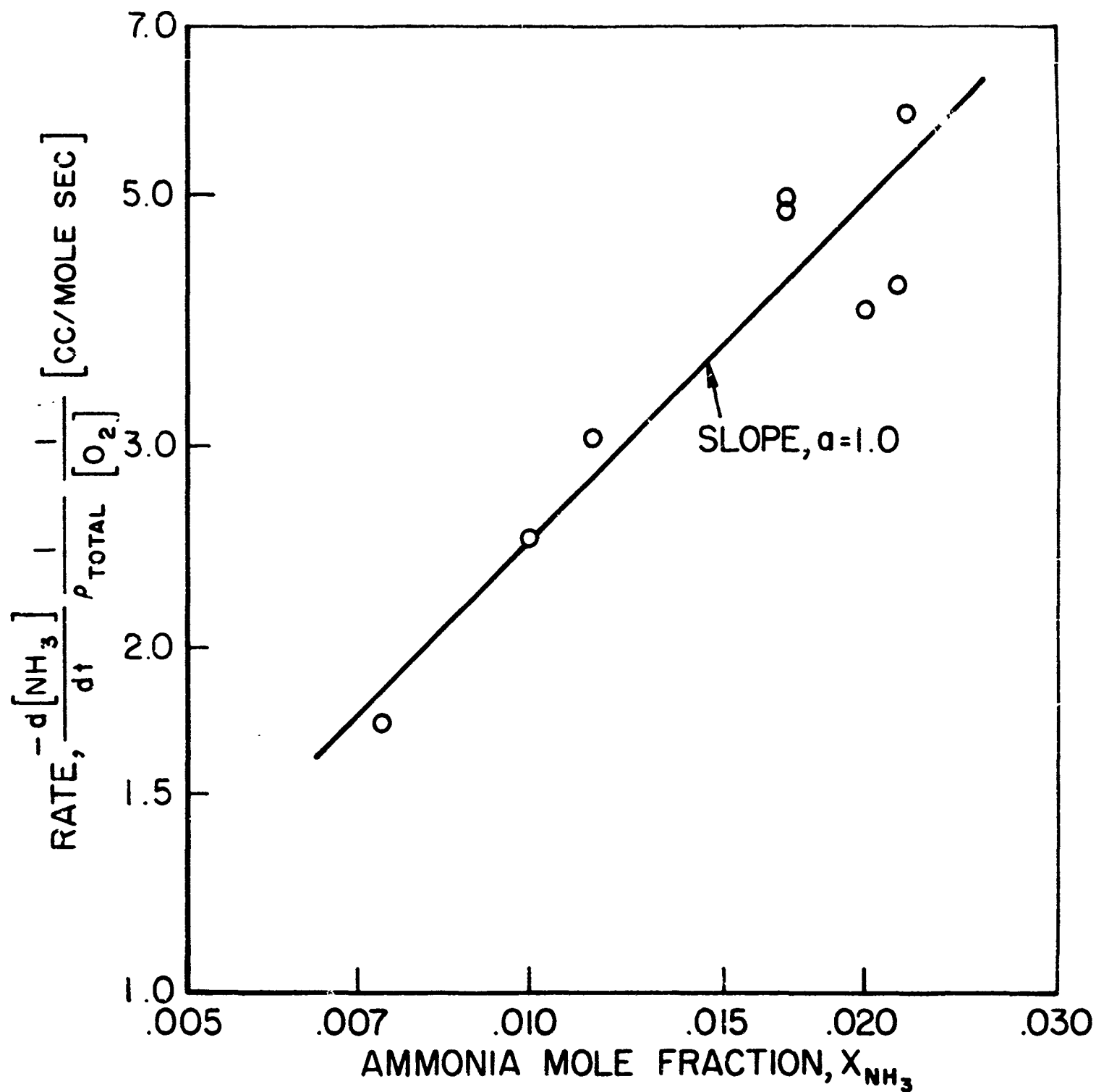
and the rate constant is found to be

$$k = 10^{14.61} \exp(-38700/RT) \quad [\text{cc mole}^{-1}\text{sec}^{-1}]$$

Because of the large excess of oxygen, assumption of a first order rate dependence upon the ammonia concentration alone gives a comparable correlation of the experimental data. The experimental parameters are summarized in Table 28 and the experimentally measured rate constants presented in Figure 61. Addition of up to 3% by volume of nitric oxide appears to slow the measured reaction rate only slightly and not as drastically as in the hydrogen/oxygen experiments.

### 5.2.3 Results of other investigators

Andrews and Gray (102) in measurements of the ammonia/oxygen flame speed at low pressures, 70mmHg, found the reaction to involve the complete oxidation of ammonia to water, for stoichiometric and oxygen rich mixtures. They found the flame speed to be independent of the pressure indicating an overall reaction order of two.



AMMONIA / OXYGEN REACTION RATES,  $T=1163^\circ\text{K}$ ,  
DEPENDENCE ON AMMONIA CONCENTRATION

FIGURE 32



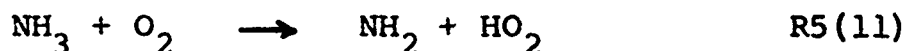
TABLE 10. Ammonia flame speeds, Andrews and Gray (102),  
70 mmHg

	H	T <sub>B</sub>	S <sub>u</sub>
	[kcal/mole]	[°K]	[cm/sec]
NH <sub>3</sub> + .75O <sub>2</sub>	75.1	2625	110
NH <sub>3</sub> + 2NO	108.1	2710	62.5

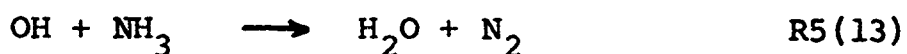
Wolfhard and Parker (103) have identified emission bands of NH<sub>2</sub>, NH, and OH in ammonia/oxygen flames. Dows, Pimentel, and Whittle (104) observed the ammonia/oxygen diffusion flame in the infra-red and detected OH as the only radical. Hussain and Norrish (105) report a failure to observe NH in studies of the explosive oxidation of ammonia for ammonia lean mixtures. From isothermal experiments at 525°C, Verwimp and van Tiggelen (106) report an overall activation energy of about 50 [kcal/mole].

#### 5.2.4 Reaction mechanism

From the observations of other investigators, a mechanism based on OH and NH<sub>2</sub> as the chain carriers seems to be indicated. The proposed mechanism is close to that suggested by Hussain and Norrish (105). The observation that high oxygen concentrations are required to obtain a reaction suggests an initiation step of



The proposed propagation reactions are analogous to those for the ammonia/nitrogen dioxide mechanism.



Additional reactions proposed are,



Application of the usual steady state analysis to the above scheme gives for the reaction rate,

$$\frac{d[\text{NH}_3]}{dt} = -k_{11} \left( 1 + \frac{k_{13}}{k_{12}} \right) [\text{NH}_3][\text{O}_2]$$

This expression has the expected first order dependence upon both the ammonia and oxygen concentrations.

### 5.3 AMMONIA/NITRIC OXIDE-OXYGEN

Attempts to obtain measurable reaction rates between ammonia and mixtures of nitric oxide and oxygen corresponding to decomposed nitrogen dioxide were unsuccessful. Reactant concentrations of up to 4%  $\text{NH}_3$  and 5%  $\text{NO} + \frac{1}{2}\text{O}_2$  in a nitrogen carrier and temperatures of up to  $1200^\circ\text{K}$  resulted in no observable exothermic reaction. These results are consistent with a similar failure to obtain reaction with ammonia/oxygen mixtures

at similar concentrations and the additional expected inhibiting effect of nitric oxide.

#### 5.4 AMMONIA/NITRIC OXIDE

Similarly, measurable reaction rates were not obtained in mixtures of ammonia and nitric oxide with concentrations of up to 4% ammonia and 5% nitric oxide in a nitrogen carrier. Maximum temperatures in these attempted experiments were 1120°K.

Andrews and Gray (102) have studied ammonia/nitric oxide flames at low pressures. They found the reaction to go to completion according to the stoichiometry



Measured flame speeds show nitric oxide to be less reactive than oxygen with ammonia (Table 10). Ammonia flame temperatures are sufficiently high to cause thermal dissociation of nitric oxide. It is difficult, therefore, to establish whether the reaction of ammonia and nitric oxide requires decomposition of nitric oxide or can proceed by way of a mechanism based on  $\text{NH}_2$  radicals present in the pyrolysis of ammonia. Unfortunately, in the present experiments, no significant pyrolysis of ammonia occurs which would allow the checking of this point. Considering the reactivity of hydrazine and nitric oxide (Section 7.4), one would expect ammonia and nitric oxide to become similarly reactive at a temperature where ammonia pyrolysis becomes significant. Jacobs (41) suggests that a temperature in excess of 1500°K is required.

### 5.5 COMPARISON OF AMMONIA REACTIONS

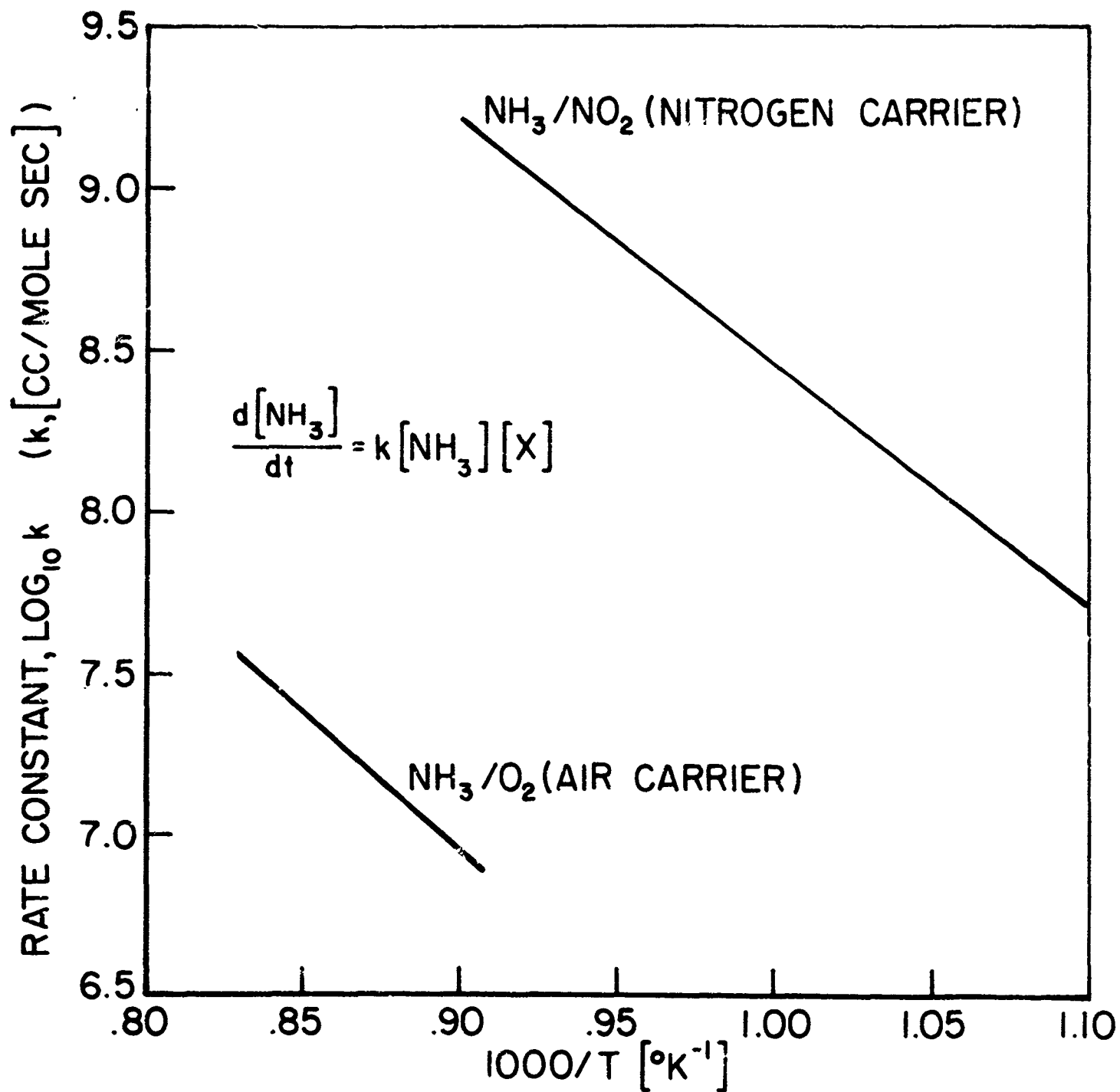
Ammonia was found to be more reactive with nitrogen dioxide than with oxygen. Since the reaction with oxygen was carried out with a large excess of oxygen while that with nitrogen dioxide was in the stoichiometric range, some care is required in comparing the reaction rate constants. Comparison based on an assumption of a first order dependence on oxygen tends to make the differences in the reaction rates seem too great because some of the oxygen serves more as a diluent than as a reactant, Figure 33. On the other hand, assumption of a zero order dependence on the oxygen concentration tends to underestimate the difference in reaction rates, Figure 34. Since it is impossible to measure the rates under conditions of similar oxidizer concentrations, the best that can be said is that the relative reaction rates of the oxidation of ammonia by nitrogen dioxide and by oxygen lie somewhere between the two values listed below.

---

TABLE 11. Relative reaction rates, ammonia at 1110°K.

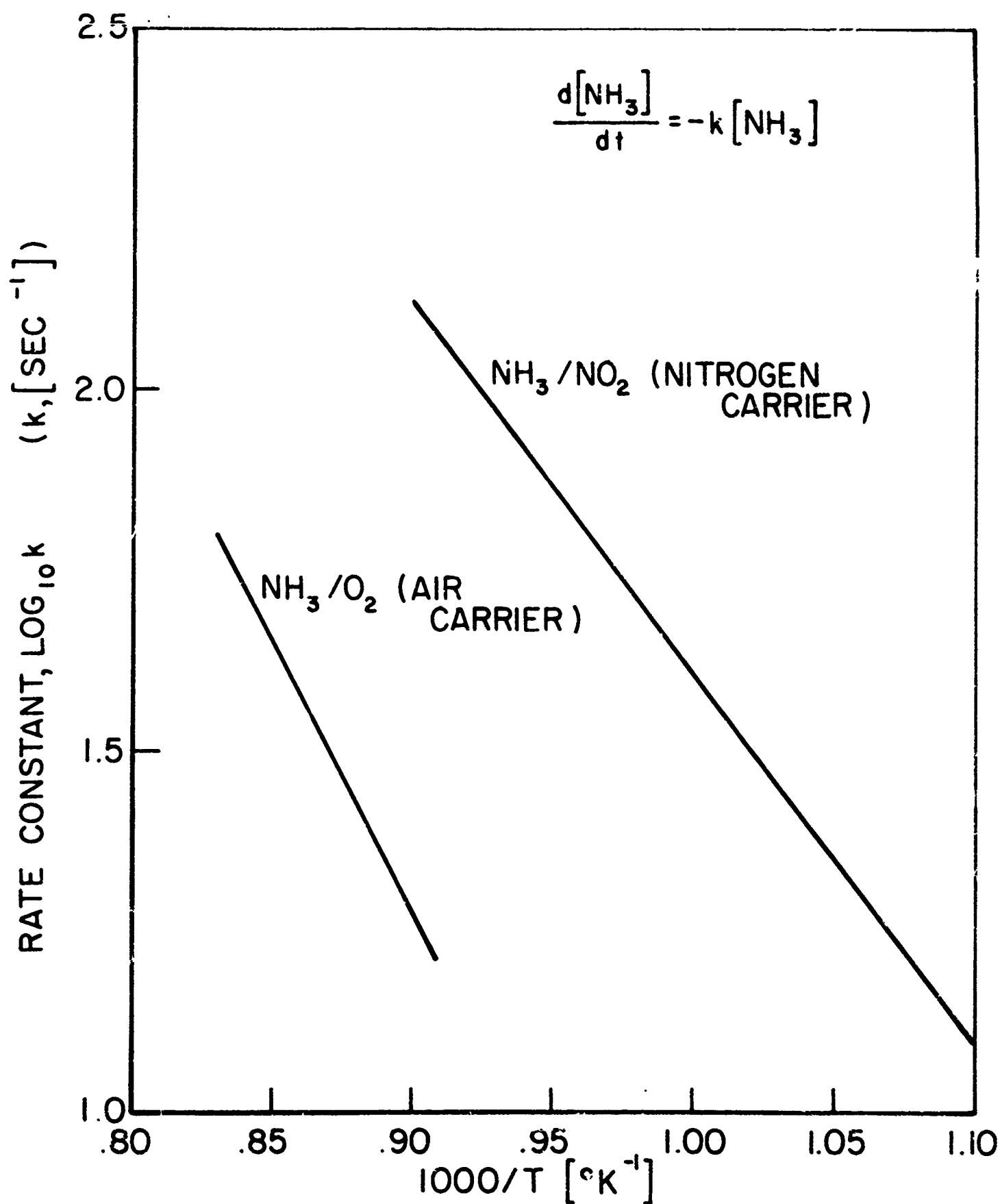
oxidizer	second order	first order
$\text{NO}_2$	180	7
$\text{O}_2$	1	1
$\text{NO} + \frac{1}{2}\text{O}_2$	no reaction	
$\text{NO}$	no reaction	

---



COMPARISON OF AMMONIA REACTION RATES,  
SECOND ORDER RATE CONSTANT

FIGURE 33



COMPARISON OF AMMONIA REACTION RATES,  
FIRST ORDER RATE CONSTANT

FIGURE 34

JP13-4055-65

The two reactions are quite similar in most respects. In both cases, observed orders with respect to the ammonia are first. The order of the ammonia/oxygen reaction with respect to the oxygen could not be determined. Other investigators have found a first order dependence. This is the same oxidizer dependence as was observed for the ammonia/nitrogen dioxide reaction. The overall activation energies are similar, 33.8 [kcal/mole] for nitrogen dioxide and 38.7 [kcal/mole] for oxygen. These similarities probably indicate that the mechanisms, particularly the chain propagation steps, are similar. A comparison of the proposed reaction mechanisms is made in Table 12.

The difference in reaction rates is attributed to the greater ease in breaking the first N-O bond in nitrogen dioxide as compared to breaking the O-O bond in molecular oxygen, 72 versus 118 [kcal/mole]. The difference in activation energies also reflects this observation. Nitrogen dioxide may be considered as a better agent for abstracting hydrogen from ammonia than oxygen. The failure to obtain reaction with nitric oxide is similarly traceable to the difficulty in breaking the  $\text{N}\equiv\text{O}$  bond.

TABLE 12: Summary of reaction mechanisms, ammonia reactions.

	$\text{NH}_3/\text{NO}_2$	$\text{NH}_3/\text{O}_2$
initiation	$\text{NH}_3 + \text{NO}_2 \rightarrow \text{HONO}^* + \text{NH}_2$	$\text{NH}_3 + \text{O}_2 \rightarrow \text{NH}_2 + \text{HO}_2$
branching		
propagation	$\text{HONO}^* \rightarrow \text{OH} + \text{NO}$ $\text{NH}_3 + \text{OH} \rightarrow \text{H}_2\text{O} + \text{NH}_2$ $\text{NO}_2 + \text{NH}_2 \rightarrow \text{HONO}^* + \text{NH}$	$\text{HNO} \rightarrow \text{H} + \text{NO}$ $\text{NH}_3 + \text{OH} \rightarrow \text{H}_2\text{O} + \text{NH}_2$ $\text{O}_2 + \text{NH}_2 \rightarrow \text{HNO} + \text{OH}$
termination	$\text{HONO}^* \xrightarrow{\text{M}} \text{HONO}$ $\text{NO}_2 + \text{NH}_2 \rightarrow \text{H}_2\text{O} + \text{N}_2$ $\text{NO}_2 + \text{NH} \rightarrow \text{HNO} + \text{NC}$ $\text{NH}_2 + \text{NH}_2 \rightarrow \text{N}_2 + \text{H}_2 + \text{H}_2$ $\text{NH} + \text{NH} \rightarrow \text{N}_2 + \text{H}_2$	$\text{NH}_2 + \text{NO} \rightarrow \text{H}_2\text{O} + \text{N}_2$



## CHAPTER 6

AMMONIA-HYDROGEN REACTIONS

As the two reactive decomposition products of hydrazine, ammonia and hydrogen were studied in a mixture consisting of a two to one volume ratio, respectively. In addition to being representative of fully decomposed hydrazine, this mixture provides information on the effect of hydrogen on the ammonia reactions, and of ammonia on the hydrogen reactions. Since the fuel in these studies is in reality a mixture of two reactants, the implicit assumption that the results apply to a single characteristic fuel (decomposed hydrazine), while useful in treating and comparing the experimental data, is not accurate. The oxidations of the two components of the fuel, being only partially coupled through any common intermediates, make interpretations of a reaction order or overall activation energy questionable. It is recognized that in some of the oxidations the hydrogen is likely to be consumed more rapidly than the ammonia. This will produce a changing hydrogen/ammonia ratio and further complicate interpretation of the results. The primary objective of the rate measurements was to establish the reaction rate of the mixture for comparison with the reaction rates of hydrogen, ammonia, and hydrazine alone. In the following discussions, the term "ammonia-hydrogen" is understood to refer to the particular composition of a two to one volume ratio.

6.1 AMMONIA-HYDROGEN/NITROGEN DIOXIDE

Since the reactions of hydrogen and of ammonia with nitrogen dioxide have approximately the same rate at the

temperatures of the present experiments (Figure 46), no division of the reaction of the mixture into separate steps is expected, nor is such a separation found.

#### 6.1.1 Stoichiometry

Also, as expected, the stoichiometry appears to follow that of the separate fuel components when reacted with nitrogen dioxide, that is, complete oxidation of the fuel to water and partial reduction of the nitrogen dioxide to nitric oxide. The stoichiometry of the mixture then is given by



The predicted heat of reaction is 77.22 (kcal/mole  $\text{NH}_3 + \frac{1}{2}\text{mole H}_2$ ) which is in good agreement with the measured heat of action of 77 (kcal/mole  $\text{NH}_3 + \frac{1}{2}\text{mole H}_2$ ).

#### 6.1.2 Experimental results

The reaction rates were measured in the 4 (inch) quartz duct using a nitrogen carrier. The experimental parameters are summarized in Table 29. Some question exists concerning the proper form of the rate equation considering the differences in the rate equations used for the fuel components separately. Summarized, these are: (1) the order with respect to hydrogen was found to be 1.4, with respect to ammonia 1.0, (2) the order with respect to nitrogen dioxide was first in both cases, however (3) an inhibiting effect of nitric oxide on the hydrogen/nitrogen dioxide reaction was detected while no pronounced inhibition of the ammonia/nitrogen dioxide

reaction by nitric oxide was noticed. A first order dependence on the nitrogen dioxide concentration and negative first order dependence on the initial nitrogen dioxide concentration (equal to the sum of the local concentration of nitrogen dioxide plus nitric oxide, see Section 4.1.2), is equivalent roughly to a zero order dependence upon the nitrogen dioxide concentration. The result holds especially if there is an excess concentration of nitrogen dioxide over the stoichiometric value. Ideally, one would write a rate equation containing two terms,

$$\frac{d[\text{NH}_3 + \frac{1}{2}\text{H}_2]}{dt} = -k_1[\text{NH}_3][\text{NO}_2] - k_2 \frac{[\text{H}]^{1.4} [\text{NO}_2]}{[\text{NO}_2] + [\text{NO}]}$$

There is no experimental basis for so separating the reaction and appears to be little basis for reconciling the difference in reaction orders for the reactions of hydrogen and ammonia taken separately. Therefore, a simple first order dependence upon both the total fuel concentration and the nitrogen dioxide concentration is selected arbitrarily

$$\frac{d[\text{NH}_3 + \frac{1}{2}\text{H}_2]}{dt} = -k[\text{NH}_3 + \frac{1}{2}\text{H}_2][\text{NO}_2]$$

The rate constant is calculated from the measured reaction rate to be

$$k = 10^{23.44} \exp(-65900/RT) \quad [\text{cc mole}^{-1}\text{sec}^{-1}]$$

The experimental data for this reaction are presented in Figure 62. Once again, no particular chemical significance

is to be attributed to this apparent activation energy because the rate equation is chosen arbitrarily.

### 6.1.3 Results of other investigators and reaction mechanism

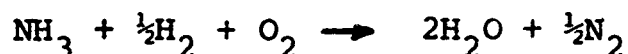
No other investigation of the reaction of ammonia-hydrogen mixtures with nitrogen dioxide, or of decomposed hydrazine, is known. Reference to the previous two chapters, Sections 4.1.5 and 5.1.4, reveals a basic similarity of the two proposed reaction mechanisms. The propagation steps of both are postulated to depend strongly upon the OH radical. The similarity between the initiation steps involving the breaking of the hydrogen bond to form HONO and the abstraction of a hydrogen atom from ammonia, also to form HONO, is noted. A detailed comparison is reserved for Chapter 8, in which an attempt is made to reconcile all of the observed reactions.

## 6.2 AMMONIA-HYDROGEN/OXYGEN

The study of ammonia-hydrogen and oxygen might be expected to result in a separation of the reaction into steps because of the widely differing rates of hydrogen and ammonia reaction with oxygen. No separation was observed. The reaction of ammonia and oxygen could be studied only in high concentrations of oxygen, obtained through the use of air as the carrier gas instead of nitrogen. Hydrogen is observed to accelerate the ammonia reaction sufficiently to allow study of the reaction at compositions only slightly oxygen rich, i.e.  $\phi_o = .5$ .

### 6.2.1 Stoichiometry

The reaction is observed to go to completion according to the stoichiometry



as is indicated by a measured heat of reaction of 106 (kcal/mole  $\text{NH}_3 + \frac{1}{2}\text{moleH}_2$ ), in good agreement with the predicted value of 104.56 (kcal/mole  $\text{NH}_3 + \frac{1}{2}\text{H}_2$ ).

### 6.2.2 Experimental results

Once again no attempt was made to determine the reaction orders. The rate equation used to reduce the experimental data was selected arbitrarily as

$$\frac{d[\text{NH}_3 + \frac{1}{2}\text{H}_2]}{dt} = -k[\text{NH}_3 + \frac{1}{2}\text{H}_2][\text{O}_2]$$

Experimental parameters are summarized in Table 30 and the experimental rate constants plotted in Figure 63. The rate constant for the above equation is found to be

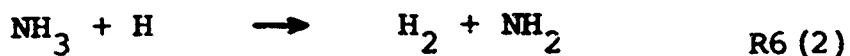
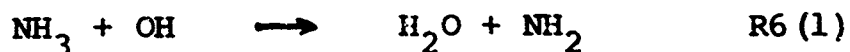
$$k = 10^{19.64} \exp (-61900/RT) \quad [\text{cc mole}^{-1}\text{sec}^{-1}]$$

While the initiation of measurable reaction between ammonia and oxygen cannot be obtained at temperatures up to 1200°K, the addition of small amounts of hydrogen,  $[\text{H}_2] / [\text{NH}_3] = .02$ , is found to produce a measurable reaction and results in the complete oxidation of the ammonia. In a somewhat similar fashion, at lower temperatures

the addition of large amounts of ammonia,  $[\text{NH}_3]/[\text{H}_2] \approx 1$ , is found to quench the hydrogen/oxygen reaction. While the initiation and acceleration of the ammonia/oxygen reaction by hydrogen appears to be independent of the hydrogen concentration,  $[\text{H}_2]$ , the retardation of the hydrogen/oxygen reaction by ammonia appears to be in proportion to the amount of ammonia added. Since initial reaction temperatures are held constant while varying amounts of ammonia are added, the effect of the ammonia is not a thermal one.

### 6.2.3 Results of other investigators and reaction mechanism

Even though the hydrogen/oxygen and ammonia/oxygen reactions have received considerable investigation, no study of mixtures of the two with oxygen is known. The reaction mechanisms of the two separate reactions are quite different, particularly in that the hydrogen/oxygen reaction is postulated to involve no chain branching. The reaction of the mixture of ammonia-hydrogen with oxygen therefore would be expected to involve a complex interaction of the two reaction mechanisms. The active intermediates of the rapid hydrogen/oxygen reaction would serve to speed the slower ammonia/oxygen reaction. The retarding effect of ammonia upon the hydrogen/oxygen reaction is expected to involve such "free radical draining" reactions as



While these reactions produce  $\text{NH}_2$  radicals, the reactions drain the chain branching radicals of the hydrogen/oxygen reaction, H and OH. Such a "draining" effect would explain the increased slowing of the hydrogen/oxygen reaction with increasing ammonia addition. One again, additional comparisons are made in Chapter 8.

### 6.3 AMMONIA-HYDROGEN/NITRIC OXIDE-OXYGEN

No measurable reaction is obtained in mixtures containing up to 3% ammonia-hydrogen and up to 4% nitric oxide-oxygen at temperatures of up to  $1150^\circ\text{K}$ . One is tempted to conclude that the effect observed is due to inhibition by nitric oxide. Even without the presence of nitric oxide, however, the oxygen concentration (less than 1.3%) and temperature levels are so low that establishment of a measurable reaction is marginal. This failure to obtain a reaction is consistent with the results of the study of the ammonia-hydrogen/oxygen reaction.

### 6.4 AMMONIA-HYDROGEN/NITRIC OXIDE

No reaction between a mixture of up to 3% ammonia-hydrogen and up to 5% nitric oxide is observable at temperatures of up to  $1150^\circ\text{K}$ , as expected. Armitage and Gray (107) have measured flame speeds for ternary mixtures of hydrogen, ammonia, and nitric oxide. They found hydrogen to inhibit the ignition and reduce the flame speed of  $\text{NH}_3 + \text{NO}$  mixtures. This observation is quite unlike the observed effect of hydrogen on the ammonia/oxygen reaction. The reaction of ammonia and nitric oxide in a flame probably involves thermal

decomposition of the ammonia, and possibly the nitric oxide, and therefore is quite different from the present observations of the ammonia/oxygen reaction in a flow reactor.

#### COMPARISON OF AMMONIA-HYDROGEN REACTIONS

Since the reaction of ammonia-hydrogen with nitrogen dioxide is observed to be much more rapid than with oxygen, and the rate measurements therefore made at different temperatures, comparison of reaction rates at a single temperature involves a large extrapolation. The rates as a function of temperature are compared in Figure 35. The relative rates at 1150°K are estimated in the following table.

TABLE 13. Relative reaction rates, ammonia-hydrogen  
( $\text{NH}_3 + \frac{1}{2}\text{H}_2$ ) at 1150°K.

<u>oxidizer</u>	<u>relative rate</u>
$\text{NO}_2$	550
$\text{O}_2$	1
$\text{NO} + \frac{1}{2}\text{O}_2$	no reaction
$\text{NO}$	no reaction



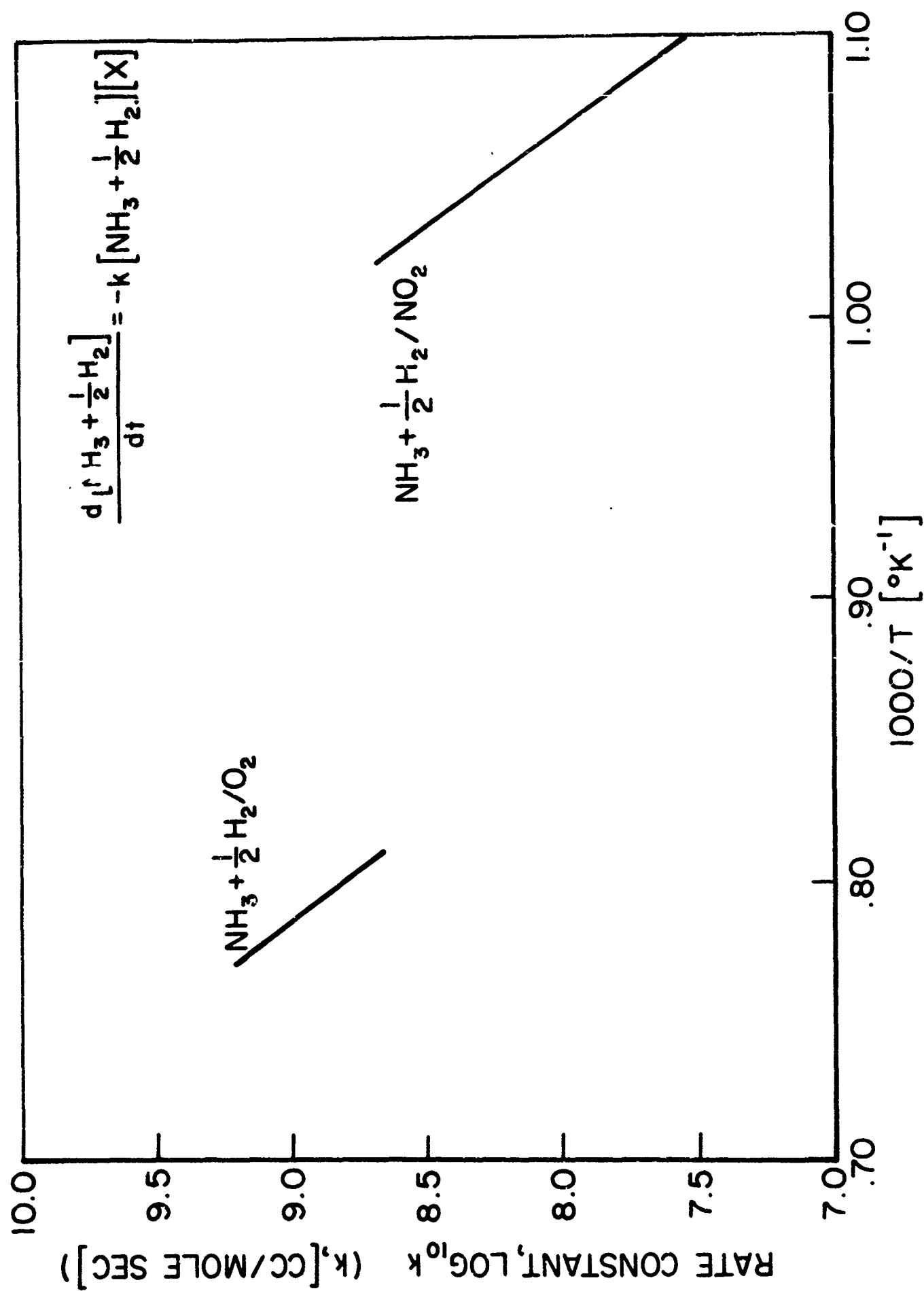


FIGURE 35

While the overall activation energies are found to be similar, 65.9 and 61.9 [kcal/mole], no great significance is attributed to the similarity because of the uncertainty in the choice of reaction orders, a rate equation, and in the meaning of the overall activation energy for such a "mixed" reactant.

CHAPTER 7     HYDRAZINE REACTIONS

Since the decomposition of hydrazine takes place at a rate which falls approximately midway within the flow reactor measuring capability, the opportunity existed to attempt to study hydrazine reactions under conditions where decomposition was not the major factor in the reaction, where decomposition occurred simultaneously with reaction, and where decomposition preceded reaction. This attempt has been successful in that examples of each type of reaction have been observed. The reactions of hydrazine with nitrogen dioxide, oxygen, decomposed nitrogen dioxide ( $\text{NO} + \frac{1}{2}\text{O}_2$ ), and nitric oxide have been studied. In combination with the previous measurements of hydrazine decomposition in the same apparatus by Eberstein (39), interpretation of the observed reaction rates, reaction orders, and overall reaction activation energies is made with particular reference to the role of hydrazine decomposition in its oxidation.

7.1     HYDRAZINE/NITROGEN DIOXIDE

Of all the reactions studied, the reaction of hydrazine and nitrogen dioxide is the only one to exhibit two distinct steps of greatly different rates. While the reaction mechanisms for the other reactions studied are recognized to involve a number of separate steps, these steps take place within the same time scale and are indistinguishable in terms of their effect upon the overall reaction rate. The reaction of hydrazine and nitrogen dioxide, however, proceeds first through a rapid reaction which is interpreted to be the reduction of the nitrogen dioxide to nitric oxide which is then followed by a second, slower reaction, the

reduction of the nitric oxide. Each of these steps is recognized to involve a number of separate reactions.

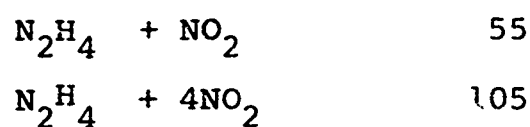
#### 7.1.1 Stoichiometry

The nature of the reactor temperature trace is direct evidence that the reaction takes place in two steps. All other reactions studied in the flow reactor exhibit monotonically increasing temperature profiles through the reaction zone (see Figure 12). The reaction of equal volumes (mole fractions) of hydrazine and nitrogen dioxide produces a temperature profile with two regions separated by a plateau or constant temperature zone (see Figure 36). The corresponding heats of reaction, which are calculated from the temperature changes, are summarized below.

---

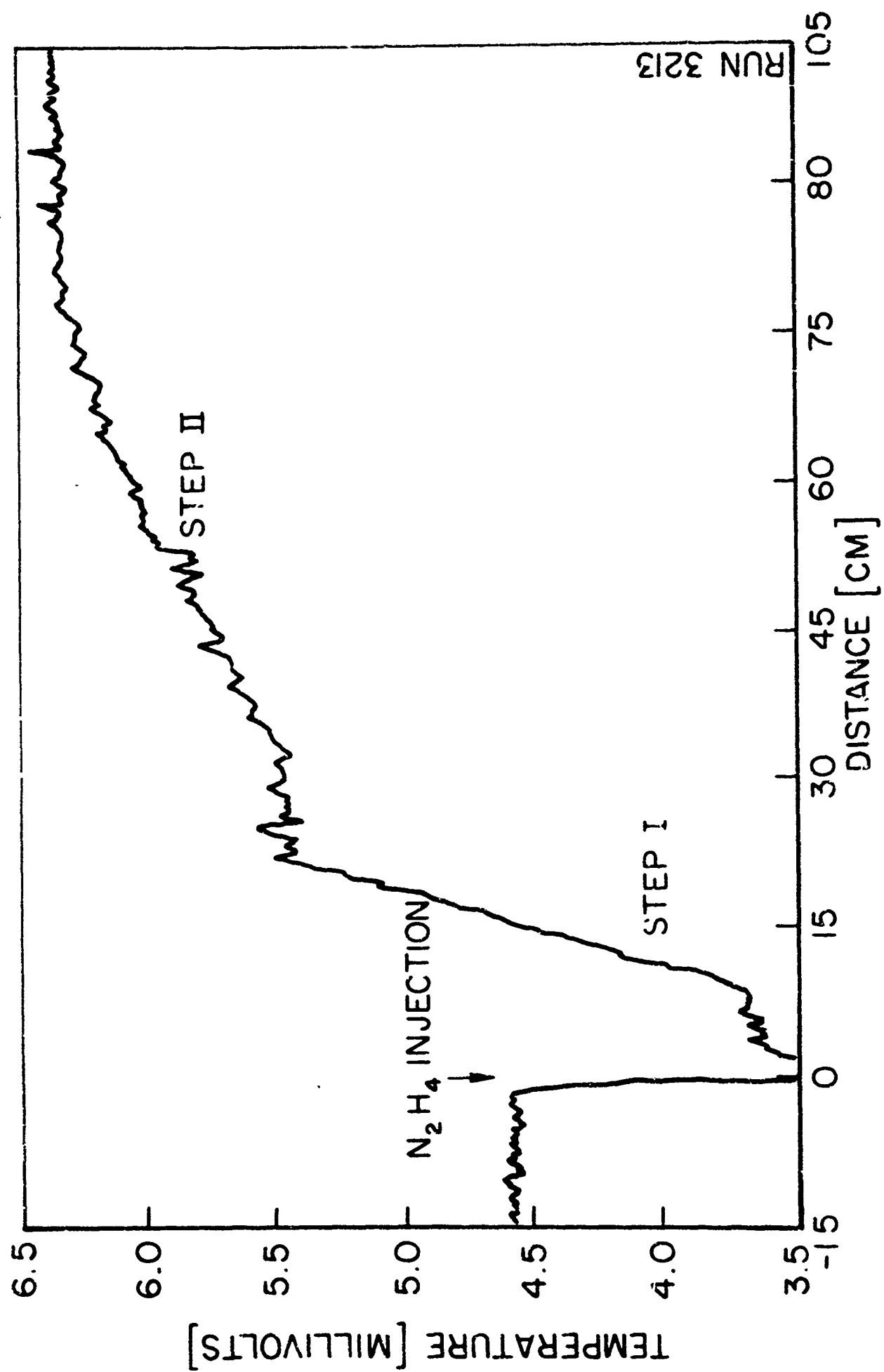
TABLE 14. Measured heats of reaction for hydrazine/  
nitrogen dioxide (kcal/mole  $\text{N}_2\text{H}_4$ )

##### step I



##### step II

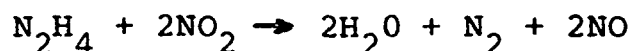




TEMPERATURE PROFILE, HYDRAZINE / NITROGEN DIOXIDE

FIGURE 36

The compositions listed above are the initial compositions and the heats of reaction therefore per initial mole of hydrazine. Since the heat of reaction usually relates to "per mole reacted," some interpretation of the above is necessary. With excess nitrogen dioxide present, the temperature profile exhibits no plateau region and all of the hydrazine is consumed in a single rapid step, step I. The measured heat of reaction for this case, 105 (kcal/mole), is close to the theoretical heat of reaction for the reaction



for which

$$\Delta H_{f298}^{\circ} = -111.0 \text{ [kcal/mole N}_2\text{H}_4\text{]}$$

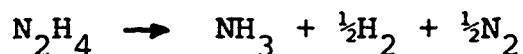
From this result and the additional observation that the plateau region approaches the final temperature as the amount of  $\text{NO}_2$  is increased and disappears at about an equivalence ratio of  $\phi = .5$ , one concludes that for the stoichiometric composition, one half of the hydrazine is consumed in each step. The step I heat of reaction is then 110 (kcal/mole  $\text{N}_2\text{H}_4$ ), calculated on the basis of the amount of hydrazine consumed, rather than the 55 (kcal/mole) calculated on the basis of the total amount of hydrazine present. Similarly, the heat of reaction for step II is now seen to be 160 (kcal/mole  $\text{N}_2\text{H}_4$ ), also based on the actual consumption of hydrazine. Complete oxidation of the hydrazine therefore does not occur according to the reaction



for which

$$\Delta H_{f298}^{\circ} = -181.5 \text{ [kcal/mole } N_2H_4]$$

The competing decomposition of hydrazine results in some of the hydrogen being trapped as molecular hydrogen or ammonia.



for which

$$\Delta H_{f298}^{\circ} = -33.8 \text{ [kcal/mole } N_2H_4]$$

The observed heat of reaction indicates that about 15% of the hydrazine decomposes without reaction. This estimate should not be considered an accurate determination because of the uncertainty in the hydrazine flow measurement. The overall heat of reaction is measured to be 135 (kcal/mole  $N_2H_4$ ), that is  $55 + 89$ , which is to be compared with the heat of reaction for the overall reaction



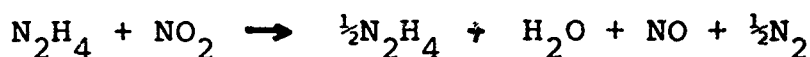
$$\Delta H_{f298}^{\circ} = 146 \text{ [kcal/mole } N_2H_4]$$

The measured rates, discussed in the following section, further indicate that step I occurs without substantial decomposition of any excess unconsummed hydrazine and that step II depends upon the decomposition of hydrazine. Addi-

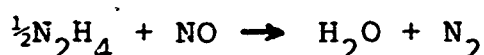
tionally, the observed behavior of the hydrazine/nitric oxide reaction corresponds closely to the step II hydrazine/nitrogen dioxide reaction.

In summary, the reaction of hydrazine and nitrogen dioxide is observed to take place in two distinct steps and is described approximately by the following overall reactions.

step I



step II



step I + step II



A detailed discussion of the plausibility of these steps in terms of a suitable reaction mechanism is presented in Section 7.1.4.

#### 7.1.2 Experimental results

Since the flow reactor is suited to the study of reactions with absolute rates occurring in the range of 10 to 1000 ( $\text{sec}^{-1}$ ), with measurements most readily obtained in the range of absolute rates of 20 to 100 ( $\text{sec}^{-1}$ ), the study of the two steps of the hydrazine/nitrogen dioxide reaction necessarily was made in two different temperature ranges. It was impossible to obtain a temperature

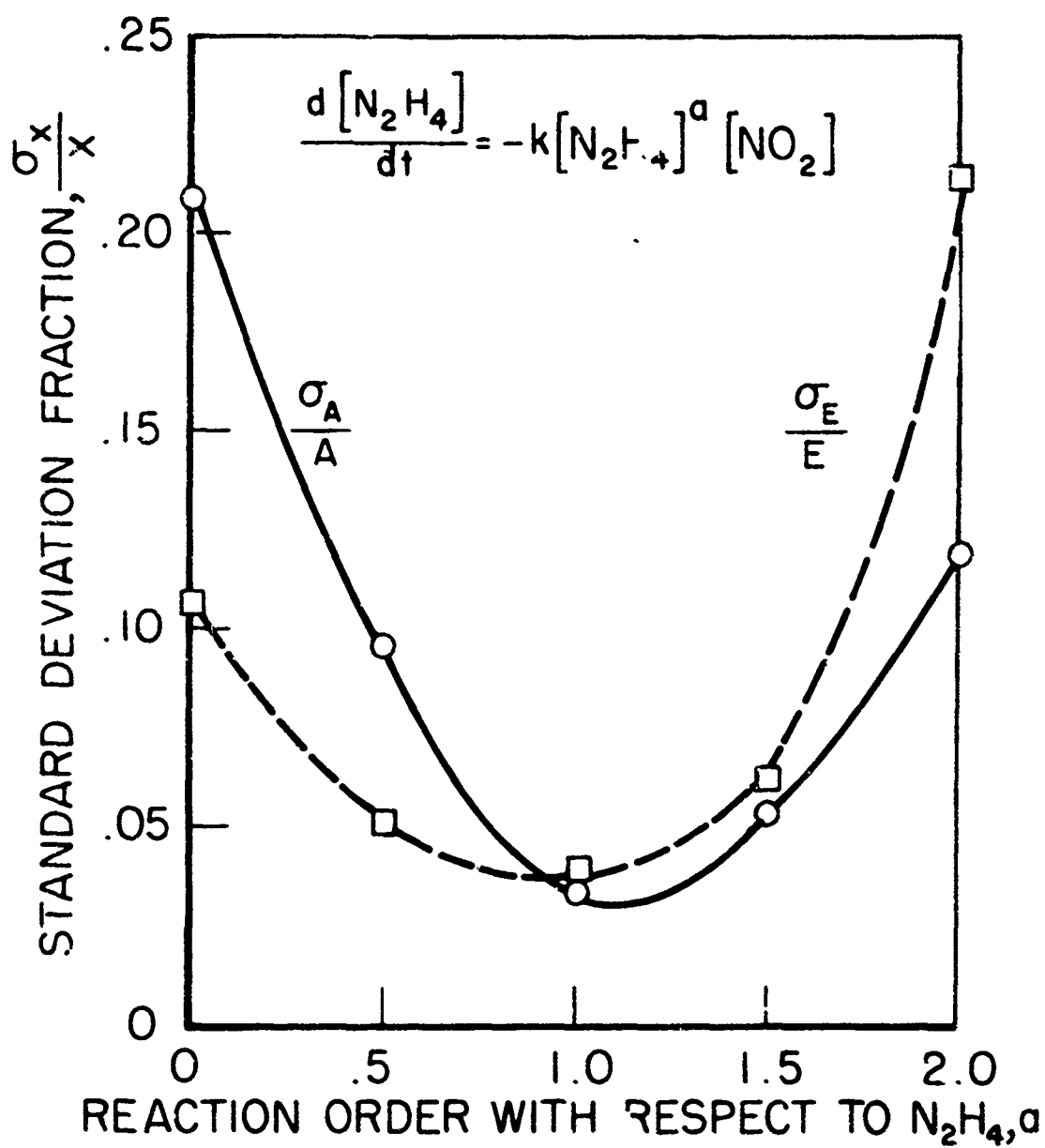


trace from a single experiment which would yield satisfactory rate measurements for both steps. Either step II of the reaction would not reach a constant temperature (as required for determination of the reaction rate) or step I would be crowded into too short a distance to allow accurate determination of the rate. After sufficient runs had been made to establish the existence of two steps in a single experiment, the two steps were studied separately. Step I of the reaction was studied at lower temperatures, using mixtures containing excess nitrogen dioxide. Step II was studied at higher temperatures, using approximately stoichiometric mixtures.

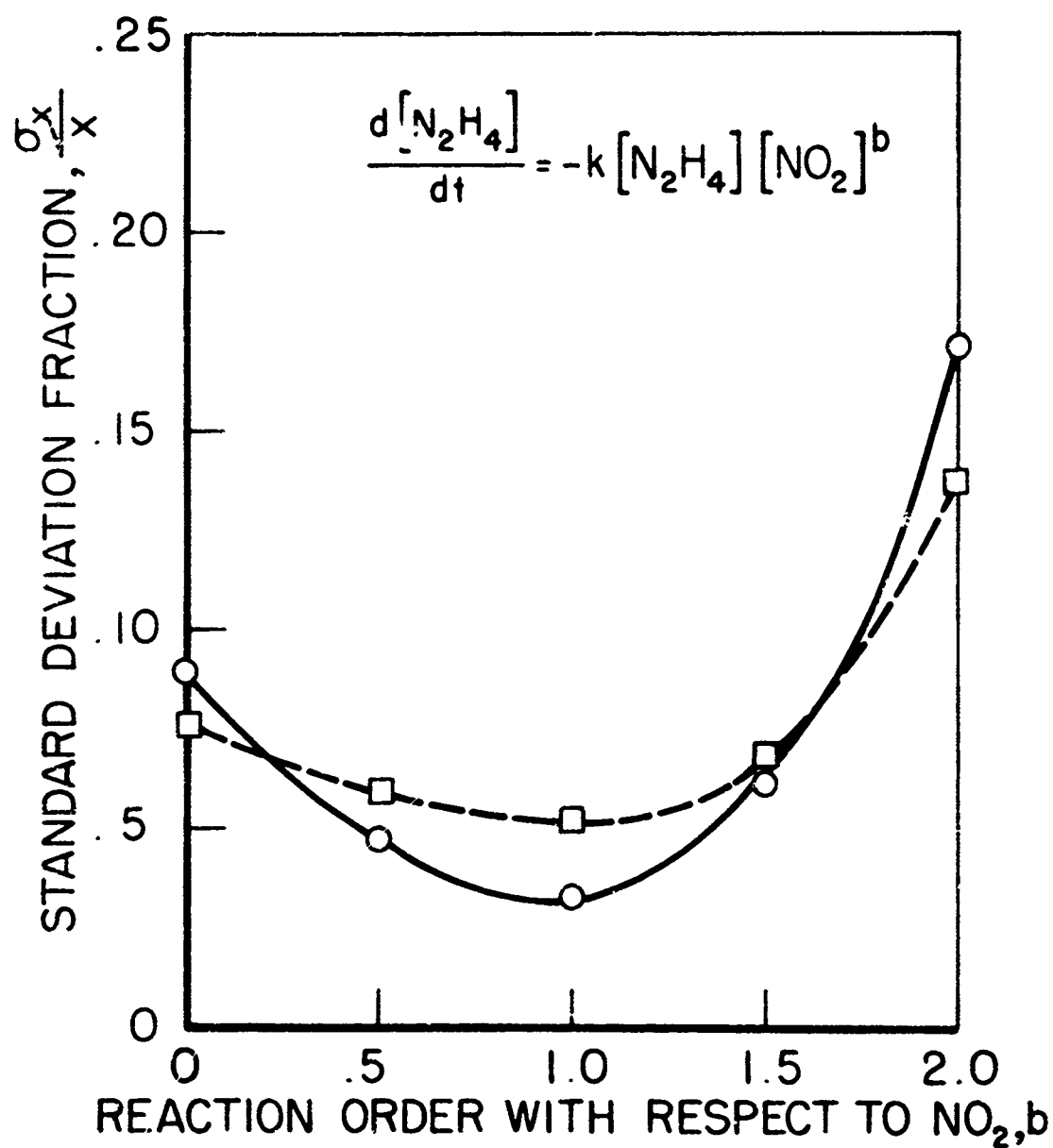
A reaction was observed, but not measured, at very low temperature, about  $400^{\circ}\text{K}$ , which produced a heavy white cloud of particles.

#### 7.1.2.1 Step I, reduction of nitrogen dioxide to nitric oxide

Sufficient experimental data were not obtainable to allow direct determination of the reaction orders from the variation of the reaction rate with reactant concentration at a given temperature. Therefore, the statistical approach, which allows the using of rates measured at all temperatures to determine the reaction orders, was employed. The method, the results of which are presented in Figures 37 and 38, gives first order dependencies upon both the hydrazine and nitrogen dioxide concentrations. Reaction rates were measured in the temperature range of  $810 \leq T \leq 888^{\circ}\text{K}$  and at equivalence ratios of  $.2 \leq \phi \leq .3$ , insuring that the hydrazine could be oxidized completely while the nitrogen dioxide was reduced only to nitric oxide. Since the experiments were conducted with approximately constant excess oxidizer concentrations, the rate



DETERMINATION OF REACTION ORDER FROM STATISTICAL CURVE FIT, HYDRAZINE / NITROGEN DIOXIDE (STEP I)



DETERMINATION OF REACTION ORDER FROM STATISTICAL CURVE FIT, HYDRAZINE / NITROGEN DIOXIDE (STEP I)

constants could be expressed satisfactorily neglecting the oxidizer concentration dependency which additionally simplifies comparison with other hydrazine reactions. That is, the standard deviation at  $b = 0$  is not much greater than at  $b = 1$  (see Figure 38). Reaction rate constants are calculated according to the rate equation

$$\frac{d[N_2H_4]}{dt} = -k[N_2H_4]$$

The experimental results, presented in Table 31 and Figure 64, yield the rate constant

$$k = 10^{8.43} \exp (-26700/RT) \quad [\text{sec}^{-1}]$$

Recall, however, that the observed rate dependency follows a second order rate equation

$$\frac{d[N_2H_4]}{dt} = -k[N_2H_4][NO_2]$$

for which

$$k = 10^{15.82} \exp (-26700/RT) \quad [(\text{mole/cc})^{-1} \text{ sec}^{-1}]$$

JP 13-4041-65

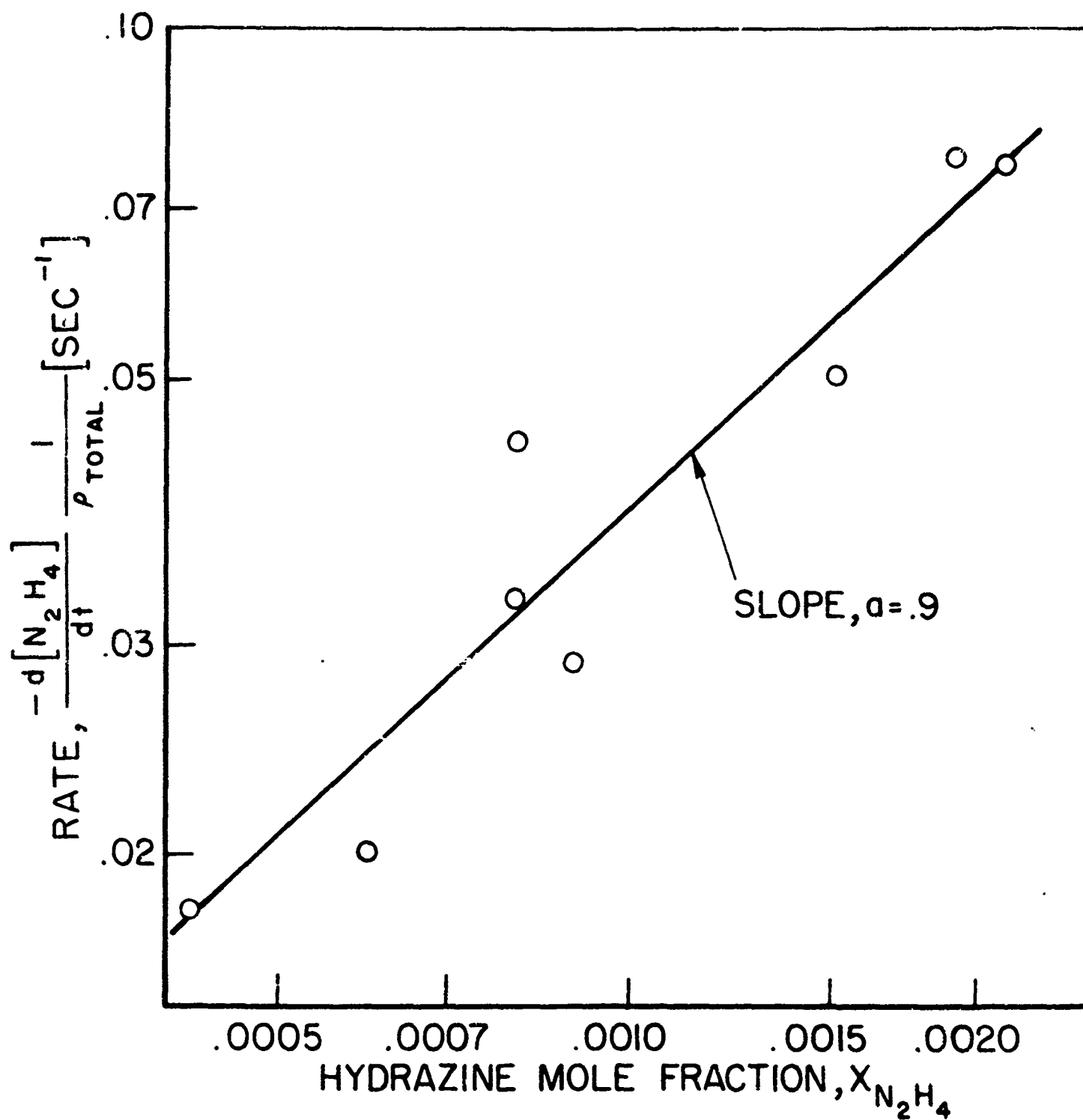
## 7.1.2.2 Step II, reduction of nitric oxide

The reaction orders for the second step of the reaction are determined directly from the variation of the reaction rate with concentration at a selected temperature. The dependence upon the hydrazine concentration is found to be slightly less than first order,  $a = .9$  (Figure 39). The dependency upon the oxidizer concentration is interpreted to be the order with respect to nitric oxide. All of the nitrogen dioxide is assumed to have been reduced to nitric oxide in the step I of the reaction. Figure 40 shows a zero order dependency,  $b = 0$ , upon the nitric oxide concentration. These results are in close agreement with the results of the investigation of the hydrazine/nitric oxide reaction. The experimental results, presented in Table 31 and Figure 65, are summarized by the following rate equation and rate constant

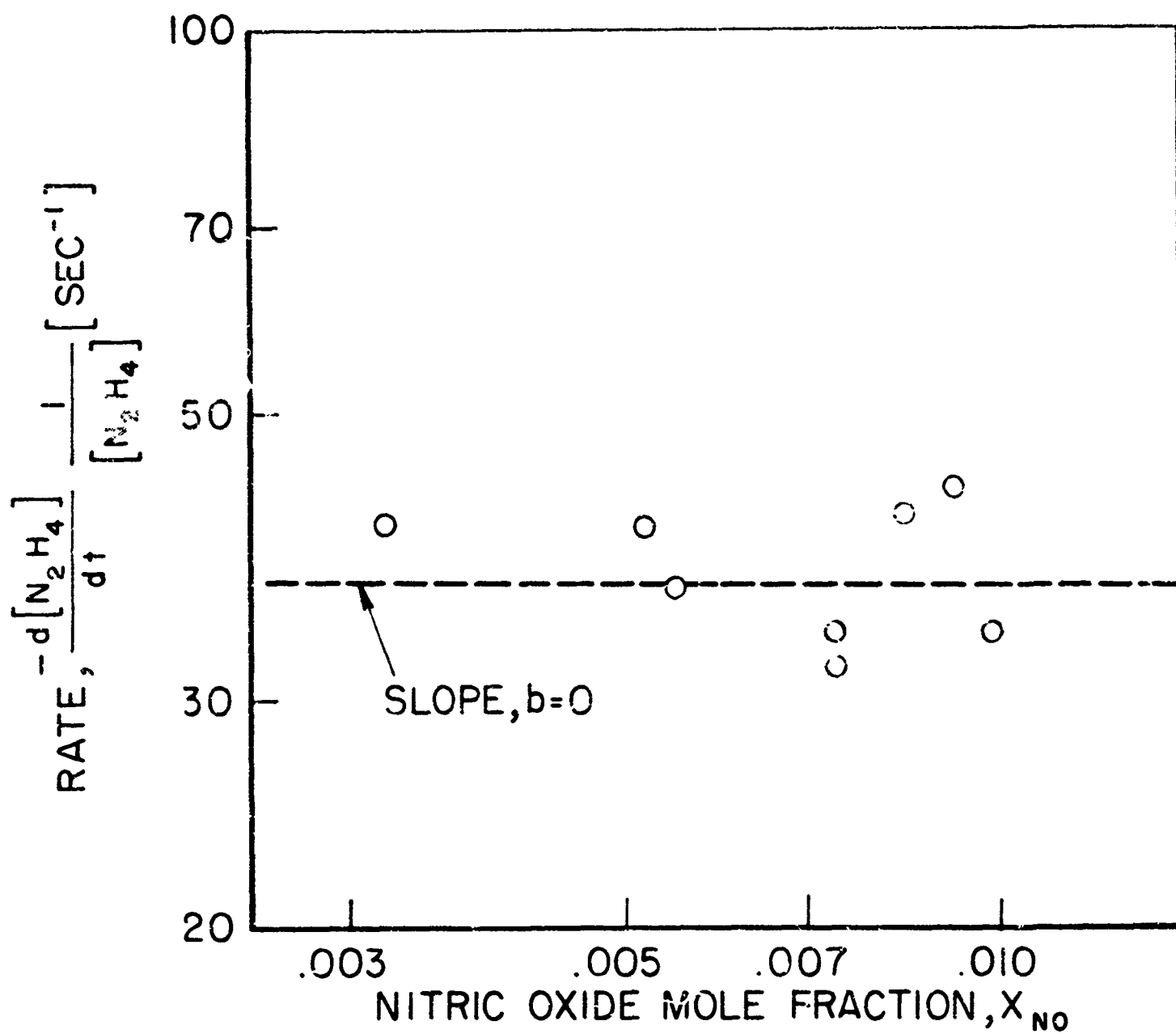
$$\frac{d[N_2H_4]}{dt} = -k[N_2H_4]$$

$$k = 10^{10.17} \exp(-39600/RT) \quad [\text{sec}^{-1}]$$

Once again, the rate constants are presented on the basis of a first order dependency upon the hydrazine concentration (rather than .9 order) to facilitate comparison and because the correlation of experimental data is almost as good for  $a = 0.9$ .



HYDRAZINE /NITROGEN DIOXIDE REACTION RATES (STEP II)  
 $T=1000^{\circ}K$ , DEPENDENCE ON HYDRAZINE CONCENTRATION



HYDRAZINE/NITROGEN DIOXIDE REACTION RATES (STEP II)  
 T = 1000°K, DEPENDENCE ON NITRIC OXIDE CONCENTRATION

FIGURE 40

### 7.1.2.3 Comparison of steps I and II

In addition to the large difference in reaction rates, other characteristics distinguish the two steps in the hydrazine/nitrogen dioxide reaction. The second step is independent of the oxidizer concentration while the first step shows a first order dependency. The first step shows an overall activation energy 13 (kcal/mole) less than for the second step, 26.7 versus 39.6 (kcal/mole). The first step occurs at a rate which is much faster than the rate of the decomposition of hydrazine. The second step occurs at approximately the same rate as "wet" hydrazine decomposition (see section 7.1.4.1 and Figure 45).

### 7.1.3 Results of other investigators

No other measurements of the hydrazine/nitrogen dioxide reaction rate are known. No premixed flame studies are known, no doubt due to the reactivity of the species at room temperature. Several investigators have studied the burning of hydrazine droplets in an equilibrium  $\text{N}_2\text{O}_4 \rightleftharpoons 2\text{NO}_2$  atmosphere. Lawver (1) reports two flame regions, an "inner decomposition flame" and an "outer oxidation flame". One would conclude that the mechanics of droplet burning are such as to preclude the existence of the step I reaction, that is, hydrazine decomposition occurs prior to contact with nitrogen dioxide. One would speculate that upon increasing pressure, transition to a step I reaction might occur. Higher pressures would collapse the flame zone and favor the second order step I reaction over the first order hydrazine decomposition and/or first order step II reaction.

UP 13-4035-65



Wasko (108) has observed the reaction of hydrazine and nitrogen tetroxide vapors at low pressures,  $10^{-4}$  mmHg and room temperature. As pressure was increased to about 1 mmHg, the reaction changed from an "explosion" to a "slower reaction," probably due to increased dilution rather than a chemical effect. Wilber et al (3) have reported preliminary results of spontaneous ignition tests of hypergolic propellant systems at low pressures and temperatures ( $10^{-2}$  mmHg and room temperature (?)), some of which included the hydrazine/nitrogen tetroxide combination. They report only two results: (1) no explosion and (2) an explosion which destroyed the reaction vessel. Perlee, Imhof, and Zabetakis (2) determined flammability limits of liquid hydrazine, monomethylhydrazine, and unsymmetrical dimethylhydrazine in nitrogen dioxide/air mixtures at one atmosphere. They observed ignition of hydrazine at  $25^{\circ}\text{C}$  at as low as 8% by volume  $\text{NO}_2$ . They also observed the reaction to produce a "white cloud of fine particles," apparently similar to the observation in the present experiments at temperature of about  $125^{\circ}\text{C}$ .

The most thorough investigation of hydrazine/nitrogen tetroxide ignition appears to have been that of Skinner, Hedley, and Snyder (4). The ignitions of both diluted vapor streams and of hydrazine droplets in an atmosphere containing nitrogen dioxide vapor were studied at temperatures of  $75^{\circ}\text{C}$ . The failure to find an inhibitor for the reaction led the investigators to conclude that the reaction mechanism was thermal rather than chain branched. The white solid produced in the pre-ignition (low temperature) reaction was identified as ammonium nitrate. In spectroscopic studies of the diffusion flame, the dominant feature was found to be the emission spectrum of  $\text{NH}_2$ . The presence of NH and OH were also detected. The analysis

of the gaseous products from a stirred reactor burning equal mole per cent of hydrazine and nitrogen dioxide (up to 6% each) in argon revealed the primary products to be nitrogen and nitric oxide with the reaction going to a maximum of 67% completion. No provision was made for detecting water.

#### 7.1.4 Reaction mechanism

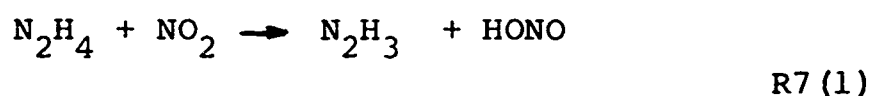
The mechanisms by which the reactions take place for the two steps are basically different. The step I reaction takes place under conditions which indicate that dissociation of the hydrazine and/or breaking of the N-N bond in the hydrazine molecule do not play a major role. The step II reaction, however, depends upon dissociation of the hydrazine, in particular, the breaking of the N-N bond.

##### 7.1.4.1 Step I, reduction of nitrogen dioxide to nitric oxide

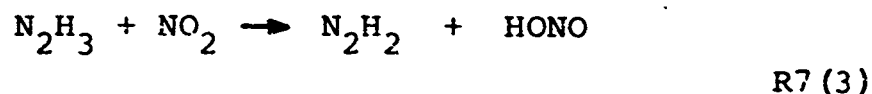
In comparing the reaction of hydrazine and nitrogen dioxide to the decomposition of hydrazine, one should note the role of water in slowing hydrazine decomposition. Eberstein (39) found that small amounts of water, (less than one per cent by volume, slowed the decomposition of hydrazine by a factor of about 10 (see Figure 45). Since in the present experiments, water is always present as a reaction product in concentrations exceeding this amount, this same inhibiting effect should be operative. The step I reaction proceeds at a rate exceeding the decomposition rates of both "wet and "dry" hydrazine. The breaking of the N-N bond in hydrazine requires 60 (kcal/mole) (14) and the decomposition of hydrazine proceeds with an

overall activation energy of about 36 (kcal/mole) (21,39). The even lower activation energy of the step I reaction, 26.7 (kcal/mole), therefore indicates that the step I reaction proceeds largely without dependence upon hydrazine decomposition or breaking of the hydrazine N-N bond.

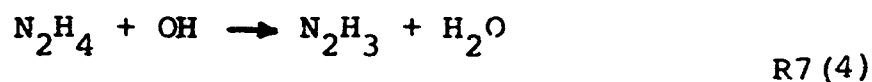
The mechanism proposed depends primarily upon the stripping of hydrogen atoms from  $N_2H_4$  and  $N_2H_3$  molecules. The susceptibility of hydrazine to such attack has been demonstrated by Gray and Thyne (26) in studies of H-atom abstraction from N-H bonds by methyl radicals. They found hydrazine to be 300 times more reactive than ammonia in this regard. The initiation step herein is postulated to involve such a hydrogen abstraction reaction to form HONO which subsequently decomposes to give OH and NO.

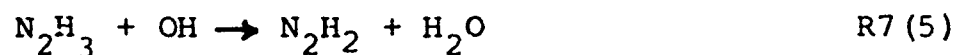


A second hydrogen abstraction should proceed almost as readily as the first

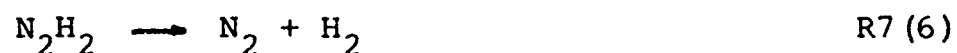


Other important reactions are postulated to be hydrogen abstraction by OH radicals,





the reactions,



and additional hydrogen abstractions by H atoms,



Taking a simplified model based on the first five reactions, R7(1) to R7(5), which are likely to be the rate controlling steps, and making the usual steady state assumption, the concentrations of the intermediates are found to be

$$[\text{OH}] = \left( \frac{k_1 k_3}{k_4 k_5} \right)^{\frac{1}{2}} [\text{NO}_2]$$

$$[\text{N}_2\text{H}_3] = \left( \frac{k_1 k_4}{k_3 k_5} \right)^{\frac{1}{2}} [\text{N}_2\text{H}_4]$$

$$[\text{HONO}] = \left\{ \frac{k_1 + \left( \frac{k_1 k_3 k_4}{k_5} \right)^{\frac{1}{2}}}{k_2'} \right\} [\text{N}_2\text{H}_4][\text{NO}_2]$$

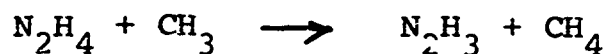
Since the specie, M, in reaction R7(2) is most likely the inert carrier nitrogen and has a nearly constant concentration, we can substitute

$$k_2^1 = k_2 [\bar{M}]$$

The reaction rate is then

$$\frac{d[N_2H_4]}{dt} = - \left\{ k_1 + \left( \frac{k_1 k_3}{k_4 k_5} \right)^{1/2} \right\} [N_2H_4][NO_2]$$

which demonstrates the experimentally observed first order dependence upon both hydrazine and nitrogen dioxide. Since one would expect the OH radical to be more effective than nitrogen dioxide in the hydrogen abstraction reactions, the second term in the rate constant is assumed to be small compared to the first. The observed rate is expected, therefore, to be characteristics of the rate of abstraction of hydrogen from hydrazine by nitrogen dioxide. As would be expected, the rate is much less than observed by Gray and Thyne (16) for the similar reaction

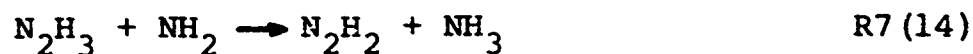
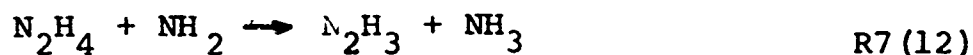


#### 7.1.4.2 Step II, reduction of nitric oxide

The observed reaction of hydrazine with nitric oxide

and the failure to observe the reaction of hydrogen or ammonia with nitric oxide has been attributed to the reactivity of nitric oxide with  $\text{NH}_2$  and  $\text{NH}$  radicals (71, 109, 25, 110). Since decomposition of hydrazine is postulated to proceed largely by the breaking of the N-N bond and thereby produce a supply of  $\text{NH}_2$  and  $\text{NH}$  radicals, the observation that the step II hydrazine/nitrogen dioxide and the hydrazine/nitric oxide reactions have the same rate as for inhibited hydrazine decomposition is consistent with the proposed mechanism. While sufficient water is present as a reaction product in the present experiments to inhibit the hydrazine decomposition, the nitric oxide, as a scavenger of  $\text{NH}_2$  and  $\text{NH}$  radicals, similarly would be expected to inhibit hydrazine decomposition. It is difficult to establish which, if either, inhibition mode predominates in the present experiments.

The decomposition of hydrazine, which was discussed in Section 2.1.2, plays a major role in the mechanism of the hydrazine/nitric oxide reaction. Important steps in hydrazine decomposition are summarized below.



The radical,  $\text{NH}$ , would participate in abstraction reactions similar to R7(12) and R7(14); however, since  $[\text{NH}] \ll [\text{NH}_2]$  (39) such reactions are of secondary importance.

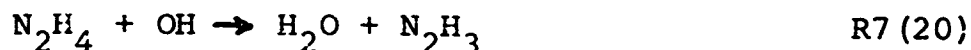
The weaker N-H bond in hydrazine, as compared to the N-H bond in ammonia or the H-H hydrogen bond, might provide a route for hydrazine/nitric oxide reaction through hydrogen abstraction to form  $\text{HNO}$ . The failure to observe a low temperature, "step I" reaction, however, contradicts this possibility. Rather, the reaction of nitric oxide and the amine radical to form nitrosamine and its subsequent decomposition are postulated,



as is a similar reaction with the amide radical,



Also postulated is the reaction



The mechanism is a complex one and does not lend itself to ready simplifications. The steady state solution may be obtained for two extreme cases involving the reaction of  $\text{N}_2\text{H}_3$ . If all  $\text{N}_2\text{H}_3$  disappears by dissociation, ie.  $k_{14}=0$ .

$$\frac{d[\text{NO}]}{dt} = -2k_{11}[\text{N}_2\text{H}_4] \left\{ 1 + \frac{k_{12}}{k_{16}} \frac{[\text{N}_2\text{H}_4]}{[\text{NO}]} \right\}$$

If, on the other hand, all  $\text{N}_2\text{H}_3$  is consumed by hydrogen abstraction, ie.  $k_{13} = 0$ ,

$$\frac{d[\text{NO}]}{dt} = -2k_{11}[\text{N}_2\text{H}_4] \left\{ \frac{1}{1 + \frac{2k_{12}}{k_{16}} \frac{[\text{N}_2\text{H}_4]}{[\text{NO}]}} \right\}$$

Since R7(16) is a radical-radical reaction and R7(12) is an abstraction reaction,  $k_{16} \gg k_{12}$ . Hence, for both cases

$$\frac{d[\text{NO}]}{dt} \approx -2k_{11}[\text{N}_2\text{H}_4]$$

Reactions R7(3) and R7(4) are probably both important. The disappearance of NO shows the observed approximately first order dependence on hydrazine and no dependence on nitric oxide. The mechanism predicts an increase in the overall activation energy compared to simple hydrazine decomposition, because of the increased role of the breaking of the 60 (kcal/mole) hydrazine N-N bond; this effect is observed.

## 7.2 HYDRAZINE/OXYGEN

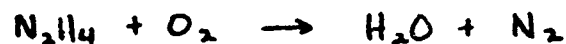
The hydrazine/oxygen reaction, unlike the previous reaction, exhibits a single characteristic reaction rate,



as, indeed, is observed for all other of the reactions studied.

### 7.2.1 Stoichiometry

The heat of reaction is measured to be 135 (kcal/mole  $N_2H_4$ ) which is in fair agreement with the heat of reaction for the complete oxidation of hydrazine

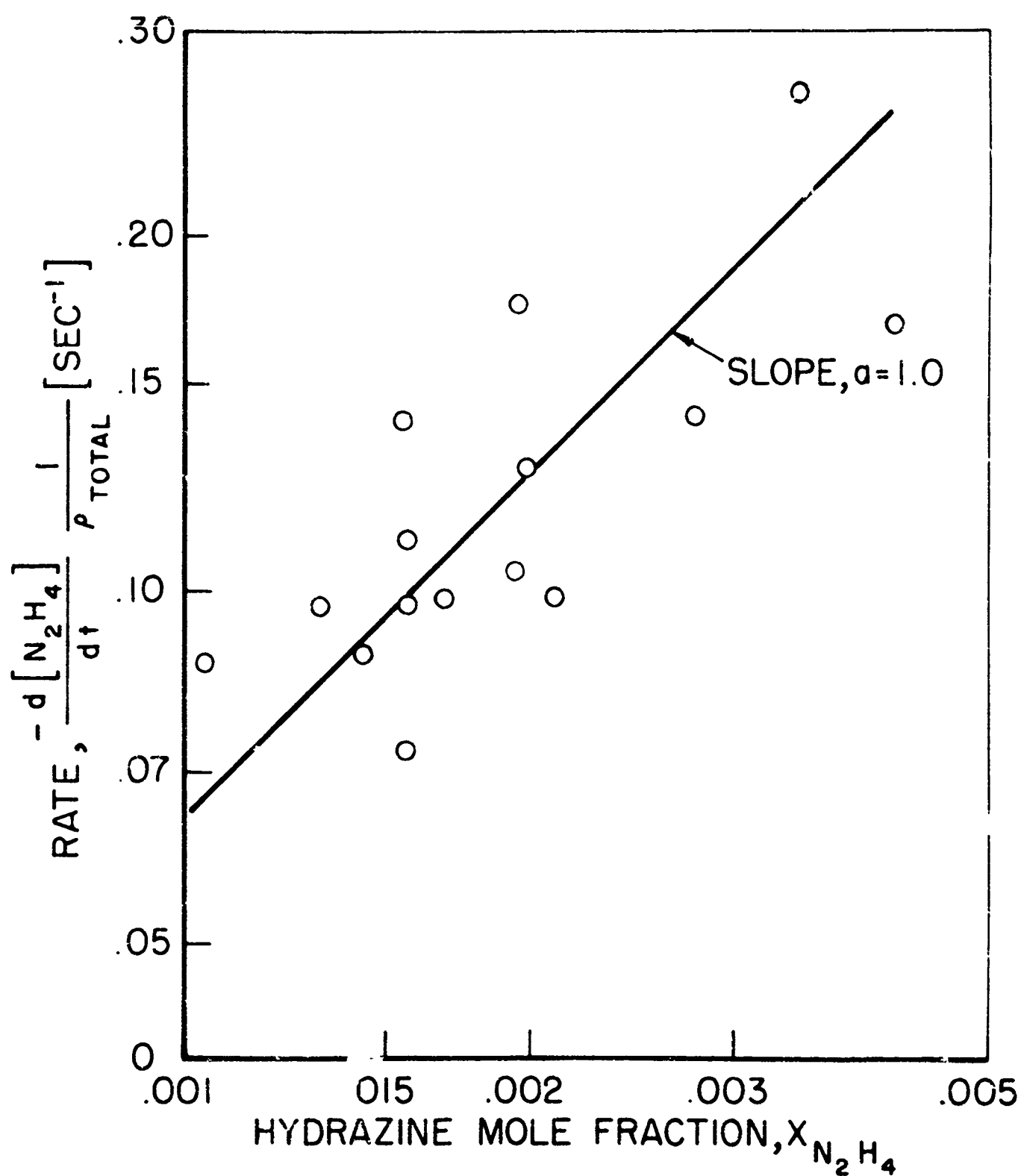


$$\Delta H_{f,298}^0 = -138.4 \text{ [kcal/mole } N_2H_4]$$

### 7.2.2 Experimental results

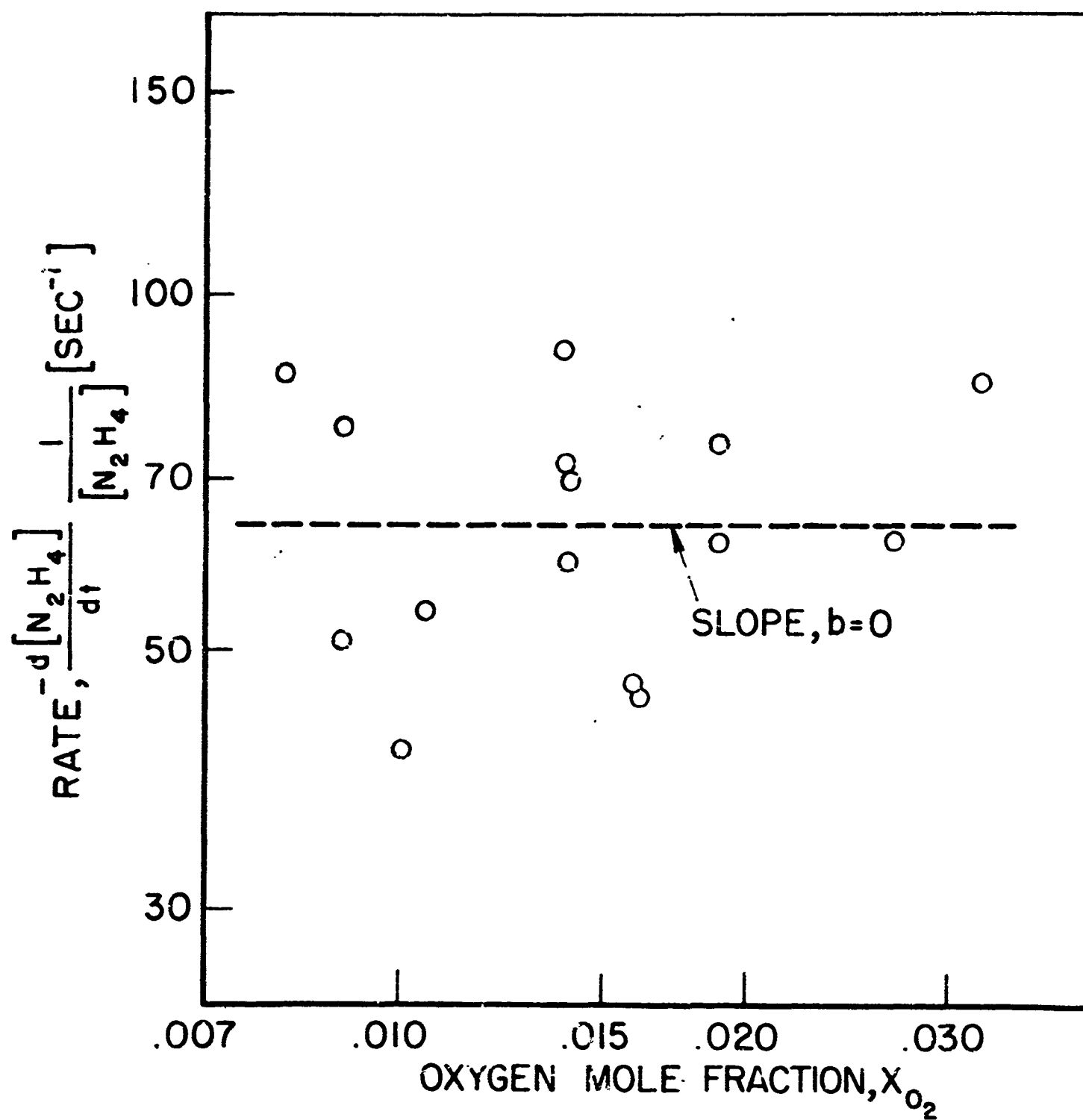
Reaction rates were measured in a four inch quartz duct at equivalence ratios of  $.2 \leq \phi \leq .5$ , or in the oxidizer rich region. The reaction order, determined from the variation in the reaction rate at  $1000^\circ K$  with the concentration of reactants, is shown to be first order with respect to the hydrazine (Figure 41) and zero order with respect to the oxygen (Figure 42). The experimental parameters and rates are summarized in Table 32 and Figure 66. According to the rate equation,

$$\frac{d[N_2H_4]}{dt} = -k[N_2H_4]$$



HYDRAZINE /OXYGEN REACTION RATES,  $T=1000^{\circ}K$ ,  
DEPENDENCE ON HYDRAZINE CONCENTRATION

FIGURE 11



HYDRAZINE/OXYGEN REACTION RATES,  $T=1000^{\circ}\text{K}$ ;  
DEPENDENCE ON OXYGEN CONCENTRATION

FIGURE 42

the rate constant is found to be

$$k = 10^{9.41} \exp(-37200/RT) \quad [\text{sec}^{-1}]$$

### 7.2.3 Results of other investigators

Gray and Lee (25) in studies of hydrazine/oxygen flames, measured flame speeds greater than those for hydrazine/nitric oxide or for the hydrazine decomposition flame. While the high heat of reaction and resulting higher temperature accounts for the greater rate of the hydrazine/oxygen flame over the hydrazine decomposition flame, their results show oxygen to be more reactive than nitric oxide with hydrazine.

TABLE 15. Hydrazine flame speeds, Gray and Lee (25), 40 mmHg

	$\Delta H_R$	$T_B$	$S_U$
	kcal/mole	$^{\circ}\text{K}$	cm/sec
$\text{N}_2\text{H}_4$ (decomposition)	33.7	1904	110
$\text{N}_2\text{H}_4 + \text{O}_2$	138.3	2700	280
$\text{N}_2\text{H}_4 + 2\text{NO}$	181.5	2745	245

They propose that the oxidation and decomposition occur simultaneously. Hussain and Norrish (105) have made spectroscopic studies of the low temperature explosive

oxidation of hydrazine induced by flash photolysis. They conclude that the major reaction "giving rise to nitrogen as a product" does not involve breaking of the N -N bond. Hall and Wolfhard (24) attribute an observed two stage hydrazine/oxygen flame to a decomposition zone followed by oxidation. The observations of Gray and Lee (25) led them to conclude, however, that a two stage process is not likely for the hydrazine/oxygen flame. No common role for the decomposition of hydrazine has been agreed upon by past investigators. While Michel and Wagner (32) report that mixture ratios of  $[O_2]/[N_2H_4] > 2$ , accelerate hydrazine decomposition, their experiments performed in a shock tube, reflect only the initiation of decomposition. Any such effect in the present studies would be masked by the inhibition of decomposition by product water.

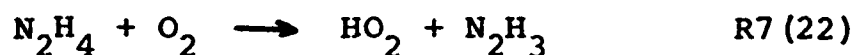
#### 7.2.4 Reaction mechanism

The present experiments indicate that decomposition and oxidation are occurring simultaneously. The reaction rate lies between that observed for hydrazine and for "wet" hydrazine and exhibits an overall activation energy close to that for hydrazine decomposition, 37.2 (kcal/mole) for the hydrazine/oxygen reaction versus 36.2 (kcal/mole) for hydrazine decomposition. That the reaction is observed to be first order with respect to hydrazine and to exhibit little dependence upon the oxygen concentration favors a strong role for hydrazine decomposition.

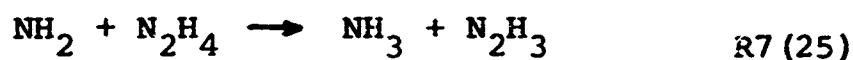
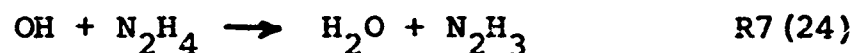
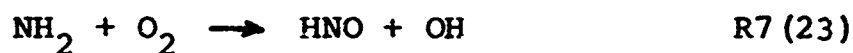
The mechanism is necessarily complex; the reactions which are felt to be the most important are discussed below. Initiation of the reaction is likely to occur primarily through fission of the hydrazine N -N bond.



In addition, the hydrogen abstraction reaction



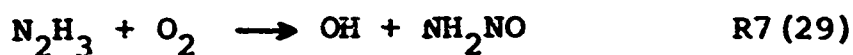
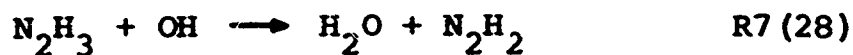
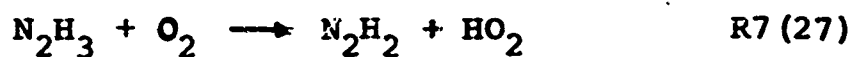
is a second initiation possibility. Propagation can then occur by



The last reaction is a step characteristic of hydrazine decomposition. Fission of the  $\text{N}_2\text{H}_3$  molecule, in the following chain branching reaction, would further add to the hydrazine decomposition character of the overall reaction

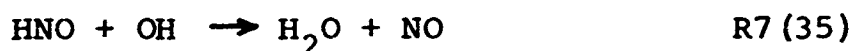
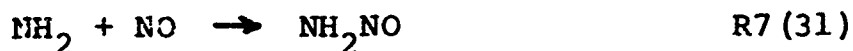


while further hydrogen abstractions from this same molecule



favor the "oxidation" character of the reaction.

Suggested possible termination reactions are



Additionally, since hydrazine decomposition will result in the formation of hydrogen and ammonia, the reactions which occur between these species and oxygen will take place also in the hydrazine/oxygen reaction.

Taking a simplified system of reactions based on equations R7(21), R7(23), R7(24), R7(25), R7(26), and R7(29) above and making the usual steady state assumption, the rate is found to be

$$\frac{d[\text{O}_2]}{dt} = -k_{21}[\text{N}_2\text{H}_4] \left\{ \frac{1 + \frac{k_{25}}{k_{27}[\text{O}_2]}}{1 + \frac{k_{24}[\text{N}_2\text{H}_4]}{k_{22}[\text{O}_2]}} \right\}$$

The steady state solution is simplified by using the disappearance of the oxidizer to describe the reaction rate, rather than the disappearance of the fuel as has been used previously. The experimental results indicate

that

$$\frac{d[N_2H_4]}{dt} \approx \frac{1}{2} \frac{d[O_2]}{dt}$$

The above expression (page 180) shows only a weak dependence on the oxygen concentration and a somewhat less than first order dependence on the hydrazine concentration, both consistent with the experimental observations.

### 7.3 HYDRAZINE/NITRIC OXIDE-OXYGEN

The reaction of decomposed nitrogen dioxide (a mixture of 2 parts nitric oxide to one part oxygen) with hydrazine was studied in an attempt to obtain direct evidence of the effect of nitrogen dioxide decomposition on its subsequent reaction with hydrazine. The decomposition of nitrogen dioxide was obtained by injection of the nitrogen dioxide upstream of the carrier gas heat exchangers.

#### 7.3.1 Stoichiometry

Because of the range of equivalence ratios studied,  $.15 \leq \phi \leq .45$ , sufficient molecular oxygen was present in all cases to effect the complete oxidation of the hydrazine and/or its decomposition products without the reaction of any of the nitric oxide. That oxygen is the primary oxidizer is evidenced by several observations. The measured heat of reaction is found to be about 130 (kcal/mole  $N_2H_4$ )



which is closer to the reaction of hydrazine and oxygen, 138 (kcal/mole  $N_2H_4$ ), than to the reaction of hydrazine and nitric oxide, 181.5 (kcal/mole  $N_2H_4$ ). No two step reaction was observed. The reaction rates are close to those of hydrazine and oxygen. The experimental results represent, then, the effect of nitric oxide on the hydrazine/oxygen reaction, according to the probable overall stoichiometry



### 7.3.2 Experimental results

Reaction rates were measured in the 4 (inch) quartz reactor duct and rate constants calculated according to a first order reaction with respect to hydrazine

$$\frac{d[N_2H_4]}{dt} = -k[N_2H_4]$$

The experimental parameters are summarized in Table 33 and the rate constants plotted in Figure 67. The rate constant expression for the above rate equation is

$$k = 10^{10.35} \exp(-39100/RT) \quad [\text{sec}^{-1}]$$

### 7.3.3 Results of other investigators and reaction mechanism

While no other investigations of the reaction of hydrazine and mixtures of nitric oxide and oxygen are known, the work on the reaction of each of the oxidizers separately with hydrazine does pertain and is discussed elsewhere in the present chapter. It is to be noted

that a mixture of nitric oxide and oxygen is peculiar to the present experiment in which the oxidizer can be held at relatively high temperature before the reaction begins. At lower induction temperatures, as associated with a premixed gas burner, the presence of oxygen would cause the conversion of nitric oxide back to nitrogen dioxide.

The reaction mechanism is postulated to be that of the hydrazine/ oxygen reaction and therefore is not repeated here. The failure of the nitric oxide to affect the reaction rate is somewhat surprising and requires some comment. By acting as a sink for  $\text{NH}_2$  radicals, nitric oxide should slow the decomposition of hydrazine and therefore slow the hydrazine/oxygen reaction. The explanation may lie in the subsequent decomposition of nitrosamine, reactions R7(17a) and R7(17b), which is postulated to produce OH and H radicals. This effective trading of  $\text{NH}_2$  radicals for OH and H radicals could reasonably account for the failure of nitric oxide to affect the hydrazine/oxygen reaction rate. It is observed that oxygen increases the hydrazine decomposition rate, probably by injecting excess radicals produced in the reaction of oxygen with the hydrazine decomposition fragments. The effect on hydrazine decomposition of OH and H radicals produced by the decomposition of nitrosamine could balance the  $\text{NH}_2$  draining effect of nitric oxide.

#### 7.4 HYDRAZINE/NITRIC OXIDE

The reaction of nitric oxide and hydrazine was discussed in section 7.1 as the "step II" of the hydrazine

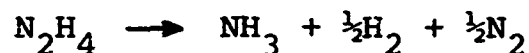
nitrogen dioxide reaction. Additional experiments were conducted "directly" upon the hydrazine/nitric oxide reaction. It was, indeed, the comparison of these two sets of experiments that led to the conclusion that the step II hydrazine/nitrogen dioxide reaction was the reaction of hydrazine and nitric oxide. The hydrazine/nitric oxide reaction is particularly interesting in that nitric oxide shows no reactivity toward hydrogen, ammonia, or mixtures of hydrogen and ammonia under conditions in which it reacts with hydrazine.

#### 7.4.1 Stoichiometry

As might be expected, the reaction fails to go to completion; the hydrogen is not oxidized completely to water. The measured heat of reaction is about 160 (kcal/mole  $\text{N}_2\text{H}_4$ ), somewhat below the predicted value of 181 (kcal/mole  $\text{N}_2\text{H}_4$ ) for the reaction



The measured heat of reaction is in agreement with that measured for the step II hydrazine/nitrogen dioxide reaction. As in that case, the observation is interpreted to indicate that some of the hydrazine is disappearing by the less energetic decomposition, 34 (kcal/mole  $\text{N}_2\text{H}_4$ ),



and that the ammonia and hydrogen so formed are not reacted. Based on the observed heat of reaction, approximately 85% of the hydrazine is consumed through reaction with nitric oxide while 15% decomposes without reaction, ie. oxidation resulting in the

appearance of hydrogen as water and ammonia as molecular nitrogen and water.

#### 7.4.2 Experimental results

Reaction orders are determined directly from the dependence of the reaction rate upon concentration at a selected reaction temperature. Dependence upon hydrazine concentration is found to be  $a = .75$ , Figure 43, and upon nitric oxide, to be  $b = 0$ , Figure 44. Initial equivalence ratios investigated are  $.3 \leq \phi_0 \leq 1.0$ . According to the rate equation,

$$\frac{d[N_2H_4]}{dt} = -k[N_2H_4]^{.75}$$

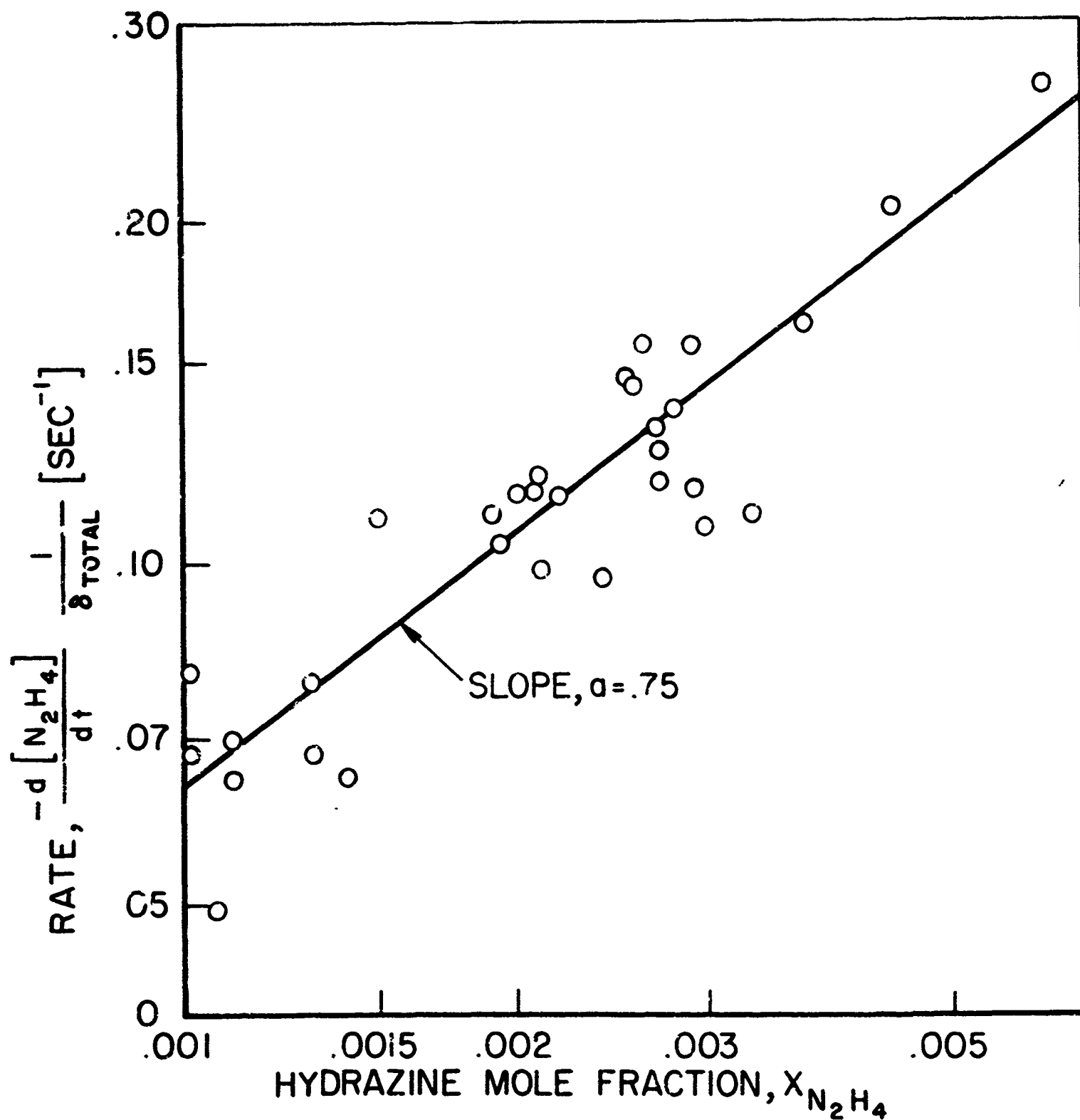
the rate constant is determined to be

$$k = 10^{6.40} \exp(-30700/RT) \quad [cc^{-.25} \text{ mols}^{.25} \text{ sec}^{-1}]$$

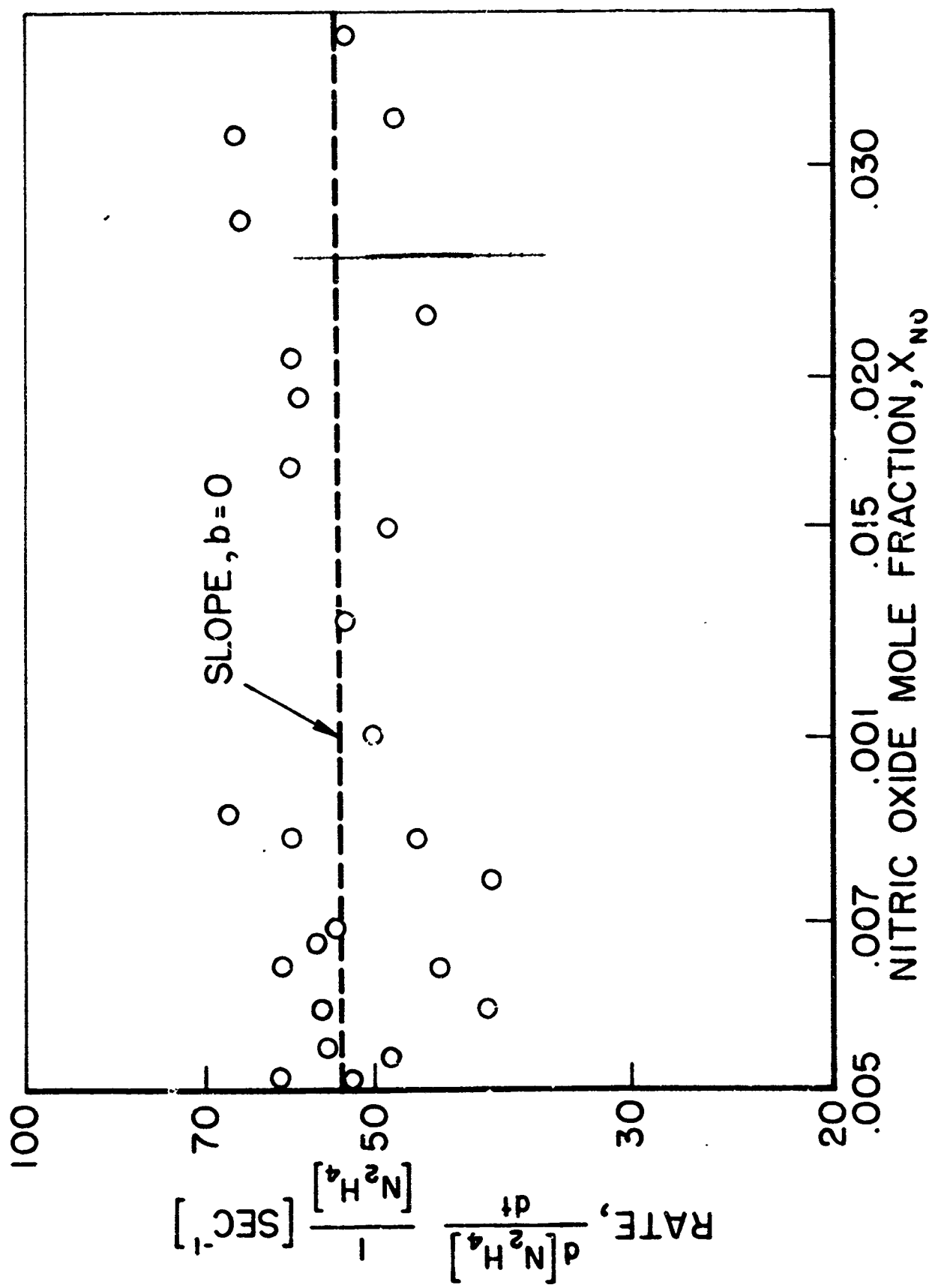
Experimental parameters are summarized in Table 34 and reaction rate constants presented in Figures 68 and 69. The measured rates and observed reaction orders are in good agreement with the step II hydrazine/nitrogen dioxide results.

#### 7.4.3 Results of other investigators

Hydrazine/nitric oxide flames have been studied by Gray and Lee (25) and by Hall and Wolfhard (24).



HYDRAZINE / NITRIC OXIDE REACTION RATES,  $T=1020^\circ K$ ,  
DEPENDENCE ON HYDRAZINE CONCENTRATION



HYDRAZINE / NITRIC OXIDE REACTION RATES,  $T=1020^{\circ}\text{K}$   
DEPENDENCE ON NITRIC OXIDE CONCENTRATION

Both pairs of investigators performed their experiments at low pressures, 40 and 30 to 150 mmHg, respectively. Gray and Lee measured flame speeds and found nitric oxide to be less reactive than oxygen. Hall and Wolfhard, from visual and spectroscopic investigations of the flame structure, concluded that a two stage reaction occurs, that is, decomposition followed by oxidation.

#### 7.4.4 Reaction mechanism

A proposed reaction mechanism has been discussed in Section 7.1.4.2. While the measured rates are approximately the same in the present reaction and the step II hydrazine/nitrogen dioxide reaction, an apparent difference in the overall activation energies exists. For hydrazine/nitric oxide and the step II hydrazine/nitrogen dioxide reactions, the overall activation energies are 45.4 and 39.6 (kcal/mole  $N_2H_4$ ), respectively, where the rate constants are both calculated on the basis of a first order dependence upon the hydrazine concentration. If the first case is calculated on the basis of a .75 order dependence upon the hydrazine concentration as is found to be more representative, the reverse trend occurs, that is 30.7 versus 39.6 (kcal/mole  $N_2H_4$ ). As an example, this state of affairs points out the difficulty in comparing overall activation energies of reactions with different reaction orders. One would expect from the proposed mechanism that the role of NO as a free radical sink would place a greater dependence upon the breaking of the N -N bond in hydrazine and therefore serve to increase the overall activation

energy for the hydrazine nitric oxide reaction. Since the rate of this reaction was measured at higher nitric oxide concentrations than the step II hydrazine/nitrogen dioxide reaction, one might expect such an increase in activation energy. That such an effect actually is occurring is difficult to establish because of the problem of comparing the overall activation energies for reactions exhibiting different orders.

The cause of the different dependence upon the hydrazine concentration also is difficult to predict from a reaction mechanism, especially since the two cases represent almost identical conditions of temperature and reactant concentrations. The product water concentration would be greater in the step II hydrazine/nitrogen dioxide than in the hydrazine/nitric oxide reaction and may account for the observed differences.

#### 7.5 COMPARISON OF HYDRAZINE REACTIONS

Because of the widely varying reaction rates of hydrazine with the different oxidizers studied, comparison at a single temperature involves substantial extrapolation, in particular of the step I hydrazine/nitrogen dioxide reaction rates. While no data were obtained which would allow accurate determination of the rate of the reaction at 1000°K, the reaction was observed to take place at this temperature at a very rapid rate and to proceed with a rate roughly as predicted by extrapolation of the rate measured in the 810 to 880°K temperature range. The reaction rates are ordered in the following table.

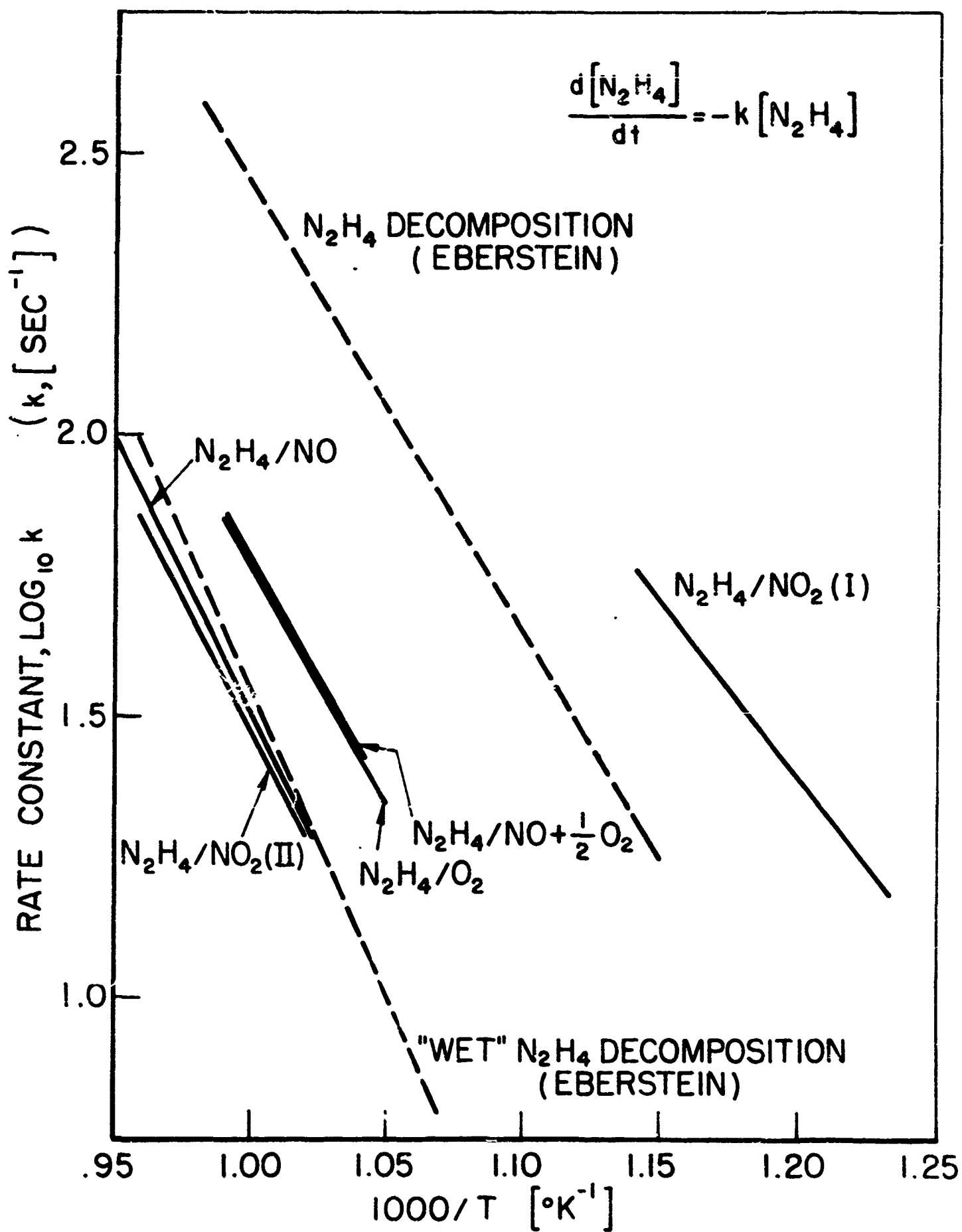


Table 16. Relative reaction rates, hydrazine reactions at 1000°K

<u>oxidizer</u>	<u>relative rate</u>
NO <sub>2</sub> (step I)	18
decomposition (39)	9
O <sub>2</sub>	2
NO + ½O <sub>2</sub>	2
decomposition "wet" (39)	1
NO	1
NO <sub>2</sub> (step II)	1

In another form, the hydrazine reaction rates as a function of temperature are compared graphically in Figure 45. For this comparison the rates for all reactions have been calculated on the basis of a first order dependence upon the hydrazine concentration. A final comparison of the observed reaction orders and overall activation energies is made in Table 17. Examination of Tables 16 and 17 and of Figure 45 in light of abbreviated versions of the proposed reaction mechanism, summarized in Table 18 reveals several interesting results.

(1) The step I reaction of hydrazine and nitrogen dioxide stands apart from the other hydrazine reactions in many respects. Its rate is the fastest of those reactions studied and exceeds the decomposition rate of hydrazine. It exhibits a much lower overall activation energy than any of the other reactions. The high reactivity of hydrazine and nitrogen dioxide is not the result of a chain branching mechanism but is attributed to the high effectiveness of nitrogen dioxide in hydrogen abstraction. Similarly, hydrazine provides a



COMPARISON OF HYDRAZINE REACTION RATES,  
NITROGEN CARRIER

TABLE 17. Comparison of reaction orders and overall activation energies, hydrazine reactions.

---

rate equation

$$\frac{d[N_2H_4]}{dt} = -k[N_2H_4]^a[X]^b$$


---

oxidizer, X	a	b	E <sub>1</sub> kcal/mole	E <sub>2</sub> kcal/mole
NO <sub>2</sub> (step I)	1.0	1.0	26.7	24.5
decomposition (141)	1.0	---	36.2	36.2
O <sub>2</sub>	1.0	0	37.2	37.2
NO + ½O <sub>2</sub>	1.0	0	39.1	39.1
decomposition "wet" (141)	1.0	---	not reported	---
NO	.75	0	30.7	45.4
NO <sub>2</sub> (step II)	.9	0	---	39.6

E<sub>1</sub>: activation energy, rate equation according to determined orders, a and b

E<sub>2</sub>: activation energy, rate equation according to first order dependence on hydrazine, a = 1, b = 0

x : oxidizer

---

TABLE 18. Summary of reaction mechanisms, hydrazine reactions

	$N_2H_4/NO_2$ step I	$N_2H_4/NO_2$ step II	$N_2H_4/O_2$	$N_2H_4$ decomposition
initiation	$N_2H_4 + NO_2 \rightarrow N_2H_3 + HONO$	$N_2H_4 \xrightarrow{M} NH_2 + NH_2$	$N_2H_4 \xrightarrow{M} NH_2 + NH_2$	$N_2H_4 \xrightarrow{M} NH_2 + NH_2$
branching		$N_2H_3 \xrightarrow{M} NH_2 + NH$	$N_2H_3 \xrightarrow{M} NH_2 + NH$	$N_2H_3 \xrightarrow{M} NH_2 + NH$
propagation	$N_2H_4 + OH \rightarrow N_2H_3 + H_2O$ $N_2H_3 + NO_2 \rightarrow N_2H_2 + HONO$ $N_2H_3 + OH \rightarrow N_2H_2 + H_2O$ $HONO \rightarrow OH + NO$ $H_2 + OH \rightarrow H_2O + H$ $NO_2 + H \rightarrow HONO$	$N_2H_4 + NH_2 \rightarrow N_2H_3 + NH_3$ $N_2H_3 + NH_2 \rightarrow N_2H_2 + NH_3$ $NO + NH_2 \rightarrow NH_2NO$ $NO + NH \rightarrow N_2 + OH$ $N_2H_4 + OH \rightarrow N_2H_3 + H_2O$ $N_2H_3 \xrightarrow{M} N_2 + H_2 + H$ $NH_2NO \rightarrow HN_2 + OH$ $HN_2 \rightarrow N_2 + H$	$NH_2 + O_2 \rightarrow HNO + OH$ $N_2H_3 + O_2 \rightarrow NH_2NO + OH$ $N_2H_4 + OH \rightarrow N_2H_3 + H_2O$ $N_2H_3 + OH \rightarrow N_2H_2 + H_2O$ $N_2H_4 + NH_2 \rightarrow N_2H_3 + NH_3$	$N_2H_4 + NH_2 \rightarrow N_2H_3 + NH_3$ $N_2H_3 \xrightarrow{M} N_2 + H_2 + H$ $N_2H_4 + H \rightarrow N_2H_3 + H_2$
termination	$N_2H_2 \rightarrow N_2 + H_2$	$N_2H_2 \rightarrow N_2 + H_2$ $NH_2NO \rightarrow H_2O + N_2$	$N_2H_2 \rightarrow N_2 + H_2$ $NH_2NO \rightarrow H_2O + N_2$ $OH + NO \rightarrow HONO$ $HNO + OH \rightarrow H_2O + NO$	$N_2H_3 + NH_2 \rightarrow NH_3 + N_2 + H_2$ $N_2H_3 + H \rightarrow H_2 + N_2 + H_2$

readily available source of hydrogen. Gray and Thynne (16, 112) found the abstraction of hydrogen by methyl radicals from hydrazine at 150°C to be 300 times faster than from ammonia and estimate the dissociation energy  $D(H-N_2H_3)$  to be about 93 (kcal/mole). The proposed mechanism for the step I reaction of hydrazine and nitrogen dioxide involves neither the fission of the N-N bond nor dissociation of hydrazine.

(2) The effect of oxygen to slow the decomposition of hydrazine is attributed to product water which has been observed by Eberstein (39) and Antoine (113, 114) to slow hydrazine decomposition. That the hydrazine/oxygen reaction proceeds more rapidly than the decomposition of "wet" hydrazine is evidence that oxidation of the hydrazine decomposition fragments occurs. That the reaction is much slower than the step I hydrazine/nitrogen dioxide reaction is attributable to the greater abstraction potential of nitrogen dioxide over oxygen. Hydrazine dissociation and oxidation proceed simultaneously.

(3) The observed step II reaction of hydrazine and nitrogen dioxide is interpreted to be the reaction of hydrazine and nitric oxide and is in good agreement with the hydrazine/nitric oxide reaction rate measurements. The similarity of the rates of these two reactions, really the same reaction, to the decomposition of "wet" hydrazine does not simply reflect the effect of product water but additionally must involve the inhibiting effect of nitric oxide on hydrazine decomposition by removal of  $NH_2$  radicals. The fission of the N-N bond in hydrazine is a prerequisite to its reaction with nitric oxide. In this sense, hydrazine decomposition precedes its oxidation by nitric oxide.

## CHAPTER 8

COMPARISON OF THE REACTIONS STUDIED: THEIR RELATION TO  
THE HYDRAZINE/NITROGEN DIOXIDE REACTION

Of the 16 reactions outlined for study, measurable reactions rates were observed for 11 while reaction rates for the remaining 5 were too slow to be measured with the flow reactor. Comparison of the measured reaction rates among the 11 reactions, while probably the most interesting relation to be noted, is difficult to resolve.

8.1 COMPARISON OF EXPERIMENTAL RESULTS

The difficulty in comparing the measured reaction rates arises both from the disparity of reaction orders among the reactions and from the difference in reaction rate itself and therefore, as a consequence of the experimental technique, differences in the temperatures at which reaction rates were measured. Fast reacting combinations were studied at low temperatures while slow reacting combinations were studied at high temperatures. Fortunately, enough overlap in the experimental parameters exists for the various reactions studied to allow qualitative and, in some cases, quantitative comparisons to be made.

8.1.1 Reaction orders

Reaction orders were determined for most of the reactions studied and do form a basis for valid comparison among reactions. As a summary, the reaction orders for the reactions studied are presented in Table 19 in terms of the exponents (orders)  $a$ ,  $b$ , and  $c$ .

TABLE 19. Summary of reaction orders for the general rate equation.

$$\text{rate} = \frac{d[\text{fuel}]}{dt} = -k[\text{fuel}]^a [\text{oxidizer}]^b [\text{x}]^c$$

oxidizer	exponent	fuel			
		$\text{N}_2\text{H}_4$	$\text{H}_2$	$\text{NH}_3$	$\text{NH}_3 + \frac{1}{2}\text{H}_2$
$\text{NO}_2$	a	1.0 <sup>(1)</sup> .9 <sup>(2)</sup>	1.4	1.0	+
	b	1.0 0	1.0	1.0	+
	c	+ +	-.8*	+	+
$\text{O}_2$	a	1.0	1.0	1.0	+
	b	0	0	1.0	+
	c	+	+	+	+
$\text{NO} + \frac{1}{2}\text{O}_2$	a	+	+	-	-
	b	+	+	-	-
	c	+	+	-	-
NO	a	.75	-	-	-
	b	0	-	-	-
	c	+	-	-	-

+ not applicable or not determined

- no reaction observed

\* for  $x = [\text{NO}] + [\text{NO}_2]$ 

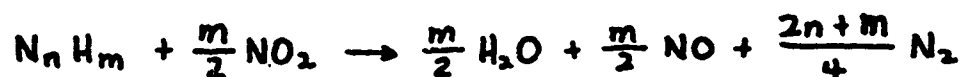
(1) step I

(2) step II

For those cases in which zero order dependencies upon the oxidizer concentration are indicated, attention is drawn to the difficulty in discerning between a true zero order dependence upon oxidizer concentration and the case involving the combination of competing direct and inverse dependencies. The hydrogen/nitrogen dioxide reaction is an example of the case in point--it is likely that this complex dependency upon several species would have gone undetected had it not been for its discovery by other investigators employing different techniques.

#### 8.1.2 Heats of reaction and stoichiometry

The measured heats of reaction serve primarily as a check on the stoichiometry of the reaction. The observed stoichiometries have a consistent pattern for each oxidizer. For all reactions, except for the hydrazine/nitric oxide reaction, complete oxidation of the fuel to water occurs. The nitrogen dioxide reactions behave according to the general stoichiometry



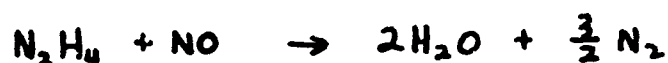
where  $N_n H_m$  is the general representation of the fuels studied. Similarly, the oxygen reactions follow the relation



The observed heat of reaction for the hydrazine/nitric oxide reaction indicates that part of the hydrazine decomposes to the products, ammonia and hydrogen (and unreactive nitrogen) which are not oxidized. Two competing stoichiometries are required to describe



this reaction.



In the flow reactor experiments approximately 85% of the hydrazine is consumed according to the first relation and the remainder according to the second. The heats of reaction as measured are presented in Table 20. These values are to be compared to the predicted values as presented in Table 6 of Chapter :

Table 20. Summary of measured heats of reaction (kcal/mole)

oxidizer	fuel			
	$\text{N}_2\text{H}_4$	$\text{H}_2$	$\text{NH}_3 + \frac{1}{2}\text{H}_2^*$	$\text{NH}_3$
$\text{NO}_2$	110	45	77	52
$\text{O}_2$	135	59	106	74
$\text{NO} + \frac{1}{2}\text{O}_2$	130	--	--	--
$\text{NO}$	160	--	--	--

\*(kcal/mole  $\text{NH}_3 + \frac{1}{2}$  mole  $\text{H}_2$ )

### 8.1.3 Reaction rates

The comparison of reaction rates for each fuel with various oxidizers has been presented in the preceding four chapters. Before attempting to order the reaction rates of all the reactions studied, it is informative to compare the

rates of each oxidizer with the various fuels. The selection of a common rate expression is required. Unfortunately, since the reactions do not show common orders, the particular selection of the rate expression can affect the apparent relative reaction rates.

An exception to this difficulty are the nitrogen dioxide reactions which all show roughly a first order dependence on both fuel and oxidizer concentrations and can be compared on the basis of a common rate expression,

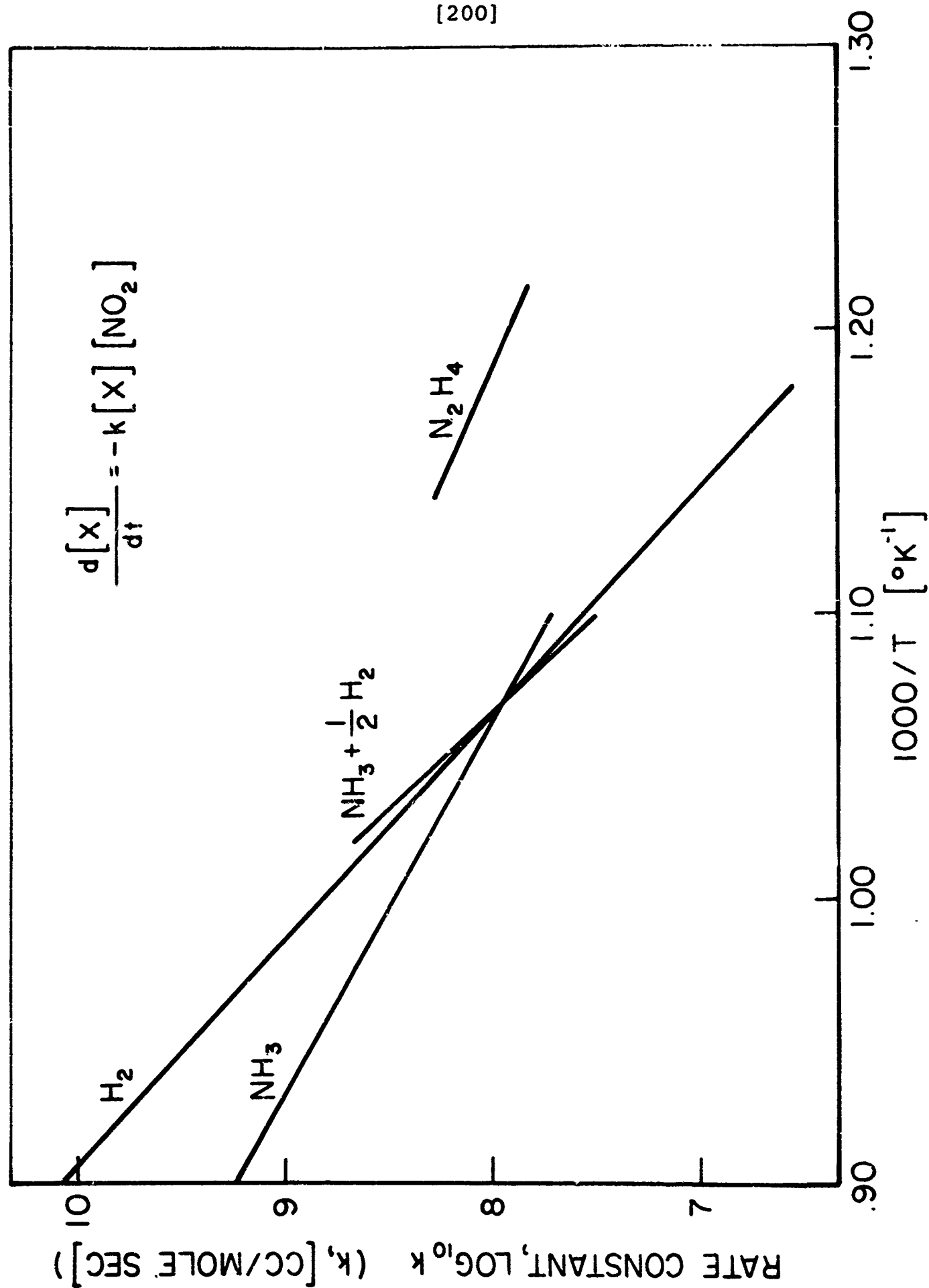
$$\frac{d[X]}{dt} = -k[X][NO_2]$$

Examination of Figure 46 in which the second order rate constants are plotted as a function of  $1/T$  reveals hydrazine to have the fastest reaction with nitrogen dioxide.

Hydrogen and the mixture of  $NH_3 + \frac{1}{2}H_2$  exhibit the same rate; at  $900^\circ K$  the ammonia reaction rate is also close to these two, while at  $1000^\circ K$ , the ammonia reaction rate is noticeably slower.

Comparison of the oxygen reaction rates are particularly difficult because of the necessity of using large excesses of oxygen to obtain measurable reactions in the case of its reaction with ammonia. In the hydrogen/oxygen reaction, large excesses of oxygen appear to slow the reaction while variations in oxygen concentration about a stoichiometric mixture produce no noticeable effect on the reaction rate. Recognizing the inherent difficulties in comparing the oxygen reaction rates, one should view Figure 47 in which a first order rate constant is presented,

$$\frac{d[X]}{dt} = -k[X]$$



COMPARISON OF NITROGEN DIOXIDE REACTION RATES

FIGURE 46

JPI 3 - 4067 - 65

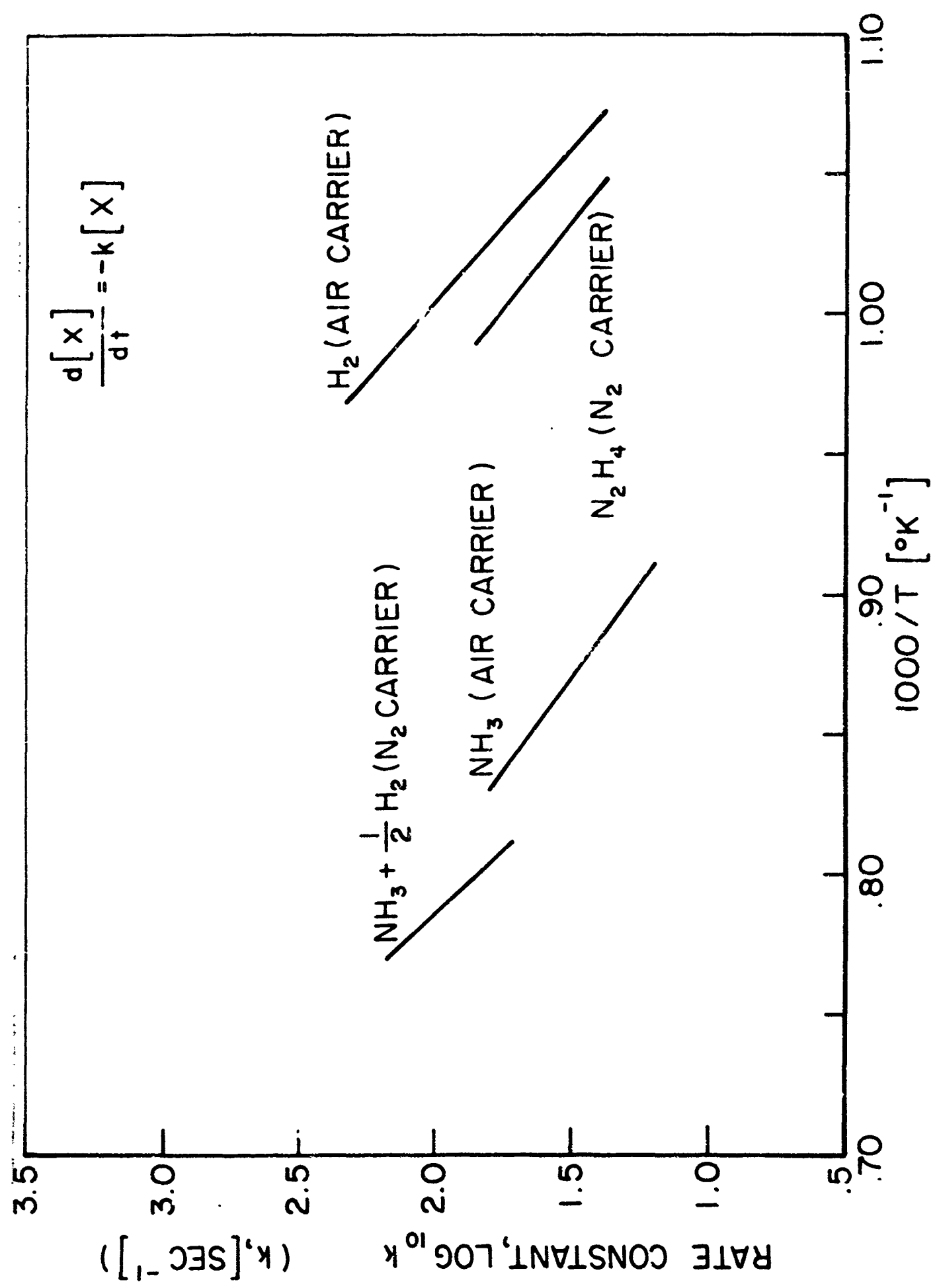


FIGURE 47

COMPARISON OF OXYGEN REACTION RATES, FIRST ORDER RATE CONSTANT

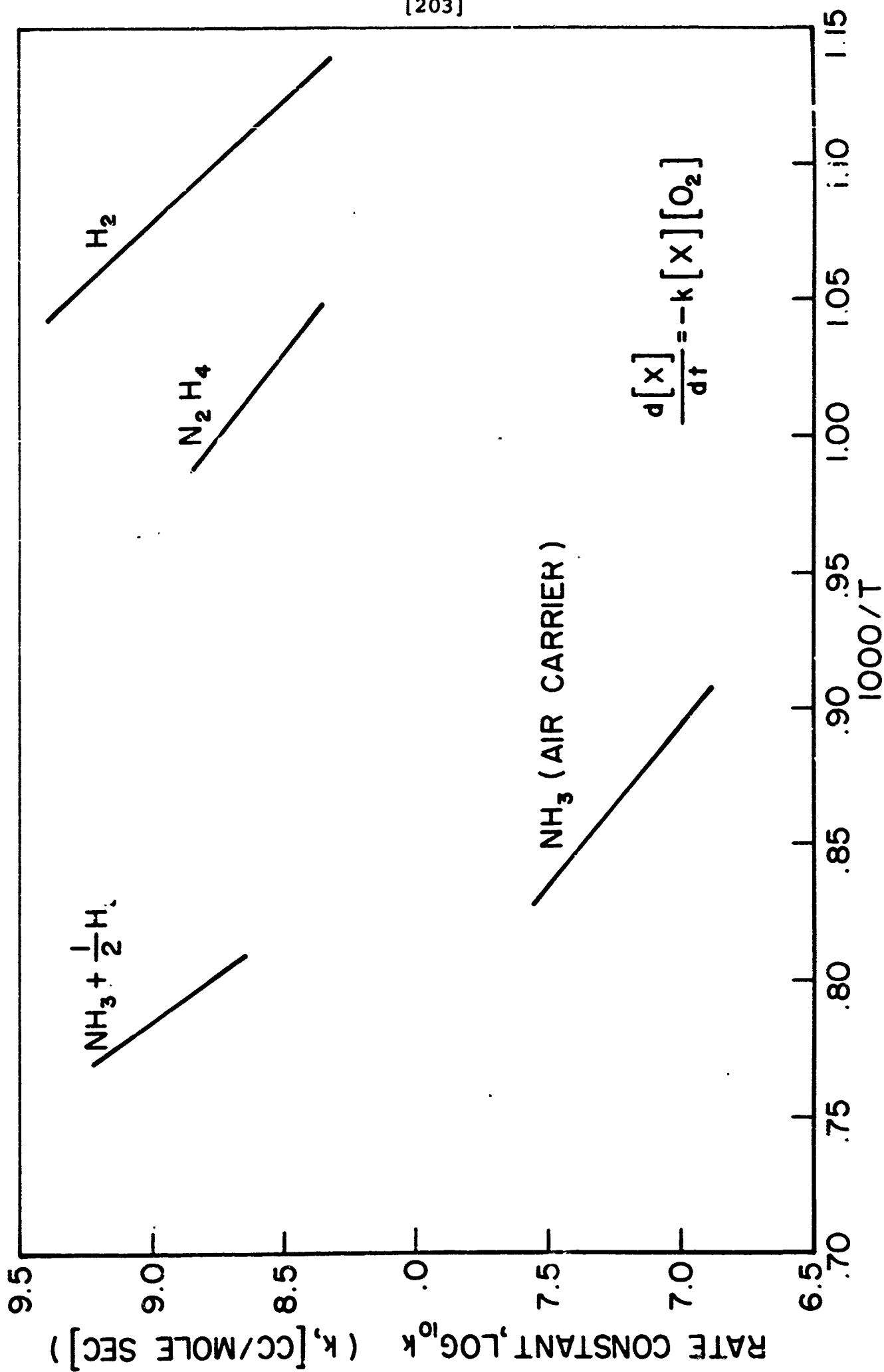
and Figure 48, in which a second order rate constant is presented,

$$\frac{d[X]}{dt} = -k[X][O_2]$$

with care for their interpretation. Hydrogen reacts most rapidly with oxygen, followed by hydrazine, ammonia-hydrogen, and ammonia, in order of decreasing reactivity.

The presence of nitric oxide, as from the decomposition of nitrogen dioxide to oxygen and nitric oxide, is found to slow the hydrogen/oxygen reaction considerably while having little effect upon the hydrazine/oxygen reaction. The two cases in which reactions are observed with decomposed nitrogen dioxide are compared in Figure 49. The inhibiting effect of nitric oxide on the hydrogen/oxygen reaction is sufficient to reverse the relative rates of the hydrogen/oxygen and hydrazine/oxygen reactions.

A composite comparison of the reaction rates is made in Table 21. Because of the enumerated difficulties in quantitatively comparing reaction rates, relative rates in this table are divided into four groups: fast, moderate, slow, and no reaction. The fast, moderate, and slow groupings represent about an order of magnitude (factor of 10) increase in reaction rate between slow and moderate and between moderate and fast. The fastest reactions are the hydrazine/nitrogen dioxide reaction and hydrogen/oxygen reaction which are found to react about 100 times faster than ammonia/oxygen and ammonia-hydrogen/oxygen. The remainder of the reactions with measurable rates were grouped with reaction rates of about 10 times the slow reactions and about 1/10 the fast reactions.



COMPARISON OF OXYGEN REACTION RATES, SECOND ORDER RATE CONSTANT

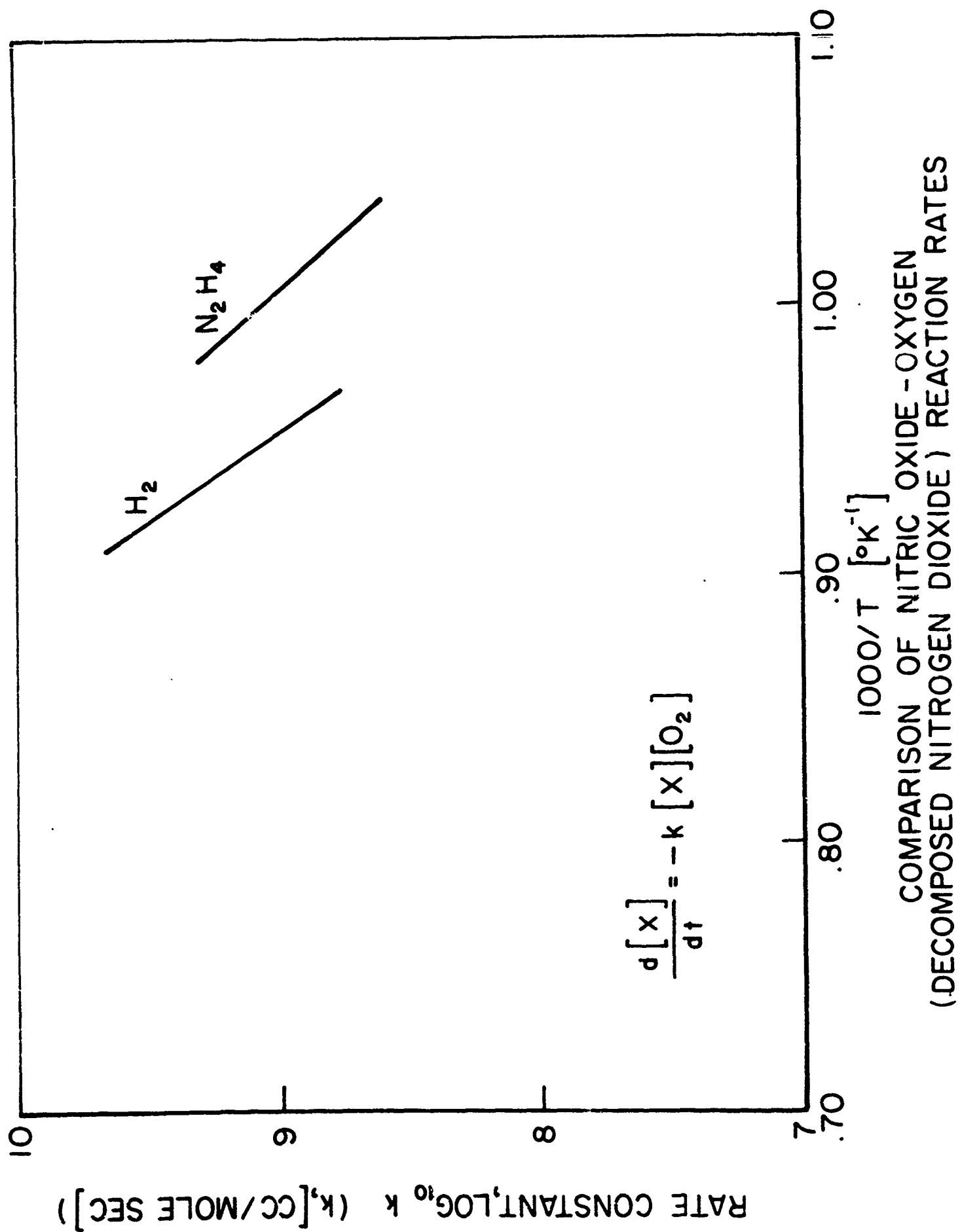


FIGURE 49

Table 21. Relative reaction rates, summary of all reactions studied, temperature range 800-1300°K.

oxidizer	fuel			
	$N_2H_4$	$H_2$	$NH_3 + \frac{1}{2}H_2$	$NH_3$
$NO_2$	fast	moderate	moderate	moderate
$O_2$	moderate	fast	slow	slow
$NO + \frac{1}{2}O_2$	moderate	moderate	no reaction	no reaction
$NO$	moderate	no reaction	no reaction	no reaction

#### 8.1.4 Overall activation energies

The overall or global activation energies for the reactions studied are summarized in Table 22. A general correlation between faster rate and lower activation energy is noted, particularly in the hydrazine and in the hydrogen columns. The overall activation energies give a clue to the dominant reaction mechanisms and are discussed in this context in Section 8.2. Attention is drawn to the effect of the selected reaction orders upon the calculated activation energies: a change in reaction order of .25 can produce as much as a 15 (kcal/mole) change in the activation energy, see, for example, Table 34. Activation energies based on common reaction orders are selected for presentation in Table 22 unless a particularly "uncommon" reaction order is indicated by the experimental results.



TABLE 22. Overall activation energies, summary of all reactions studied [kcal/mole]

oxidizer	fuel			
	$N_2H_4$	$H_2$	$NH_3 + \frac{1}{2} H_2$	$NH_3$
$NO_2$	26.7	46.2	48.2	33.8
$O_2$	37.2	38.2	48.3	38.7
$NO + \frac{1}{2} O_2$	39.1	68.6		
$NO$	45.4			

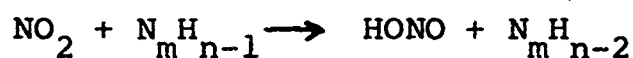
## 8.2 COMPARISON OF REACTION MECHANISMS

The reaction mechanisms presented have been shown in most cases to possess steady state solutions which agree with the observed reaction orders. While the proposed mechanisms seem to have complexity as their primary common feature, some simple relations among the different mechanisms can be noted. Attention is focused primarily on the reduction of nitrogen dioxide and on the oxidation of hydrazine.

### 8.2.1 Oxidation by nitrogen dioxide

Nitrogen dioxide was found to be measurably reactive with all of the fuels studied, at least to the extent of reduction to nitric oxide. A similarity

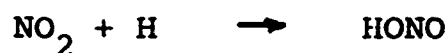
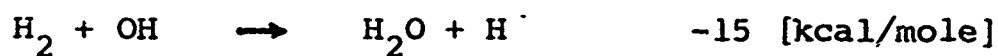
can be noted in the dominant propagation reactions of the reaction of nitrogen dioxide with hydrogen, ammonia, and hydrazine. As suggested by an analogous observation for the oxidation of ammonia and hydrazine by oxygen made by Hussain and Norrish (105), the following general propagation scheme is noted.



This general propagation reaction appears in the following pairs of reactions.

hydrogen

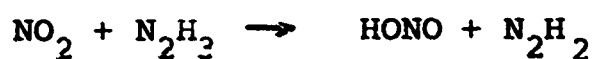
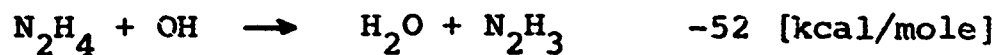
$\Delta H_{f298}^\circ$



ammonia



hydrazine



The common molecular intermediate, HONO, while relatively stable, will subsequently undergo the branching reaction



While NO is properly classified as a radical, it appears here as a stable specie and does not undergo further reaction.

An additional correlation of the reaction rates and overall activation energies with the nature of the first hydrogen abstraction reaction is noted. The similarity in reaction rates for ammonia and hydrogen with nitrogen dioxide is in agreement with the similar exothermicities of their respective hydrogen abstraction reactions and similar bond dissociation energies, which are 104 [kcal/mole] for both the fission of the hydrogen molecule and the breaking of the first N-H bond in ammonia. The higher reaction rate for hydrazine than for ammonia is consistent with a weaker N-H bond and hence a better potential for hydrogen abstraction.

#### 8.2.2 The oxidation of hydrazine

The measured reaction rates, reaction orders, and overall activation energies for the oxidation of hydrazine by nitrogen dioxide, oxygen, and nitric oxide are distinctively different and represent distinctively different reaction mechanisms. The reaction of hydrazine and nitrogen dioxide already has been described as a rapid hydrogen abstraction reaction, occurring without the decomposition of the hydrazine. The remaining reactions involve the decomposition of hydrazine, either as a parallel reaction or as a prerequisite reaction.

The lower reaction rate of oxygen than nitrogen dioxide is traceable to the greater effectiveness of nitrogen dioxide as a hydrogen abstractor. It is difficult to establish from the observations whether the slower reaction of hydrazine/oxygen than of pure hydrazine decomposition is due to a slowing effect of the hydrazine decomposition by the product water, as observed by Eberstein (39), or is merely a result of a requirement that the hydrazine pyrolysis occur before it can react with oxygen. The observed reaction rate of hydrazine and oxygen is greater than the rate observed for the decomposition of "wet" hydrazine. The water concentration of "wet" hydrazine is less than that produced early in the hydrazine/oxygen reaction. This observation seems to indicate that complete dissociation of hydrazine to ammonia, hydrogen, and nitrogen is not a prerequisite of its reaction with oxygen. The similarity in overall activation energies of hydrazine decomposition and the hydrazine/oxygen reaction, however, does support the importance of a role of hydrazine decomposition in its reaction with oxygen.

The still slower reaction of hydrazine and nitric oxide depends on the decomposition of hydrazine to form reactive  $\text{NH}_2$ , possibly also  $\text{NH}$ , radicals. It is concluded that complete pyrolysis of the hydrazine to ammonia, hydrogen, and nitrogen cannot occur to a great extent because these species are not reactive with nitric oxide at the experimental conditions. The failure of nitric oxide to affect the hydrazine/oxygen and ammonia/oxygen reaction rates (and probably the hydrazine/nitrogen dioxide reaction rate as well) appears anomalous considering the likely role of  $\text{NO}$  as a  $\text{NH}_2$

radical sink and its inhibiting effect on the hydrogen/oxygen reaction. One explanation is that oxygen and nitrogen dioxide are even more reactive with  $\text{NH}_2$  radicals than nitric oxide, making the presence of NO unnoticed. Another explanation is that the inhibiting effect of NO on the hydrogen/oxygen reaction is tied to the removal of H atoms by the formation of HNO and that H atoms are not important intermediates in the other reactions.

The oxidation of hydrazine has been shown to follow no particular pattern but to depend upon the oxidizing agent. Reactions have been observed in which oxidation proceeds without pyrolysis, in which oxidation and pyrolysis are concluded to proceed simultaneously, and in which pyrolysis is a prerequisite to oxidation. The reaction of hydrazine and nitrogen dioxide is characterized by a unique two step process, the reduction of nitrogen dioxide to nitric oxide followed by the reduction of the nitric oxide. The reaction rates for these two steps differ by a factor of 13.

### 8.2.3 Other comments on reaction mechanisms

One peculiar observation is the failure of nitric oxide and ammonia to react, even in the presence of oxygen. The oxidation of ammonia would seem to provide a source of  $\text{NH}_2$  radicals apparently required for the reduction of nitric oxide. While it is understandable that initiation of the ammonia/nitric oxide reaction would be difficult, as indeed even the ammonia/oxygen reaction is observed to be, one might expect that the ammonia/nitric oxide reaction would be sustained in the presence of the ammonia/oxygen reaction. Once again the explanation may lie in the competition between  $\text{O}_2$

and NO for  $\text{NH}_2$  radicals. Experimental results seem to indicate that oxygen is more reactive with  $\text{NH}_2$  than is nitric oxide.

The high reaction rate of hydrogen and oxygen is attributed to a chain branched reaction mechanism. Of the reactions studied, only the hydrogen/oxygen reaction has been proposed to involve chain branching.

### 8.3 THE EFFECT OF NITROGEN DIOXIDE DECOMPOSITION UPON ITS SUBSEQUENT REACTION

It has been argued already that the decomposition of nitrogen tetroxide to nitrogen dioxide is sufficiently rapid to insure that it occurs in most gas phase combustions before any reduction reaction. While the decomposition of nitrogen dioxide to nitric oxide and oxygen is a much slower process, its occurrence in a combustion reaction is possible.

In all reactions observed, the decomposition of nitrogen dioxide to nitric oxide and molecular oxygen is found to slow its subsequent reaction. Since nitric oxide is a reaction product in the reduction of nitrogen dioxide, the decomposition of nitrogen dioxide should not affect the heat of reaction. High temperatures, sufficient to produce thermal decomposition of the nitric oxide, apparently are required for the complete reduction of nitrogen dioxide, except where hydrazine is the reducing agent. In this case, complete reduction of the nitrogen dioxide is possible, even at moderate temperatures. The rate of the complete reduction of nitrogen dioxide appears to be unaffected by the decomposition of the nitrogen dioxide as the rate controlling process is the reduction of the nitric oxide, whether it is formed as a decomposition product or as a reaction intermediate. Unlike the flow

reactor, in a combustor producing large temperature increases (as is the function of most combustors), the first step of the hydrazine/nitrogen dioxide reaction would provide a sufficient temperature rise to accelerate the second step of the reaction to the point where it possibly would not be rate controlling.

A second form of nitrogen dioxide decomposition should be mentioned. The term "decomposed nitrogen dioxide" has been used to refer to nitrogen dioxide which has undergone decomposition to nitric oxide and molecular oxygen prior to mixing with the fuel. If the nitrogen dioxide undergoes decomposition in the presence of the fuel, the decomposition intermediates, nitric oxide and atomic oxygen, would be available for oxidation of the fuel. Because of the reactivity of atomic oxygen, such "concurrent thermal decomposition" would not slow the reaction rate of nitrogen dioxide. In the reactions studied, thermal decomposition of nitrogen dioxide was slower than the nitrogen dioxide/fuel reaction. Any such "concurrent thermal decomposition" that might occur during the reaction process should be treated as a step in the reaction mechanism.

#### 8.4 THE EFFECT OF HYDRAZINE DECOMPOSITION UPON ITS SUBSEQUENT REACTION

As was anticipated, in all cases studied, the pyrolysis of hydrazine to ammonia, hydrogen, and nitrogen acts to slow or prevent its subsequent reaction. On the other hand, its decomposition to the extent of the breaking of the N-N bond apparently is required for reaction with nitric oxide.

The complete pyrolysis of hydrazine to ammonia, hydrogen, and nitrogen slows its reaction with nitrogen dioxide by a factor of about 6. The complete pyrolysis of nitrogen dioxide to nitric oxide and molecular oxygen slows its reaction with hydrazine by a factor of about 10. The reaction of completely pyrolyzed hydrazine and completely pyrolyzed nitrogen dioxide is too slow to be studied in the flow reactor. This failure to obtain a reaction indicates a reaction rate which is at least 1000 times smaller than the reaction rate of hydrazine and nitrogen dioxide.

\* \* \*

In summary, the homogeneous gas phase kinetics of the reaction of hydrazine and nitrogen dioxide were studied by experimental investigation of a number of related reactions. Interpretation of measured reaction orders, reaction rates, and overall activation energies was provided through the postulation of reaction mechanisms. Reactant pyrolysis in the hydrazine/nitrogen dioxide reaction was demonstrated to control the nature of the reaction.



REFERENCES

1. Lawver, B. R., "Some observations on the combustion of  $N_2H_4$  droplets," AIAA Preprint 65-355, Annual Meeting, July 1965, San Francisco, California.
2. Perlee, H. E., Imhof, A. C., Zabetakis, M. G., "Flammability Characteristics of hydrazine fuels in nitrogen tetroxide atmospheres," Journal of Chemical and Engineering Data 7, 377-379 (1962).
3. Wilber, P. C., Merrigan, M. A., Choudhury, P.R., Vango, S.P., Lee, W., "On the spontaneous ignition of hypergolic propellant systems at low pressures and temperatures," Western States Combustion Institute Meeting, Paper Number 64-29, October 26-27, 1964
4. Skinner, G. B., Hedley, W. H., Snyder, A.D., "Mechanism and chemical inhibition of the hydrazine-nitrogen tetroxide reaction," ASD-TDR-62-1041, December 1962.
5. Murray, R. C., Hall, A. R., "Flame speeds in hydrazine vapor in mixtures of hydrazine and ammonia with oxygen," Transactions of the Faraday Society 47, 743-751 (1951).
6. Liquid Propellant Manual, Applied Physics Laboratory, Johns Hopkins University (1961).
7. Kit, B., Evered, D. S., Rocket Propellant Handbook, (The Macmillan Company, New York).
8. "Performance and properties of liquid propellants," Aerojet-General Corporation, March 1961.
9. Hodgman, Charles E., editor, Handbook of Chemistry and Physics, 44th Edition, (Chemical Rubber Publishing Company, Cleveland, 1962).
10. Audrieth, L. F., Ogg, B. A., The Chemistry of Hydrazine, (Wiley, New York, 1951).
11. JANAF Thermochemical Tables, (The Dow Chemical Company, Midland, Michigan, 1965).
12. Jolly, W. L., The Inorganic Chemistry of Nitrogen, (Benjamin, New York, 1964).

13. Rosser, W. A., Wise, H., "The gas-phase oxidation of ammonia by nitrogen dioxide," JPL PR 20-273, September 15, 1955.
14. Dibeler, V. H., Franklin, J. L., Reese, R. M., "Electron impact studies of hydrazine and the methyl-substituted hydrazines," Journal of the American Chemical Society 81, 68-73 (1959).
15. McHale, E. T., Know, B. E., Palmer, H. B., "Determination of the decomposition kinetics of hydrazine using a single-pulse shock tube," Tenth Symposium (International) on Combustion, 341-351, (The Combustion Institute, Pittsburgh, 1965).
16. Gray, P. Thyne, J. C. J., "Arrhenius parameters for elementary combustion reactions: H-atom abstraction from N-H bonds," Tenth Symposium (International) on Combustion, 435-443, (The Combustion Institute, Pittsburgh, 1965).
17. Gilbert, M., "The hydrazine flame," JPL PR 20-318, July 1957.
18. Gilbert, M., Altman, D., "Mechanism and flame speed for hydrazine decomposition," JPL PR 20-278, 1955.
19. Gilbert, M., "An approximate treatment of hydrazine decomposition in laminar, non-isothermal flow," JPL-PR 20-336, July 1957.
20. Gray, P., Lee, J. C. Leach, H. A., Taylor, D. C., "The propagation and stability of the decomposition flame of hydrazine," Sixth Symposium (International) on Combustion, 255-263, (Reinhold, New York, 1956).
21. Gray, P., Lee, J. C., Spencer, M., "Combustion, flame and explosion of hydrazine and ammonia. Spontaneous ignition of pure gaseous hydrazine," Combustion and Flame 7, 315-322 (1963).
22. Adams, G.K., Cook, G. B., "The effect of pressure on the mechanism and speed of the hydrazine decomposition flame," Combustion and Flame 4, 9-18 (1960).
23. Adams, G. K., Stocks, G. W., "The combustion of hydrazine," Fourth Symposium (International) on Combustion, 239-248, (Williams and Wilkins, Baltimore, 1953).

24. Hall, A. R., Wofhard, H. G., "Hydrazine decomposition flames at subatmospheric pressures," Faraday Society Transactions 52, 1520-1525 (1956).
25. Gray, P., Lee, J. C., "Recent studies of the oxidation and decomposition flames of hydrazine," Seventh Symposium (International) on Combustion, 61-67, (Butterworths, London, 1959).
26. Vanpee, M., Wolfhard, H. G., Clark, A.H., "Flame studies of high energy fuels and oxidizers: hydrazine-diborane, oxygen-diborane, oxygen-hydrazine and hydrazine decomposition flames," Thiokol Chemical Corporation, Reaction Motors Division, RMD-1-P, October 1961.
27. Pauling, Linus, The Nature of the Chemical Bond, 3rd edition, (Cornell University Press, Ithaca, New York, 1960).
28. Herzberg, Gerhard, Molecular Spectra and Molecular Structure I. Spectra of Diatomic Molecules, 2nd edition, (Van Nostrand, Princeton, 1950).
29. Schexnayder, C. J. Jr., "Tabulated values of bond dissociation energies, ionization potentials, and electron affinities for some molecules found in high-temperature reactions," NASA TN D-1791, May 1963.
30. Laidler, K. J., Reaction Kinetics, Volume 1, Homogeneous Gas Reactions, (Pergamon, Oxford, 1963).
31. Moelwyn-Hughes, E. A., Physical Chemistry, (Pergamon Press, New York, 1961).
32. Michel, K. W., Wagner, H. G.G., "The pyrolysis and oxidation of hydrazine behind shock waves," Tenth Symposium (International) on Combustion, 353-364, (The Combustion Institute, Pittsburgh, 1965).
33. Moberly, W. H., "Shock tube study of hydrazine decomposition," Journal of Physical Chemistry 66, 366-368 (1962).
34. Jost, A., Michel, K. W., Troe, J., Wagner, H. G., "Detonation and shock-tube studies of hydrazine and nitrous oxide," ARL 63-157, September 1963.
35. Diesen, R. W., "Mass spectral studies of kinetics behind shock waves. Thermal dissociation of hydrazine," Journal of Chemical Physics 39, 2121-2127 (1963).

36. Jost, W., "Investigation of gaseous detonations and shock wave experiments with hydrazine," ARL 62-330, April 1962.
37. Michel, W.W., Wagner, H.G., "Untersuchung des thermischen Zerfalls und der Oxydation von Hydrazin mit Stosswellen," A. Phys. Chem. 35, 4-6 (1962).
38. Eberstein, I., Glassman, I., "The gas-phase decomposition of hydrazine and its methyl derivatives," Tenth Symposium (International) on Combustion, 365-374, (The Combustion Institute, Pittsburgh, 1965).
39. Eberstein, I., "The gas phase decomposition of hydrazine propellants," Princeton University, Department of Aerospace and Mechanical Sciences, Technical Report 708 (1964).
40. Liquid Propellant Safety Manual, Liquid Propellant Information Agency, Applied Physics Laboratory, Johns Hopkins University, October 1958.
41. Jacobs, T. A., "Shock tube measurements of the homogeneous rate of decomposition of  $\text{NH}_3$  in  $\text{NH}_3$ -Ar mixtures," Eight Symposium (International) on Combustion, 151-154, (Williams and Wilkins, Baltimore, 1962).
42. Carrington, T., Davidson, N., "Shock waves in chemical kinetics: The rate of dissociation of  $\text{N}_2\text{O}_4$ ," Journal of Physical Chemistry 57, 418-427 (1953).
43. Wegener, P.P., Marte, J.E., Thiel, C., "Study of supersonic flows with chemical reactions: Measurements of rate constants of the reaction  $\text{N}_2 + \text{N}_2\text{O}_4 \rightarrow \text{N}_2 + 2\text{NO}_2$  at low reactant concentration," JPL PR 20-349, June 19, 1958.
44. Wegener, P.P., "Measurements of rate constants of fast reactions in a supersonic nozzle," Journal of Chemical Physics 28, 724-725 (1958).
45. Giauque, W.F., Kemp, J.D., "The entropies of nitrogen tetroxide and nitrogen dioxide. The heat capacity from 15°K to the boiling point. The heat of vaporization and vapor pressure. The equilibria  $\text{N}_2\text{O}_4 \rightleftharpoons 2\text{NO}_2 \rightleftharpoons 2\text{NO} + \text{O}_2$ ," Journal of Chemical Physics 6, 40-52 (1938).
46. Patty, Frank A., "In organic compounds of oxygen, nitrogen, and carbon," Industrial Hygiene and Toxicology, Frank A. Patty, editor, Vol. II, Toxicology, David W. Fassett and Don D. Irish, Editors, Chapter XXV, (Interscience Publishers, New York, 1962).

47. Gray, P., Yoffee, A. D., "The reactivity and structure of nitrogen dioxide," Chemical Reviews 55, 1069-1154 (1955).
48. Rosser, W.A. Jr., Wise, H., "Thermal decomposition of nitrogen dioxide," Journal of Chemical Physics, 493-494 (1956).
49. Ashmore, P.G., Burnett, M.G., "Concurrent molecular and free radical mechanisms in the thermal decomposition of nitrogen dioxide," Transactions of the Faraday Society 58, 253-261 (1962).
50. Wise, H., French, M.F., "Reaction kinetics of rocket propellant gases: I. Rate of decomposition of nitric oxide at elevated temperatures," JPL PR 9-46, March 27, 1950.
51. Wise, H., French, M.F., "Reaction kinetics of rocket propellant gases: II. Effect of reaction products and mechanism of thermal decomposition of nitric oxide," JPL PR 20-150, October 1951.
52. Crocco, L., Glassman, I., Smith, I.E., "Kinetics and mechanism of ethylene oxide decomposition at high temperatures," Journal of Chemical Physics 31, 506-510 (1959).
53. Swigart, R. J., "A study of the kinetics of the hydrogen-oxygen reaction in a new flow reactor," Department of Aeronautical Engineering Report No. 432, Princeton University, 15 August 1958.
54. Glassman, I., Eberstein, I. J., "Turbulence effects in chemical reaction kinetics measurements," AIAA Journal 1, 1424-1426 (1963).
55. Cookson, R. A., Dunham, P. G., Kilham, J.K., "Non-catalytic coatings for thermocouples," Combustion and Flame 8, 168-170 (1964).
56. "The handling and storage of liquid propellants," Office of the Director of Defense Research and Engineering, March 1961.
57. "Industrial hydrazine, handling and storage," Olin Mathieson Chemical Corporation.
58. Liberto, R.R., "Titan II storable propellant handbook, revision B," Bell Aerosystems Company 8182-933004, AFBSD-TR-62-2, March 1963.

59. McGonigle, R. J., "Large scale handling of nitrogen tetroxide," Nitrogen Division, Allied Chemical Corporation.
60. McGonigle, R. J., "Mixed oxides of nitrogen--properties and handling," Allied Chemical Corporation.  
  
"Nitrogen tetroxide," Nitrogen Division, Allied Chemical Corporation, Product Development Booklet NT-1.  
  
"Nitrogen tetroxide," Nitrogen Division, Allied Chemical Corporation.
63. Nalimov, V.V. (translated by Prasenjit Basu, M. Williams, editor), The Application of Mathematical Statistics to Chemical Analysis, (Addison-Wesley, Reading, Massachusetts, 1963).
64. Pierson, R. H., Fletcher, A.N., Gantz, E. St. C., "Catalog of infrared spectra for qualitative analysis of gases," Analytical Chemistry 28, 1218-1239 (1956).
65. Netusil, W.F., Proffit, R. L., Enloe, J.D., "Development of a system to identify rocket exhaust products and determine thermodynamic functions," Rocketdyne R-5878, October 1964.
66. Rosser, W.A. Jr., Wise, H., "Kinetics of the reaction between hydrogen and nitrogen dioxide," Journal of Chemical Physics 26, 571-576 (1957).
67. Rosser, W.A., Wise, H., "The rate of reaction of hydrogen and nitrogen dioxide," Journal of physical chemistry 65, 532-534 (1961).
68. Rosser, W. A., Wise, H., "Kinetics of the reaction between hydrogen and nitrogen dioxide," JPL PR20-282, December 21, 1955.
69. Ashmore, P.G., Levitt, B.P., "Thermal reaction between hydrogen and nitrogen dioxide. Part 3. Further experimental work on the kinetics: reaction mechanism," Transactions of the Faraday Society 53, 945-954 (1957).
70. Ashmore, P.G., Levitt, H.P., "Thermal reaction between hydrogen and nitrogen dioxide. Part 2. Experimental work on the kinetics of the reactions," Transactions of the Faraday Society 52, 835-848 (1956).

71. Wolfhard, H.G., Parker, W.G., "Spectra and combustion mechanism of flames supported by the oxides of nitrogen," Fifth Symposium (International) on Combustion, 718-728, (Reinhold, New York, 1955).
72. Clyne, M.A.A., Thrush, B.A., "Reaction of nitrogen dioxide with hydrogen atoms," Transactions of the Faraday Society 57, 2176-2187 (1961).
73. Benson, Sidney W., The Foundation of Chemical Kinetics, (McGraw-Hill, New York, 1960).
74. Lewis, B., von Elbe, G., Combustion, Flames and Explosions of Gases, 2nd edition, (Academic Press, New York, 1961).
75. Minkoff, G.J., Tipper, C.F.H., Chemistry of Combustion Reactions, (Butterworths, London, 1962).
76. Patch, R.W., "Prediction of composition limits for detonation of hydrogen-oxygen-diluent mixtures," ARS Journal 31, 46-51 (1961).
77. Nicholls, J.A., Adamson, T.C. Jr., Morrison, R.B., "Ignition time delay of hydrogen-oxygen-diluent mixtures at high temperatures," AIAA Journal 1, 2253-2257 (1963).
78. Miyama, H., Takeyama, T., "Kinetics of hydrogen-oxygen reaction in shock waves," Journal of Chemical Physics 41, 2287-2290 (1964).
79. Schott, G.L., Kinsey, J.L., "Kinetic studies of hydroxyl radicals in shock waves. II. Induction times in the hydrogen-oxygen reaction," Journal of Chemical Physics 29, 1177-1182 (1958).
80. Rhodes, R.P., Chriss, D.E., "A preliminary study of stationary shock induced combustion with hydrogen-air mixtures," Arnold Engineering Development Center TN-61-36, July 1961.
81. Ruegg, F.W., Dorsey, W.W., "A missile technique for the study of detonation waves," Journal of Research of the National Bureau of Standards 66C, 51-58 (1962).
82. Strehlow, R.A., Cohen, A., "Initiation of detonation," Physics of Fluids 5, 97-101 (1962).

83. Fujimoto, Shiro, "Chemical reaction in a shock wave. I. The ignition delay of a hydrogen-oxygen mixture in a shock tube," Bulletin of the Chemical Society of Japan 36, 1233-1236 (1963).
84. Mullaney, G.J., Ku, P.H., Botch, W.D., "Determination of induction times in one-dimensional detonation ( $H_2$ ,  $C_2H_2$ , and  $C_2H_4$ )," AIAA Journal 3, 873-875 (1965).
85. Mullaney, G.J., Arave, R., "Determination of induction times in one-dimensional detonations," Boeing Scientific Research Laboratories, DI-82-0324, Flight Sciences Laboratory Report No. 87, December 1963.
86. Skinner, G.B., Ringrose, G.H., "Ignition delays of a hydrogen-oxygen-argon mixture at relatively low temperatures," Journal of Chemical Physics 42, 2190-2192 (1965).
87. Norrish, R.G.W., Porter, G., "Spectroscopic studies of the hydrogen-oxygen explosion initiated by the flash photolysis of nitrogen dioxide," Proceedings of the Royal Society of London 210, 439-460 (1952).
88. Willbourn, A.H., Hinshelwood, C. N., "The mechanism of the hydrogen-oxygen reaction I. The third explosion limit," Proceedings of the Royal Society 185A, 353-380 (1946).
89. Momtchiloff, I.N., Taback, E.D., Buswell, R.F., "Kinetics in hydrogen-air flow systems. I. Calculation of ignition delays for hypersonic ramjets," Ninth Symposium (International) on Combustion, 220-230, (Academic Press, New York, 1963).
90. Tuesday, C.S., Boudart, M., "Vibrational relaxation times by the impact tube method," Princeton University Chemical Kinetic Project Technical Note No. 7, OSR-TN-55-67 (1955).
91. Dixon-Lewis, G., Williams, A., "The rate of heat release in some slow burning hydrogen-oxygen flames", Combustion and Flame 8, 249-255 (1964).
92. Ashmore, P.G., "Induction periods and limits of ignition in sensitized ignitions of hydrogen and oxygen," Faraday Society Transactions 51, 1090-1104 (1955).
93. Ashmore, P.G., Catalysis and Inhibition of Chemical Reactions, (Butterworths, London, 1963).



94. Crist, R.H., Wertz, J.E., "Kinetics of the oxidation of hydrogen sensitized by nitrogen dioxide," Journal of Chemical Physics 7, 719-724 (1939).
95. Skinner, G.B., work reported on at Combustion Instability Conference, Patrick AFB, Florida, June 1965.
96. Trotman-Dickenson, A.F., Gas Kinetics, (Butterworths, London, 1955).
97. Clement, M.J.Y., Ramsay, D.A., Canadian Journal of Physics 39, 205 (1961), as quoted in reference 107.
98. Ashmore, P.G., Tyler, B.J. "Reaction of hydrogen atoms with nitrogen dioxide," Transactions of the Faraday Society 58, 1108-1116 (1962).
99. Falk, F., Pease, R.N., "An initial report on the stoichiometry and kinetics of the gas phase reaction of nitrogen dioxide and ammonia," Journal of the American Chemical Society 76, 4746-4747 (1954).
100. Falk, Felix, "Stoichiometry and kinetics of the gas phase reaction of nitrogen dioxide and ammonia," Princeton University, Chemistry Department thesis, University Microfilm Number 13691 (1956).
101. Frost, A.A., Pearson, R.G., Kinetics and Mechanism, 2nd Edition, (Wiley, New York, 1962).
102. Andrews, D.G.R., Gray, P., "Combustion of ammonia supported by oxygen, nitrous oxide or nitric oxide. Laminar flame propagation at low pressures in binary mixtures," Combustion and Flame 8, 113-126 (1964).
103. Wolfhard, H. G., Parker, W.G., "A spectroscopic investigation of the structure of diffusion flames," Proceedings of the Physical Society, London A65, 2-19 (1952).
104. Dows, D.A., Whittle, E., Pimentel, G.C., "Infrared emission and absorption in an ammonia oxygen diffusion flame," Journal of Chemical Physics 23, 499-502 (1955).
105. Hussain, D., Norrish, R.G.W., "Explosive oxidation of ammonia and hydrazine studies by kinetic spectroscopy," Proceedings of the Royal Society 373A, 145-164 (1963).

106. Verwimp, J., van Tiggelen, A., "Etude experimental de l'oxydation lente II. Reaction de melanges d'ammoniac et d'oxygene," Bulletin Socaete Chim. Belg. 62, 205-222 (1953).
107. Armitage, J.W., Gray, P., "Flame speeds and flammability limits in the combustion of ammonia: ternary mixtures with hydrogen, nitric oxide, nitrous oxide or oxygen," Combustion and Flame 9, 173-184 (1965).
108. Washko, Robert A., "Reaction of hydrazine and nitrogen tetroxide in a low pressure environment," AIAA Journal 1, 1919-1920 (1963).
109. Gray, P., Spencer, M., "Thermal explosions in the oxidation of hydrazine by nitric oxide and nitrous oxide," Transactions of the Faraday Society 59, 879-885 (1963).
110. Adams, G.K., Parker, W.G., Wolfhard, H.G., "Radical reactions of nitric oxide in flames," Faraday Society Discussions No. 14, 97-103 (1953).
111. Semenov, N.N., Some Problems in Chemical Kinetics and Reactivity, Volume I, translated by Michel Boudart, (Princeton University Press, Princeton, New Jersey, 1958).
112. Gray, P., Thyne, J.C.J., "Kinetics of hydrogen abstraction from hydrazine, ammonia and trideuteroammonia," Faraday Society Transactions 60, 1947-1952 (1964).
113. Antoine, A.C., "The mechanism of burning of liquid hydrazine," Eight Symposium (International) on Combustion, 1057-1059 (Williams and Wilkins, Baltimore, 1962).
114. Antoine, A.C., "The effect of some additives on the burning rate of liquid hydrazine," Combustion and Flame 6, 364-365 (1962).
115. Kline, S.J., McClintock, F.A., "The description of uncertainties in single sample experiments," Mechanical Engineering, 3-8, January 1953.
116. Beighley, C.M., "Storables still renew interest," Missiles and Rockets, 30-33, February 15, 1960.
117. "Performances theoreques des melanges d'ergols pour reacteurs," Rocketdyne.

118. Johnston, S.A., Mathias, E.A., Hanzel, P.C., Schieler, L., "Propellant performance and gas composition handbook," Aerospace Corporation, DCAS-TDR-62-2, January 1962.
119. Johnston, S.A., Cook, E.A., Hansel, P.C., Schieler, L., "Propellant performance and gas composition handbook, Supplement I," Aerospace Corporation, DCAS-TDR-62-2 supplement I, October 1962.
120. Cook, E.A., Johnston, S.A., Schieler, L., "Propellant performance and gas composition handbook, supplement II," Aerospace Corporation, DCAS-TDR-62-2, supplement II, November 1963.
121. Wanhainen, J.P. DeWitt, R.L., Ross, P.S., "Performance of a low-thrust storable-bipropellant rocket at very low chamber pressure," NASA TN D-678, March 1961.
122. Zeleznik, F.J., Gordon, S., "A general IBM 704 or 7090 computer program for computation of chemical equilibrium compositions, rocket performance, and Chapman-Jouget detonations," NASA TN D-1454, October 1962.
123. Gordon, S., Zeleznik, F.J., "A general IBM 704 or 7090 computer program for computation of chemical equilibrium compositions, rocket performance, and Chapman-Jouquet detonations, supplement I--assigned area-ratio performance," NASA TN D-131, 1959.
124. Rollbuhler, R.J., Tomazic, W.A., "Comparison of  $N_2H_4-N_2O_4$  and  $N_2H_4-ClF_3$  in small scale rocket chambers," NASA TN D-131, 1959.
125. Chilenski, J.J., Lee, D.H., "An experimental investigation of the performance of the nitrogen tetroxide-hydrazine system in the oxidizer-rich and fuel-rich regions," JPL TR 32-312, 12 March 1962.
126. Lee, D.H., "Performance calculations for monopropellant hydrazine and monopropellant hydrazine-hydrazine nitrate mixtures," JPL TR 32-348, 3 December 1962.
127. Elverum, G.W. Jr., Staudhammer, P., "The effect of rapid liquid-phase reactions on injector design and combustion in rocket motors," JPL PR 30-4, August, 1959.

NOMENCLATURE

<u>symbol</u>	<u>quantity</u>	<u>dimensions</u>
A	exponent of preexponential factor in Arrhenius expression for the rate constant $k = 10^A T^m \exp(-E/RT)$	
[A]	concentration of species A	moles/cc
a	reaction order with respect to fuel or reducing reactant	
$A_t$	throat area	$\text{cm}^2$
$\text{\AA}$	Angstrom unit, $10^{-8}$ [cm]	
b	reaction order with respect to oxidizer or oxidizing reactant	
$C_p$	specific heat at constant pressure	$\text{cal/mole}^\circ\text{K}$
$C_v$	specific heat at constant volume	$\text{cal/mole}^\circ\text{K}$
$C^*$	characteristic velocity	ft/sec
c	reaction order with respect to initial concentration of oxidizer	
d	bulk density	gm/cc
D	bond dissociation energy	kcal/mole
E	activation energy	cal/mole
$E^*$	effective activation energy	cal/mole
E	bond energy	kcal/mole
$\Delta F_f^\circ$	free energy of formation	kcal/mole
[F]	fuel concentration	gm/cc
$g_c$	gravitational acceleration constant, 980 [cm/sec <sup>2</sup> ]	$\text{cm/sec}^2$
$\Delta H_R$	enthalpy of reaction	kcal/mole fuel
$\Delta H_f^\circ_{298}$	standard enthalpy of formation at 298.16°K	kcal/mole
$\Delta H_f^\circ_T$	standard enthalpy of formation at temperature, T	kcal/mole

$I_{sp}$	specific impulse	sec
$k$	rate constant	(depends on overall rate equation order)
$k_n$	nth order rate constant	$(cc/mole)^{n-1} sec^{-1}$
$k_o$	reference rate constant	
$\dot{m}$	mass flow rate	gm/sec
$MW$	molecular weight	gm/gm-mole
$n$	reaction order	
$n$	number of moles	
$O/F$	oxidizer to fuel ratio (by weight), also "r"	
$[O]$	oxidizer concentration	gm/cc
$P_c$	chamber pressure	pounds/in <sup>2</sup>
$Q$	heat of reaction	cal/mole fuel
$R$	universal gas constant, 1.9869	cal/mole <sup>o</sup> K
$R$	reaction rate	
$R'$	reduced reaction rate	sec <sup>-1</sup>
$r$	mixture ratio, mass oxidizer/mass fuel, also "O/F"	
$S^o$	absolute entropy	cal/mole <sup>o</sup> K
$t$	time	sec
$t_{1/2}$	reaction half-time, time for reaction to proceed to 50% completion	sec
$T$	temperature	<sup>o</sup> K
$u$	uncertainty in measured or calculated quantity	
$x$	mole fraction	
$x$	distance	cm
$\gamma$	ratio of specific heats, $C_p/C_v$	
$\xi$	reaction ratio	
	$\frac{(\text{fuel/oxidizer})}{(\text{fuel/oxidizer})_{\text{reaction stoichiometry}}}$	

$\phi$	equivalence ratio	
	$\frac{(\text{fuel/oxidizer})}{(\text{fuel/oxidizer})_{\text{standard stoichiometry}}}$	
$\rho$	molar density	moles/cc
$\rho_{\text{total}}$	total molar density	moles/cc
$\sigma_x$	standard deviation of x	
$\sigma_{m_l}$	ratio of moles of material m consumed to reactant l consumed	
$\sigma_{p_l}$	ratio of moles of product p produced to reactant l consumed	

subscripts

f	final
i	specie index
m	atom number
n	atom number
o	initial

# APPENDIX A. SUMMARY OF EXPERIMENTAL PARAMETERS, ARRHENIUS PARAMETERS, AND EXPERIMENTAL RATE DATA

The reaction rates measured in the flow reactor are converted to rate constants,  $k$ , through a general rate equation of the form,

$$\frac{d[A]}{dt} = -k[A]^a[B]^b[C]^c \quad \text{EA (1)}$$

The convention used throughout is that,

- A: concentration of fuel (or reducing reactant)
- B: concentration of oxidizer (or oxidizing reactant)
- C: concentration of species C, observed to affect the reaction rate

All concentrations are expressed in (moles/cc). The rate constant will then have the dimensions

$$\frac{(\text{moles/cc})^{-(a+b+c-1)}}{\text{sec}}^{-1}$$

In the summary of experimental parameters the following are identified:

- (1) reactor duct size and material
- (2) range of temperatures over which experimental rates were obtained
- (3) range of initial equivalence ratios (The local composition, upon which the rate constant is calculated, will vary greatly from that indicated by the initial equivalence ratio. As the reaction approaches completion, the local equivalence ratio will approach infinity or

zero depending upon whether the initial value of the equivalence ratio was greater than or less than one. It is, of course, assumed that one of the reactants is fully consumed at "completion.")

- (4) range of initial fuel concentrations
- (5) number of experimental data points

To obtain the temperature dependence of the rate constant, the calculated rate constants are fit by the method of least squares to the following, Arrhenius, rate expression.

$$k = 10^A T^m \exp (-E/RT)$$

In addition to the Arrhenius parameters, A and E, the uncertainties in A and E, expressed at their respective standard deviations, are tabulated.

For each combination of reactants and duct in which rate measurements were made, the logarithm (base 10) of the experimental rate constant is plotted as a function of  $1000/T$ . The particular rate equation used, EA(1), is identified by the exponents a,b,c. The exponent "m" is the temperature dependence of the pre-exponential part of the Arrhenius rate constant, for which a value of zero is used throughout Appendix A. In the computer plots, the asterisk (\*) refers to a single datum point. Multiple data points, that is, grid regions in which several data points are grouped, are indicated by the number of data points, that is, the symbols 2 to 9. If the number of data points exceeds 9, the symbol "\$" is used. Note that the number "1" always indicates a grid line and not a single datum point. The lines drawn through the experimental points are the least squares curve fit lines.



TABLE 23. Summary of hydrogen/nitrogen dioxide reaction rate constants

rate equation $\frac{d[H_2]}{dt} = -k \frac{[H_2]^{1.4} [NO_2]}{[NO_2] + [NO]}$ $k = 10^A \exp (-E/RT) \quad [ (\text{mole/cc})^{-.4} \text{sec}^{-1} ]$		
duct diameter [in]	2	4
duct material	quartz	quartz
T [°K]	890-1110	850-1090
$\phi_o$	.33-2.4	0.7-5.5
$[H_2]_o \times 10^7$ [moles/cc]	1.8-10.6	2.5-9.6
data points	271	455
E [kcal/mole]	+48.0	+46.2
$\sigma_E$ [kcal/mole]	0.8	0.6
A	14.91	14.26
$\sigma_A$	.18	.15

[231]

HYDROGEN/NITROGEN DIOXIDE REACTION KINETICS  
2 (INCH) QUARTZ DUCT, NITROGEN CARRIER

LOG10(RATE CONSTANT) M= 0.00 A= 1.40 B= 1.00 C=-1.00 271 POINTS

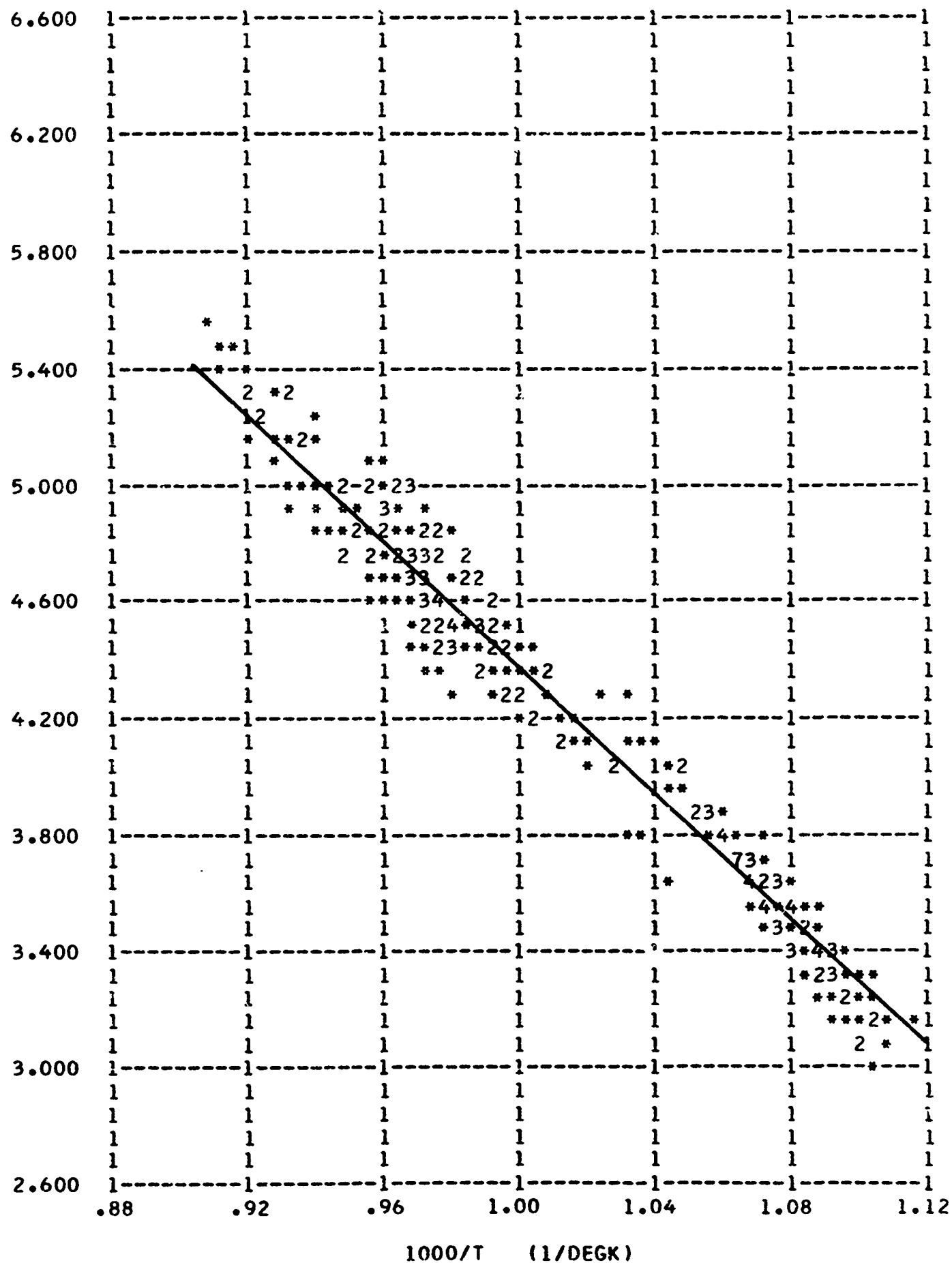


FIGURE 50

HYDROGEN/NITROGEN DIOXIDE REACTION KINETICS  
4 (INCH) QUARTZ DUCT, NITROGEN CARRIER

LOG10(RATE CONSTANT) M= 0.00 A= 1.40 B= 1.00 C=-1.00 455 POINTS

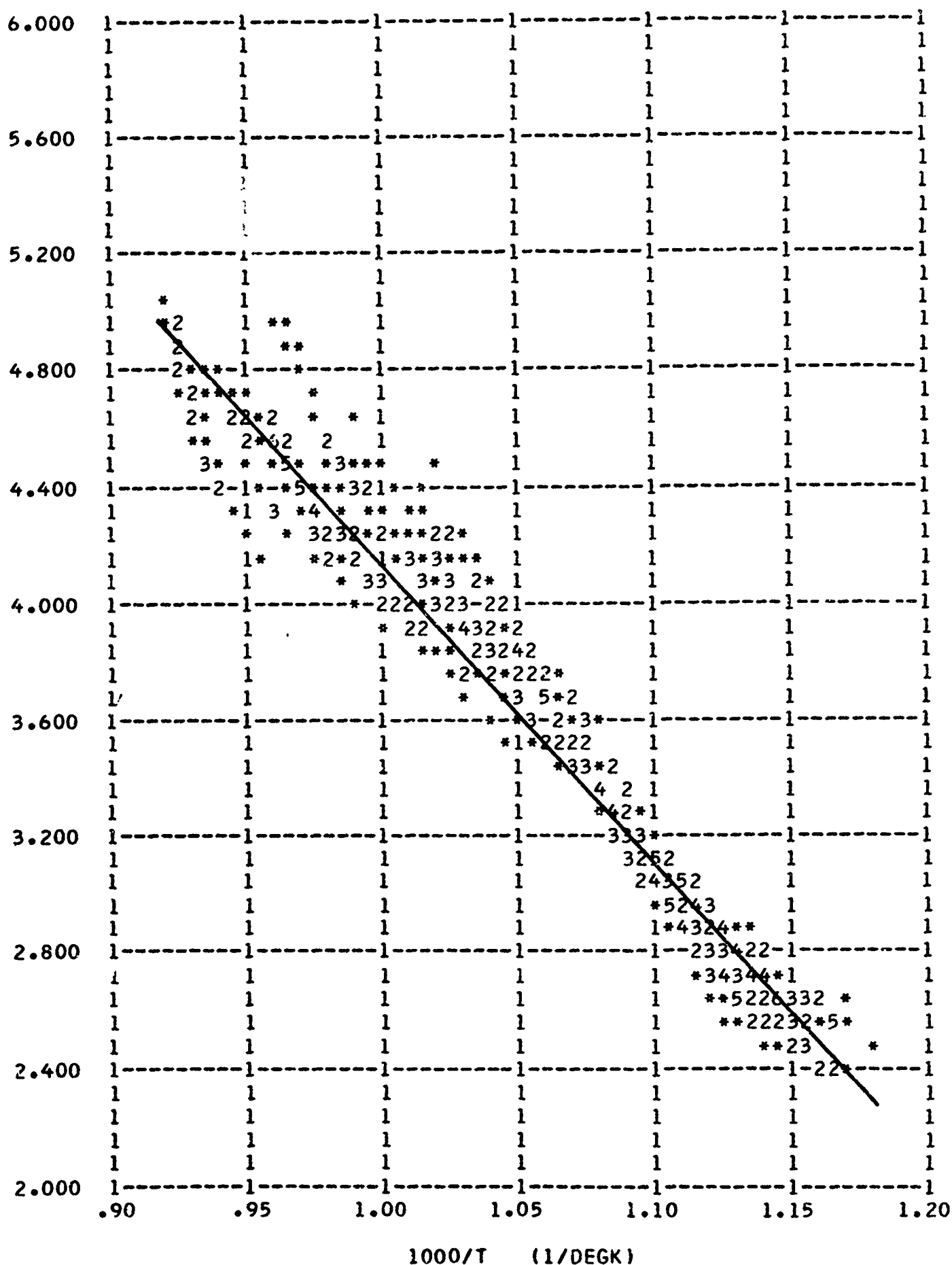


FIGURE 51

TABLE 24. Summary of hydrogen/oxygen reaction rate constants,  
near stoichiometric (nitrogen carrier)

rate equation $\frac{d[H_2]}{dt} = -k[H_2]$ $k = 10^A \exp(-E/RT) \quad [\text{sec}^{-1}]$		
duct diameter [in]	2	4
duct material	quartz	quartz
T [°K]	915-980	880-960
$\phi_O$	.3-1.0	.25-1.3
$[H_2]_O \times 10^7$ [moles/cc]	1.5-4.7	1.1-2.7
data points	21	198
E [kcal/mole]	+37.8	+38.2
$\rho_E$ [kcal/mole]	6.7	1.4
A	11.15	10.96
$\rho_A$	1.55	.34

[234]

HYDROGEN/OXYGEN REACTION KINETICS  
2 (INCH) QUARTZ DUCT, NITROGEN CARRIER

LOG10(RATE CONSTANT) M= 0.00 A= 1.00 B= 0.00 C= 0.00 21 POINTS

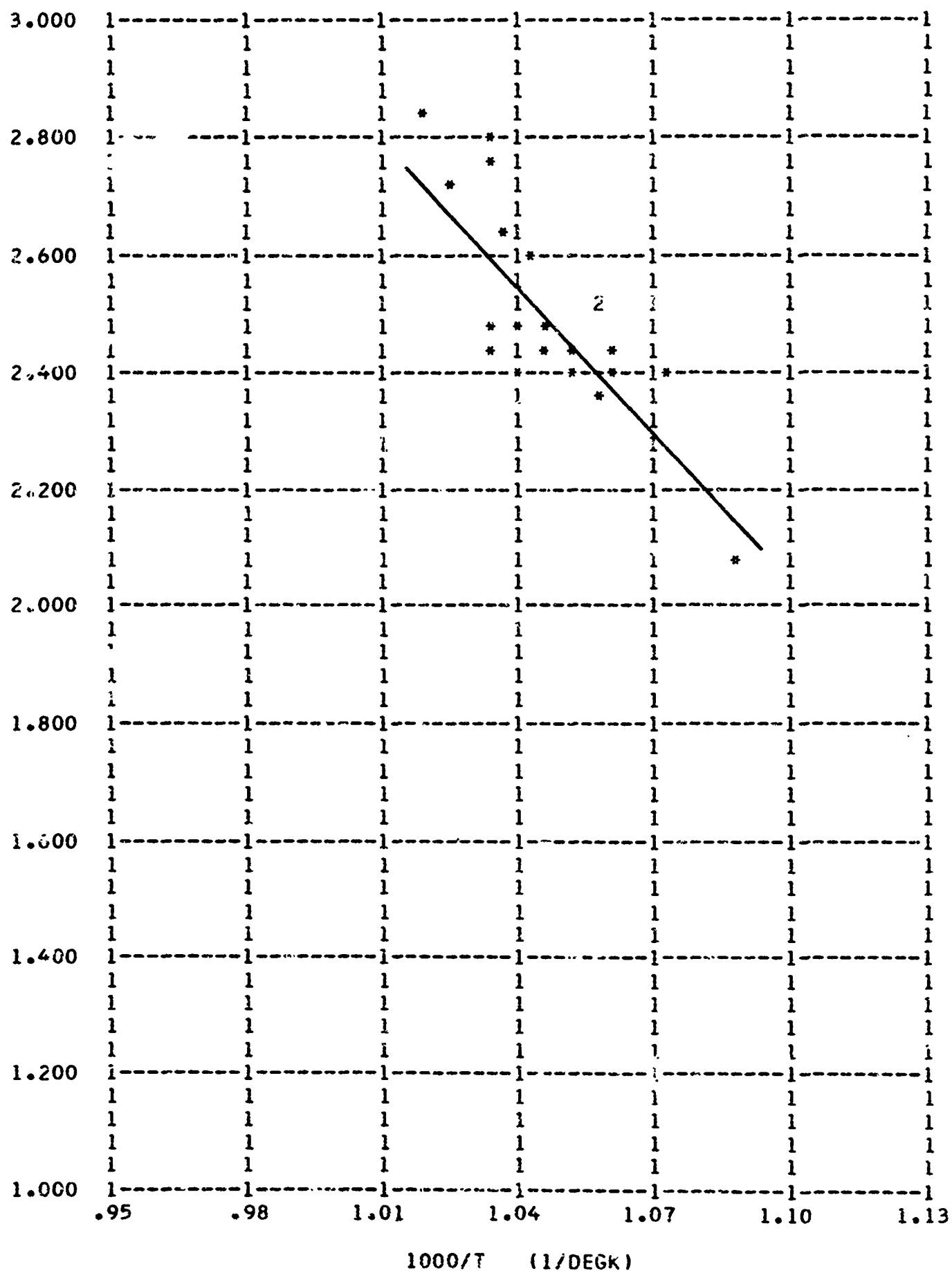


FIGURE 52

HYDROGEN/OXYGEN REACTION KINETICS  
4 (INCH) QUARTZ DUCT, NITROGEN CARRIER

LOG10(RATE CONSTANT) M= 0.00 A= 1.00 B= 0.00 C= 0.00 198 POINTS

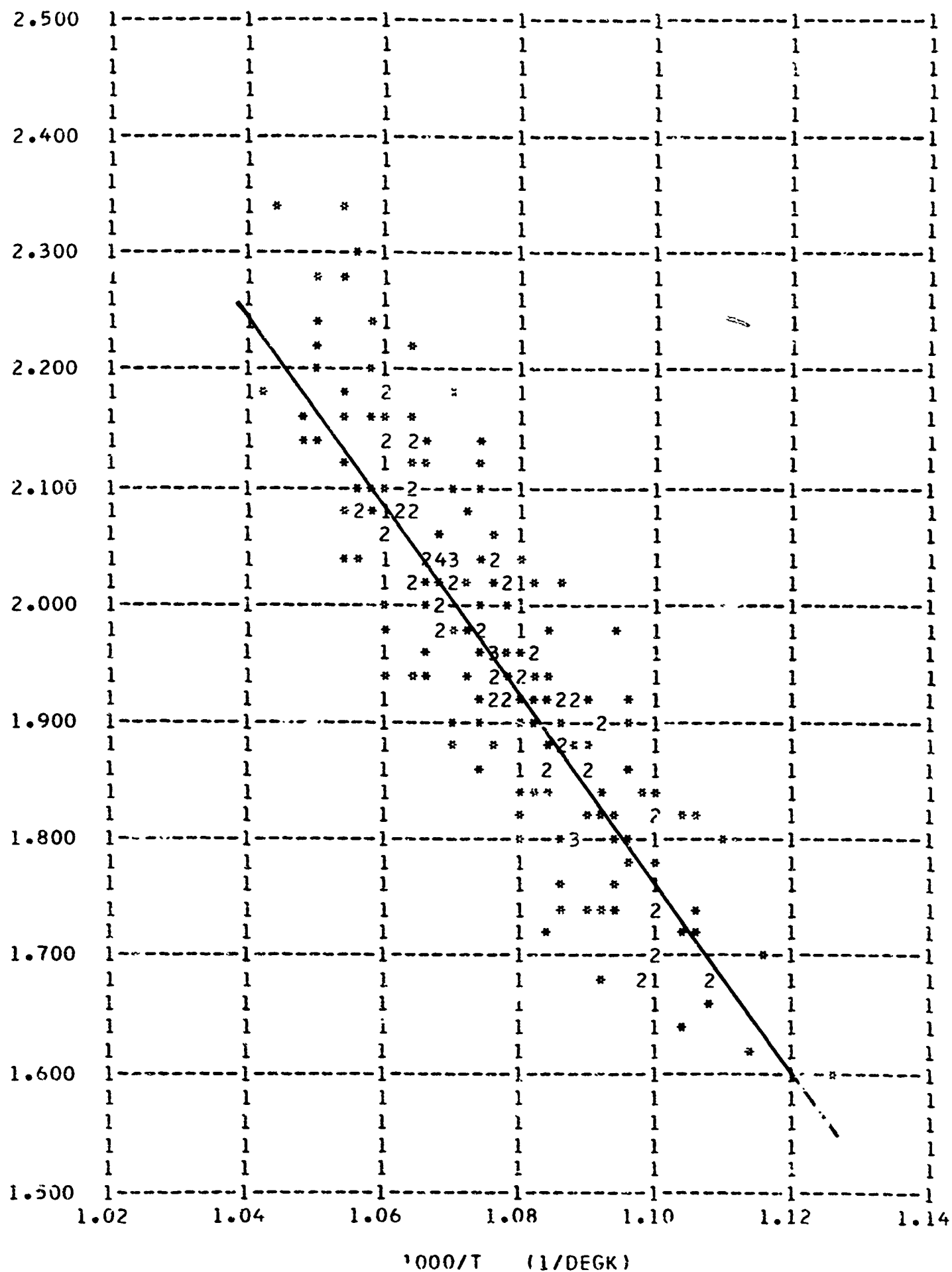


FIGURE 53

TABLE 25. Summary of hydrogen/oxygen reaction rate constants  
excess oxygen (air carrier)

rate equation $\frac{d[H_2]}{dt} = -k[H_2]$ $k = 10^A \exp(-E/RT) \quad [\text{sec}^{-1}]$				
duct diameter [in]	2	3	4	3 3/8
duct material	quartz	quartz	quartz	stainless steel
T [°K]	900-1050	920-1020	930-1040	920-1030
$\phi_o$	.031-.062	.026-.124	.031-.062	.031-.050
$[H_2]_o \times 10^7$ [moles/cc]	1.7-3.0	1.3-6.0	1.7-3.0	1.7-2.5
data points	108	26	106	102
E [kcal/mole]	+36.2	+39.8	+39.5	+38.2
$\sigma_E$ [kcal/mole]	1.6	3.6	1.6	1.3
A	10.42	11.15	10.71	10.62
$\sigma_A$	.35	.81	.35	.30

[237]

HYDROGEN/OXYGEN REACTION KINETICS  
2 (INCH) QUARTZ DUCT, AIR CARRIER

LOG10(RATE CONSTANT) M= 0.00 A= 1.00 B= 0.00 C= 0.00 108 POINTS

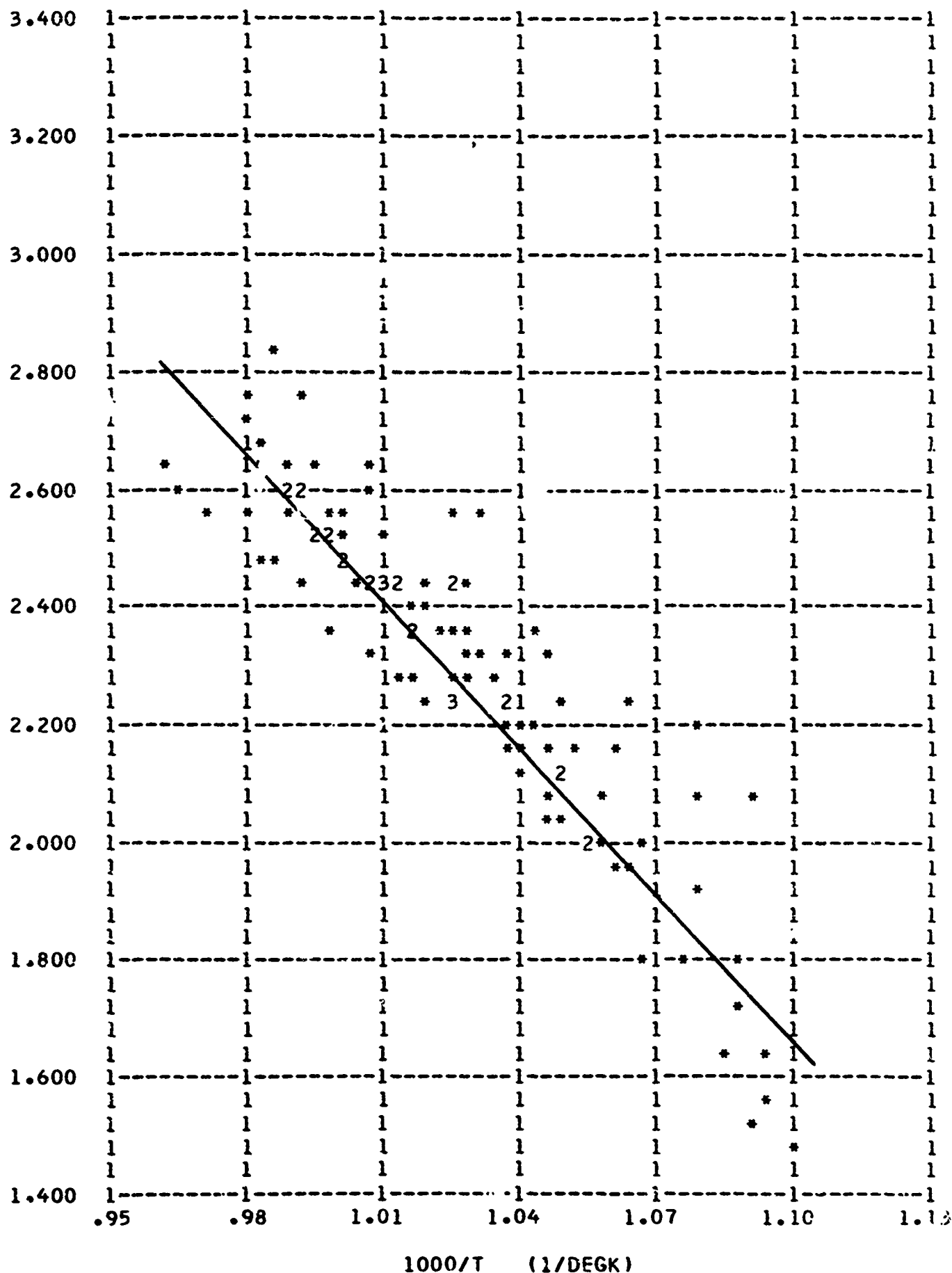


FIGURE 54



HYDROGEN/OXYGEN REACTION KINETICS  
3 (INCH) QUARTZ DUCT, AIR CARRIER

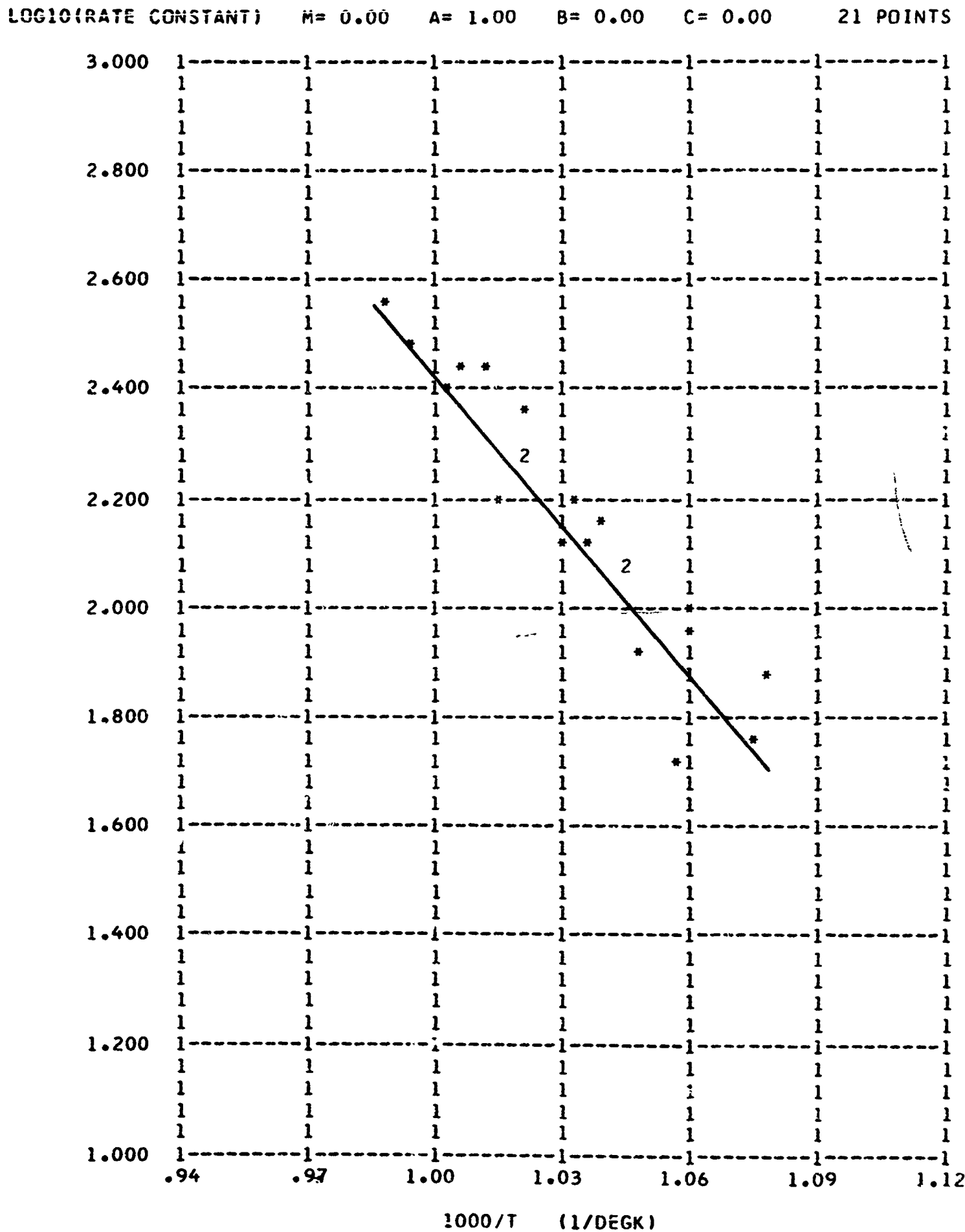


FIGURE 55

HYDROGEN/OXYGEN REACTION KINETICS  
4 (INCH) QUARTZ DUCT, AIR CARRIER

LOG10(RATE CONSTANT) M= 0.00 A= 1.00 B= 0.00 C= 0.00 107 POINTS

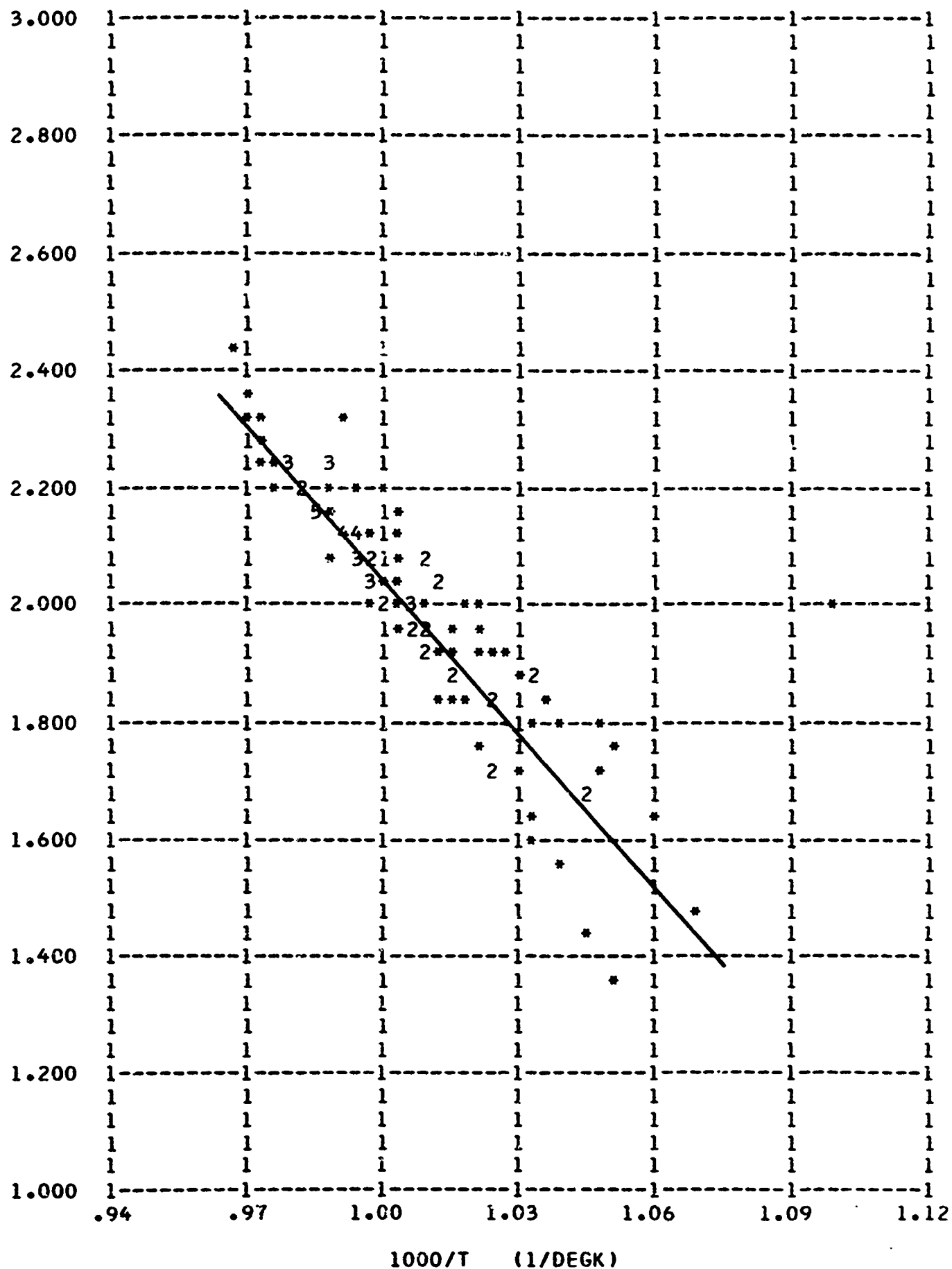


FIGURE 56

[240]

HYDROGEN/OXYGEN REACTION KINETICS  
3.375 (INCH) STAINLESS STEEL DUCT, AIR CARRIER

LOG10(RATE CONSTANT) M= 0.00 A= 1.00 B= 0.00 C= 0.00 102 POINTS

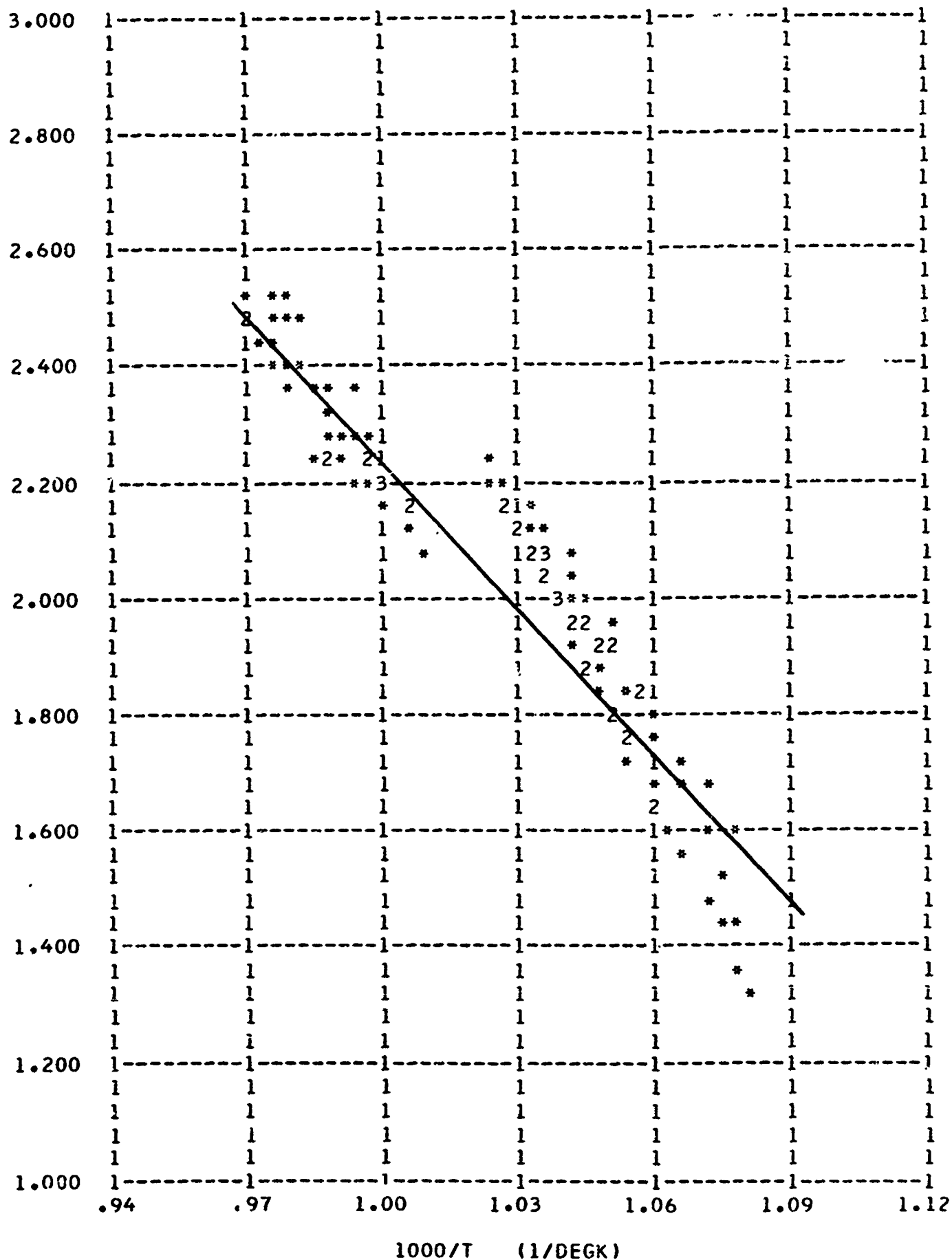


FIGURE 57

TABLE 26. Summary of hydrogen/nitric oxide-oxygen reaction rate constants,  $\text{H}_2/\text{NO} + \frac{1}{2}\text{O}_2$ , nitrogen carrier

rate equation $\frac{d[\text{H}_2]}{dt} = -k[\text{H}_2]^a[\text{O}_2]^b[\text{NO}]^c$		
a	1.4	1.0
b	1.0	0
c	-1.0	0
$k = 10^A \exp(-E/RT)$		
	[ (moles/cc) $^{-.4}$ sec $^{-1}$ ]	[sec $^{-1}$ ]
duct diameter [in]	2	
duct material	quartz	
T [°K]	1030-1100	
$\phi_o$	.44-.64	
$\xi_o$	.88-1.29	
$[\text{H}_2] \times 10^7$ [moles/cc]	2.1-4.6	
data points	69	
E [kcal/mole]	+98.3	+68.6
$\sigma_E$ [kcal/mole]	5.8	5.6
A	25.71	16.46
$\sigma_A$	1.18	1.14

HYDROGEN/NITROGEN DIOXIDE (DECOMPOSED) REACTION KINETICS  
2 (INCH) QUARTZ DUCT, NITROGEN CARRIER, OXIDIZER INJECTION PORT 4

LOG10(RATE CONSTANT) M= 0.00 A= 1.40 B= 1.00 C=-1.00 69 POINTS

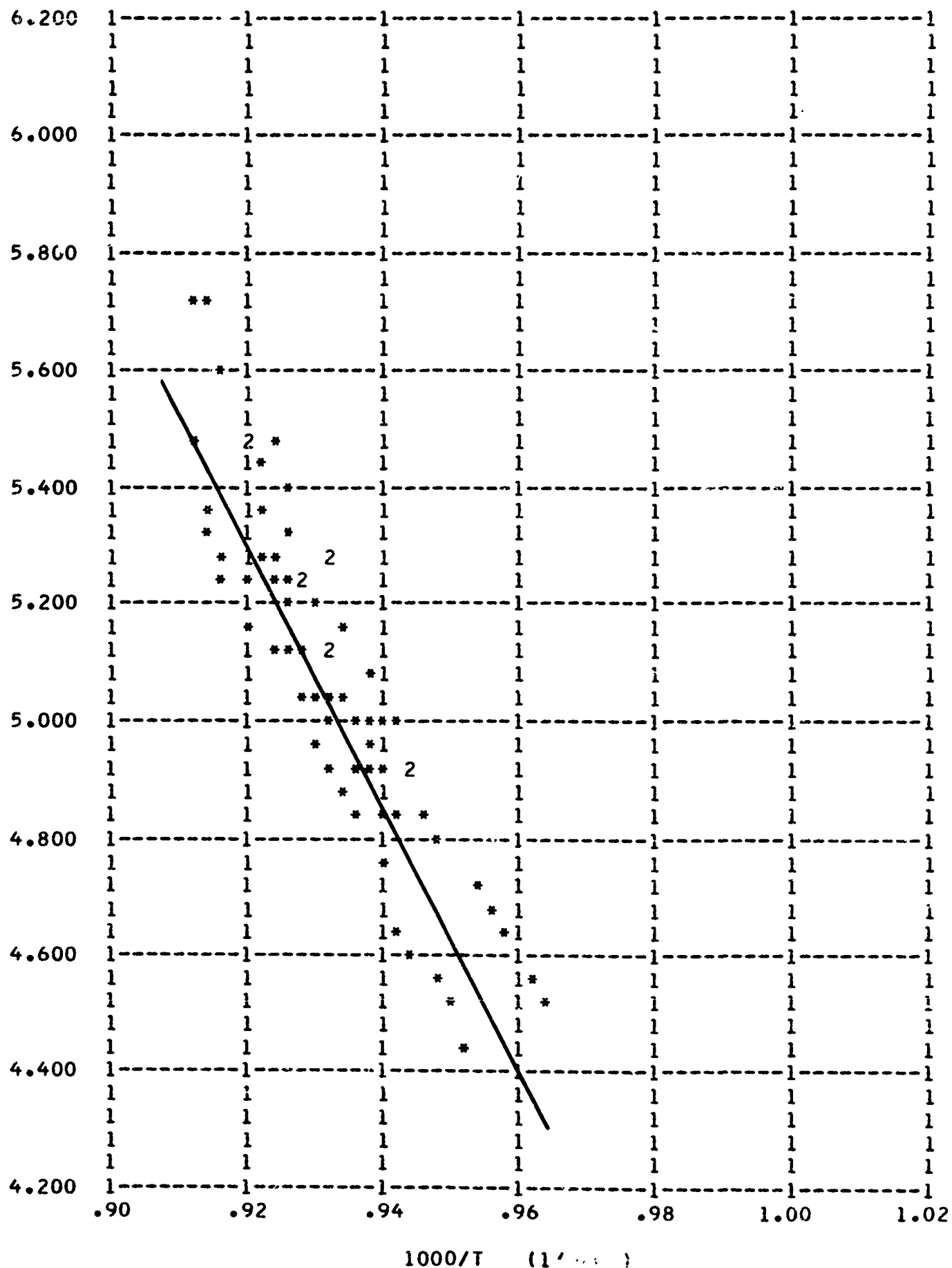


FIGURE 58

TABLE 27. Summary of ammonia/nitrogen dioxide reaction rate constants, nitrogen carrier

rate equation $\frac{d[\text{NH}_3]}{dt} = -k[\text{NH}_3][\text{NO}_2]$ $k = 10^A \exp(-E/RT)$ [cc/mole sec]		
duct diameter [in]	2	4
duct material	quartz	quartz
T [°K]	900-1080	880-1110
$\phi_o$	.27-6.8	.37-6.0
$\xi_o$	.54-13.6	.74-12.0
$[\text{NH}_3]_o \times 10^7$ [moles/cc]	.61-4.5	.61-3.4
data points	187	324
E [kcal/mole]	+41.8	+33.8
$\sigma_E$ [kcal/mole]	1.5	1.1
A	17.63	15.85
$\sigma_A$	.34	.25

AMMONIA/NITROGEN DIOXIDE REACTION KINETICS  
2 (INCH) QUARTZ DUCT, NITROGEN CARRIER

LOG10(RATE CONSTANT) M= 0.00 A= 1.00 B= 1.00 C= 0.00 187 POINTS

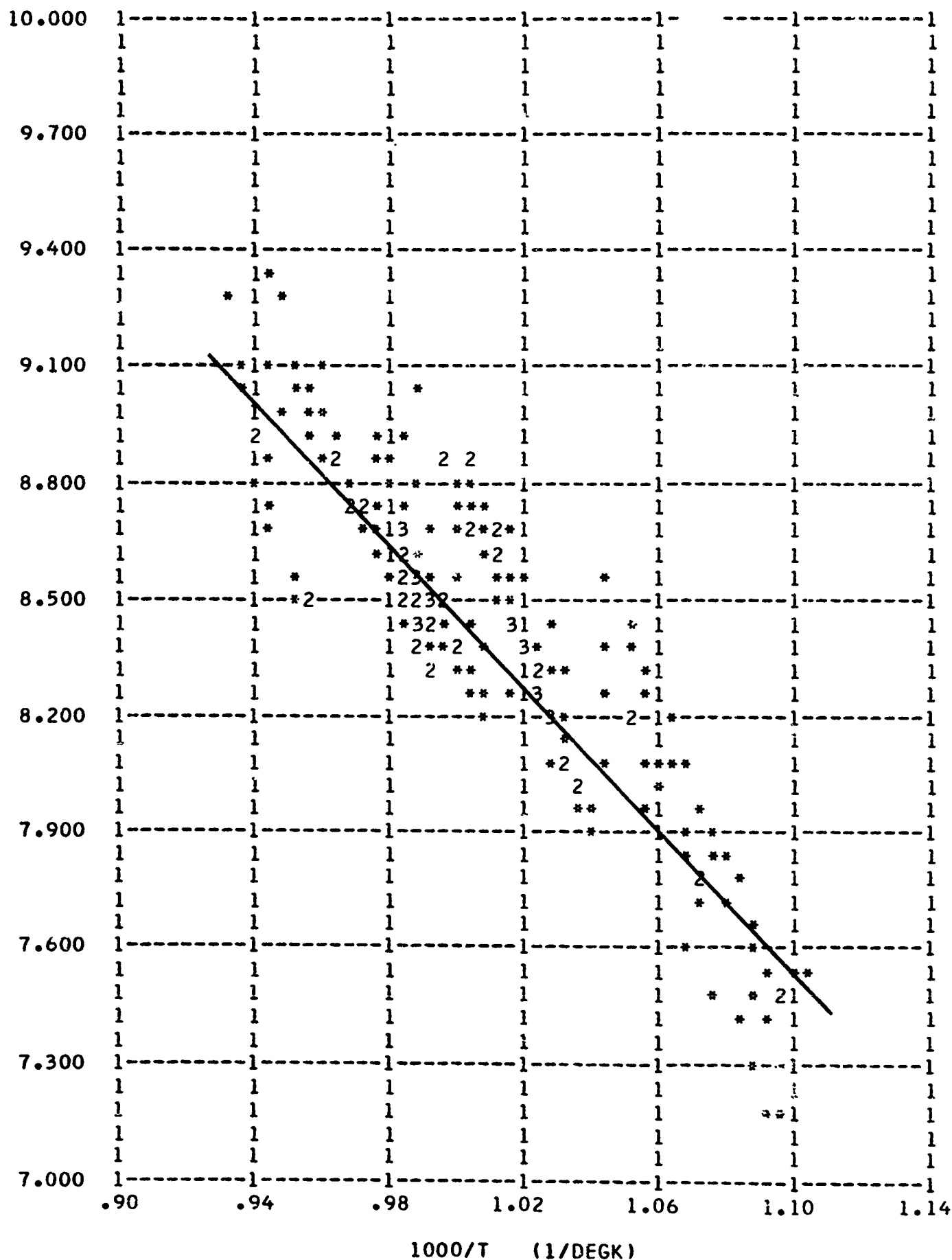


FIGURE 59

[245]

AMMONIA/NITROGEN DIOXIDE REACTION KINETICS  
4 (INCH) QUARTZ DUCT, NITROGEN CARRIER

LUG10(RATE CONSTANT) M= 0.00 A= 1.00 B= 1.00 C= 0.00 324 POINTS

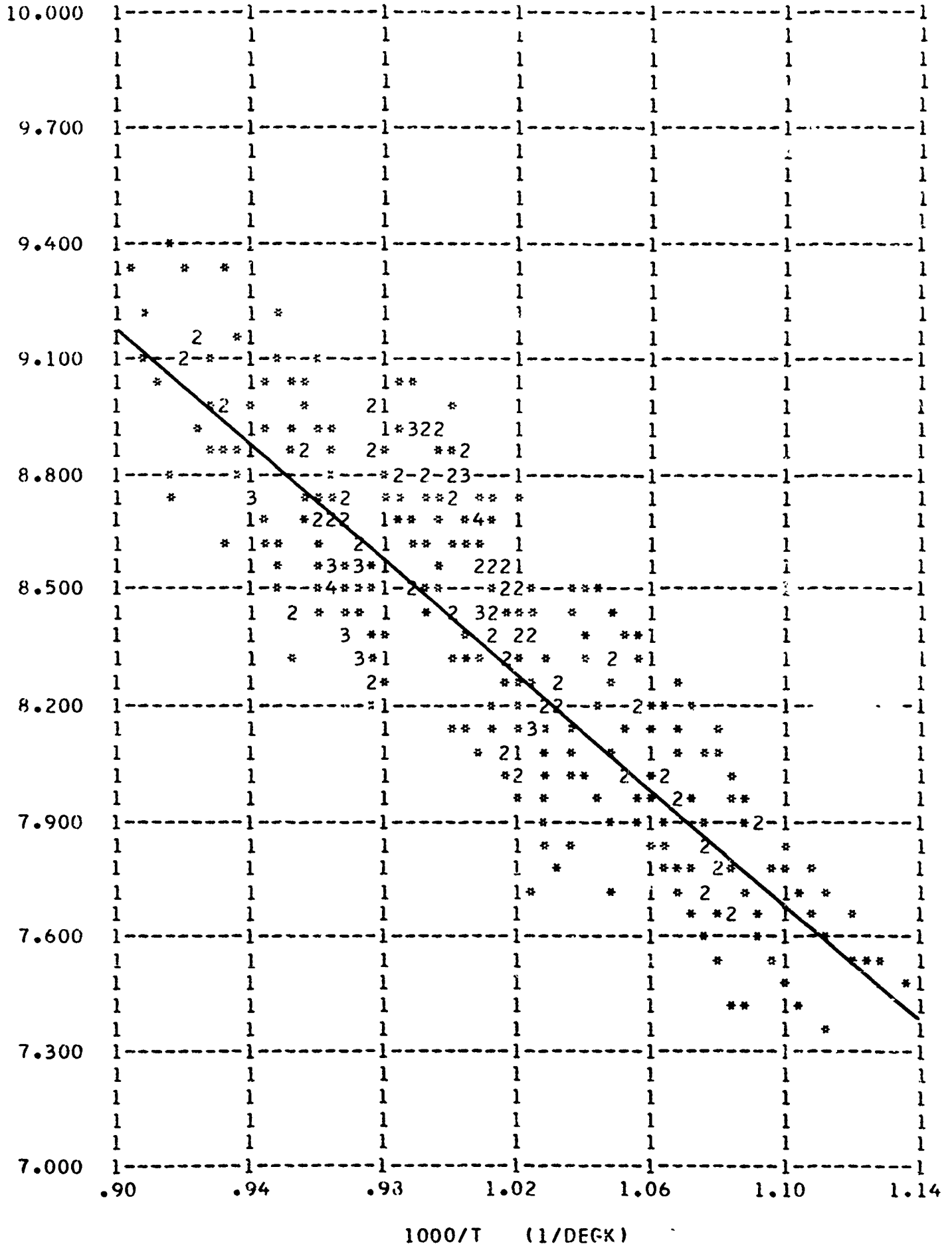


FIGURE 60



TABLE 28. Summary of ammonia/oxygen reaction rate constants, air carrier

rate equation $\frac{d[NH_3]}{dt} = -k[NH_3]^a [O_2]^b$		
a	1.0	1.0
b	1.0	0
$k = 10^A \exp (-E/RT)$		
	[cc/mole cc]	[sec <sup>-1</sup> ]
duct diameter[in]	4	
duct material	quartz	
T[°K]	1110-1210	
$\phi_o$	.12-.16	
$[NH_3]_o \times 10^{-7}$ [moles/cc]	3.8-7.0	
data points	72	
E [kcal/mole]	+38.7	+34.5
$\rho_E$ [kcal/mole]	3.1	3.1
A	14.61	8.10
$\rho_A$	.59	.59

[247]

AMMONIA/OXYGEN REACTION KINETICS  
4 (INCH) QUARTZ DUCT, AIR CARRIER

LOG10(RATE CONSTANT) M= 0.00 A= 1.00 B= 1.00 C= 0.00 72 POINTS

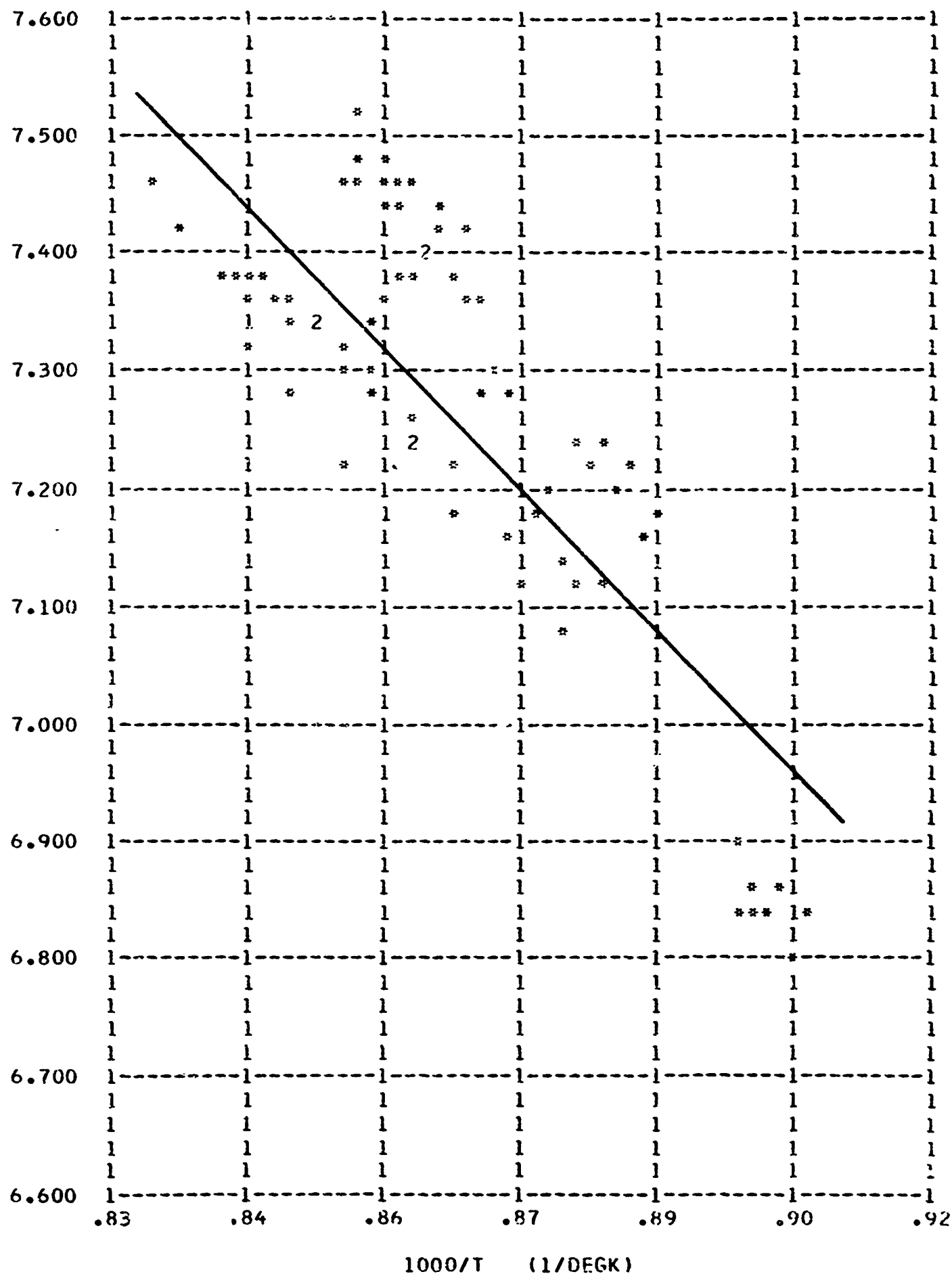


FIGURE 61

TABLE 29. Summary of ammonia-hydrogen/nitrogen dioxide reaction rate constants, nitrogen carrier

rate equation $\frac{d[\text{NH}_3 + \frac{1}{2}\text{H}_2]}{dt} = -k[\text{NH}_3 + \frac{1}{2}\text{H}_2]^a[\text{NO}_2]^b$		
a	1.0	1.0
b	1.0	0
$k = 10^A \exp(-E/RT)$		
	(cc/mole sec)	(sec <sup>-1</sup> )
duct diameter [in]	4	
duct material	quartz	
T [°K]	910-980	
$\phi_0$	.24-.5	
$\xi_0$	.58-1.0	
$[\text{NH}_3 + \frac{1}{2}\text{H}_2]_0 \times 10^7$ [moles/cc]	1.1-2.0	
data points	96	
E [kcal/mole]	+65.9	+48.2
$\sigma_E$ [kcal/mole]	3.9	1.8
A	23.44	12.63
$\phi_A$	.91	.41

[249]

AMMONIA+HYDROGEN(2-1)/NITROGEN DIOXIDE REACTION KINETICS  
4 (INCH) QUARTZ DUCT, NITROGEN CARRIER

LOG10(RATE CONSTANT) M= 0.00 A= 1.00 B= 1.00 C= 0.00 96 POINTS

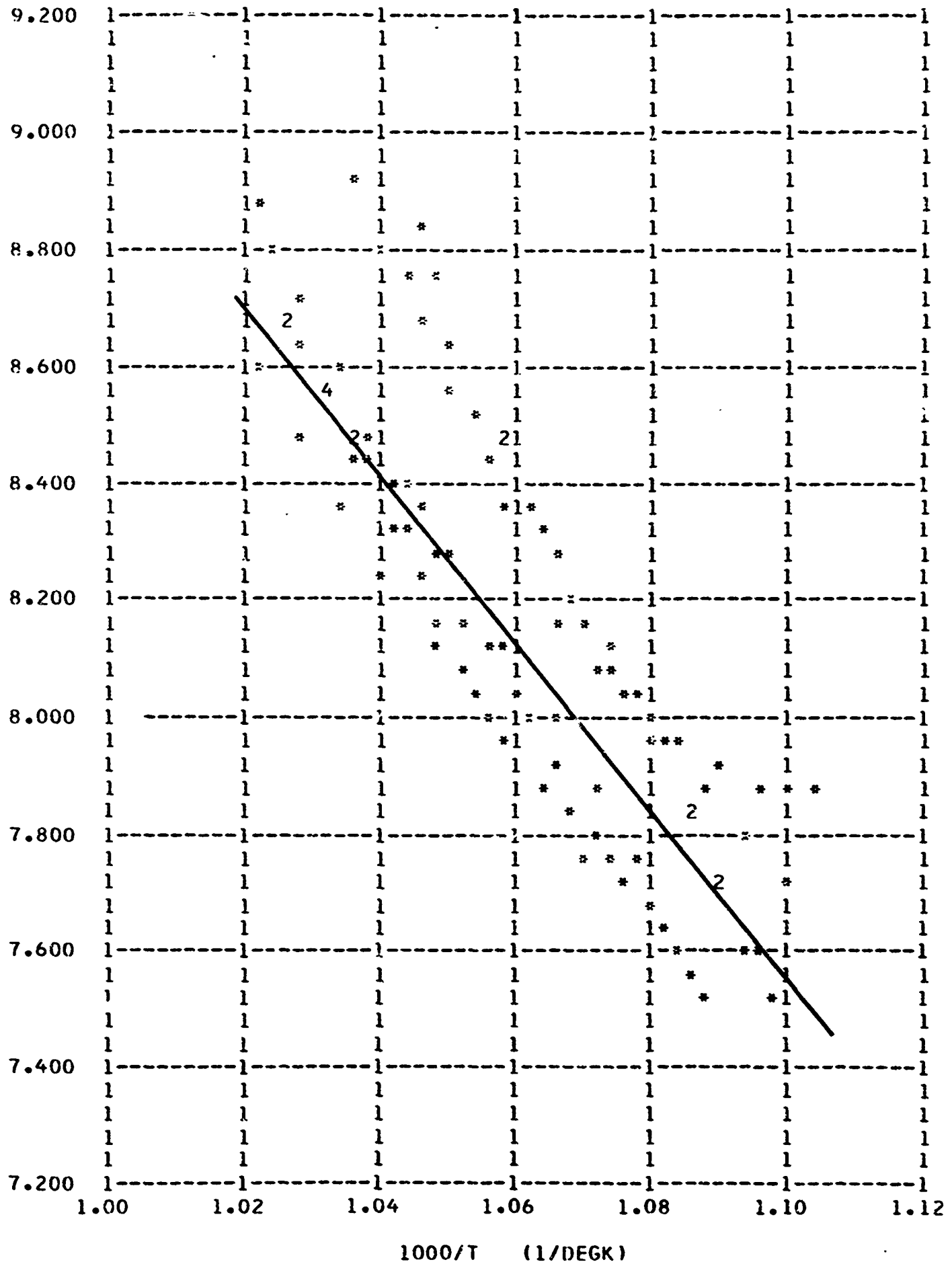


FIGURE 62

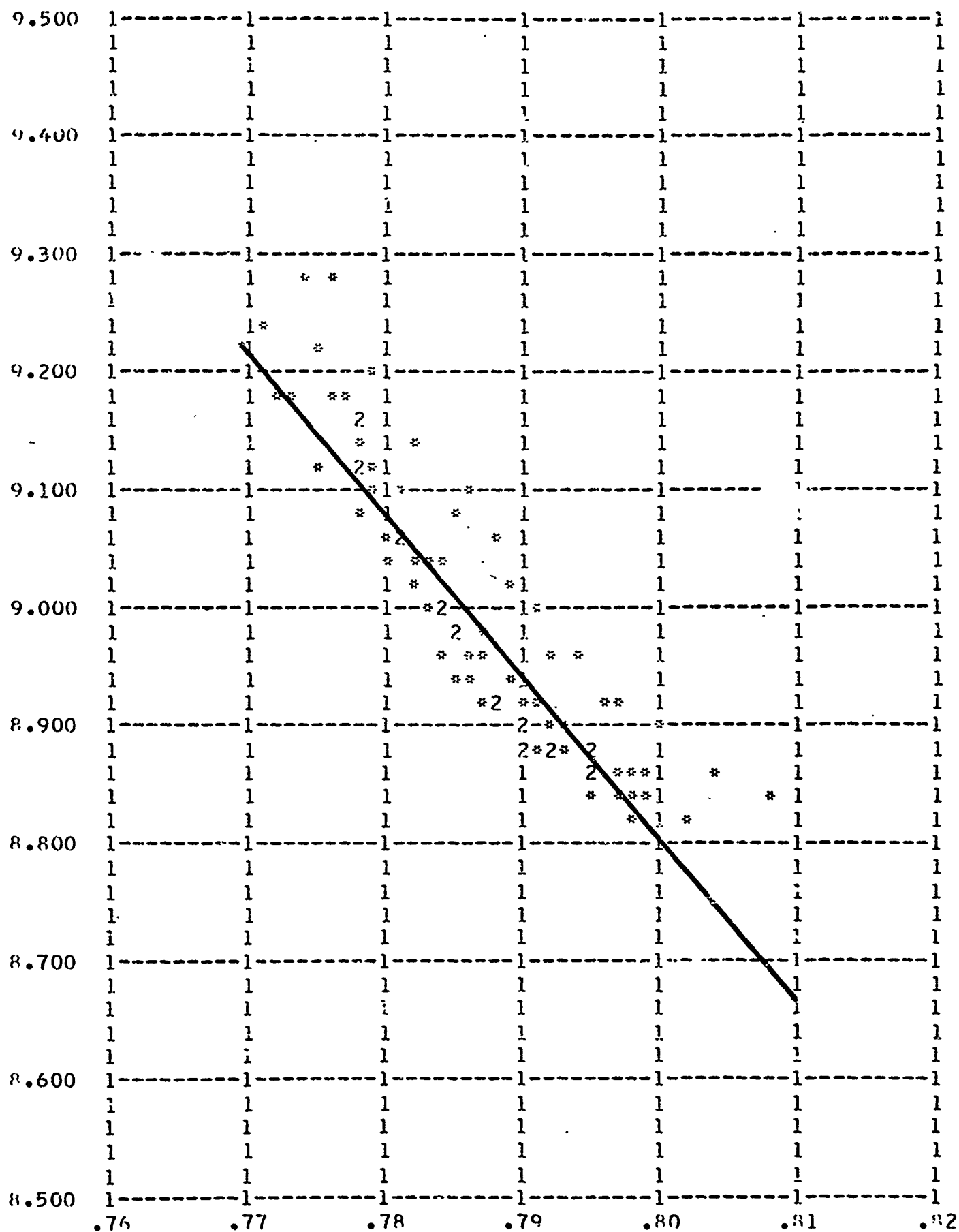
TABLE 30. Summary of ammonia-hydrogen/oxygen reaction rate constants, nitrogen carrier

rate equation $\frac{d[\text{NH}_3 + \frac{1}{2}\text{H}_2]}{dt} = -k[\text{NH}_3 + \frac{1}{2}\text{H}_2]^a[\text{O}_2]^b$		
a	1.0	1.0
b	1.0	0
$k = 10^A \exp (-E/RT)$		
	[cc/mole sec]	[sec <sup>-1</sup> ]
duct diameter [in]	4	
duct material	quartz	
T [°K]	1230-1300	
$\phi_0$	.28-.5	
$[\text{NH}_3 + \frac{1}{2}\text{H}_2]_0 \times 10^7$ [moles/cc]	.6-.9	
data points	80	
E [kcal/mole]	+61.9	+48.3
$\sigma_E$ [kcal/mole]	3.4	3.9
A	19.64	10.28
$\sigma_A$	.72	.84

[251]

ACQUINIA+HYDROGEN(2=1)/OXYGEN REACTION KINETICS  
4 (INCH) QUARTZ DUCT, NITROGEN CARRIER

LOG10(RATE CONSTANT) H= 0.00 A= 1.00 B= 1.00 C= 0.00 80 POINTS



1000/T (1/D°GK)

FIGURE 63

TABLE 31. Summary of hydrazine/nitrogen dioxide reaction rate constants, nitrogen carrier

rate equation $\frac{d[N_2H_4]}{dt} = -k [N_2H_4]$ $k = 10^A \exp (-E/RT) \quad [sec^{-1}]$		
	step I reduction of NO <sub>2</sub> to NO	step II reduction of NO
duct diameter [in]	4	
duct material	quartz	
T [°K]	810-880	980-1040
$\phi_o$	.2-.3	.3-1.0
$[N_2H_4]_o \times 10^7$ [moles/cc]	1.0	.4-1.2
data points	56	256
E [kcal/mole]	+26.7	+39.6
$\sigma_E$ [kcal/mole]	1.1	2.6
A	8.43	10.17
$\sigma_A$	.28	.55

[253]

HYDRAZINE/NITROGEN DIOXIDE REACTION KINETICS  
4 (INCH) QUARTZ DUCT, NITROGEN CARRIER

LOG10(RATE CONSTANT) M= 0.00 A= 1.00 B= 0.00 C= 0.00 56 POINTS

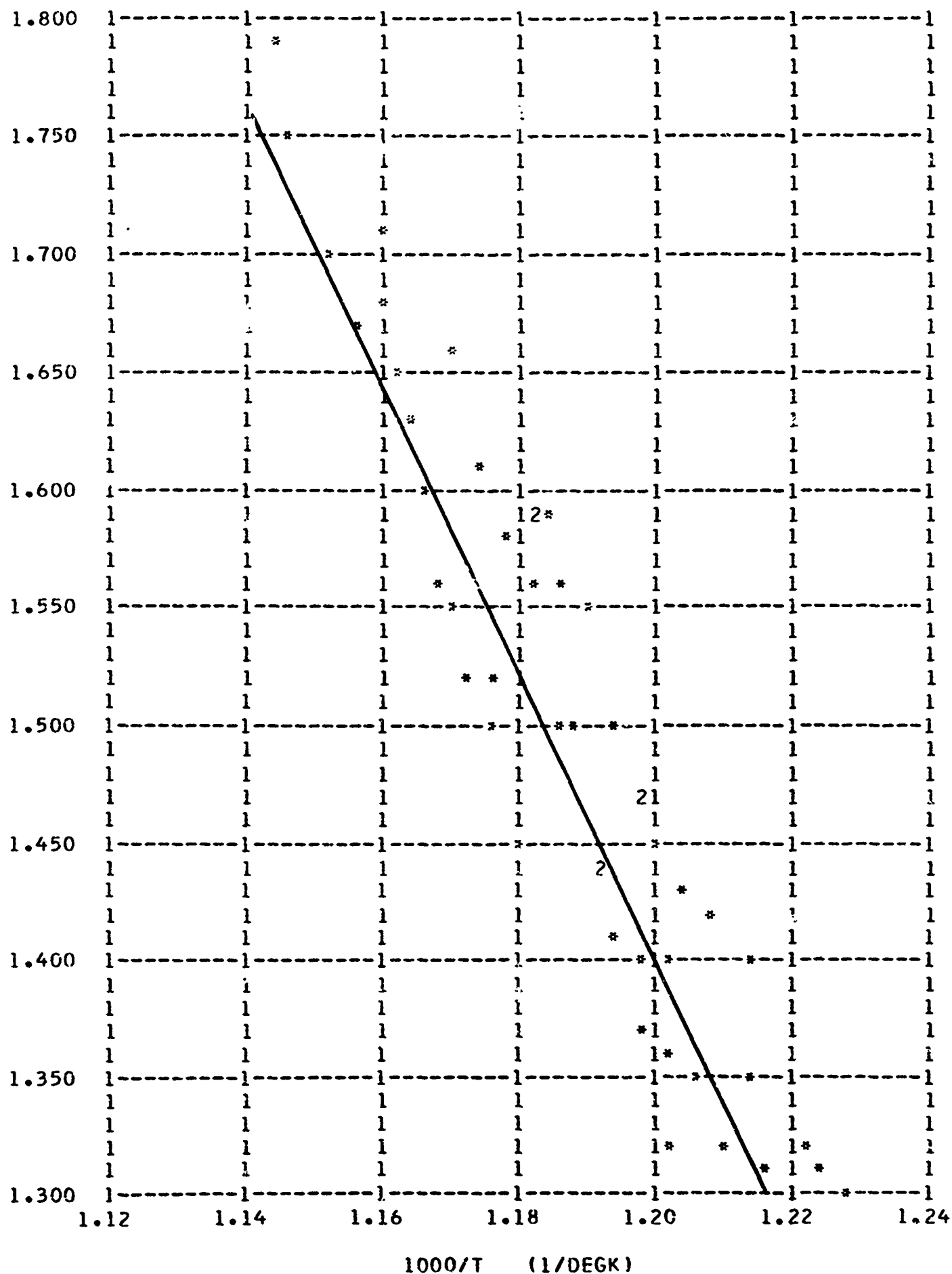


FIGURE 64



HYDRAZINE/NITROGEN DIOXIDE REACTION KINETICS  
4 (INCH) QUARTZ DUCT, NITROGEN CARRIER

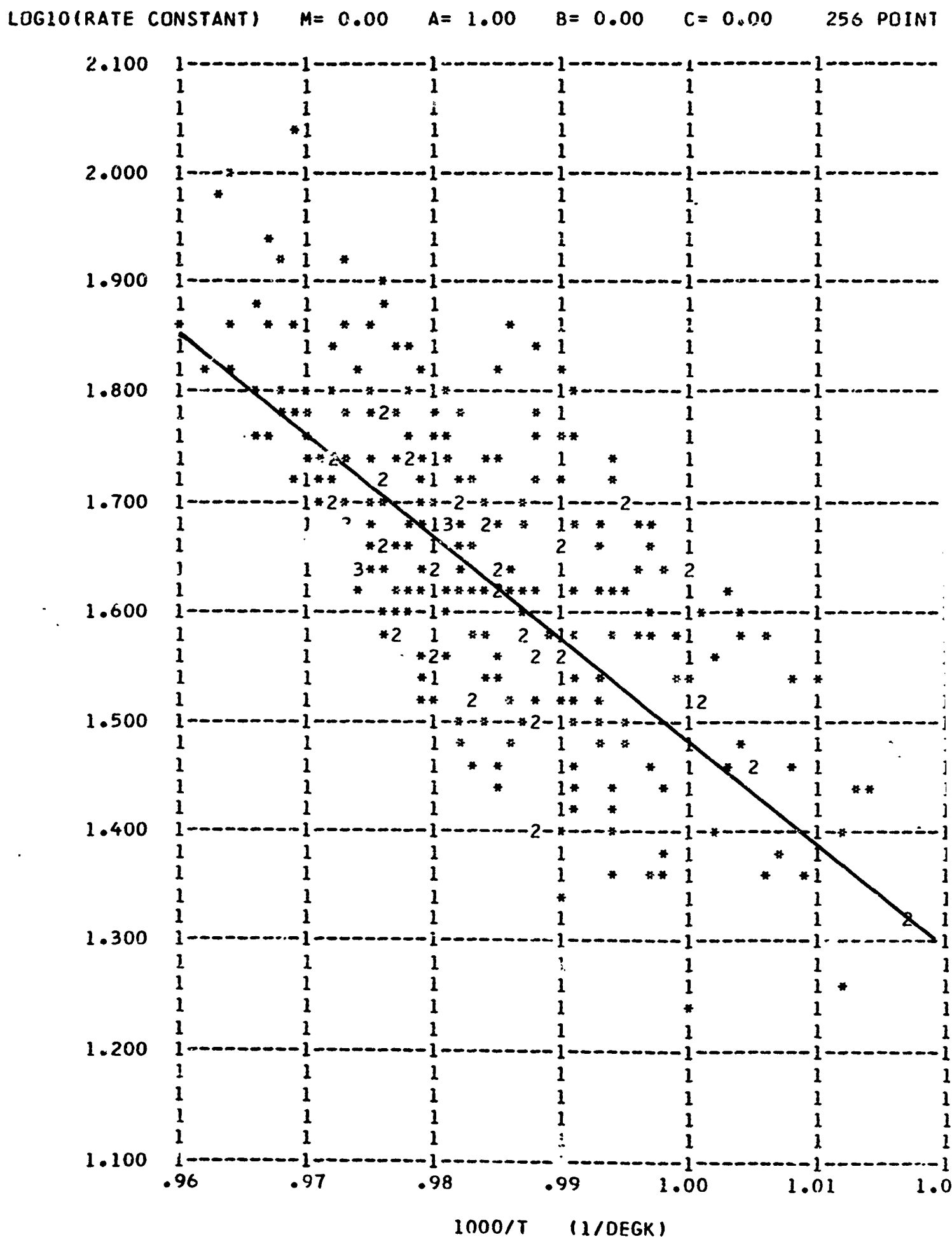


FIGURE 65

TABLE 32. Summary of hydrazine/oxygen reaction rate constants, nitrogen carrier

rate equation $\frac{d[N_2H_4]}{dt} = k [N_2H_4]$ $k = 10^A \exp (-E/RT) \quad [sec^{-1}]$	
duct diameter [in]	4
duct material	quartz
T [°K]	950-1010
$\phi_o$	.2-.5
$[N_2H_4]_o \times 10^7$ [moles/cc]	.6-1.4
data points	1.83
E [kcal/mole]	+37.2
$\sigma_E$ [kcal/mole]	2.4
A	9.91
$\sigma_A$	.54

HYDRAZINE/OXYGEN REACTION KINETICS  
4 (INCH) QUARTZ DUCT, NITROGEN CARRIER

LOG10(RATE CONSTANT) M= 0.00 A= 1.00 B= 0.00 C= 0.00 183 POINTS

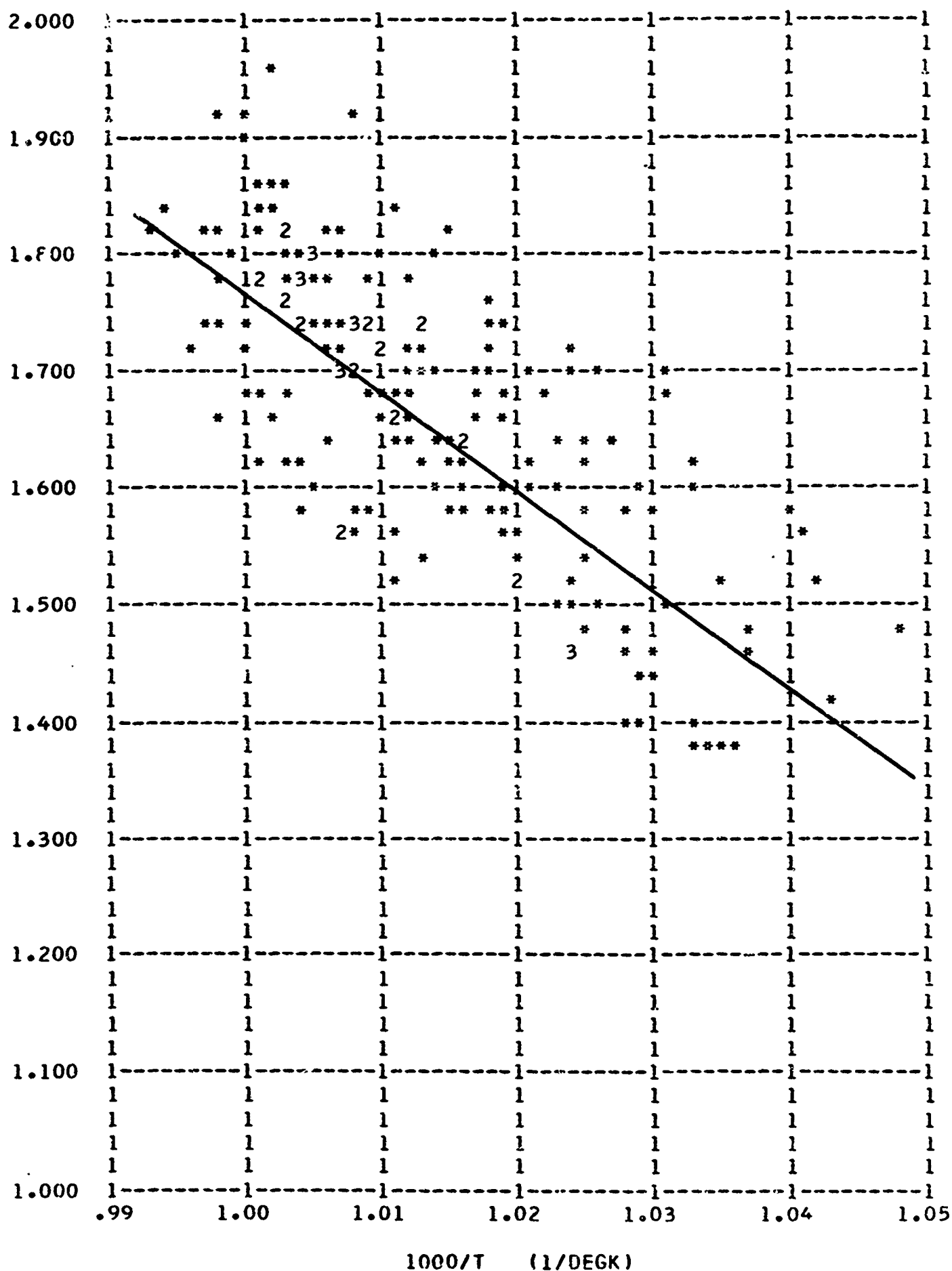


FIGURE 66

TABLE 33. Summary of hydrazine/decomposed nitrogen dioxide rate constants, nitrogen carrier

rate equation $\frac{d[N_2H_4]}{dt} = -k[N_2H_4]$ $k = 10^A \exp (-E/RT) \quad [\text{sec}^{-1}]$	
duct diameter [in]	4
duct material	quartz
T [°K]	960-1020
$\phi_o$	.15-.45
$[N_2H_4]_o \times 10^7$ [moles/cc]	.35-.50
data points	44
E [kcal/mole]	+39.1
$\sigma_E$ [kcal/mole]	2.3
A	10.35
$\sigma_A$	.50

HYDRAZINE/DECOMPOSED NITROGEN DIOXIDE REACTION KINETICS  
4 (INCH) QUARTZ DUCT, NITROGEN CARRIER

LOG10(RATE CONSTANT) M= 0.00 A= 1.00 B= 0.00 C= 0.00 44 POINTS

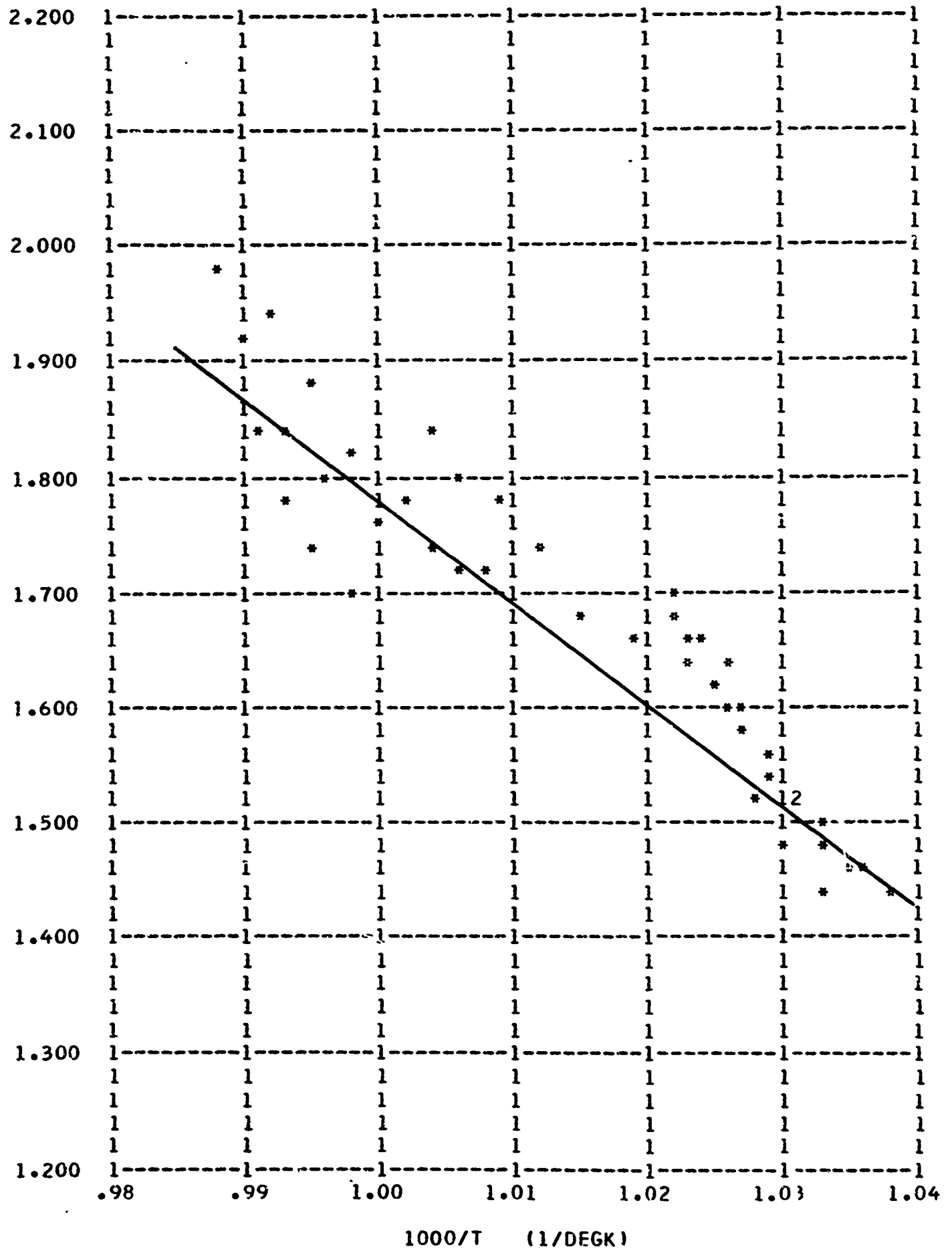


FIGURE 67

TABLE 34. Summary of hydrazine/ nitric oxide reaction rate constants, nitrogen carrier

rate equation $\frac{d[N_2H_4]}{dt} = -k [N_2H_4]^a$		
a	1.00	0.75
$k = 10^A \exp (-E/RT)$		
	$[\text{sec}^{-1}]$	$[(\text{moles/cc})^{-.75} \text{sec}^{-1}]$
duct diameter [in]	2	
duct material	quartz	
T[°K]	980-1060	
$\phi_o$	.3-1.0	
$[N_2H_4]_o \times 10^7 [\text{moles/cc}]$	.5-.7	
data points	243	
E[kcal/mole]	+45.4	+30.7
$\sigma_E$ [kcal/mole]	1.5	1.2
A	11.48	6.40
$\rho_A$	.32	.27

[260]

HYDRAZINE/NITRIC OXIDE REACTION KINETICS  
4 (INCH) QUARTZ DUCT, NITROGEN CARRIER

LOG10(RATE CONSTANT) M= 0.00 A= 1.00 B= 0.00 C= 0.00 241 POINTS

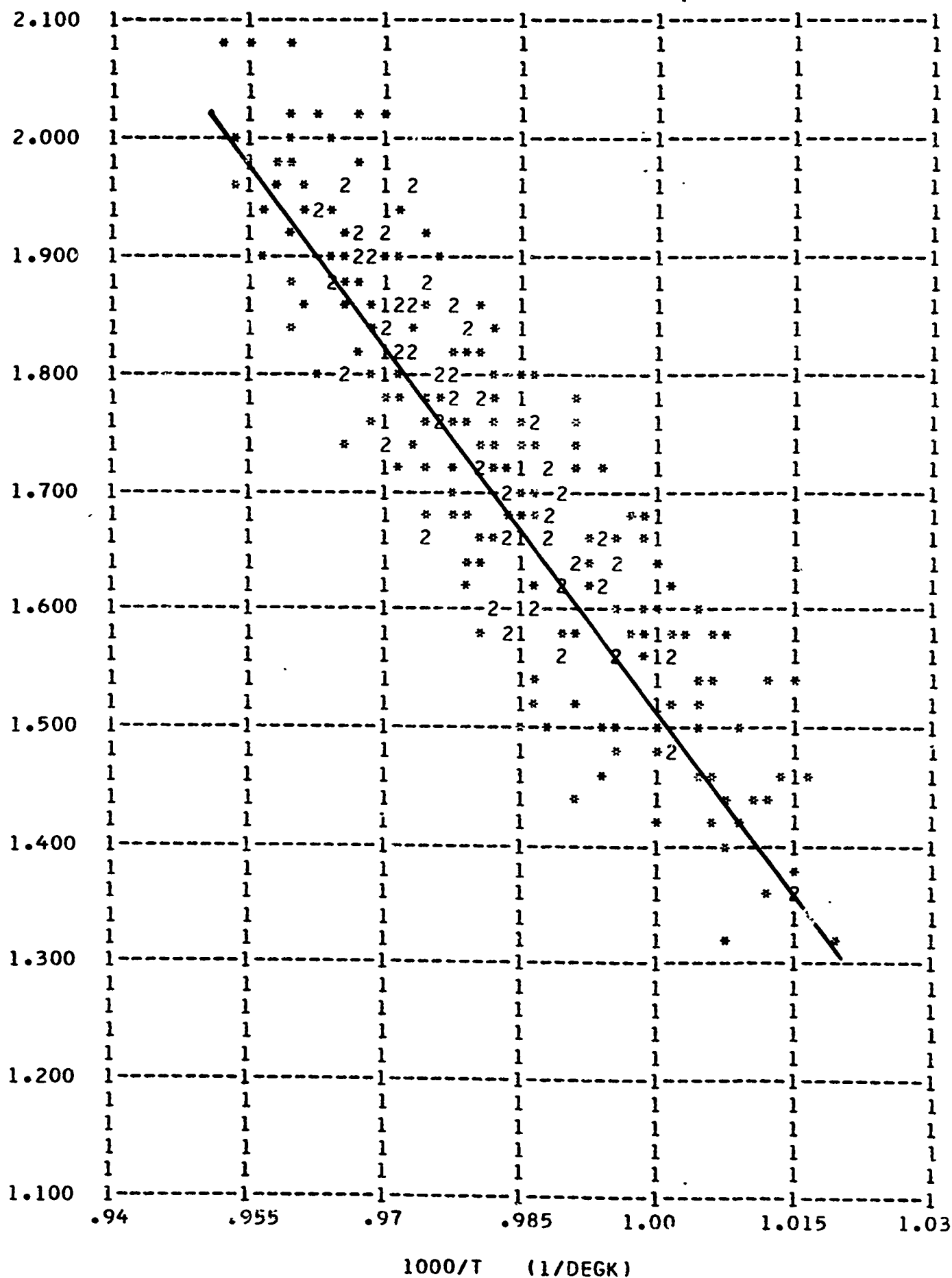


FIGURE 68

HYDRAZINE/NITRIC OXIDE REACTION KINETICS  
4 (INCH) QUARTZ DUCT, NITROGEN CARRIER

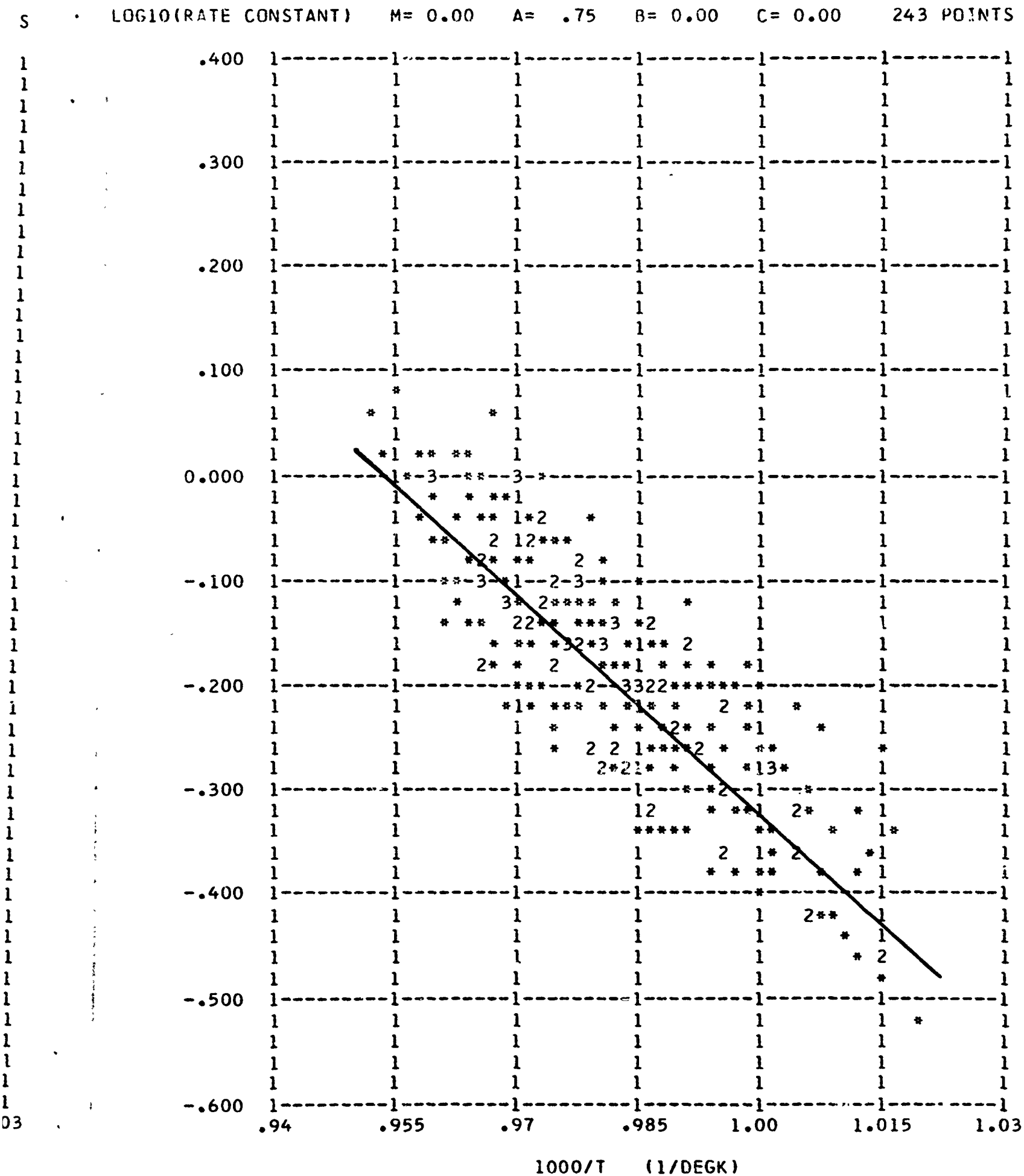


FIGURE 69



## APPENDIX B. DERIVATIONS

B.1 Determination of the rate constant from the reaction rate

It was shown in Section 3.1.1 that the reaction rate can be determined from the measured quantities as

$$\frac{d[A_1]}{dt} = -[A_1]_0 \frac{T_0 T_f}{T^2(T_f - T_0)} \frac{dT}{dt}$$

EB (1)

The general rate equation is

$$\frac{d[A_1]}{dt} = -k \prod_{i=1}^m A_i^{n_i}$$

EB (2)

The convention is adopted that reactant  $A_1$  is chosen to be that reactant which is consumed first. Equating EB (1) and EB (2) gives

$$k = \frac{[A_1]_0}{\prod_{i=1}^m A_i^{n_i}} \frac{T_0 T_f}{T^2(T_f - T_0)} \frac{dT}{dt}$$

EB (3)

The concentration of reactant  $A_1$  is assumed proportional to the temperature change, so that

$$[A_1] = [A_1]_0 \frac{T_f - T}{T_f - T_0} \frac{T_0}{T}$$

The ratio  $T_0/T$  represents the change in density or total concentration, with temperature. Also mole fractions are introduced.

$$x_i = \frac{[A_i]}{\rho}$$

The product term now becomes

$$\prod_{i=1}^m A_i^{n_i} = \rho^{\left(\sum_{i=1}^m n_i\right)} \prod_{i=1}^m x_i^{n_i}$$

$$= [A]_0 \frac{T_f - T}{T_f - T_0} \frac{T_0}{T} \rho^{-1 + \sum_{i=1}^m n_i} x^{n_1-1} \prod_{i=2}^m x_i^{n_i}$$

EB (4)

Substituting EB (4) into EB (3) gives

$$k = \left( \rho^{-1 + \sum_{i=1}^m n_i} x^{n_1-1} \prod_{i=2}^m x_i^{n_i} \right)^{-1} \frac{T_f}{T} \frac{1}{T_f - T} \frac{dT}{dt}$$

EB (5)

The determination of the various  $x_i$  depends on the initial conditions and extent of reaction. For the concentration of reactants,

$$x_1 = x_{10} \frac{T_f - T}{T_f - T_0}$$

$$x_2 = x_{20} - (x_{10} - x_1) \sigma_{21}$$

•  
•  
•

$$x_m = x_{m0} - (x_{10} - x_1) \sigma_{m1}$$

where

$$\sigma_{m1} = \frac{\text{moles reactant } m \text{ consumed}}{\text{moles reactant } 1 \text{ consumed}}$$

For the products

$$x_p = (x_{10} - x_1) \sigma_{p1}$$

where

$$\sigma_{p1} = \frac{\text{moles product p produced}}{\text{moles reactant 1 consumed}}$$

or if the specie  $A_c$  is of constant concentration

$$X_c = X_{c0}$$

The assumptions explicit and implicit in thus calculating the rate constant can be shown to result in errors which are small compared to the experimental uncertainties. Since in all cases there exists a large non-reactive carrier dilution, fluid properties vary little through the reaction zone, as is important in justification of the assumption of constant specific heat. The change in specific heat with temperature, which also is neglected, is only about 2% for a given run. The change in density with a net change in the number of moles of gas as brought about by the reaction is accounted for, but is also a small effect.

B.2 Estimation of the uncertainty in the reaction rate constant from the uncertainties in the measured quantities

The reaction rate constant for an nth order reaction with a reaction rate depending upon the concentration of a single specie, or for an overall reaction order of n with a reaction ratio,  $\xi = 1.0$ , is given by

$$k = \text{constant } T_f \frac{(T_f - T_o)^{n-1}}{(T_f - T)^n} \frac{dT}{dx} V_o$$

EB (6)

Following the method of reference (115), the uncertainty in the rate constant is approximately

$$u_k \approx \left\{ \left( \frac{\partial k}{\partial T_f} u_{T_f} \right)^2 + \left( \frac{\partial k}{\partial (T_f - T_o)} u_{T_f - T_o} \right)^2 + \left( \frac{\partial k}{\partial (T_f - T)} u_{T_f - T} \right)^2 + \left( \frac{\partial k}{\partial \left( \frac{dT}{dx} \right)} u_{\frac{dT}{dx}} \right)^2 + \left( \frac{\partial k}{\partial V_o} u_{V_o} \right)^2 \right\}^{\frac{1}{2}}$$

EB (7)

The relative uncertainty is given by dividing the above expression by  $k$  to give

$$\frac{u_k}{k} = \left\{ \sum_{i=1}^m \left( \frac{1}{k} \frac{\partial k}{\partial y_i} u_{y_i} \right)^2 \right\}^{\frac{1}{2}}$$

EB (8)

The terms in parentheses are recognized to be the partial logarithmic derivatives

$$\frac{\partial \ln k}{\partial y_i} u_{y_i}$$

and can be evaluated from EB (4) as

$$\frac{\partial \ln k}{\partial T_f} u_{T_f} = \frac{u_{T_f}}{T_f}$$

$$\frac{\partial \ln k}{\partial (T_f - T_0)} u_{T_f - T_0} = (n-1) \frac{u_{T_f - T_0}}{T_f - T_0}$$

$$\frac{\partial \ln k}{\partial (T_f - T)} u_{T_f - T} = -n \frac{u_{T_f - T}}{T_f - T}$$

$$\frac{\partial \ln k}{\partial \left( \frac{dT}{dx} \right)} u_{\frac{dT}{dx}} = \frac{u_{\frac{dT}{dx}}}{\frac{dT}{dx}}$$

$$\frac{\partial \ln k}{\partial V_0} u_{V_0} = \frac{u_{V_0}}{V_0}$$

The terms  $(T_f - T_o)$  and  $(T_f - T)$  are treated as measured quantities because uncertainties in the temperature are likely to be systematic rather than random so that

$$u_{T_f - T_o} < u_{T_f} \text{ or } u_{T_o}$$

The relative uncertainties in the measured quantities are estimated to be

$$\frac{u_{T_f}}{T_f} = .01$$

$$\frac{u_{T_f - T_o}}{T_f - T_o} = .10$$

$$\frac{u_{T_f - T}}{T_f - T} = .10 \text{ to } .50$$

The higher value for the last uncertainty corresponds to the data taken near the end of the reaction zone where  $T$  approaches  $T_f$ . The "tail end" of the data, about the last 10 degree temperature rise of the reaction, is always discarded because of this difficulty.

$$\frac{u_{\frac{dT}{dx}}}{\frac{dT}{dx}} = .05$$

$$\frac{u_{V_0}}{V_0} = .05$$

The uncertainties in the rate constant can be estimated from EB (8). For a first order reaction the uncertainties are 12 to 51% and for a second order reaction, from 24 to 100%.



### B.3 The relation between reaction rate and reaction time

For a non-isothermal reaction, the calculation of a reaction time must involve consideration of the change in the rate "constant" with temperature. Similarly, in non-isothermal experiments in which a reaction time is measured, the temperature dependence of this reaction time requires careful interpretation.

Consider a first order reaction whose rate is given by

$$\frac{dx}{dt} = -kx$$

EB (9)

where

$$x = \frac{[A]}{[A]_0} \quad \text{fraction of reactant A unreacted}$$

$[A]$  concentration of reactant A

$[A]_0$  initial concentration of reactant A

$k$  rate constant

It is further assumed that the rate constant is expressible in the Arrhenius form

$$k = 10^A \exp (-E/RT)$$

EB (10)

[2/1]

and that the temperature is linearly dependent upon the fraction of A reacted

$$T = T_f - (T_f - T_0)x$$

or

$$\frac{T}{T_0} = \frac{T_f}{T_0} - \frac{T_f - T_0}{T_0} x$$

EB (11)

The rate "constant" may now be written in terms of the fraction unreacted as

$$k = 10^A \exp \left( - \frac{E}{RT_0} \frac{T_0}{T} \right)$$

$$= 10^A \exp \left( - \frac{E}{RT_0} \frac{1}{\frac{T_f}{T_0} - \left( \frac{T_f}{T_0} - 1 \right) x} \right)$$

EB (12)

This is equivalent to writing the rate constant in terms of the initial temperature, as

$$k = 10^A \exp \left( - \frac{E^*}{RT_0} \right)$$

EB (13)

where the "effective" activation energy,  $E^*$ , is defined as

$$E^* = \frac{E}{\frac{T_f}{T_0} - \left(\frac{T_f}{T_0} - 1\right) x}$$

EB (14)

For an exothermic reaction

$$\frac{T_f}{T_0} > 1$$

$$x \leq 1$$

so that from EB (14) we see that

$$E^* \leq E$$

EB (15)

For a reaction in which there is a temperature rise, the "effective" activation energy, that is, the activation energy corresponding to isothermal reaction at temperature  $T_0$ , is less than that appearing in the Arrhenius expression. Experiments in which the extent of reaction is determined as a function of an initial temperature,

but for which there is a temperature rise during the experiment, will result in fictiously low activation energies, and fictiously high rates. In highly diluted reactions, or in reactions whose progress is measured before significant temperature rise occurs, this effect is negligible.

The extent of reaction may be determined for a non-isothermal first order reaction by integration of equation EB(9) to give

$$t_i = \int_{x_i}^1 \frac{1}{k} \frac{dx}{x}$$

or

$$t_i = 10^{-A} \int_{x_i}^1 \exp\left(\frac{E}{RT_0} \frac{1}{\frac{T_f}{T_0} - \left(\frac{T_f}{T_0} - 1\right)x}\right) \frac{dx}{x}$$

EB (16)

For an isothermal reaction,  $T = T_f = T_0$ ,

$$t_i = 10^{-A} \ln \frac{1}{x_i} \exp\left(\frac{E}{RT}\right)$$

EB (17)

The reaction half time is

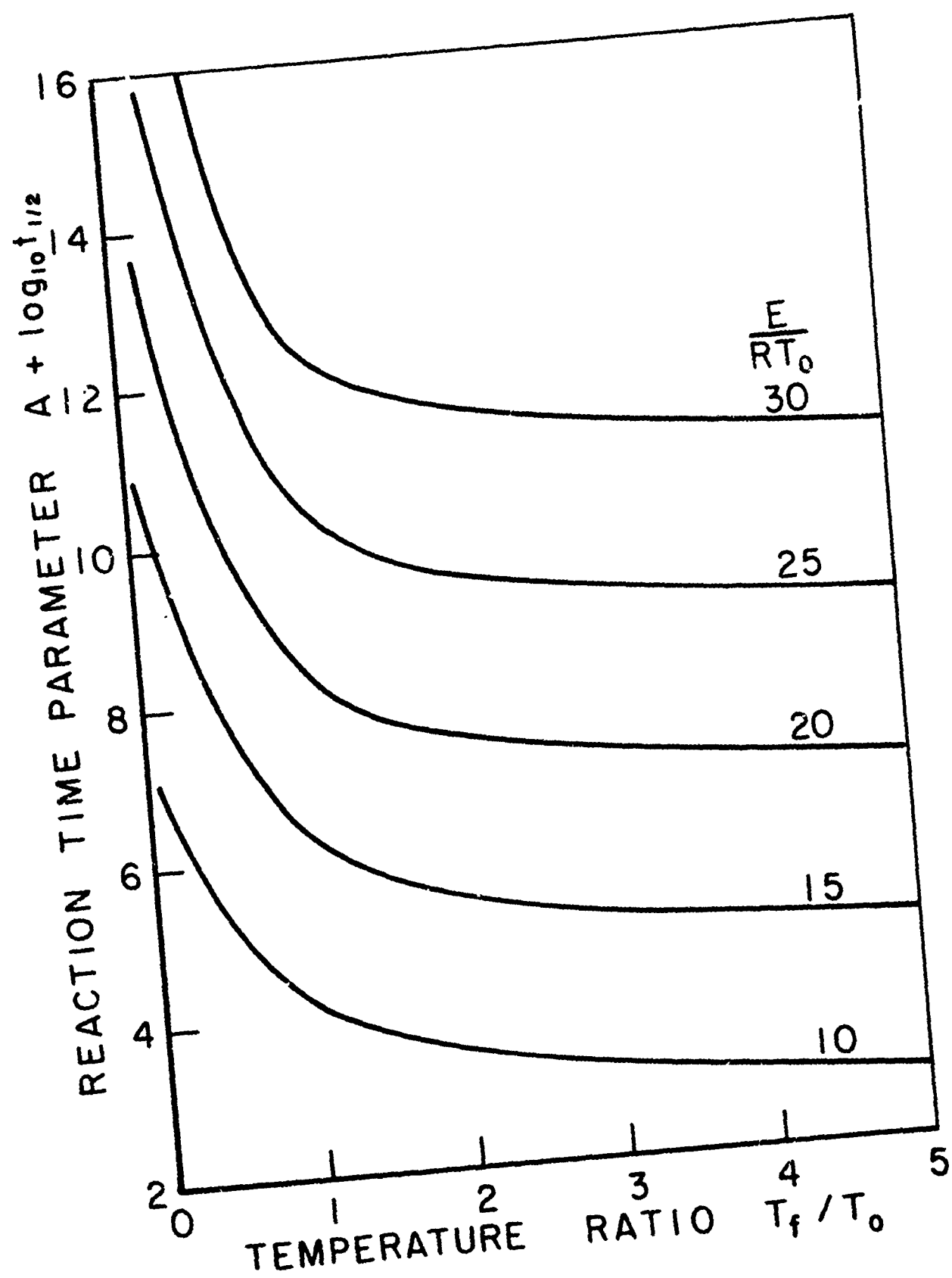
$$t_{\frac{1}{2}} = \frac{\ln 2}{k}$$

EB (18)

or a "time constant" for the reaction can be defined by the time to go to  $1 - \frac{1}{e}$  or 63% of completion ,

$$t_{1-\frac{1}{e}} = \frac{1}{k}$$

For a non-isothermal reaction, the determination of a reaction time is more difficult. Integration of EB(16) was carried out numerically for the non-isothermal case and the results are presented for the particular case of the time required to reach one-half completion of the reaction, Figure 70.



REACTION HALF-TIME FOR A FIRST ORDER  
REACTION WITH TEMPERATURE CHANGE

FIGURE 70

## APPENDIX C. DATA REDUCTION AND ANALYSIS PROGRAMS

The FORTRAN statements of the data reduction and analysis programs written for an IBM 1620 computer with 40000 bit core storage and on-line printer are presented in this appendix. Five different programs are required, primarily because of machine size limitations, but also to facilitate data handling.

Part 1: Determination of flow rates

Experimental measurements are transformed into flow parameters through application of appropriate calibration tables and correction for temperature, pressure, and molecular weight effects. Molar flow rates, mole fractions, equivalence and reaction ratios are calculated.

Part 2: Determination of rates

The output of Part 1 is combined with the temperature profile information and reaction rates are calculated. Rate constants according to four different prescribed reaction rate equations are calculated. The output consists of a printed record of the rate constant information and a punched output for use in the following three parts of the data reduction program.

Part 3: Minima and maxima

The output of the previous part is searched and the extreme values of the rate constants and temperatures determined.

#### Part 4: Plot program

The base 10 logarithms of the rate constants are plotted as a function of reciprocal temperature for each of the rate equations. The plotting subroutine itself is not presented but is available in both SPS and FORTRAN language forms from the Computing Group, Guggenheim Laboratories, Forrestal Research Center, Princeton, New Jersey.

#### Part 5: Statistical analysis of rate data

The output of Part 3 is analyzed statistically to produce at least squares best fit to a linear relation between the logarithm of the rate constant and the reciprocal temperature. The preexponential factor and overall activation energy of the Arrhenius rate expression are determined as are the standard deviations in these two constants.

Sample outputs of Parts 1 and 2 are presented at the end of this appendix.



[278]

FLOW REACTOR DATA REDUCTION PROGRAM, PART 1  
SP14.1.2  
ROBERT F SAWYER

# DETERMINATION OF FLOW RATES

DIMENSION NT(11),TX(11,5),TY(11,5),X(11),Y(11),IT(11),DYDX(11)  
DIMENSION ABC(11,10),DATE(5),CC(9),CX(11),WDOT(4),VDDOT(4),XV(4)  
DIMENSION DUCT(10),L(11)  
COMMON TX,TY,NT,Y,IT,DYDX

## DIMENSION CONVENTIONS

### INPUT

REFERENCE TEMPERATURES	DEGK
REFERENCE PRESSURES	ATMA
DUCT DIAMETER	IN
MANOMETER READINGS	IN HG
PRESSURES	PSIG
TEMPERATURES	DEGF
BASE TEMPERATURE	MV

### OUTPUT

TEMPERATURE	DEGK
PRESSURE	ATMA
AREA	CM2
FLOW RATE	MOLE/SEC

## CONSTANTS

C1 EQUIVALENCE CONSTANT O/F STOIC  
C2 CHART CONSTANT  
C3 MOLE INCREASE CONSTANT MOLE PRODUCTS/MOLE REACTANTS  
C4 REACTION CONSTANT O/F CONSUMED  
C5 OXIDIZER INJECTION PORT  
C6 DILUENT INJECTION LOCATION (0=MANIFOLD, 1=EVAPORATOR)  
C7 MEAN SPECIFIC HEAT, (CAL/MOLE-DEGK)  
C8 HEAT OF REACTION(PER MOLE OF FUEL)/SPECIFIC HEAT(BULK)  
C9 OXIDIZING CARRIER FRACTION

## INPUT OF TABLES

TABLE NUMBER 1  
TABLE NUMBER 2 CARRIER ORIFICE  
TABLE NUMBER 3 CARRIER TEMPERATURE  
TABLE NUMBER 4 DILUENT ORIFICE  
TABLE NUMBER 5 DILUENT TEMPERATURE  
TABLE NUMBER 6  
TABLE NUMBER 7 FUEL ORIFICE  
TABLE NUMBER 8 FUEL TEMPERATURE  
TABLE NUMBER 9  
TABLE NUMBER 10 OXIDIZER ORIFICE  
TABLE NUMBER 11 OXIDIZER TEMPERATURE

READ 900, NNT  
DO 100 NTBL=1,NNT  
READ 901, (ABC(NTBL,I),I=1,10),NT(NTBL)

```

MNT=NT(NTBL) [279]
READ 902, (TX(NTBL,I),TY(NTBL,I),I=1,MNT)
100 CONTINUE
C
C INPUT OF HEADINGS
C
READ 912,DATE
READ 910
READ 911
C
C INPUT OF PRELIMINARY DATA
C
READ 956, CC
READ 956, CTR,CMWR,DTR,DMWR,FTR,FMWR,OTR,OMWR
READ 956, DPR,FPR
READ 920, C,CMW,D,DMW,F,FMW,O,OMW
READ 921, DUCT,DUCTD
PUNCH 957, (CC(I),I=1,8)
NCC5=CC(5)
C
C CONVERT DUCT DIAMETER TO CENTIMETERS, CALCULATE AREA
C
XDUCTD=2.54*DUCTD
DUCTA=3.1416*XDUCTD**2/4.
C
C PRELIMINARY OUTPUT
C
PRINT 950, DATE
PRINT 910
PRINT 911
PRINT 951
DO 200 NTBL=1,NNT
PRINT 952, NTBL,(ABC(NTBL,I),I=1,10)
MNT=NT(NTBL)
PRINT 953, (TX(NTBL,I),TY(NTBL,I),I=1,MNT)
200 CONTINUE
PRINT 955
PRINT 957, CC
PRINT 956, CTR,CMWR,DTR,DMWR,FTR,FMWR,OTR,OMWR
PRINT 956, DPR,FPR
PRINT 920, C,CMW,D,DMW,F,FMW,O,OMW
PRINT 954, (DUCT(I),I=1,10),XDUCTD
C
C INPUT TARE DATA
C
READ 922, NRUN,CX
C
C OUTPUT TARE DATA
C
PRINT 970
PRINT 963
PRINT 967, CX(2),CX(6),CX(9),CX(10)
PRINT 968, CX(3),CX(5),CX(8),CX(11)
PRINT 969, CX(4),CX(7)
C
C INPUT RUN DATA
C
111 READ 922, NRUN,X
IF(NRUN-11111)112,100,112

```

```

C
C      OUTPUT RUN DATA
C
112 PRINT 960, DATE
    PRINT 910
    PRINT 911
    PRINT 961, NRUN
    PRINT 962, X(1)
    PRINT 982, NCC5
    PRINT 963
    PRINT 964, C,D,F,O
    PRINT 965, CMW,DMW,FMW,OMW
    PRINT 966
    PRINT 967, X(2),X(6),X(9),X(10)
    PRINT 968, X(3),X(5),X(8),X(11)
    PRINT 969, X(4),X(7)

C
C      TARE CORRECTIONS
C
    DO 210 I=1,11
      X(I)=X(I)-CX(I)
210 CONTINUE

C
C      PRELIMINARY CALCULATIONS
C
C      CONVERT TO DEGK AND ATMOSPHERES
C
    X(2)=(X(2)+14.69)/14.69
    X(3)=(X(3)+459.74)/1.8
    X(5)=(X(5)+459.74)/1.8
    X(6)=(X(6)+14.69)/14.69
    X(8)=(X(8)+459.74)/1.8
    X(9)=(X(9)+14.69)/14.69
    X(10)=(X(10)+14.69)/14.69
    X(11)=(X(11)+459.74)/1.8

C
C      TEMPERATURE CALIBRATIONS
C
    I=3
    CALL INTER(X,I)
    X(I)=Y(I)
    I=5
    CALL INTER(X,I)
    X(I)=Y(I)
    I=8
    CALL INTER(X,I)
    X(I)=Y(I)
    I=11
    CALL INTER(X,I)
    X(I)=Y(I)

C
C      OUTPUT CORRECTED INPUTS
C
    PRINT 971
    PRINT 977, X(2),X(6),X(9),X(10)
    PRINT 978, X(3),X(5),X(8),X(11)
    PRINT 969, X(4),X(7)

C
C      FLOW CALCULATIONS

```

```

C      X(4)=X(4)**.5
      X(7)=X(7)**.5
      I=2
      CALL INTER(X,I)
      I=4
      CALL INTER(X,I)
      I=7
      CALL INTER(X,I)
      I=10
      CALL INTER(X,I)

C
C      MASS FLOW RATES
C
      WDOT(1)=Y(2)*((CMW/CMWR)*(CTR/X(3)))**.5
      WDOT(2)=Y(4)*((DMW/DMWR)*(DTR/X(5))*(X(6)/DPR))**.5
      WDOT(3)=Y(7)*((FMW/FMWR)*(FTR/X(8))*(X(9)/FPR))**.5
      WDOT(4)=Y(10)*((OMW/OMWR)*(OTR/X(11)))**.5

C
C      MOLE FLOW RATES
C
      VDOT(1)=WDOT(1)/CMW
      VDOT(2)=WDOT(2)/DMW
      VDOT(3)=WDOT(3)/FMW

C
C      CORRECTION FOR DILUENT INJECTION INTO EVAPORATOR
C
      VDOT3=VDOT(3)
      IF(CC(6))229,229,220
220  VDOT(3)=WDOT(3)/(DMW+FMW)*2.
      VDOT3=VDOT(3)-VDOT(2)
229  VDOT(4)=WDOT(4)/OMW
      TVDOT=VDOT(1)+VDOT(2)+VDOT3+VDOT(4)

C
C      MOLE FRACTIONS
C
      DO 230 I=1,4
230  XV(I)=VDOT(I)/TVDOT

C
C      EQUIVALENCE RATIO
C
      VDOT4=VDOT(4)+CC(9)*VDOT(1)
      ER=CC(1)*VDOT3/VDOT4
      RR=CC(4)*VDOT3/VDOT4

C
C      OUTPUT FLOW CALCULATIONS
C
      PRINT 972
      PRINT 973, WDOT
      PRINT 974, VDOT
      PRINT 975, XV
      PRINT 976, ER
      PRINT 981, RR

C
C      DETERMINE AND PRINT PARAMETERS OUTSIDE RANGE OF TABLES
C
      II=0
      DO 240 I=1,NN7
      IF(IT(I))241,240,241

```

```

241 II=II+1
    L(II)=I
240 CONTINUE
    IF(II)250,250,245
245 PRINT 980,(L(JJ),JJ=1,II)
250 CONTINUE

```

C

C

C

CORRECT MOLE FRACTIONS

XV(3)=VDOT3/TVDOT

XV(4)=VDOT4/TVDOT

C

C

C

OUTPUT FOR PART 2

PUNCH 979, NRUN,X(1),TVDOT,CTR,RR,XV(3),XV(4),DUCTA

GO TO 111

C

C

C

FORMATS

900 FORMAT(I5)

901 FORMAT(10A4,I5)

902 FORMAT(2F10.0)

910 FORMAT(72H

1 )

911 FORMAT(72H

1 )

912 FORMAT(5A4)

920 FORMAT(4(A4,6X,F10.0))

921 FORMAT(10A4,F10.0)

922 FORMAT(I5,11F5.0)

950 FORMAT(1H1,51X,5A4//)

951 FORMAT(//38H TABLES OF CALIBRATIONS AND OTHER DATA)

952 FORMAT(//15H TABLE NUMBER I2,3X,10A4//)

953 FORMAT(2(10X,F10.4))

954 FORMAT(///1X10A4,5X,10HDIAMETER =F6.2,2X,4H(CM)//)

955 FORMAT(//10H CONSTANTS//)

956 FORMAT(8F10.4)

957 FORMAT(7F10.4,F10.3)

960 FORMAT(42H1CHEMICAL KINETICS FLOW REACTOR DATA SHEET10X5A4//)

961 FORMAT(//11H RUN NUMBER56XI5//)

962 FORMAT(//25H PROBE BASE (MV)41XF6.3)

963 FORMAT(30X7HCARRIER5X7HDILUENT7X4HFUEL5X8HOXIDIZER//)

964 FORMAT(9H CHEMICAL23X4(A4,8X))

965 FORMAT(17H MOLECULAR WEIGHT13X4(F6.2,6X)//)

966 FORMAT(6H INPUT)

967 FORMAT(25H PRESSURE (PSIG)5X4(F6.1,6X))

968 FORMAT(25H TEMPERATURE (DEGF)5X4(F6.0,6X))

969 FORMAT(25H MANUMETER (INHG)17X2(F6.2,6X)//)

970 FORMAT(11H TARE INPUT//)

971 FORMAT(10H CORRECTED)

972 FORMAT(11H CALCULATED)

973 FORMAT(25H FLOW RATE (GM/SEC)3X4(F8.4,4X))

974 FORMAT(25H FLOW RATE (MOLE/SEC)3X4(F8.5,4X))

975 FORMAT(16H MOLE FRACTION13X4(F7.5,5X)//)

976 FORMAT(18H EQUIVALENCE RATIO48XF6.3)

977 FORMAT(25H PRESSURE (ATMA)5X4(F6.2,6X))

978 FORMAT(25H TEMPERATURE (DEGK)5X4(F6.0,6X))

979 FORMAT(I5,7E10.3)

980 FORMAT(42H RANGE OF THE FOLLOWING TABLE(S) EXCEEDED 11I3//)

[283]

981 FORMAT(15H REACTION RATIO51XF6.3//)  
982 FORMAT(24H OXIDIZER INJECTION PORT47XI1//)

C

END

SUBROUTINE INTER(X,I)

C

INTERPOLATES AND EXTRAPOLATES IN CALIBRATION TABLES

C

DIMENSION NT(11),TX(11,5),TY(11,5),X(11),Y(11),IT(11),DYDX(11)

COMMON TX,TY,NT,Y,IT,DYDX

NNT=NT(I)

DO 11 J=1,NNT

IF(X(I)-TX(I,J))10,10,11

11 CONTINUE

C

IT = -1 X TOO LARGE

C

IT = 0 X IN TABLE

C

IT = 1 X TOO SMALL

J=J-1

IT(I)=-1

GO TO 22

10 IF(J-1)20,20,21

20 IT(I)=1

GO TO 24

21 IT(I)=0

22 DX=TX(I,J)-TX(I,J-1)

DY=TY(I,J)-TY(I,J-1)

DYDX(I)=DY/DX

IF(IT(I))23,26,26

26 Y(I)=(X(I)-TX(I,J-1))/DX\*DY+TY(I,J-1)

GO TO 99

23 Y(I)=(X(I)-TX(I,J))/DX\*DY+TY(I,J)

GO TO 99

24 DX=TX(I,J+1)-TX(I,J)

DY=TY(I,J+1)-TY(I,J)

DYDX(I)=DY/DX

Y(I)=(X(I)-TX(I,J))/DX\*DY+TY(I,J)

99 RETURN

END

\*\*\*\*\*

```

C      FLOW REACTOR DATA REDUCTION PROGRAM, PART 2
C      SP14.2.4
C      ROBERT F SAWYER
C
C      DETERMINATION OF RATES
C
C      SENSE SWITCH 1    SUPPRESS PRINT
C      SENSE SWITCH 2    SUPPRESS PUNCH
C      SENSE SWITCH 3    USE INPUT INITIAL TEMPERATURE, OTHERWISE
C                        CALCULATES A VALUE FROM C8
C
C      DIMENSION CONVENTIONS
C
C      TEMPERATURES          DEGK
C      THERMOCOUPLE          MV, 0 DEGK BASE
C      AREA                  CM2
C      FLOW RATE              MOLE/SEC
C      SLOPES, CHART          ABSOLUTE
C      SLOPES, OUTPUT        DEGK/CM
C      VELOCITY              CM/SEC
C      RATE, R1              1/SEC
C      RATE, R2 THRU R5      ((CM3/MOLE)**(A+B+C-1))/(SEC DEGK**M)
C      DENSITY               MOLES/CM3
C      HEAT OF REACTION      CAL/MOLE FUEL REACTED
C
C      DIMENSION      T(20),S(20),Y(20),TT(20),RT(20),SS(20),DYDX(20)
C      DIMENSION      X(20),DATE(5),FR(20)
C      DIMENSION      V(20),R(20),TR(20),XV(4),RL(5,20),RR(5,20)
C      DIMENSION      TX(1,80),TY(1,80),NT(20),IT(20)
C      DIMENSION      ABC(1,10)
C      DIMENSION      CC(4,5)
C      COMMON         TX,TY,NT,Y,IT,DYDX
C
C      INPUT THERMOCOUPLE TABLE
C
C      READ 901, (ABC(1,I),I=1,10),NT(1)
C      MNT=NT(1)
C      READ 902, (TX(1,I),TY(1,I),I=1,MNT)
C
C      OUTPUT TABLE
C
C      J=1
C      PRINT 952, J,ABC
C      PRINT 953, (TX(1,I),TY(1,I),I=1,MNT)
C
C      INPUT HEADINGS
C
C      READ 910
C      READ 911
C      101 READ 912,(DATE(I),I=1,5)
C
C      INPUT CONSTANTS
C
C      READ 918, C1,C2,C3,C4,C5,C6,C7,C8
C      READ 919, CC
C
C      PUNCH CONSTANTS

```

```

C      IF(SENSE SWITCH 2)100,99
99 PUNCH 919, CC
C
C
C      INPUT DATA FROM DATA REDUCTION PROGRAM, FIRST PART
C
100 READ 977, NRUN,X(1),TVDOT,CTR,ER,XV(3),XV(4),DUCTA
    IF(NRUN-11111)102,101,102
102 CONTINUE
C
C      INPUT CHART DATA
C
    I=0
311 I=I+1
    READ 922, NDUM,T(I),S(I)
    T(I)=T(I)+X(1)
    IF (NDUM)310,311,311
310 NI=I
    VC=22400.*TVDOT/DUCTA/CTR
    DO 320 I=1,NI
    X(1)=T(I)
    CALL INTER(X,1)
    TT(I)=Y(1)
    DYDX(I)=DYDX(1)
320 CONTINUE
C
C      HEAT OF REACTION
C
    IF(ER-1.)315,315,316
315 HOR=C7*(TT(NI)-TT(1))/XV(3)
    GO TO 317
316 HOR=C7*(TT(NI)-TT(1))/XV(4)
    HOR=HOR*C4
317 CONTINUE
C
C      CALCULATION OF INITIAL TEMPERATURE
C
    IF(SENSE SWITCH 3)327,324
324 IF(ER-1.)325,325,326
325 TT(1)=TT(NI)-C8*XV(3)
    GO TO 327
326 TT(1)=TT(NI)-C8*XV(4)/C4
327 CONTINUE
C
    DO 330 I=1,NI
    RT(I)=1./TT(I)*1000.
    SS(I)=C2*S(I)*DYDX(I)
    CD=(TT(I)-TT(1))/(TT(NI)-TT(1))
    V(I)=VC*TT(I)
C
C      CALCULATION OF FIRST ORDER RATE, R1
C
    IF(SS(I))322,322,321
321 R(I)=SS(I)*V(I)*TT(NI)/TT(I)/(TT(NI)-TT(1))
    RR(1,I)=R(I)*TT(I)**(-CC(1,1))
    AR=RR(1,I)
    RL(1,I)=LOGF(AR)/2.30
    GO TO 330

```



```

322 R(I)=0.
    RR(1,I)=0.
    RL(1,I)=0.
330 CONTINUE
C
C    FRACTION NOT REACTED
C
    DO 350 I=1,NI
350 FR(I)=(TT(NI)-TT(I))/(TT(NI)-TT(1))
C
C    CALCULATION OF RATES, R2 THRU R5
C
    IF(ER-1.)390,390,395
C
C    OXIDIZER RICH CASE
C
390 DO 401 I=1,NI
    XV3=XV(3)*FR(I)+1.E-20
    XV4=XV(4)-(XV(3)-XV3)*C4
    RHO=273./TT(I)/22400.
    DO 400 M=2,5
    EC1=CC(2,M)-1.
    EC2=CC(2,M)+CC(3,M)+CC(4,M)-1.
    XVC=1./(XV3**EC1*XV4**CC(3,M)*RHO**EC2 *XV(4)**CC(4,M))
400 RR(M,I)=XVC*R(I)*TT(I)**(-CC(1,M))
401 CONTINUE
    GO TO 420
C
C    FUEL RICH CASE
C
395 DO 411 I=1,NI
    XV4=XV(4)*FR(I)+1.E-20
    XV3=XV(3)-(XV(4)-XV4)/C4
    RHO=273./TT(I)/22400.
    DO 410 M=2,5
    EC1=CC(3,M)-1.
    EC2=CC(2,M)+CC(3,M)+CC(4,M)-1.
    XVC=1./(XV3**CC(2,M)*XV4**EC1*RHO**EC2 *XV(4)**CC(4,M))
410 RR(M,I)=XVC*R(I)*TT(I)**(-CC(1,M))
411 CONTINUE
420 CONTINUE
C
C    TAKE LOG10(RATES)
C
    DO 431 I=1,NI
    DO 430 M=2,5
    IF(R(I))421,422,421
421 AR=RR(M,I)
    RL(M,I)=LOGF(AR)/2.30
    GO TO 430
422 RR(M,I)=0.
    RL(M,I)=0.
430 CONTINUE
431 CONTINUE
C
C    REVERSE SENSE OF FRACTION REACTED
C
    DO 439 I=1,NI
439 FR(I)=1.-FR(I)

```

C  
C  
C

## PRINT OUTPUT

```

IF(SENSE SWITCH 1)440,435
435 PRINT 960, (DATE(I),I=1,5)
PRINT 910
PRINT 911
PRINT 961, NRUN
PRINT 940, HOR
PRINT 927
PRINT 928
PRINT 929
PRINT 931, (I,T(I),TT(I),S(I),SS(I),V(I),FR(I),I=1,NI)
PRINT 930
PRINT 941, (CC(1,M),M=1,5)
PRINT 942, (CC(2,M),M=1,5)
PRINT 943, (CC(3,M),M=1,5)
PRINT 944, (CC(4,M),M=1,5)
PRINT 933
PRINT 935
PRINT 934, (I,RT(I),(RR(M,I),M=1,5),I=1,NI)
PRINT 945

```

C  
C  
C

## PUNCH PLOT CARDS

```

440 IF(SENSE SWITCH 2)100,700
700 DO 701 I=1,NI
IF(R(I))701,701,702
702 PUNCH 978, NRUN,RT(I),(RL(M,I),M=1,5)
701 CONTINUE

```

C

GO TO 100

C  
C  
C

## FORMATS

```

901 FORMAT(10A4,I5)
902 FORMAT(2F12.0)
910 FORMAT(72H
1
)
911 FORMAT(72H
1
//)
912 FORMAT(5A4)
918 FORMAT(8F10.5)
919 FORMAT (4F10.5)
922 FORMAT(15,11F5.0)
927 FORMAT(16H FLOW CONDITIONS/)
928 FORMAT(3X5HPOINT6X1HT9X1HT12X1HS9X1HS 9X1HV10X2HFR/)
929 FORMAT(14X2HMOV7X4HDEGK10X1H-7X4HD/CM6X6HCM/SEC8X1H-/)
930 FORMAT(//15H RATE CONSTANTS/)
931 FORMAT(I7,F10.3,F11.1,F11.2,F11.3,F11.1,F11.4)
933 FORMAT(3X5HPOINT2X6H1000/T7X2HR19X2HR29X2HR39X2HR49X2HR5/)
934 FORMAT(I7,F9.4,2XE10.3,1XE10.3,1XE10.3,1XE10.3,1XE10.3)
935 FORMAT(10X6H1/DEGK8X1H*10X1H*10X1H*10X1H*10X1H*)
940 FORMAT(28H HEAT OF REACTION (CAL/MOLE)34XF10.0/)
941 FORMAT (6X1HM8X5F11.2)
942 FORMAT (6X1HA8X5F11.2)
943 FORMAT (6X1HB8X5F11.2)
944 FORMAT (6X1HC8X5F11.2/)
945 FORMAT(//3X69H* RATE CONSTANT DIMENSIONS=((CM3/MOLE)**(A+B+C-1))/

```

[288]

```
1(SEC DEGR**M) )
952 FORMAT(/15H TABLE NUMBER 12,3X,10A4//)
953 FORMAT(2(10X,F10.4))
960 FORMAT(42H1CHEMICAL KINETICS FLOW REACTOR DATA SHEET10X5A4//)
961 FORMAT(11H RUN NUMBER56X15//)
977 FORMAT(15,7E10.3)
978 FORMAT(110,6F10.5)
```

C

END

SUBROUTINE INTER(X,I)

C

INTERPOLATES AND EXTRAPOLATES IN CALIBRATION TABLES

C

C

DIMENSION TX(1,80),TY(1,80),NT(20),Y(20),IT(20),DYDX(20)

DIMENSION X(20)

COMMON TX,TY,NT,Y,IT,DYDX

NNT=NT(I)

DO 11 J=1,NNT

IF(X(I)-TX(I,J))10,10,11

11 CONTINUE

C

IT = -1 X TOO LARGE

C

IT = 0 X IN TABLE

C

IT = 1 X TOO SMALL

J=J-1

IT(I)=-1

GO TO 22

10 IF(J-1)20,20,21

20 IT(I)=1

GO TO 24

21 IT(I)=0

22 DX=TX(I,J)-TX(I,J-1)

DY=TY(I,J)-TY(I,J-1)

DYDX(I)=DY/DX

IF(IT(I))23,26,26

26 Y(I)=(X(I)-TX(I,J-1))/DX\*DY+TY(I,J-1)

GO TO 99

23 Y(I)=(X(I)-TX(I,J))/DX\*DY+TY(I,J)

GO TO 99

24 DX=TX(I,J+1)-TX(I,J)

DY=TY(I,J+1)-TY(I,J)

DYDX(I)=DY/DX

Y(I)=(X(I)-TX(I,J))/DX\*DY+TY(I,J)

99 RETURN

END

\*\*\*\*\*~\*\*\*\*\*

C FLOW REACTOR DATA REDUCTION PROGRAM, PART 3  
 C SP14.3.3  
 C ROBERT F SAWYER  
 C FINDS MINIMA AND MAXIMA FOR PLOT ROUTINE

C  
 C  
 C SENSE SWITCH SETTINGS  
 C SS 1 PRINTS PLOT CARDS  
 C SS 2 PUNCHES PLOT CARDS  
 C

DIMENSION C(4,5)  
 DIMENSION X(6),XMIN(6),XMAX(6)  
 X=0  
 3=0  
 100 I=1,6  
 )=0.  
 MIN(I)=1.E+20  
 100 XMAX(I)=-1.E+20  
 READ 903  
 READ 904  
 READ 905  
 READ 906  
 READ 906  
 READ 906  
 READ 906  
 READ 906  
 READ 906  
 PRINT 907  
 PRINT 903  
 PRING 904  
 READ 902, C  
 IF(SENSE SWITCH 1)500,501  
 500 PRINT 900,(K,B,(C(M,N),N=1,5),M=1,4)  
 501 IF(SENSE SWITCH 2)510,511  
 510 PUNCH 903  
 PUNCH 904  
 PUNCH 905  
 PUNCH 902, C  
 511 CONTINUE  
 101 READ 900, NRUN,X  
 IF(NRUN)300,300,105  
 105 K=K+1  
 IF(SENSE SWITCH 1) 400,401  
 400 PRINT 900, NRUN,X  
 401 IF(SENSE SWITCH 2)410,411  
 410 PUNCH 900, NRUN,X  
 411 CONTINUE  
 DO 200 I=1,6  
 IF(X(I)-XMIN(I))110,111,111  
 110 XMIN(I)=X(I)  
 111 IF(X(I)-XMAX(I))200,200,120  
 120 XMAX(I)=X(I)  
 200 CONTINUE  
 GO TO 101  
 300 PRINT 901  
 PRINT 900, K,XMIN  
 PRINT 900, K,XMAX  
 GO TO 99  
 900 FORMAT(I10,6F10.5)

[290]

```
901 FORMAT(38H MINIMA AND MAXIMA OF DATA PLOT POINTS//)
902 FORMAT(4F10.5)
903 FORMAT(72H
1      )
904 FORMAT(72H
1      )
905 FORMAT(72H
1      )
906 FORMAT(1H )
907 FORMAT(1H1)
END
```

\*\*\*\*\*

```
C   FLOW REACTOR DATA REDUCTION PROGRAM, PART 4
C   SP14.4.1
C   ROBERT F SAWYER
C
C   PLOT PROGRAM
C
C   SENSE SWITCH SETTINGS
C
C   ALL OFF      PLOTS RATES R1 THRU R5 IN SEQUENCE, RETURNS TO
C                 READ NEW SET OF PLOT CARDS
C
C   ON           SENSE SWITCH SETTINGS ARE READ AS A BINARY NUMBER
C                 (1234) WHICH IS CONVERTED TO ITS DECIMAL
C                 EQUIVALENT, N, THEN RATE TYPE R(N) IS PLOTTED
C
C   DIMENSION    X(300),Y(5,300),YY(300)
C   DIMENSION    YMAX(5),YMIN(5),NY(5)
C   DIMENSION    AX(20),C(4,5)
C
C
C   99 READ 900
C   READ 901
C   READ 912
C   READ 902, XMAX,XMIN,NX
C   READ 902, (YMAX(I),YMIN(I),NY(I),I=1,5)
C   I=1
C   READ 918, C
100 READ 910, NRUN,X(I),(Y(J,I),J=1,5)
    IF(NRUN)102,102,101
101 I=I+1
    GO TO 100
102 N=I
    J=0
    K=0
103 CALL SENSE (M)
    J=M
```

[291]

```
      IF(J)120,110,120
110 K=K+1
      J=K
120 CONTINUE
      DO 200 I=1,N
200 YY(I)=Y(J,I)
      YYMIN=YMIN(J)
      YYMAX=YMAX(J)
      NN=NY(J)
      PRINT 900
      PRINT 901
      PRINT 913, (C(I,J),I=1,4),N
      CALL PLOT(X,XMAX,XMIN,NX,YY,YYMAX,YYMIN,NN,N)
C
C      LABEL ABSCISSA
C
      XNX=NX
      DX=(XMAX-XMIN)/XNX
      AX(1)=XMIN
      MX=NX+1
      DO 300 I=2,MX
300 AX(I)=AX(I-1)+DX
      PRINT 911,(AX(I),I=1,MX)
      PRINT 912
      IF(K)301,103,301
301 IF(K-5)110,99,110
C
C      FORMATS
C
900 FORMAT(72H1
1
)
901 FORMAT(72H
1
)
902 FORMAT(2F10.5,I10)
910 FORMAT(I10,6F10.5)
911 FORMAT( 5X11F10.2)
912 FORMAT( 72H
1
)
913 FORMAT(/21H LOG10(RATE CONSTANT)5X2HM=F10.4,5X2HA=F10.4,5X2HB=F10.
14,5X2HC=F10.4,13X15,7H POINTS/)
918 FORMAT(4F10.0)
      END

C      ROBERT F SAWYER
C
      SUBROUTINE SENSE(N)
C
C      SENSE SWITCH SETTINGS
C
C      READS SENSE SWITCHES AS BINARY NUMBER (1234)
C
      N1=0
      IF(SENSE SWITCH 1)100,101
100 N1=8
101 N2=0
```

[292]

```
      IF(SENSE SWITCH 2)110,111
110 N2=4
111 N3=0
      IF(SENSE SWITCH 3)120,121
120 N3=2
121 N4=0
      IF(SENSE SWITCH 4)130,131
130 N4=1
131 N=N1+N2+N3+N4
      RETURN
      END
```

\*\*\*\*\*>\*\*\*^t\*\*\*>\*\*\*\*\*

```
C      FLOW REACTOR DATA REDUCTION PROGRAM, PART 5
C      SP14.5.1
C      ROBERT F SAWYER
C
C      STATISTICAL ANALYSIS OF RATE DATA
C
C      TERMINATES ON BLANK CARD
C
C      SENSE SWITCH 1      SUPRESS PRINT
C      SENSE SWITCH 2      READ OR PUNCH PARTIAL SUMS FOR RESTART
C      SENSE SWITCH 3      CONTINUE AFTER PUNCHING PARTIAL SUMS,
C                           OTHERWISE STARTS NEW SET OF RUNS
C
C      DIMENSION      NNRUN(100),T(20),Y(5,20),X(20)
C      DIMENSION      SYR(5),SY2R(5),SXYR(5)
C      DIMENSION      SUMCR(5),SUMBR(5),SUMCR2(5),SUMBR2(5)
C      DIMENSION      CR(5),SCR(5),BR(5),SBR(5)
C      DIMENSION      CTR(5),SCTR(5),BTR(5),SBTR(5)
C      DIMENSION      CTP(5),SCTP(5),BTP(5),SBTP(5)
C      DIMENSION      SYTP(5),SY2TP(5),SXYTP(5)
C      DIMENSION      AYR(5),SR(5),AYTP(5),STP(5)
C      DIMENSION      NNRUN(20),CZ(4,5)
C      DIMENSION      RCR(5),RBR(5),RCTR(5),RBTR(5),RCTP(5),RBTP(5)
C      COMMON NI,NR,NP,X,Y,SXTP,SX2TP,SYTP,SY2TP,SXYTP,SUMCR,SUMBR,
1SUMCR2,SUMBR2
C      COMMON CR,SCR,BR,SBR,CTR,SCTR,BTR,SBTR,CTP,SCTP,BTP,SBTP
C
C      SET CONSTANTS
C
C      Z=1.9864
C      S=1./LOGF(10.)
C
C      INPUT OF PRELIMINARY DATA
C
195 READ 902
      READ 905
      READ 906
```

[293]

```
      READ 903, CZ
      IF (SENSE SWITCH 2) 180, 181
180  READ 940, NI, NR, NP, SXT, SX2T, (SYT(J), SY2T(J), SXYT(J), SUMCR(J),
      SUMBR(J), SUMCR2(J), SUMBR2(J), J=1, 5)
      GO TO 189
181  NI=0
      NR=0
      NP=0
      SXT=0.
      SX2T=0.
      DO 182 I=1, 5
      SYT(J)=0.
      SY2T(J)=0.
      SXYT(J)=0.
      SUMCR(J)=0.
      SUMBR(J)=0.
      SUMCR2(J)=0.
182  SUMBR2(J)=0.
189  K=1
      GO TO 390
```

C  
C  
C

INPUT TEMPERATURES AND RATES

```
194  NRUN(1)=NRUN(NI+1)
      T(1)=T(NI+1)
      DO 192 I=1, 5
192  Y(I, 1)=Y(I, NI+1)
      J=2
196  READ 900, NRUN(J), T(J), (Y(I, J), I=1, 5)
      IF (NRUN(J)) 199, 199, 197
197  IF (J-1) 1971, 1971, 198
1971 J=2
      GO TO 196
198  IF (NRUN(J)-NRUN(J-1)) 199, 1981, 199
1981 J=J+1
      GO TO 196
199  NI=J-1
      NNRUN(K)=NRUN(NI)
      NK=NK
      K=K+1
```

C  
C  
C

SUMMATION OF POINTS AND RUNS

```
NR=NR+1
NP=NP+NI
```

C  
C  
C

RECASTING OF DATA

```
DO 210 I=1, NI
DO 211 J=1, 5
211 Y(J, I)=2.30*Y(J, I)
210 X(I)=T(I)/1000.
```

C  
C  
C

STATISTICAL ANALYSIS

CALL STAT

C  
C  
C

CALCULATIONS



```

DO 350 J=1,5
CR(J)=CR(J)*Z
SCR(J)=SCR(J)*Z
DUM=SCR(J)/CR(J)
RCR(J)=ABSF(DUM)
BR(J)=BR(J)*S
SBR(J)=SBR(J)*S
DUM=SBR(J)/BR(J)
RBR(J)=ABSF(DUM)
350 CONTINUE
GO TO 393
360 DO 370 J=1,5
CTR(J)=CTR(J)*Z
SCTR(J)=SCTR(J)*Z
DUM=SCTR(J)/CTR(J)
RCTR(J)=ABSF(DUM)
BTR(J)=BTR(J)*S
SBTR(J)=SBTR(J)*S
DUM=SBTR(J)/BTR(J)
RBTR(J)=ABSF(DUM)
CTP(J)=CTP(J)*Z
SCTP(J)=SCTP(J)*Z
DUM=SCTP(J)/CTP(J)
RCTP(J)=ABSF(DUM)
BTP(J)=BTP(J)*S
SBTP(J)=SBTP(J)*S
DUM=SBTP(J)/BTP(J)
RBTP(J)=ABSF(DUM)
370 CONTINUE
GO TO 400
C
C   OUTPUT
C
390 IF(SENSE SWITCH 1)196,391
391 PRINT 902
PRINT 905
PRINT 911
PRINT 912
PRINT 911
PRINT 914, ((CZ(M,N),N=1,5),M=1,4)
PRINT 911
PRINT 911
J=1
GO TO 196
393 PRINT 915, NNRUN(NK)
IF(SENSE SWITCH 1) 196,394
394 PRINT 911
PRINT 916, CR
PRINT 917, SCR
PRINT 923, RCR
PRINT 918, BR
PRINT 919, SBR
PRINT 924, RBR
PRINT 911
PRINT 911
IF(NRUN(NI+1))360,360,194
400 CONTINUE
IF(SENSE SWITCH 1)420,407
407 PRINT 902

```

[295]

```
PRINT 905
PRINT 911
PRINT 912
PRINT 911
IF(NK-9)403,401,401
403 PRINT 920, NR, (NNRUN(K),K=1,NK)
GO TO 406
401 PRINT 920, NR, (NNRUN(K),K=1,9)
IF(NK-9)404,406,404
404 PRINT 921, (NNRUN(K),K=10,NK)
406 PRINT 911
PRINT 914, ((CZ(M,N),N=1,5),M=1,4)
PRINT 911
PRINT 916, CTR
PRINT 917, SCTR
PRINT 923, RCTR
PRINT 918, BTR
PRINT 919, SBTR
PRINT 924, RBTR
PRINT 911
PRINT 911
PRINT 922, NP
PRINT 911
PRINT 916, CTP
PRINT 917, SCTP
PRINT 923, RCTP
PRINT 918, BTP
PRINT 919, SBTP
PRINT 924, RBTP
PRINT 911
420 CONTINUE
IF(SENSE SWITCH 2)430,195
430 PUNCH 940,NI,NR,NP,SXTP,SX2TP,(SYTP(J),SY2TP(J),SXYTP(J),SUMCR(J),
1SUMBR(J),SUMCR2(J),SUMBR2(J),J=1,5)
IF(SENSE SWITCH 3)390,195
900 FORMAT(I10,6F10.5)
902 FORMAT(72H
1
)
903 FORMAT(4F10.5)
905 FORMAT(72H
1
)
906 FORMAT(6(/))
910 FORMAT(1H1)
911 FORMAT(1H )
912 FORMAT( 54H STATISTICAL ANALYSIS OF CHEMICAL KINETICS RATE DATA )
914 FORMAT(28X5F9.4)
915 FORMAT(6X10HRUN NUMBERI6)
916 FORMAT(6X12HE (CAL/MOLE)10X5F9.0)
917 FORMAT(6X18HSIGMA E (CAL/MOLE)4X5F9.0)
918 FORMAT(6X12HA 10X5F9.3)
919 FORMAT(6X12HSIGMA A 10X5F9.3)
920 FORMAT(6X11HSUMMARY OF I3,5H RUNS9I5)
921 FORMAT(25X9I5)
922 FORMAT(6X11HSUMMARY OF I4,7H POINTS)
923 FORMAT(6X11H(SIGMA E)/E11X5F9.4)
924 FORMAT(6X11H(SIGMA A)/A11X5F9.4)
940 FORMAT(3I5/(6E12.5))
END
```

```

C      STATISTICAL ANALYSIS SUBROUTINE
      SUBROUTINE STAT
      DIMENSION      NNRUN(100),T(20),Y(5,20),X(20)
      DIMENSION      SYR(5),SY2R(5),SXYR(5)
      DIMENSION      SUMCR(5),SUMBR(5),SUMCR2(5),SUMBR2(5)
      DIMENSION      CR(5),SCR(5),BR(5),SBR(5)
      DIMENSION      CTR(5),SCTR(5),BTR(5),SBTR(5)
      DIMENSION      CTP(5),SCTP(5),BTP(5),SBTP(5)
      DIMENSION      SYTP(5),SY2TP(5),SXYTP(5)
      DIMENSION      AYR(5),SR(5),AYTP(5),STP(5)
      COMMON NI,NR,NP,X,Y,SXTP,SX2TP,SYTP,SY2TP,SXYTP,SUMCR,SUMBR,
1SUMCR2,SUMBR2
      COMMON CR,SCR,BR,SBR,CTR,SCTR,BTR,SBTR,CTP,SCTP,BTP,SBTP

C      RUN SUMMATIONS
C
C      SXR=0.
      SX2R=0.
      DO 90 J=1,5
      SYR(J)=0.
      SY2R(J)=0.
90  SXYR(J)=0.
      DO 100 I=1,NI
      SXR=SXR+X(I)
      SX2R=SX2R+X(I)**2
100 CONTINUE
      DO 110 J=1,5
      DO 110 I=1,NI
      SYR(J)=SYR(J)+Y(J,I)
      SY2R(J)=SY2R(J)+Y(J,I)**2
      SXYR(J)=SXYR(J)+X(I)*Y(J,I)
110 CONTINUE

C      TOTAL POINT SUMMATION
C
C      SXTP=SXTP+SXR
      SX2TP=SX2TP+SX2R
      DO 120 J=1,5
      SYTP(J)=SYTP(J)+SYR(J)
      SY2TP(J)=SY2TP(J)+SY2R(J)
      SXYTP(J)=SXYTP(J)+SXYR(J)
120 CONTINUE

C      CONVERT RUN AND POINT NUMBERS
C
C      ANI=NI
      ANR=NR
      ANP=NP

C      RUN CURVE FIT
C
      AXR=SXR/ANI
      DO 130 J=1,5
      CR(J)=(ANI*SXYR(J)-SXR*SYR(J))/(ANI*SX2R-SXR**2)
      AYR(J)=SYR(J)/ANI

```

[297]

```
BR(J)=AYR(J)-CR(J)*AXR
SR(J)=((SY2R(J)-SYR(J)**2/ANI-((SXYR(J)-SXR*SYR(J)/ANI)**2)/(SX2R-
1SXR**2/ANI))/(ANI-2.))**.5
SCR(J)=SR(J)*(1./(SX2R-ANI*AXR**2))**.5
SBR(J)=SR(J)*(SX2R/(ANI*SX2R-SXR**2))**.5
```

130 CONTINUE

C  
C  
C  
C  
C

RUN SUMMARY

TOTAL RUN SUMMATION

```
DO 140 J=1,5
SUMCR(J)=SUMCR(J)+CR(J)
SUMBR(J)=SUMBR(J)+BR(J)
SUMCR2(J)=SUMCR2(J)+CR(J)**2
SUMBR2(J)=SUMBR2(J)+BR(J)**2
```

C  
C  
C

AVERAGES

```
CTR(J)=SUMCR(J)/ANR
BTR(J)=SUMBR(J)/ANR
```

C  
C  
C

STANDARD DEVIATIONS

```
SCTR(J)=((SUMCR2(J)-SUMCR(J)**2/ANR)/(ANR-1.000001))**.5
SBTR(J)=((SUMBR2(J)-SUMBR(J)**2/ANR)/(ANR-1.000001))**.5
```

140 CONTINUE

C  
C  
C

POINT SUMMARY

```
AXTP=SXTP/ANP
DO 150 J=1,5
CTP(J)=(ANP*SXYTP(J)-SXTP*SYTP(J))/(ANP*SX2TP-SXTP**2)
AYTP(J)=SYTP(J)/ANP
BTP(J)=AYTP(J)-CTP(J)*AXTP
STP(J)=((SY2TP(J)-SYTP(J)**2/ANP-((SXYTP(J)-SXTP*SYTP(J)/ANP)**2)/
1(SX2TP-SXTP**2/ANP))/(ANP-2.))**.5
SCTP(J)=STP(J)*(1./(SX2TP-ANP*AXTP**2))**.5
SBTP(J)=STP(J)*(SX2TP/(ANP*SX2TP-SXTP**2))**.5
```

150 CONTINUE

RETURN  
END

[2981]

## CHEMICAL KINETICS FLOW REACTOR DATA SHEET

15 MAY 1964

NITROGEN DIOXIDE/HYDROGEN REACTION RATE STUDY  
 ROBERT F SAWYER, GUGGENHEIM LABORATORIES

RUN NUMBER 387

PROBE BASE (MV) 6.100  
 OXIDIZER INJECTION PORT 2

	CARRIER	DILUENT	FUEL	OXIDIZER
CHEMICAL MOLECULAR WEIGHT	N2 28.01	N2 28.01	H2 2.01	NO2 46.00
INPUT				
PRESSURE (PSIG)	152.0	58.0	21.6	40.6
TEMPERATURE (DEGF)	115.	80.	85.	394.
MANOMETER (INHG)		2.00	10.30	
CORRECTED				
PRESSURE (ATMA)	11.34	4.94	2.47	3.76
TEMPERATURE (DEGK)	321.	300.	303.	468.
MANOMETER (INHG)		2.00	10.30	
CALCULATED				
FLOW RATE (GM/SEC)	14.4795	1.0072	.0624	.3990
FLOW RATE (MOLE/SEC)	.51683	.03595	.03098	.00867
MOLE FRACTION	.87237	.06068	.05230	.01463

EQUIVALENCE RATIO 1.786

REACTION RATIO 3.572

## CHEMICAL KINETICS FLOW REACTOR DATA SHEET

15 MAY 1964

NITROGEN DIOXIDE/HYDROGEN REACTION RATE STUDY  
ROBERT F SAWYER, GUGGENHEIM LABORATORIES

RUN NUMBER

387

HEAT OF REACTION (CAL/MOLE)

42530.

## FLOW CONDITIONS

POINT	T	T	S	S	V	FR
	MV	DEGK	-	D/CM	CM/SEC	-
1	5.800	893.3	0.00	0.000	570.3	0.0000
2	6.100	919.7	1.32	2.077	587.2	.3057
3	6.170	925.8	1.26	1.983	591.1	.3761
4	6.290	936.2	1.19	1.856	597.7	.4965
5	6.301	937.2	1.11	1.731	598.3	.5075
6	6.368	943.0	1.08	1.685	602.0	.5744
7	6.429	948.2	1.03	1.593	605.3	.6347
8	6.485	953.0	.99	1.531	608.4	.6901
9	6.540	957.7	.93	1.438	611.4	.7445
10	6.590	961.9	.82	1.268	614.1	.7939
11	6.635	965.7	.73	1.119	616.5	.8381
12	6.678	969.4	.66	1.012	618.9	.8803
13	6.800	979.7	0.00	0.000	625.5	1.0000

## RATE CONSTANTS

M	0.00	0.00	0.00	0.00	0.00
A	0.00	1.00	1.20	1.40	1.60
B	0.00	1.00	1.00	1.00	1.00
C	0.00	-1.00	-1.00	-1.00	-1.00

POINT	1000/T	R1	R2	R3	R4	R5
	1/DEGK	*	*	*	*	*
1	1.1193	0.000E-99	0.000E-99	0.000E-99	0.000E-99	0.000E-99
2	1.0872	2.165E+01	6.625E-00	1.150E+02	1.997E+03	3.468E+04
3	1.0800	2.301E+01	7.193E-00	1.256E+02	2.193E+03	3.830E+04
4	1.0680	2.669E+01	8.673E-00	1.529E+02	2.697E+03	4.757E+04
5	1.0669	2.545E+01	8.299E-00	1.465E+02	2.586E+03	4.564E+04
6	1.0604	2.866E+01	9.551E-00	1.695E+02	3.009E+03	5.343E+04
7	1.0546	3.157E+01	1.073E+01	1.916E+02	3.419E+03	6.101E+04
8	1.0493	3.577E+01	1.240E+01	2.223E+02	3.986E+03	7.147E+04
9	1.0441	4.076E+01	1.440E+01	2.594E+02	4.674E+03	8.420E+04
10	1.0395	4.456E+01	1.602E+01	2.899E+02	5.247E+03	9.495E+04
11	1.0354	5.009E+01	1.830E+01	3.325E+02	6.041E+03	1.097E+05
12	1.0315	6.124E+01	2.273E+01	4.145E+02	7.561E+03	1.378E+05
13	1.0206	0.000E-99	0.000E-99	0.000E-99	0.000E-99	0.000E-99

\* RATE CONSTANT DIMENSIONS=((CM3/MOLE)\*\*(A+B+C-1))/(SEC DEGK\*\*M)

APPENDIX D. INFRARED SPECTRA AND MASS SPECTROSCOPIC ANALYSIS  
OF GAS SAMPLES

The infrared spectra of some typical gas samples taken from the flow reactor are presented. Included are the following,

ammonia/nitrogen dioxide reaction products,  
excess nitrogen dioxide, Figure 71

hydrogen/nitrogen dioxide reaction products,  
excess nitrogen dioxide, Figure 72

The infrared spectrum of a nitric oxide sample also is presented, Figure 73. Impurities of nitrous oxide and carbon dioxide are detected.

The results of mass spectrometric analysis of some flow reactor gas samples are summarized in Table 35.

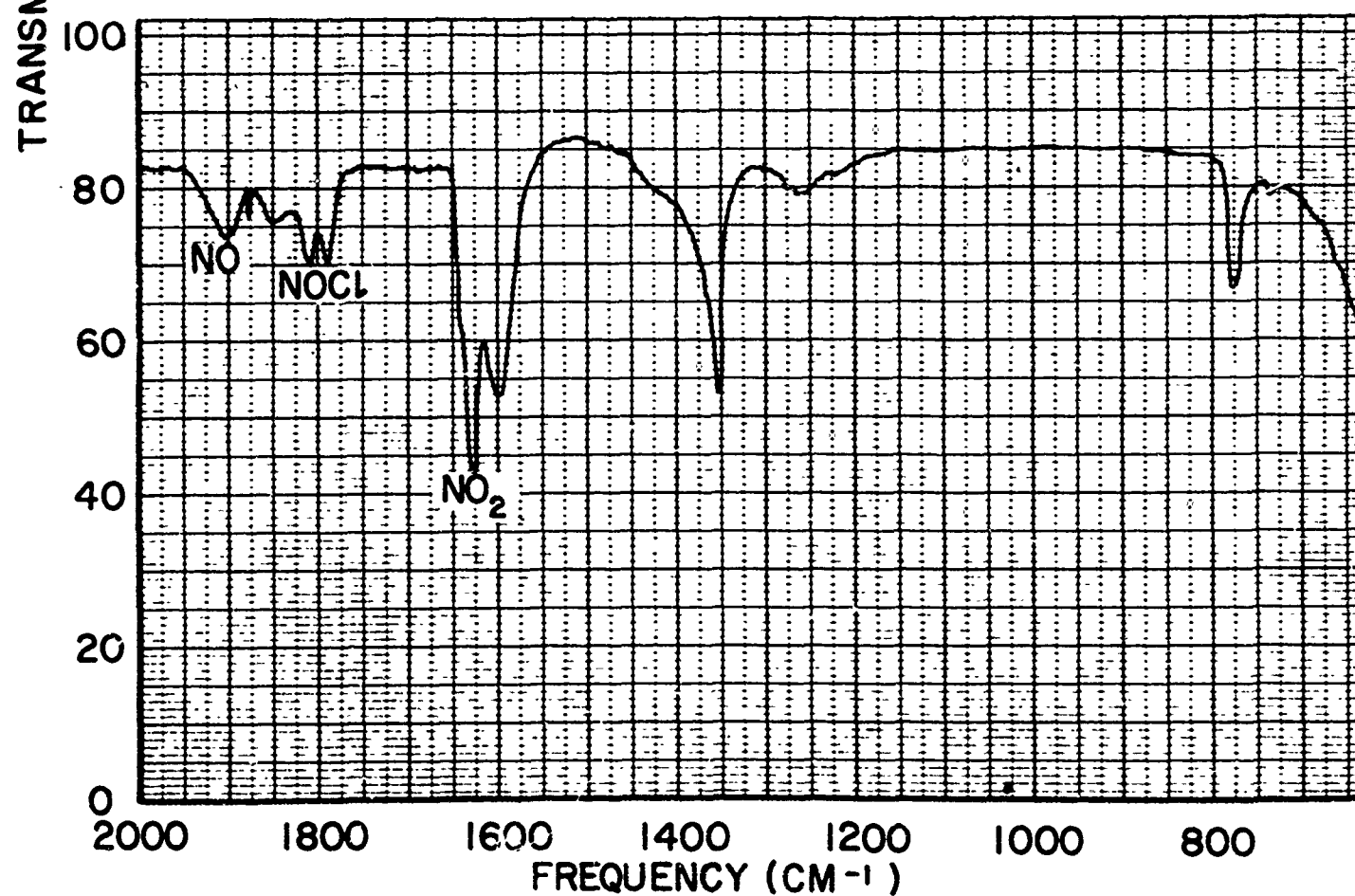
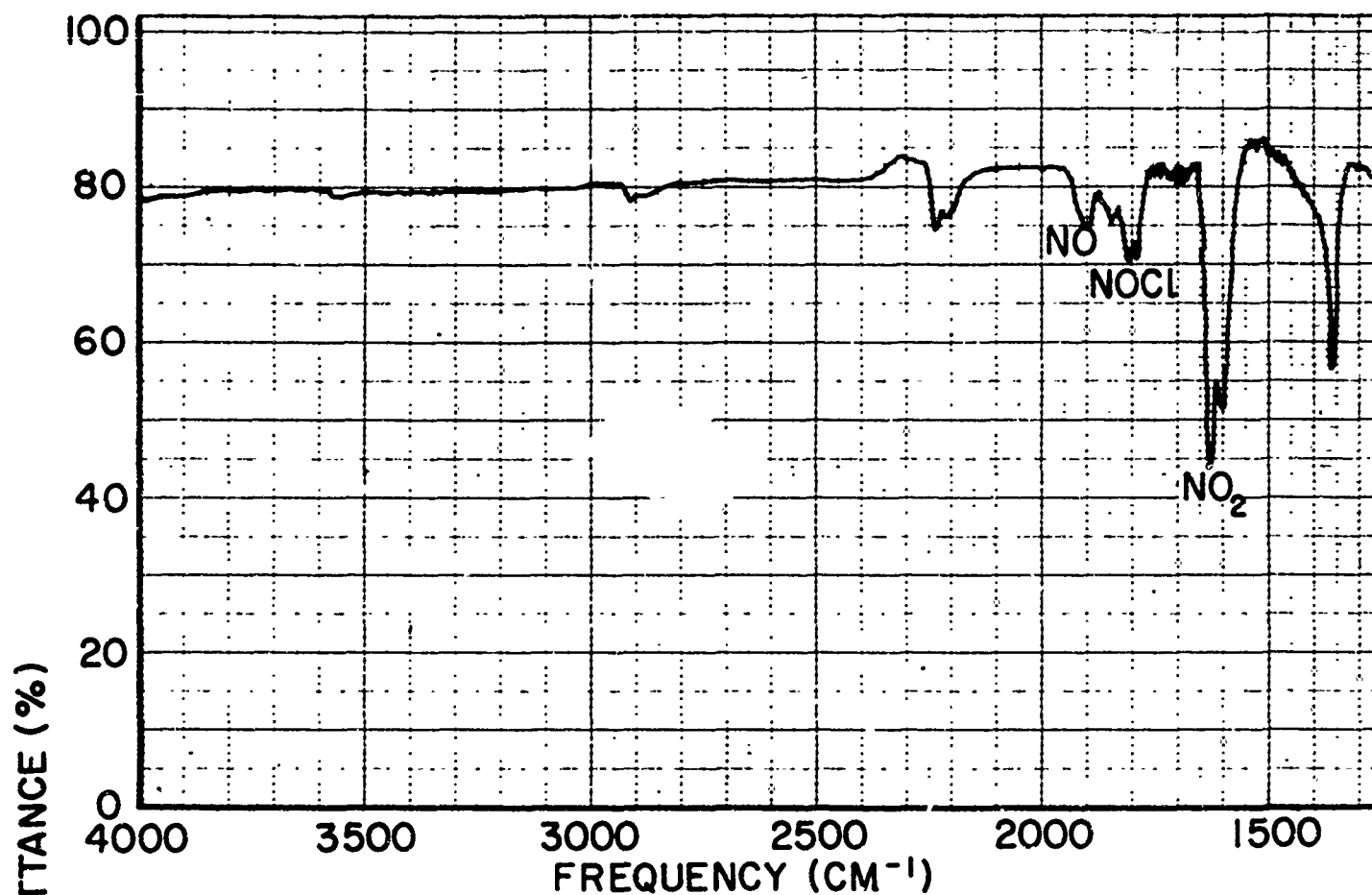
TABLE 35. Mass spectrometric analysis of gas samples

<u>sample</u>	<u>composition</u>
nitric oxide	NO > .9995*
nitrogen	N <sub>2</sub> > .9998*
hydrogen/nitrogen dioxide reaction products	O <sub>2</sub> < .0001 Ar < .0001 CO <sub>2</sub> .0002 H <sub>2</sub> O .0005 H <sub>2</sub> .0280 NO .0140 N <sub>2</sub> .9571*
ammonia/nitrogen dioxide reaction products	O <sub>2</sub> --- Ar --- CO <sub>2</sub> --- H <sub>2</sub> O .0002 H <sub>2</sub> < .0001 NO .0350 N <sub>2</sub> .9647*

---

\* by difference

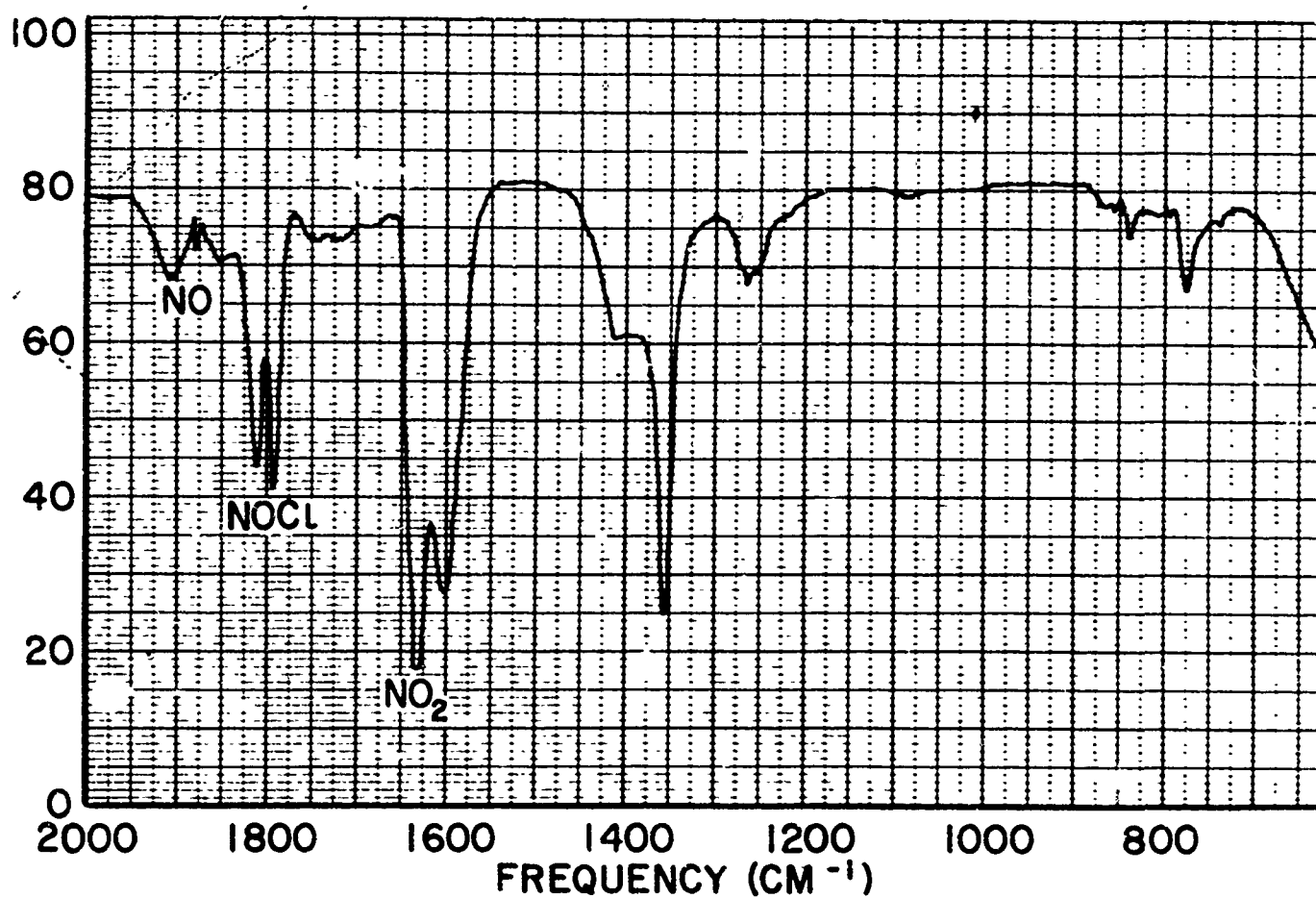
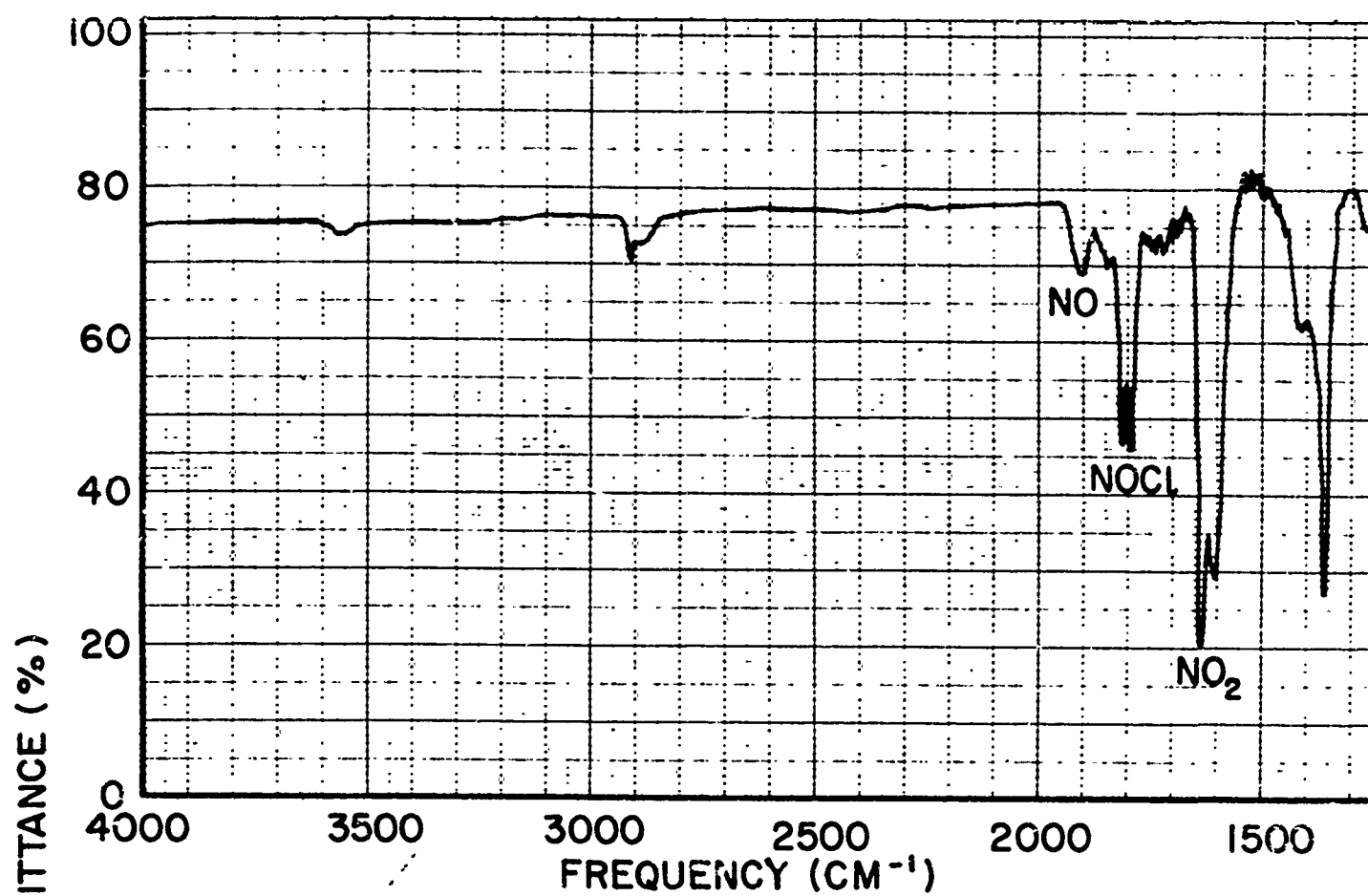




INFRARED SPECTRUM, AMMONIA / NITROGEN DIOXIDE,  
EXCESS NITROGEN DIOXIDE

FIGURE 71

JPI3-4077-65

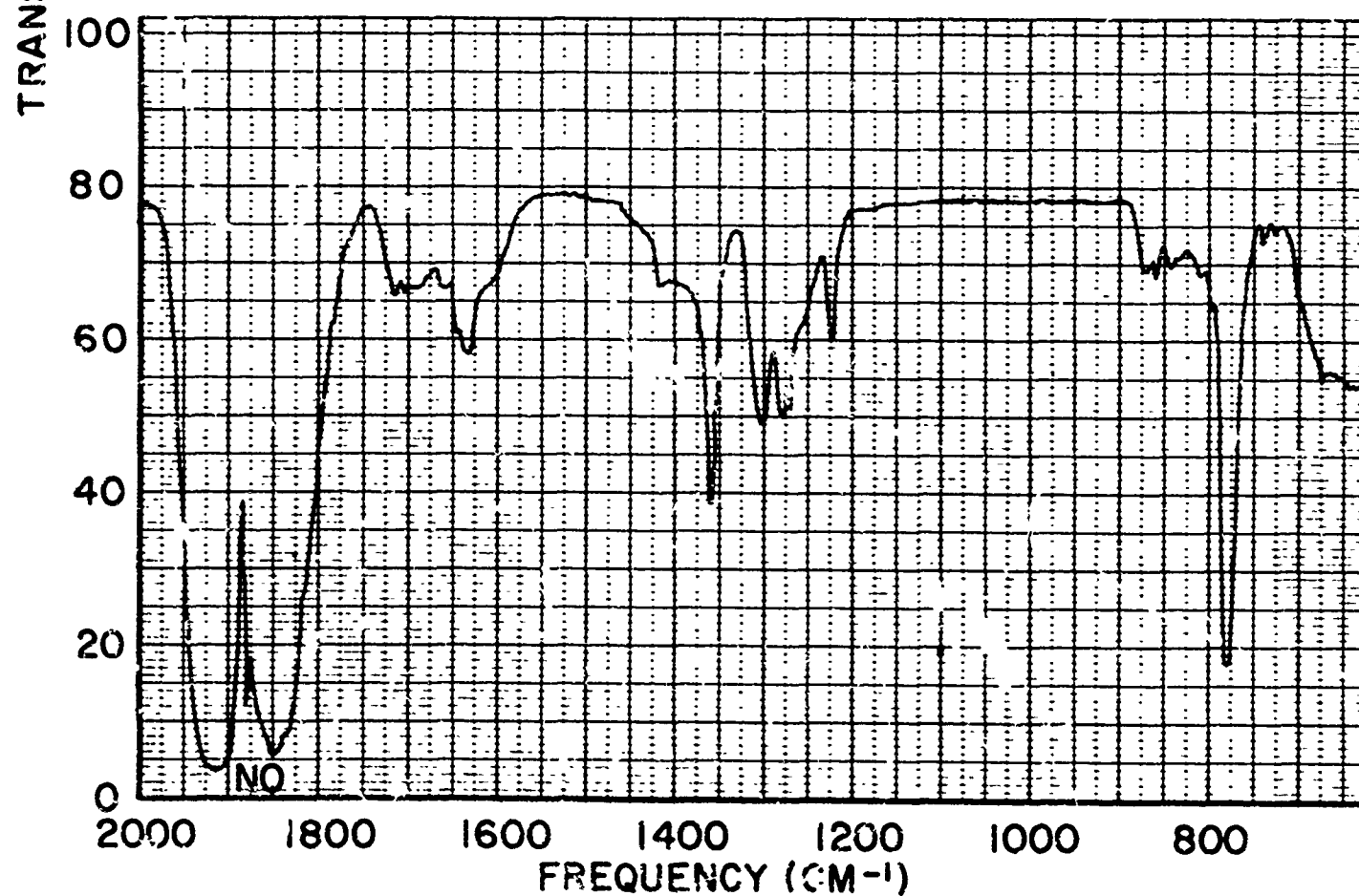
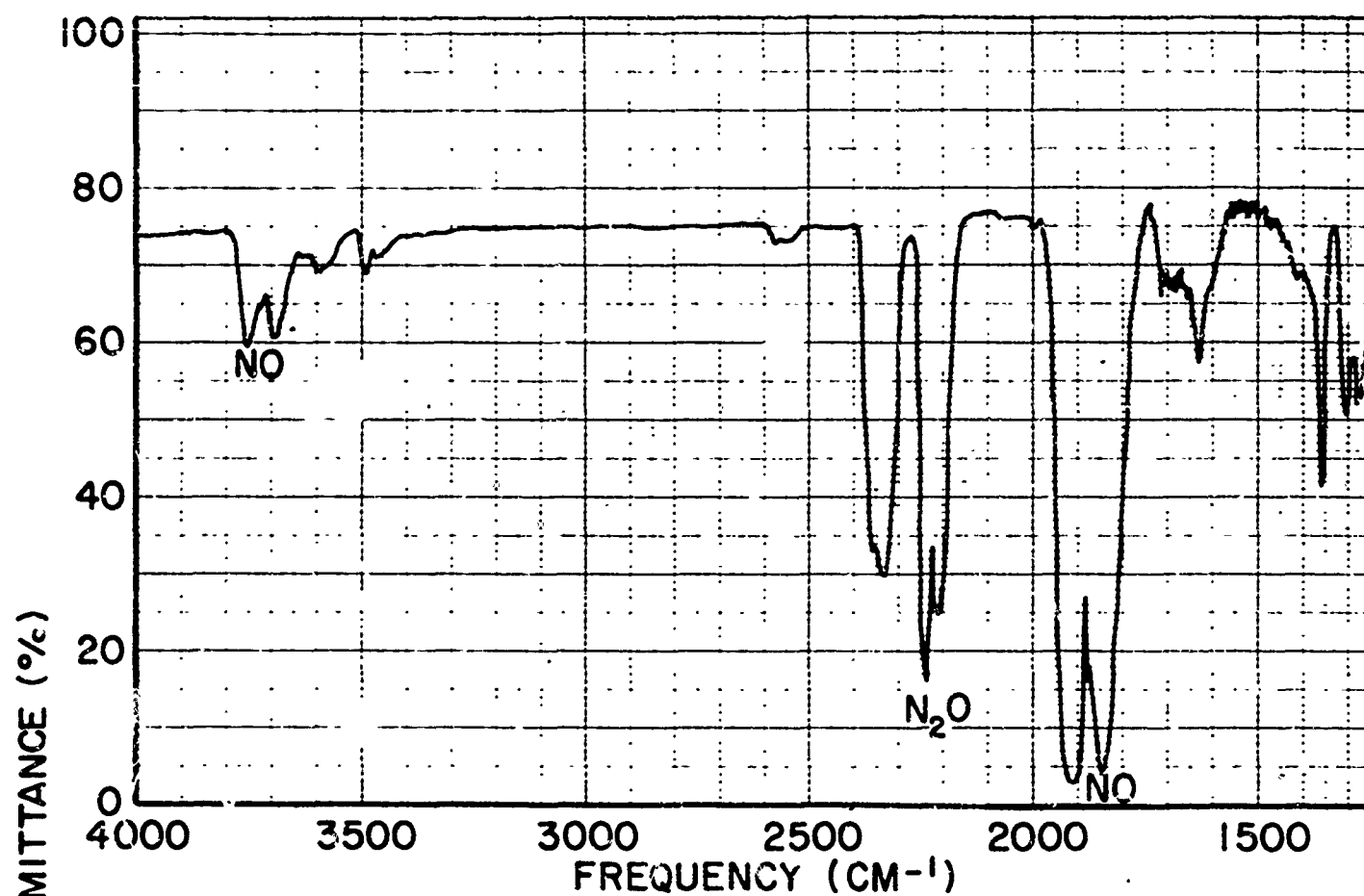


INFRARED SPECTRUM, HYDROGEN / NITROGEN DIOXIDE,  
EXCESS NITROGEN DIOXIDE

FIGURE 72

VP13-4071-03

VP13-4070



INFRARED SPECTRUM, NITRIC OXIDE

FIGURE 73

APPENDIX E.      HYDRAZINE/NITROGEN TETROXIDE AS ROCKET  
                         PROPELLANTS

The attractiveness of hydrazine and nitrogen tetroxide as a rocket propellant combination lies both in their physical properties and in their thermochemical performance.

E.1 General properties

Properties of the hydrazine/nitrogen tetroxide combination which contribute to their attractiveness as rocket propellants are listed below.

(1) Storability: Both propellants are suited to long term storage at ambient conditions.

(2) Performance: The combination offers a specific impulse and density which makes it rival the cryogenic combination of liquid oxygen and RP-1 (a kerosene blend) in performance in a missile system (116). The specific impulses at a chamber pressure of 1000 (psia) and an equilibrium expansion to 1 (atm) pressure of several propellant combinations are listed below for comparison.

JP13-4076-65

TABLE 36. Theoretical performance of some common propellants  
(117,118,119,120) (equilibrium expansion from 1000  
to 14.7 psia)

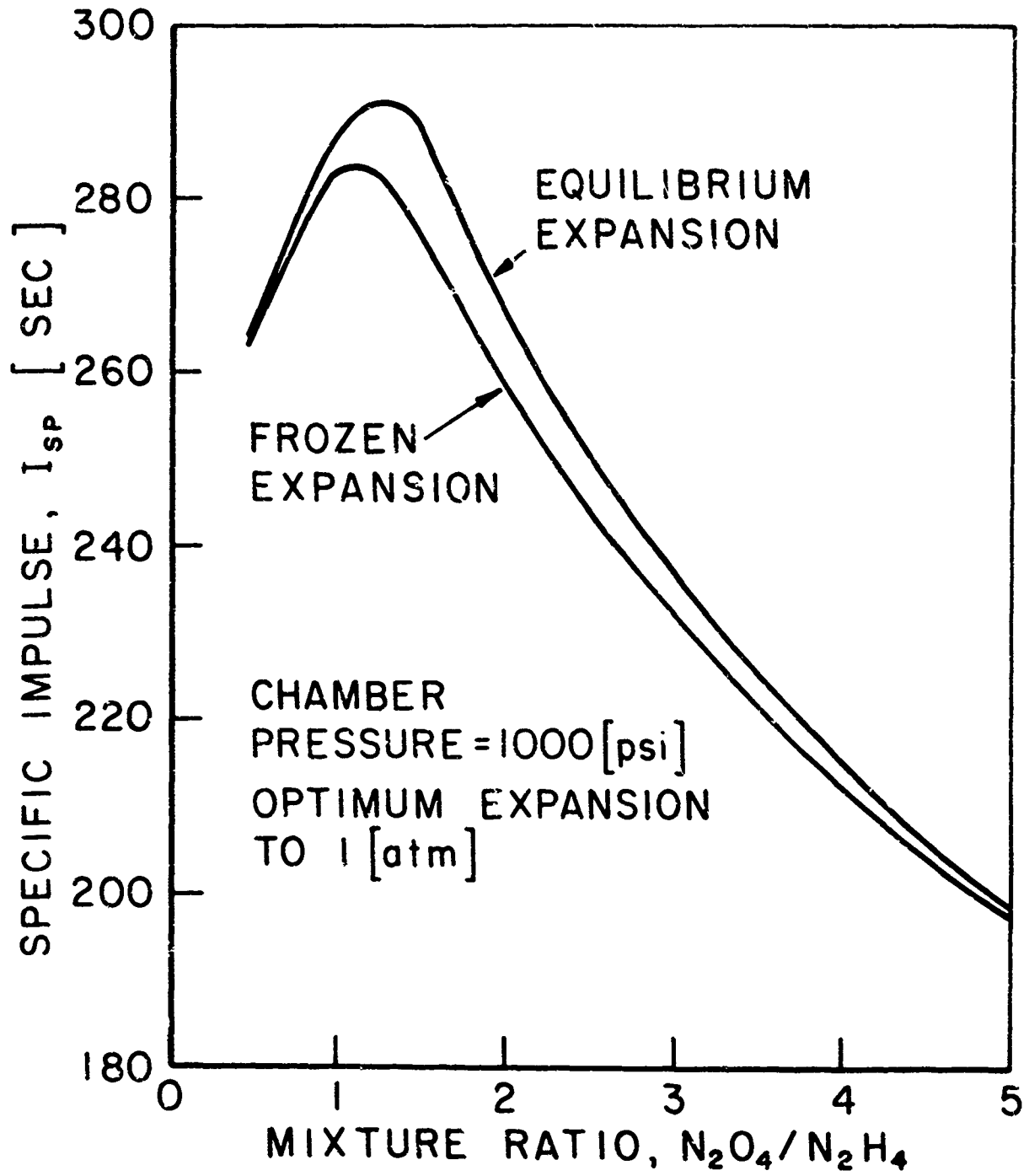
propellant	mixture ratio	bulk density	specific impulse
	r	d	sp
	-	gm/cc	sec
$N_2O_4/N_2H_4$	1.35	1.21	291
$H_2O_2/N_2H_4$	2.00	1.25	285
$ClF_3/N_2H_4$	2.79	1.49	292
$O_2/RP-1$	2.45	1.02	301
$O_2/H_2$	4.00	0.28	391
$N_2O_4/NH_3$	2.02	1.06	269
$N_2O_4/RP-1$	4.08	1.26	276
$N_2O_4/UDMH$	2.65	1.17	286
$N_2O_4/MMH$	2.19	1.21	238
$B_5H_9/N_2H_4$	1.27		328
$N_2O_4/B_5H_9$	3.30		303
$N_2O_4/N_2H_4/30\% Al$	0.40		301

(3) Ignition: The combination is hypergolic and therefore requires no ignition device. Ignition has been found to take place at pressures of less than 1 (mmHg) (108,3). Combustion has been started and sustained in a rocket chamber at 1.5 (psia) (121).

## E.2 Theoretical performance

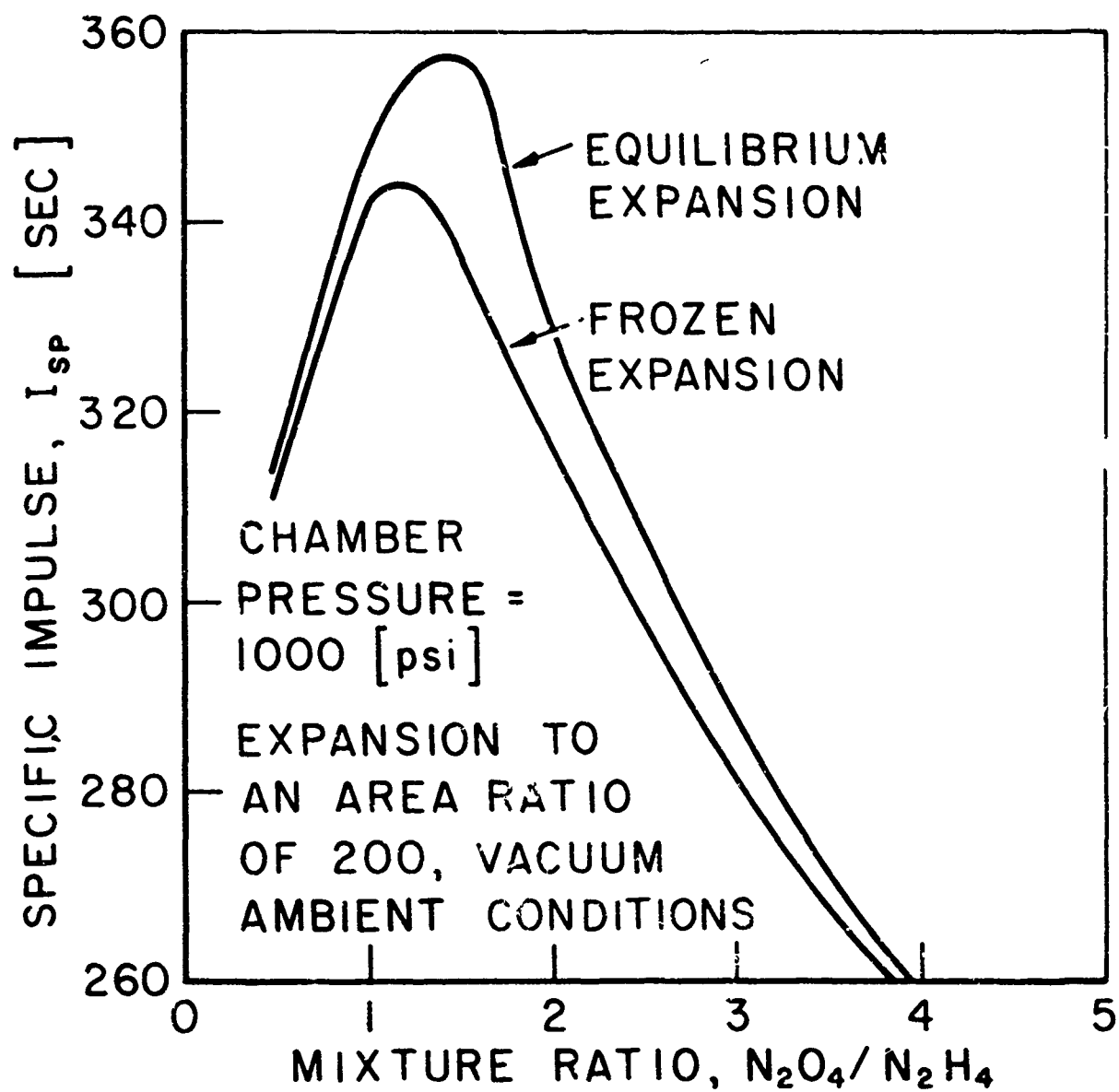
The theoretical performance of hydrazine/nitrogen tetroxide as rocket propellants was calculated using the equilibrium thermodynamics computer program of Zelenik and Gordon (122, 123). Specific impulse as a function of mixture ratio for equilibrium composition and frozen composition expansions are plotted for "sea level" conditions, ie. optimum expansion to 1 (atm) pressure with 1 (atm) ambient pressure, and for "space" conditions, ie. expansion to an area ratio of 200 with vacuum ambient conditions, in Figures 74 and 75, respectively. As is the case with most rocket propellants, the optimum mixture ratio shifts from a fuel rich mixture for frozen expansion toward the stoichiometric value of  $O/F = 1.44$  for equilibrium expansion. Equilibrium expansion allows recovery of energy stored in dissociated species thereby favoring the mixture ratio giving maximum energy release, near stoichiometric.

Some of the parameters of the equilibrium reaction of liquid hydrazine and liquid nitrogen tetroxide at a mixture ratio of  $O/F = 1.5$  are summarized below.



THEORETICAL SPECIFIC IMPULSE  
NITROGEN TETROXIDE / HYDRAZINE

FIGURE 74



THEORETICAL SPECIFIC IMPULSE  
NITROGEN TETROXIDE / HYDRAZINE

JP-3-JPR4020-65



TABLE 37. Combustion parameters,  $\text{N}_2\text{H}_4/\text{N}_2\text{O}_4$ , O/F = - 5.

pressure	1000 (psia)
combustion temperature	3248 ( $^{\circ}\text{K}$ )
enthalpy	114.6 (cal/gm)
molecular weight	21.6
specific heat ratio, $\gamma$	1.149
characteristic velocity, $c^*$	5745 (ft/sec)
composition	mole fraction
$\text{H}_2\text{O}$	.475
$\text{N}_2$	.404
$\text{H}_2$	.043
OH	.036
$\text{O}_2$	.018
NO	.013
H	.008
C	.004

The theoretical characteristic velocity is plotted as a function of the mixture ratio in Figure 76. Defined as

$$c^* = \frac{p_c A_t}{\dot{m}}$$

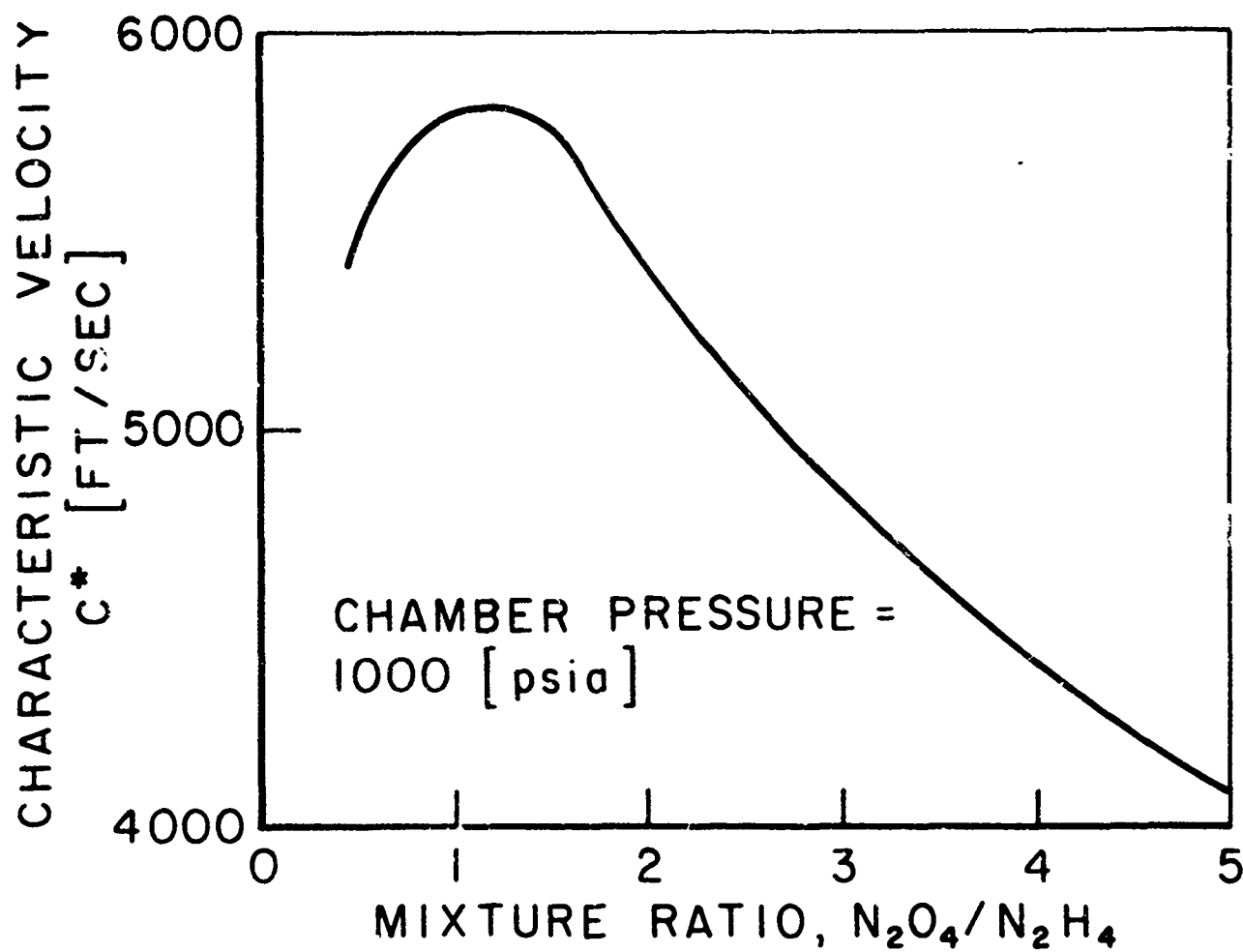
experimentally measured characteristic velocities, as compared to the theoretical value, are useful rocket propulsion parameters representative of the efficiency of the combustion process.

### E.3 Experimental performance

Several investigators have shown the experimental performance of hydrazine/nitrogen tetroxide to be close to that theoretically predicted.

Rollbuhler and Tomazic (124) obtained maximum characteristic velocities,  $c^*$ , of 5790 (feet/sec) at a mixture ratio of 1.04 in a 300 (pound) thrust chamber at a pressure of 300 (psia). This is 99% of the theoretical equilibrium value. In comparing these results with those obtained for hydrogen/chlorine trifluoride, they concluded that the dissociation of nitrogen tetroxide to nitrogen dioxide was largely complete before combustion and contributed to enhancing propellant vaporization and reaction. Chlorine tribluoride would not and did not show this behavior.

In a much smaller rocket at low combustion pressure, 25 (pounds) thrust at a chamber pressure of 10 (psia), Wanhainen, DeWitt, and Ross (121) obtained a maximum characteristic velocity of 5200 (ft/sec) (or 92% of the

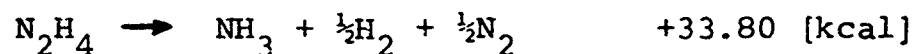


THEORETICAL CHARACTERISTIC VELOCITY  
NITROGEN TETROXIDE/HYDRAZINE

theoretical value) at a mixture ratio of 1.0.

Chilenski and Lee (125) studied hydrazine/nitrogen tetroxide in an approximately 100 (pound) thrust chamber at pressures of 300 to 500 (psia). In particular, they investigated performance at low, 0 to 0.55, and high, 5.9 to 13.0, mixture ratios,  $r$ . In the fuel rich region they obtained performances in excess of those theoretically predicted. They attributed this result to a lack of endothermic ammonia decomposition. In the oxidizer rich region, they obtained performances below the predicted values. They attributed this performance to the lack of exothermic dissociation of the nitrogen oxides.

The effect of the non-equilibrium behavior of hydrazine decomposition whereby



instead of the equilibrium decomposition

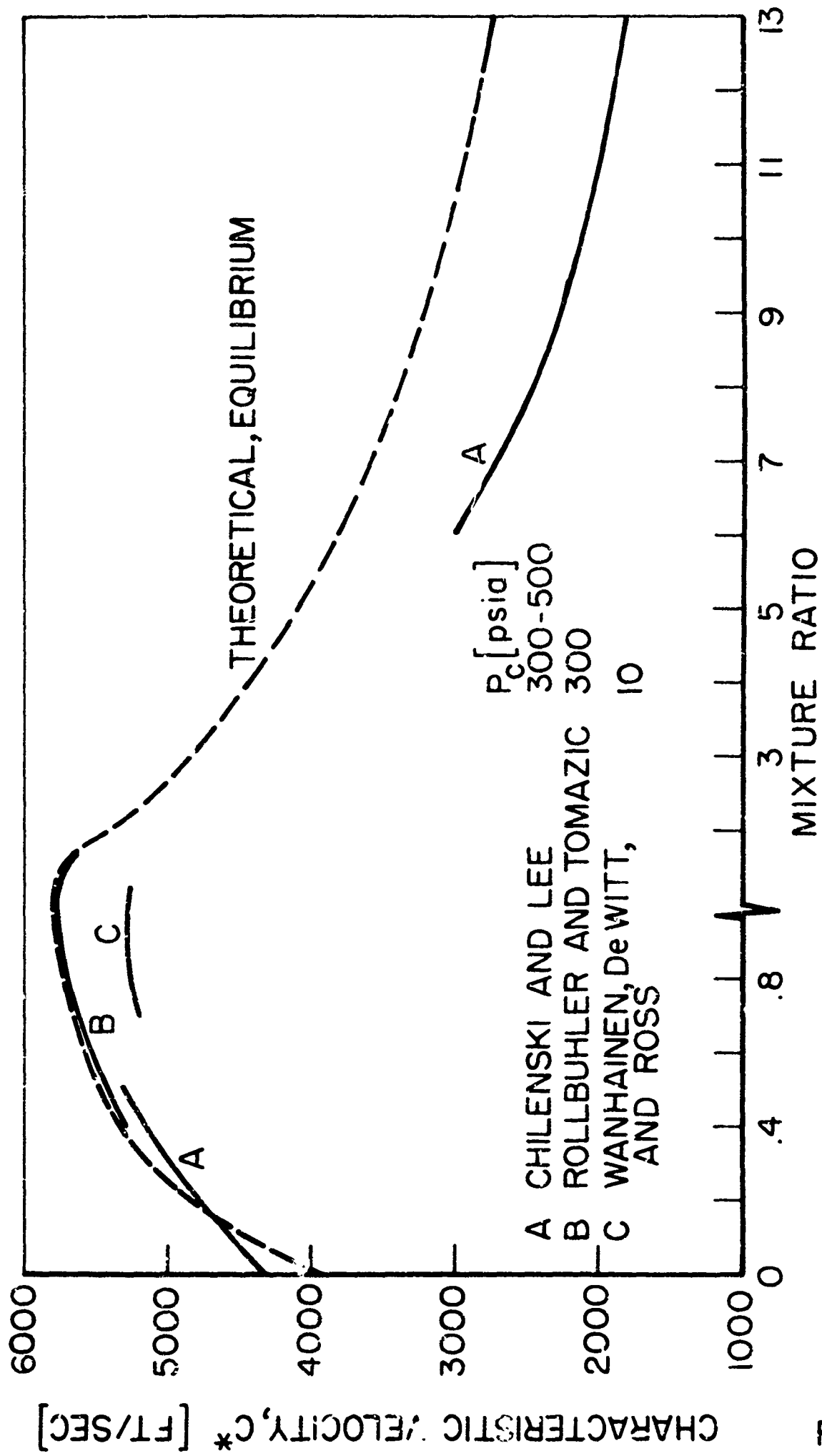


to give higher than theoretically predicted performance has been noted before, see, for example, (126).

Elverum and Stauhammer (127) studied the combustion of hydrazine and nitrogen tetroxide at 40, 80, and 800 pounds thrust levels at pressures between 200 and 300 psia. They obtained performance of up to 98% of theoretical characteristic velocity but noted the necessity of obtaining rapid and complete mixing to prevent hydrazine vapor

expulsions. Low performance was observed where poor liquid phase mixing was obtained. They attributed this effect to an inhibition of liquid phase mixing by rapid initial reaction [which seems to be a rather circuitous argument].

Experimental performances in terms of characteristic velocity are compared in Figure 77. The theoretical characteristic velocity curve is for a pressure of 300 (psia). While characteristic velocity drops only slightly with decreasing chamber pressure, the low pressure experimental results (curve C) should be compared with a theoretical value somewhat less than that in the figure. Away from the optimum mixture ratio (1.31), non-equilibrium effects cause the experimental results to diverge from the theoretical predictions. The low performance at low pressure is probably due to low injection velocities and poor mixing rather than any effect on the chemical reaction.



EXPERIMENTAL PERFORMANCE, HYDRAZINE / NITROGEN TETROXIDE

UNCLASSIFIED  
Security Classification

DOCUMENT CONTROL DATA - R&D		
1 ORIGINATOR'S REPORT NUMBER <b>Princeton University Department of Aerospace &amp; Mechanical Sciences Princeton, New Jersey 08540</b>		2 SECURITY CLASSIFICATION <input checked="" type="checkbox"/> Unclassified Other Specify _____
3 REPORT TITLE <b>THE HOMOGENEOUS GAS PHASE KINETICS OF REACTIONS IN THE HYDRAZINE-NITROGEN TETROXIDE PROPELLANT SYSTEM</b>		
4 DESCRIPTIVE NOTES (Type of report and inclusive dates) <input checked="" type="checkbox"/> Scientific Report <input type="checkbox"/> Final Report <input type="checkbox"/> Journal Article <input type="checkbox"/> Proceedings <input type="checkbox"/> Book		
5 AUTHOR(S) (Last name, first name, initial) <b>Sawyer Robert F</b>		
6 REPORT DATE AS PRINTED <b>1965</b>	7A TOTAL NO OF PAGES <b>336</b>	7B NO OF REFS <b>127</b>
8A CONTRACT OR GRANT NO <b>AF 49(638)1268</b>	9A ORIGINATOR'S REPORT NUMBER(S) (if given) <b>TR 761</b>	
B PROJECT NO <b>9711-01</b>	9B OTHER REPORT NUMBER(S) (Any other numbers that may be assigned this report) <b>AFOSR 66-0855</b>	
C 61445014	AD	
10 AVAILABILITY/LIMITATION NOTICES <b>Distribution of this document is unlimited</b>		<input checked="" type="checkbox"/> Available from DDC <input type="checkbox"/> Available from CFSTI <input type="checkbox"/> Available from Source <input type="checkbox"/> Available Commercially
11 SUPPLEMENTARY NOTES (Citation)		12 SPONSORING MILITARY ACTIVITY <b>AF Office of Scientific Research (SREP) Office of Aerospace Research Washington, D. C. 20333</b>
13 ABSTRACT <p>The reaction of hydrazine and nitrogen tetroxide is affected strongly by reactant decompositions. Hydrazine can decompose to hydrogen, ammonia, and nitrogen. Nitrogen tetroxide can decompose to nitrogen dioxide, nitric oxide, oxygen, and nitrogen. The gas phase homogeneous reactions of hydrazine, hydrogen, ammonia, and hydrogen/ammonia mixtures with nitrogen dioxide, oxygen, nitric oxide, and oxygen/nitric oxide mixtures were studied in an adiabatic flow reactor at temperatures of from 800 to 1300°K. Heats of reaction, reaction orders, and reaction rates were determined for 11 reactions involving combinations of the above reactants. Arrhenius rate constants were calculated and overall activation energies determined from the measured reaction rates. The reaction of hydrogen and oxygen is about ten times more rapid than the reaction of hydrogen and nitrogen dioxide. The hydrogen/nitrogen dioxide reaction produces nitric oxide which inhibits the further oxidation of hydrogen. Ammonia reacts about ten times more rapidly with nitrogen dioxide than with oxygen. Hydrazine and nitrogen dioxide react with a two step behavior: the rapid reduction of nitrogen dioxide to nitric oxide is followed by a slower reduction of the nitric oxide. The first step occurs with out hydrazine decomposition. The second step requires the decomposition of hydrazine. The reaction of hydrazine and oxygen occurs with simultaneous decomposition and oxidation.</p>		

14.

## KEY WORDS

Hydrazine  
 Nitrogen Tetroxide  
 Nitrogen Dioxide  
 Hydrogen  
 Oxygen  
 Arsenia  
 Nitric Oxide  
 Reaction Rates  
 Gas Phase Reactions  
 Reaction Kinetics  
 Adiabatic Flow Reactor  
 Arrhenius Rate Constants  
 Combustion Reactions  
 Reaction Mechanisms  
 Combustion Kinetics

## LINK A

ROLE

WT

## LINK B

ROLE

WT

## LINK C

ROLE

WT

## INSTRUCTIONS

1. ORIGINATING ACTIVITY: Enter the name and address of the contractor, subcontractor, grantee, Department of Defense activity or other organization (Corporate author) issuing the report.

2a. REPORT SECURITY CLASSIFICATION: Enter the overall security classification of the report. Indicate whether "Restricted Data" is included. Marking is to be in accordance with appropriate security regulations.

2b. GROUP: Automatic downgrading is specified in DoD Directive 5200.10 and Armed Forces Industrial Manual. Enter the group number. Also, when applicable, show that optional markings have been used for Group 3 and Group 4 as authorized.

3. REPORT TITLE: Enter the complete report title in all capital letters. Titles in all cases should be unclassified. If a meaningful title cannot be selected without classification, show title classification in all capitals in parenthesis immediately following the title.

4. DESCRIPTIVE NOTES: If appropriate, enter the type of report, e.g., interim, progress, summary, annual, or final. Give the inclusive dates when a specific reporting period is covered.

5. AUTHOR(S): Enter the name(s) of author(s) as shown on or in the report. Enter last name, first name, middle initial. If military, show rank and branch of service. The name of the principal author is an absolute minimum requirement.

6. REPORT DATE: Enter the date of the report as day, month, year, or month, year. If more than one date appears on the report, use date of publication.

7a. TOTAL NUMBER OF PAGES: The total page count should follow normal pagination procedures, i.e., enter the number of pages containing information.

7b. NUMBER OF REFERENCES: Enter the total number of references cited in the report.

9a. CONTRACT OR GRANT NUMBER: If appropriate, enter the applicable number of the contract or grant under which the report was written.

8a, 8b, & 8c. PROJECT NUMBER: Enter the appropriate military department identification, such as project number, sub-project number, system numbers, task number, etc.

9a. ORIGINATOR'S REPORT NUMBER(S): Enter the official report number by which the document will be identified and controlled by the originating activity. This number must be unique to this report.

9b. OTHER REPORT NUMBER(S): If the report has been assigned any other report numbers (either by the originator or by the sponsor), also enter this number(s).

10. AVAILABILITY/LIMITATION NOTICES: Enter any limitations on further dissemination of the report, other than

those imposed by security classification, using standard statements such as:

(1) "Qualified requesters may obtain copies of this report from DDC."

(2) "Foreign announcement and dissemination of this report by DDC is not authorized."

(3) "U. S. Government agencies may obtain copies of this report directly from DDC. Other qualified DDC users shall request through

(4) "U. S. military agencies may obtain copies of this report directly from DDC. Other qualified users shall request through

(5) "All distribution of this report is controlled. Qualified DDC users shall request through

If the report has been furnished to the Office of Technical Services, Department of Commerce, for sale to the public, indicate this fact and enter the price, if known.

11. SUPPLEMENTARY NOTES: Use for additional explanatory notes.

12. SPONSORING MILITARY ACTIVITY: Enter the name of the departmental project office or laboratory sponsoring (paying for) the research and development. Include address.

13. ABSTRACT: Enter an abstract giving a brief and factual summary of the document indicative of the report, even though it may also appear elsewhere in the body of the technical report. If additional space is required, a continuation sheet shall be attached.

It is highly desirable that the abstract of classified reports be unclassified. Each paragraph of the abstract shall end with an indication of the military security classification of the information in the paragraph, represented as (TS), (S), (C), or (U).

There is no limitation on the length of the abstract. However, the suggested length is from 150 to 225 words.

14. KEY WORDS: Key words are technically meaningful terms or short phrases that characterize a report and may be used as index entries for cataloging the report. Key words must be selected so that no security classification is required. Identifiers, such as equipment model designation, trade name, military project code name, geographic location, may be used as key words but will be followed by an indication of technical context. The assignment of links, roles, and weights is optional.